

UNIVERSIDADE FEDERAL DO PARANÁ

CAROLINE KUKOLJ



ANÁLISE PROTEÔMICA E METABOLÔMICA DE *Azospirillum brasiliense* FP2 E
SEU MUTANTE *ntrC* EM CONDIÇÕES DE ALTO E BAIXO AMÔNIO

CURITIBA

2018

CAROLINE KUKOLJ

ANÁLISE PROTEÔMICA E METABOLÔMICA DE *Azospirillum brasiliense* FP2 E
SEU MUTANTE *ntrC* EM CONDIÇÕES DE ALTO E BAIXO AMÔNIO

Tese apresentada ao Programa de Pós Graduação em Ciências – Bioquímica, Setor de Ciências Biológicas, Universidade Federal do Paraná, como requisito parcial à obtenção do título de Doutor em Ciências – Bioquímica.

Orientador: Emanuel Maltempi de Souza
Co-orientador: Glaucio Valdameri

CURITIBA

2018

Universidade Federal do Paraná. Sistema de Bibliotecas.
Biblioteca de Ciências Biológicas.
(Rosilei Vilas Boas – CRB/9-939).

Kukolj, Caroline

Análise Proteômica e metabolômica de *Azospirillum brasiliense* FP2 e seu mutante ntrc em condições de alto e baixo amônio. / Caroline Kukolj. – Curitiba, 2018.

215 f. : il.

Orientador: Emanuel Maltempi de Souza.

Coorientador: Glaucio Valdameri.

Tese (Doutorado) – Universidade Federal do Paraná, Setor de Ciências Biológicas. Programa de Pós-Graduação em Ciências – Bioquímica.

1. *Azospirillum brasiliense*. 2. Proteínas. 3. Nitrogênio. 4. Bactérias nitrificantes. I. Título. II. Souza, Emanuel Maltempi de. III. Valdameri, Glaucio. IV. Universidade Federal do Paraná. Setor de Ciências Biológicas. Programa de Pós-Graduação em Ciências – Bioquímica.

CDD (20. ed.) 589.9

TERMO DE APROVAÇÃO

Os membros da Banca Examinadora designada pelo Colegiado do Programa de Pós-Graduação em CIÊNCIAS (BIOQUÍMICA) da Universidade Federal do Paraná foram convocados para realizar a arguição da Tese de Doutorado de **CAROLINE KUKOLJ**, intitulada: **ANÁLISE PROTEÔMICA E METABOLÔMICA DE AZOSPIRILLUM BRASILENSE FP2 E SEU MUTANTE NTRC EM CONDIÇÕES DE ALTO E BAIXO AMÔNIO**, após terem inquirido a aluna e realizado a avaliação do trabalho, são de parecer pela sua APROVAÇÃO no rito de defesa.

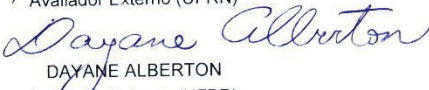
A outorga do título de Doutor está sujeita à homologação pelo colegiado, ao atendimento de todas as indicações e correções solicitadas pela banca e ao pleno atendimento das demandas regimentais do Programa de Pós-Graduação.

Curitiba, 17 de Dezembro de 2018.


EMANUEL MALTEMPI DE SOUZA
Presidente da Banca Examinadora


ROSE ADELE MONTEIRO
Avaliador Interno (UFPR)


GUSTAVO ANTONIO DE SOUZA
Avaliador Externo (UFRN)


DAYANE ALBERTON
Avaliador Externo (UFPR)

*Aos meus pais, Dorli e
Michael, com todo meu
amor e gratidão, dedico...*

RESUMO

O gênero *Azospirillum* inclui microrganismos de vida livre capazes de colonizar e promover o crescimento de gramíneas e cereais, como milho, sorgo, trigo, arroz e aveia. O *Azospirillum* é capaz de fixar nitrogênio e se associar às raízes dessas plantas, podendo transferir parte do nitrogênio fixado ao vegetal (aproximadamente 10% das necessidades da planta). Dentre as 16 espécies descritas para o gênero, *Azospirillum brasiliense* é a mais estudada. O sistema *ntr* regula o metabolismo de nitrogênio em *A. brasiliense*, incluindo os genes responsáveis pela fixação. Esse sistema é composto pelas proteínas codificadas pelos genes *glnD*, *glnB*, *glnZ*, *ntrB* e *ntrC*. A proteína GlnD é capaz de sensoriar a glutamina intracelular e agir como uridililtransferase (Utase/UR) em resposta aos níveis de nitrogênio. Em condições de limitação de nitrogênio, GlnD adiciona grupos uridilil (UMP) às proteínas PII, GlnB e GlnZ, na presença de ATP e 2-oxoglutarato. GlnB uridililada não interage com a histidina kinase NtrB, que, na sua forma livre, fosforila NtrC. NtrC ativa a transcrição de genes em resposta aos níveis de nitrogênio de maneira dependente de sigma 54 (RpoN). NtrB e NtrC compõem um sistema de dois componentes, no qual NtrB é capaz de fosforilar NtrC quando o nitrogênio intracelular é baixo. Por outro lado, a presença de nitrogênio resulta na defosforilação e consequente inativação de NtrC. O regulon NtrC já foi estabelecido em estudos anteriores para diversos organismos, incluindo *Escherichia coli*, *Sinorhizobium meliloti* e *Pseudomonas putida*. Esses estudos mostraram a função global regulatória de NtrC nesses organismos e sugerem que esse ativador está envolvido na expressão de genes relacionados a transporte e catabolismo de compostos nitrogenados, assim como na regulação central de redes metabólicas. Em *A. brasiliense*, NtrC atua como ativador transcricional de *glnB*/*glnA*, *glnZ* e outros operons envolvidos em assimilação de nitrogênio. Em baixo nitrogênio, a transcrição de *glnB* aumenta em cinco vezes através da ação de NtrC e de maneira dependente do promotor sigma 54 de *glnB*. Além disso, GlnB é capaz de modular sua própria expressão, uma vez que controla a atividade de NtrB e, consequentemente, NtrC. GlnB uridililada é essencial para a atividade de NifA, ativador transcricional dos genes *nif*. Essa regulação é independente de NtrC, pois mutantes *ntrC* são capazes de fixar nitrogênio. NtrC também regula *glnZ*, que tem sua expressão aumentada sob limitação de nitrogênio. Em *A. brasiliense*, GlnZ não está envolvido na atividade de NtrB-NtrC, contrário ao que ocorre em *E. coli*. O metabolismo geral do nitrogênio em *A. brasiliense* compreende uma cascata complexa e não totalmente elucidada. O objetivo deste trabalho é utilizar uma abordagem proteômica e metabolômica para avaliar a resposta de *A. brasiliense* FP2 e seu mutante *ntrC* cultivados em baixo e alto amônio, a fim de elucidar possíveis novos alvos de NtrC. Foi possível obter uma lista de proteínas que respondem ao baixo amônio na estirpe selvagem e mutante, possibilitando uma melhor compreensão da regulação do metabolismo de nitrogênio nesse organismo e também definir novos alvos de NtrC. Foi sugerida a participação de NtrC na resposta a estresse oxidativo e na capacidade de promoção de crescimento em plantas, especialmente para os parâmetros relacionados à raiz.

Palavras-chave: *Azospirillum brasiliense*. PII. Sistema *ntr*. Nitrogênio. NtrC. FP2.

ABSTRACT

The *Azospirillum* genus includes free-living microorganisms able to colonize and promote the growth of important cereals and grasses, such as maize, sorghum, wheat, rice and oat. *Azospirillum* is able to fix nitrogen in association with plant roots and transfer to plant part of the N fixed (about 10% of the plant needs). Among 16 *Azospirillum* species described, *Azospirillum brasilense* is the most studied. The *ntr* system regulates nitrogen metabolism in *A. brasilense*, including nitrogen fixation. This system is composed of the proteins encoded by the genes *glnD*, *glnB*, *glnZ*, *ntrB* and *ntrC*. The GlnD protein is able to sense intracellular glutamine and acts as an uridylyltransferase/uridylyl-removing enzyme (UTase/UR) in response to nitrogen levels. Under limiting nitrogen conditions, GlnD adds uridylyl groups (UMP) to the PII proteins, GlnB and GlnZ, in the presence of ATP and 2-oxoglutarate. Uridylylated GlnB cannot interact with the histidine kinase NtrB, which, in its free form, is able to phosphorylate NtrC. NtrC is an enhancer binding protein that controls the transcription of nitrogen regulated promoters, in a sigma 54 (RpoN) factor dependent manner. NtrB and NtrC compose a two-component system in which NtrB is capable of phosphorylating NtrC when nitrogen levels are low. On the other hand, the presence of nitrogen results in dephosphorylation and subsequent inactivation of NtrC. Previous studies defined the NtrC regulon for a number of organisms, including *Escherichia coli*, *Sinorhizobium meliloti* and *Pseudomonas putida*. These studies showed the global regulatory function of NtrC in these organisms and suggested that NtrC is involved in the expression of genes related to transport and catabolism of nitrogen compounds, as well as regulation of central metabolic networks. In *Azospirillum brasilense*, NtrC acts as a transcriptional activator of *glnB*/*glnA*, *glnZ* and other operons involved in nitrogen assimilation. In a nitrogen limiting condition, transcription of *glnB* increased five-fold mediated by the action of phosphorylated NtrC acting at the *glnB* sigma 54 factor dependent promoter, thus GlnB is able to regulate its own expression, since it controls the activity of NtrB and, consequently, NtrC. Uridylylated GlnB is essential for the activity of NifA, the transcriptional activator of *nif* genes. This regulation is independent of NtrC, as evidenced by the fact that *ntrC* mutants are able to fix nitrogen. NtrC also regulates *glnZ* and its expression is increased under limiting nitrogen. In *A. brasilense*, GlnZ was not found to be involved in the activity of NtrB-NtrC, in contrast to what occurs in *E. coli*. The general nitrogen metabolism in *A. brasilense* comprises a complex and yet not fully elucidated regulatory cascade. The aim of this work was to contrast the proteomic and metabolomic responses in *A. brasilense* FP2 and its *ntrC* mutant when grown in high and low nitrogen. The goal was to better understand the nitrogen metabolism regulation in this organism and to also find new targets for the transcriptional activator NtrC. It was determined a list of proteins that respond the low ammonium condition in the wild type and in the mutant, leading to a better understanding of the nitrogen metabolism regulation in this organism and also define new targets for NtrC. It was suggested that NtrC participates in the oxidative stress response and in the ability to promote plant growth, especially for the parameters related to the root.

Keywords: *Azospirillum brasilense*. PII. *Ntr* system. Nitrogen. NtrC. FP2.

LISTA DE FIGURAS

- FIGURE 1 - GROWTH CURVE OF *Azospirillum brasiliense* FP2 AND *ntrC* UNDER HIGH AND LOW NITROGEN. The arrows indicate the time points where samples were collected for lc/ms/ms and metabolomic analysis. Values represent the mean of four independent experiments..... 42
- FIGURE 2 - WESTERN BLOTT ANALYSIS OF GlnB AND GlnZ EXPRESSION IN *Azospirillum brasiliense* FP2 GROWN IN HIGH AND LOW NITROGEN. 1. INDICATES THE PURIFIED PROTEIN, 2 & 3. INDICATE TREATMENT WITH LOW AND HIGH NITROGEN IN THE WILD TYPE FP2, RESPECTIVELY..... 43
- FIGURE 3 - (A) HIERARCHICAL CLUSTERING ANALYSIS DISPLAYED AS A HEAT MAP OF PROTEINS FROM *A. brasiliense* FP2 AND ITS ISOGENIC MUTANT *ntrC* UNDER HIGH AND LOW NITROGEN. The rows represent individual proteins and the columns are the samples. Proteins that changed in abundance are indicated in red and green, respectively. The proteins that were not changed are indicated in black. The intensity of the colors increased as the difference in abundance increased. (B) PCA of the protein samples showing separation between bacterial strains and treatments..... 44
- FIGURE 4 - FUNCTIONAL CLASSIFICATIONS OF DIFFERENTIALLY EXPRESSED PROTEINS UNDER LOW AND HIGH NITROGEN IN *A. brasiliense* FP2..... 45
- FIGURE 5 - FUNCTIONAL CLASSIFICATION OF DIFFERENTIALLY EXPRESSED PROTEINS IN *A. brasiliense ntrC* UNDER HIGH AND LOW NITROGEN..... 46
- FIGURE 6 - VENN DIAGRAM OF DIFFERENTIALLY ABUNDANT PROTEINS THAT ARE UPREGULATED UNDER LOW NITROGEN TREATMENT IN *A. brasiliense* FP2 AND THE MUTANT *ntrC*..... 47
- FIGURE 7 - KEGG CLASSIFICATION FOR THE CANDIDATE PROTEINS LIKELY INDUCED BY NTRC. Pathways that showed at least 3 induced proteins are shown in the figure..... 48
- FIGURE 8 - (A) HEAT MAP SHOWING ABUNDANCES OF ALL METABOLITES IN ALL SAMPLES. Each bar represents a metabolite colored by its abundance intensities on normalized scale from blue (decreased level) to red (increased level). The samples are showed in triplicates. (B) PCA ANALYSIS FOR ALL METABOLITE SAMPLES. (C) HIERARCHICAL CLUSTERING ANALYSIS BASED ON THE METABOLITE ABUNDANCE PROFILES FOR ALL SAMPLES..... 52
- FIGURE 9 - HEAT MAP SHOWING ABUNDANCES OF ALL METABOLITES IN *A. brasiliense* FP2 HIGH AND LOW NITROGEN. Each bar represents a metabolite colored by its abundance intensities. The samples are showed in triplicates..... 53

FIGURE 10 - INTEGRATED PROTEOMICS AND METABOLOMICS DATA IN PERCENTAGE OF COVERAGE FOR <i>A. brasiliense</i> BIOLOGICAL PATHWAYS. (A) COVERAGE OF THE TEN MOST AFFECTED PATHWAYS IN THE WILD TYPE LOW AND HIGH N. (B) COVERAGE OF THE TEN MOST AFFECTED PATHWAYS IN THE MUTANT UNDER LOW AND HIGH NITROGEN.....	57
FIGURE 11 - <i>S. viridis</i> GROWTH PROMOTION FOR EACH <i>A. brasiliense</i> STRAIN COMPARED TO THE UN-INOCULATED CONTROL. BARS ARE MEAN OF N = X +- SE. Asterisk represents p-value = 0.01** and 0.001***.....	60
FIGURE 12 - CELL SURVIVAL RATE OF THE <i>A. brasiliense</i> FP2 AND <i>ntrC</i> , IN HIGH AND LOW NITROGEN, UNDER DIFFERENT CONCENTRATIONS OF H ₂ O ₂	62
FIGURE 13 - TRANSCRIPTIONAL VALIDATION OF PROTEOMIC DATA USING RT-qPCR ASSAYS. THE VALUE OF FOLD CHANGE ON THE Y-AXIS INDICATES THE RATIO OF EITHER PROTEIN OR mRNA LEVEL IN THE <i>A. brasiliense</i> FP2 HIGH N WHEN COMPARED TO THE LOW N.....	64
FIGURE 14 - RELATIVE EXPRESSION OF SELECTED GENES COMPARED TO THE CONTROL <i>A. brasiliense</i> FP2 LOW N. Asterisk represents p-value = 0.05*; 0.01** and 0.001***	65
FIGURE 15 - KEGG PATHWAY CLASSIFICATION FOR UPREGULATED PROTEINS IN <i>A. brasiliense</i> FP2 IN RESPONSE TO NITROGEN LIMITATION. Bars indicate the percentage of coverage for each pathway.....	96
FIGURE 16 - COG CLASSIFICATION FOR PUTATIVE PROTEINS REGULATED BY <i>NtrC</i>	107
FIGURE 17 - GROWTH CURVE UNDER DIFFERENT CONCENTRATIONS OF H ₂ O ₂ BASED ON OD ₆₀₀ . The arrows indicate the point when H ₂ O ₂ was added.....	108
FIGURE 18 - GROWTH CURVE UNDER DIFFERENT CONCENTRATIONS OF H ₂ O ₂ BASED ON CFU COUNT.	109
FIGURE 19 - ROOT COLONIZATION OF WILD TYPE AND MUTANT STRAIN. Twenty days after inoculation the number of CFU was determined.....	140
FIGURA 20 - ELETROFORESE EM GEL DE AGAROSE DOS FRAGMENTOS AMPLIFICADOS COM PRIMERS PARA <i>glnZ</i> (F/R) e <i>glnB</i> (F2/R2).....	164
FIGURA 21 - CONFIRMAÇÃO DA ESTIRPE LHNTRC5. 1. LHNTRC5 em 20mM de amônio. 2. FP2 em 20mM de amônio. 3. LHNTRC5 em 20mM de NaNO ₃ . 4. FP2 em 20mM de NaNO ₃	164

FIGURA 22 - CURVA DE CRESCIMENTO DAS ESTIRPES ESTUDADAS EM 20mM DE CLORETO DE AMÔNIO E EM 5mM DE GLUTAMINA. O nome da estirpe é seguido da fonte de nitrogênio, sendo N para 20mM de cloreto de amônio e G para 5mM de glutamina.....	165
FIGURA 23 - CURVA DE CRESCIMENTO DAS ESTIRPES ESTUDADAS EM 20mM E 2mM DE CLORETO DE AMÔNIO. O nome da estirpe é seguido da concentração de nitrogênio, sendo + para 20mM de cloreto de amônio e - para 2mM.....	166
FIGURA 24 - CURVA DE CRESCIMENTO.....	168
FIGURA 25 - FLUORESCÊNCIA DE CADA CULTURA EM FUNÇÃO DE DO ₆₀₀	169
FIGURA 26 - NÚMERO DE CÉLULAS POR TEMPO DAS ESTIRPES ESTUDADAS.....	169
FIGURA 27 - PERFIL DE CRESCIMENTO DAS BACTÉRIAS INOCULADAS EM LACTATO ADICIONADO DE 1, 5 E 10% DE LB.....	170
FIGURA 28 - PERFIL DE CRESCIMENTO DE CADA ESTIRPE EM ALTO (+N) E BAIXO (-N) NITROGÊNIO.....	171
FIGURA 29 - WESTERN BLOT DE <i>A. brasiliense</i> FP2 E <i>ntrc</i> EM ALTO E BAIXO NITROGÊNIO.....	172
FIGURA 30 - GEL 2-D TESTE 1, UTILIZANDO PROTOCOLO RECOMENDADO PELO FABRICANTE.....	174
FIGURA 31 - GEL 2-D TESTE 2. Amostra não tratada com CleanUp.....	175
FIGURA 32 - GEL 2-D TESTE 3. Amostra tratada com CleanUp.....	175
FIGURA 33 - GEL 2-D TESTE 4.....	176
FIGURA 34 - GEL 2-D TESTE 5.....	176
FIGURA 35 - GEL 2-D TESTE 7.....	177
FIGURA 36 - GEL 2-D TESTE 8.....	177
FIGURA 37 - GEL 2-D TESTE 9.....	178
FIGURA 38 - NÚMERO DE PROTEÍNAS DIFERENCIAIS IDENTIFICADAS EM CADA COMPARAÇÃO. A condição de alto nitrogênio está representada por +N e de baixo por -N.....	179
FIGURA 39 - GRÁFICO DE VENN COM O NÚMERO DE PROTEÍNAS INDUZIDAS EM FP2 E <i>ntrC</i> EM BAIXO NITROGÊNIO.....	203
FIGURA 40 - CLASSIFICAÇÃO KEGG DO GRUPO DE PROTEÍNAS COM POTENCIAL REGULAÇÃO POR NtrC.....	204

- FIGURA 41 - DEZ VIAS MAIS AFETADAS NAS ESTIRPES SELVAGEM E MUTANTE EM ALTO NITROGÊNIO. Os resultados incluem análise proteômica e metabolômica e estão representados em porcentagem de cobertura da via..... 213
- FIGURA 42 - DEZ VIAS MAIS AFETADAS NAS ESTIRPES SELVAGEM E MUTANTE EM BAIXO NITROGÊNIO. Os resultados incluem análise proteômica e metabolômica e estão representados em porcentagem de cobertura da via..... 214
- FIGURA 43 – EXPRESSÃO RELATIVA DOS GENES SELECIONADOS COMPARADOS AO CONTROLE *A. brasiliense* FP2 BAIXO N. Asteriscos representam p-value = 0.05*; 0.01** and 0.001***..... 215

LISTA DE TABELAS

TABLE 1 - NUMBER OF DIFFERENTIALLY EXPRESSED PROTEINS FOR EACH COMPARISON.....	43
TABLE 2 - PROTEINS WITH A SIGMA 54 MOTIF IN THE PROMOTER REGION OF THEIR CORRESPONDENT GENES.....	63
TABLE 3 - PRIMERS USED FOR RT-qPCR ANALYSIS.....	73
TABLE 4 - DIFFERENTIAL PROTEINS BETWEEN <i>A. brasiliense</i> FP2 LOW AND HIGH N.....	74
TABLE 5 - KEGG PATHWAY CLASSIFICATION FOR DIFFERENTIAL PROTEINS IN <i>A. brasiliense</i> FP2 IN RESPONSE TO NITROGEN LIMITATION.....	91
TABLE 6 - DIFFERENTIAL PROTEINS BETWEEN <i>A. brasiliense ntrC</i> LOW AND HIGH NITROGEN.....	97
TABLE 7 - CANDIDATE PROTEINS TO BE INDUCED BY NtrC.....	103
TABLE 8 - NtrC REGULATION CANDIDATES INVOLVED IN THE QUORUM SENSING PATHWAY	110
TABLE 9 - NtrC REGULATION CANDIDATES INVOLVED IN THE OXIDATIVE STRESS RESPONSE	110
TABLE 10 - TOTAL METABOLITES, RETENTION TIMES AND ABUNDANCES IN EACH TREATMENT AND TRIPPLICATES.....	111
TABLE 11 - DIFFERENTIAL METABOLITES IN <i>A. brasiliense</i> FP2 HIGH AND LOW NITROGEN.....	119
TABLE 12 - DIFFERENTIAL METABOLITES IN <i>A. brasiliense ntrC</i> HIGH AND LOW NITROGEN.....	121
TABLE 13 - KEGG DISTRIBUTION OF PROTEOME AND METABOLOMICS DATA FOR <i>A. brasiliense ntrC</i> HIGH AND LOW NITROGEN.....	123
TABLE 14 - KEGG DISTRIBUTION OF PROTEOME AND METABOLOMICS DATA FOR <i>A. brasiliense</i> FP2 HIGH AND LOW NITROGEN.....	127
TABLE 15 - PLANT ASSAY.....	132
TABELA 16 - TEMPOS DE GERAÇÃO EM HORAS DAS ESTIRPES ESTUDADAS EM 20mM DE CLORETO DE AMÔNIO E EM 5mM DE GLUTAMINA.....	166

TABELA 17 - TEMPOS DE GERAÇÃO EM HORAS DAS ESTIRPES ESTUDADAS EM 20mM E 2mM DE CLORETO DE AMÔNIO.....	167
TABELA 18 - CONCENTRAÇÕES OBTIDAS NA DOSAGEM DE PROTEÍNAS.....	173
TABELA 19 - RENDIMENTO OBTIDO NA DOSAGEM DE PROTEÍNAS.....	173
TABELA 20 - PROGRAMA DE FOCALIZAÇÃO UTILIZADO NO TESTE 6.....	177
TABELA 21 - PROTEÍNAS DIFERENCIAIS ENTRE <i>A. brasiliense</i> FP2 E O MUTANTE <i>ntrC</i> EM BAIXO NITROGÊNIO.....	179
TABELA 22 - PROTEÍNAS DIFERENCIAIS ENTRE <i>A. brasiliense</i> FP2 E O MUTANTE <i>ntrC</i> EM ALTO NITROGÊNIO.....	191
TABELA 23 - PROTEÍNAS COM POSSÍVEIS SÍTIOS DE LIGAÇÃO DE NtrC NA REGIÃO PROMOTORA DOS SEUS GENES. Em verde estão as bases que apresentaram similaridade com o motivo utilizado na busca.....	206
TABELA 24 - PROTEÍNAS COM POSSÍVEIS SÍTIOS DE LIGAÇÃO DE SIGMA 54 NA REGIÃO PROMOTORA DOS SEUS GENES. Em verde estão as bases que apresentaram similaridade com o motivo utilizado na busca. As proteínas em negrito apresentam também possível sítio de ligação de NtrC.....	207
TABELA 25 - DIFFERENTIAL METABOLITES BETWEEN <i>A. brasiliense</i> FP2 AND <i>ntrC</i> UNDER HIGH NITROGEN.....	210
TABELA 26 - DIFFERENTIAL METABOLITES BETWEEN <i>A. brasiliense</i> FP2 AND <i>ntrC</i> UNDER LOW NITROGEN.....	211

SUMÁRIO

1. INTRODUÇÃO.....	15
1.1 REVISÃO BIBLIOGRÁFICA.....	16
1.1.2 <i>Azospirillum</i>	16
1.1.3 Proteínas P _{II} no metabolismo de nitrogênio.....	17
1.1.4 Sistema <i>ntr</i> e NtrC.....	21
1.1.5 Proteômica.....	24
1.1.6 Metabolômica.....	28
2. MANUSCRITO.....	33
2.1 ABSTRACT.....	33
2.2 INTRODUCTION.....	34
2.3 EXPERIMENTAL SECTION.....	35
2.3.1 Bacterial strains and growth conditions.....	35
2.3.2 Protein extraction.....	36
2.3.3 Western blot analysis.....	36
2.3.4 Label free quantitative LC-MS/MS analysis.....	36
2.3.5 Determination of intracellular metabolites by GC-MS and data analysis.....	37
2.3.6 Pathways analysis.....	38
2.3.7 Plant colonization assay: Seed sterilization, germination conditions, plant inoculation, and plant growth conditions.....	39
2.3.8 Plant growth promotion measurements, statistical analysis and bacterial quantification.....	39
2.3.9 Oxidative stress response analysis.....	40
2.3.10 Analysis of the promoter region for putative genes regulated by NtrC.....	40
2.3.11 RNA isolation, cDNA synthesis and quantitative RT-PCR.....	40
2.4 RESULTS AND DISCUSSION.....	41
2.4.1 Bacterial growth under limiting nitrogen.....	41
2.4.2 Western blot analysis of GlnB and GlnZ abundance in <i>A. brasilense</i> as a function of nitrogen availability.....	42
2.4.3 Proteomic data overview.....	43

2.4.4 Proteomic profile of <i>A. brasiliense</i> FP2 in response to nitrogen limitation.....	44
2.4.5 Proteins regulated by nitrogen availability in <i>A. brasiliense ntrC</i>	46
2.4.6 Identification of proteins likely to belong to the NtrC regulon.....	47
2.4.7 Metabolomic profiling of <i>A. brasiliense</i>	51
2.4.8 Metabolomic changes in <i>A. brasiliense</i> FP2 in response to nitrogen limitation.....	53
2.4.9 Metabolomic changes in the <i>A. brasiliense ntrC</i> mutant in response to nitrogen limitation.....	55
2.4.10 Proteome and metabolomics integration using pathway analysis.....	55
2.4.11 Effects of <i>A. brasiliense</i> FP2 and <i>ntrC</i> mutant strains on <i>S. viridis</i> growth.....	58
2.4.12 Oxidative stress response.....	61
2.4.13 Analysis of the promoter region for putative genes regulated by NtrC	62
2.4.14 mRNA levels of selected genes using RT-qPCR.....	63
2.4.15 qRT-PCR analyses of the differentially expressed genes.....	64
2.5 CONCLUSION.....	65
2.6 ACKNOWLEDGMENTS.....	65
2.7 REFERENCES.....	66
2.8 MATERIAL SUPLEMENTAR.....	73
3 CONSIDERAÇÕES FINAIS.....	141
4 CONCLUSÕES.....	144
REFERÊNCIAS.....	146
APÊNDICE 1.....	163
Linhagens bacterianas, meios de cultura e condições de crescimento.....	163
Confirmação das estirpes estudadas.....	163
Avaliação do perfil de crescimento das estirpes estudadas e definição das condições de baixo e alto nitrogênio.....	165
Confirmação das condições de alto e baixo nitrogênio.....	171
Padronização do protocolo de extração de proteínas.....	172
Padronização da isoeletrofocalização em tiras de 24cm e pH 4-7.....	174
Análise do proteoma de <i>A. brasiliense</i> FP2 e seu mutante <i>ntrc</i> em alto e baixo nitrogênio.....	178
Análise bioinformática.....	205

Análise metabolômica.....	209
Integração de proteoma e metaboloma utilizando análise de vias KEGG.....	212
Análise qRT-PCR de genes diferencialmente expressos.....	214

1. INTRODUÇÃO

O gênero *Azospirillum* tem sido estudado há mais de 40 anos devido a associação mutuamente benéfica com gramíneas. Suas propriedades de promoção do crescimento vegetal, tais como a fixação biológica do nitrogênio e a liberação de hormônios são bem conhecidas e interessantes economicamente. O melhor entendimento da regulação do metabolismo de nitrogênio nesse organismo pode levar futuramente à seleção de estirpes mais eficientes em promover o crescimento vegetal, com potencial contribuição para culturas de interesse econômico, como milho, arroz e trigo. Estudos anteriores demonstraram que os mecanismos de regulação e controle do processo de fixação e metabolismo de nitrogênio, além dos possíveis alvos moleculares do ativador transcracional NtrC e das proteínas P_{II}, embora bastante estudados, não estão totalmente elucidados. Nesse contexto, abordagens amplas, como proteômica e metabolômica, constituem importantes ferramentas e possibilitam o estudo da organização e controle das vias metabólicas de *A. brasiliense*, incluindo a atividade de enzimas que catalisam etapas específicas do metabolismo nitrogênio.

O objetivo geral deste trabalho foi determinar o proteoma e metaboloma de *Azospirillum brasiliense* FP2 e seu mutante *ntrC* em alto e baixo amônio. O objetivo é gerar um panorama das proteínas e metabólitos diferencialmente expressos encontrados nessas estirpes a fim de investigar mais detalhadamente aspectos ainda não elucidados do metabolismo e sinalização de níveis de nitrogênio neste organismo, especialmente relacionados ao papel de NtrC. A escolha desse mutante levou em consideração o importante papel dessa proteína no processo de regulação do metabolismo de nitrogênio e sua capacidade de responder a diferentes estímulos. Além disso, a conservação e distribuição de NtrC em procariotos permite que seja feita uma correlação com os sistemas regulatórios de outras espécies.

Este trabalho será dividido em duas partes, a primeira em forma de artigo de periódico, contendo a primeira versão do manuscrito a ser submetido para a revista *Journal of Proteome Research*, e a outra em forma de apêndice, incluindo dados obtidos não apresentados no artigo, além de experimentos essenciais para definição e modificação da estratégia inicial de trabalho.

No projeto proposto inicialmente seria utilizada a técnica de 2D-DIGE (*Differential Gel Electrophoresis*) para comparar os perfis proteicos de *A. brasiliense* FP2 e seus mutantes *glnB*, *glnZ*, *glnBglnZ* e *ntrC* em alto e baixo nitrogênio. A estratégia incluía a marcação de amostras com diferentes sondas fluorescentes (CyDye), permitindo a detecção de duas condições em um mesmo gel. Os géis bidimensionais seriam comparados e as proteínas diferencialmente expressas identificadas por espectrometria de massas MALDI-Tof/Tof. Os géis obtidos nessa etapa não apresentaram boa resolução das bandas, especialmente as da parte ácida, portanto, após sucessivas tentativas de protocolos de isoeletrofocalização, essa estratégia foi alterada. Na nova estratégia, foi estabelecida uma colaboração com o Dr. Gustavo Antônio de Souza, da unidade de espectrometria da Universidade de Oslo, na Noruega, para a análise proteômica *shotgun label-free* (LC-MS/MS). Com essa técnica, é possível a análise direta de misturas complexas, gerando um perfil global das proteínas presentes na amostra. Por ser uma técnica mais sensível, menor quantidade de proteína pode ser detectada e um maior número de compostos é identificado em relação à análise utilizando gel.

Os experimentos que levaram à modificação da estratégia inicial estão sumarizados no apêndice desde trabalho, bem como dados obtidos que não foram incluídos no manuscrito.

1.1 REVISÃO BIBLIOGRÁFICA

1.1.2 *Azospirillum*

Há um grande interesse no entendimento do metabolismo de bactérias que promovem o crescimento vegetal e incrementam a produtividade de plantas através da fixação biológica do nitrogênio, devido ao aumento da demanda por alimentos e à busca por alternativas ao uso de fertilizantes, cuja produção é de alto custo econômico e ambiental. Dentre os organismos fixadores de nitrogênio atmosférico, as espécies do gênero *Azospirillum* são as mais estudadas (REIS, 2000) e compreendem bactérias que podem ser de vida livre ou colonizar a superfície ou o interior de raízes de cereais e gramíneas, como milho, sorgo, trigo, arroz e aveia, promovendo crescimento da planta (BASHAN *et al.*, 2004). A fixação de nitrogênio nessas bactérias é um processo altamente regulado, devido à estequiometria da

reação demonstrada abaixo, que requer alta energia e é catalisada pelo complexo enzimático nitrogenase.



Além disso, condições ambientais favoráveis, como baixos níveis de nitrogênio e oxigênio são necessárias.

1.1.3 Proteínas P_{II} no metabolismo de nitrogênio

As proteínas responsáveis pela biossíntese e montagem do complexo nitrogenase são codificadas pelos genes *nif* (CHUBATSU *et al.*, 2012), cuja expressão é regulada pelo sistema *ntr*, que controla o metabolismo geral do nitrogênio e compreende uma cascata regulatória complexa e ainda não totalmente elucidada. Na maioria dos diazotróficos, a expressão dos genes *nif* é dependente do ativador transcripcional NifA (LI *et al.*, 2011). Em *Azospirillum brasilense*, NifA é controlado por proteínas transdutoras de sinal da família P_{II}, GlnB e GlnZ (HUERGO *et al.*, 2008). Essas proteínas são capazes de sofrer modificações covalentes reversíveis por uridililação em resposta aos níveis de nitrogênio intracelular, sendo que tanto a forma livre, quanto a uridililada podem interagir com outras proteínas e modular suas atividades (HUERGO *et al.*, 2008). A uridililação de GlnB e GlnZ e a consequente transferência de informação para outros componentes do sistema *ntr* representa um ponto chave na cascata regulatória do metabolismo do nitrogênio, entretanto, a lista de alvos das proteínas P_{II} ainda não foi totalmente descrita (HUERGO *et al.*, 2013).

Em *A. brasilense*, o gene *glnB* está em um operon com *glnA*, que codifica a enzima glutamina sintetase (GS), necessária para assimilação de amônio (DE ZAMAROCZY *et al.*, 1990). Em *E. coli*, a GS pode sofrer modificação covalente reversível por adenililação, catalisada pela adenililtransferase (ATase), sendo que em excesso de nitrogênio a GS é altamente adenililada, e consequentemente inativada, por intermédio das P_{II} desuridililadas, enquanto que em baixo nitrogênio a maior parte da GS permanece desadenililada e ativa (DE ZAMAROCZY *et al.*, 1996; NINFA & JIANG, 2005). A atividade de ATase é controlada pelas proteínas P_{II} em

resposta aos níveis de nitrogênio intracelular, porém, em *A. brasiliense*, isso não foi observado (DE ZAMAROCZY, 1998).

Em condições de limitação de nitrogênio, a concentração de glutamina intracelular é baixa e a proteína GlnD de *A. brasiliense* atua como uridilil transferase (UTase), adicionando grupos uridilil (UMP) às proteínas P_{II}, GlnB e GlnZ, na presença de ATP e 2-oxoglutarato (JIANG *et al.*, 1998). Na forma uridililada, GlnB não interage com a proteína NtrB, deixando-a livre para catalisar a fosforilação de NtrC (JIANG & NINFA, 1999). NtrB e NtrC compõem um sistema de dois componentes, sendo que, sob baixa concentração de nitrogênio, NtrB transfere um grupo fosforil para o ativador transcrecional NtrC (NINFA *et al.*, 1993). NtrC fosforilado é capaz de ativar a transcrição de genes responsáveis pela assimilação de nitrogênio por fontes alternativas, por exemplo nitrato (ARCONDÉGUY, JACK e MERRICK, 2001). Em *Klebsiella pneumoniae*, NtrC fosforilada ativa a transcrição dos genes *glnA*, *amtB* (que codifica um transportador de amônia), *glnK* (codifica uma proteína ortóloga à GlnZ de *A. brasiliense*) e *nifA* (ZHANG *et al.*, 2005).

Por outro lado, em condições de excesso de nitrogênio, a proteína GlnD liga-se à glutamina e atua como removedora de grupos uridilil (UR), deixando as P_{II} livres, desuridililadas. Nessa condição, GlnB interage com NtrB impedindo a fosforilação de NtrC, que permanece inativo (JIANG & NINFA, 1999).

Além da resposta a glutamina, as proteínas P_{II} também estão sujeitas a regulação alostérica pela ligação direta dos efetores 2-oxoglutarato e ATP. As P_{II} são homotriméros que apresentam um sítio de ligação para ATP e um sítio para 2-oxoglutarato em cada monômero. A ligação de uma molécula de 2-oxoglutarato a um monômero das P_{II} ocorre de forma dependente da ligação prévia de uma molécula de ATP (FOKINA *et al.*, 2010). A ligação da primeira molécula de 2-oxoglutarato faz com que a afinidade pelos outros sítios diminua e as ligações subsequentes tornem-se mais difíceis (JIANG & NINFA, 2009). Dessa forma, o trimero GlnB ou GlnZ livre, só irá se ligar a mais de uma molécula de 2-oxoglutarato quando a concentração intracelular deste for alta, ou seja, em baixos níveis de nitrogênio intracelular. Nestas condições, GlnB pode ser uridililada e perder afinidade por NtrB, que fica livre para fosforilar e ativar NtrC (KAMBEROV *et al.*, 1995). Além disso, GlnB saturada com 2-oxoglutarato também inibe a ligação com a ATase,

consequentemente a GS permanece desadenililada e ativa (JIANG *et al.*, 1998). Em *E. coli*, GlnK (GlnZ de *A. brasiliense*) apresenta efeito similar em resposta aos níveis de 2-oxoglutarato (ATKINSON & NINFA, 1999). Portanto, presença de ATP e 2-oxoglutarato é indispensável para que GlnB e GlnZ possam ser uridililadas e a capacidade de interagir com suas proteínas alvo é diretamente influenciada pela combinação dos efetores ligados e pelo estado de uridililação (JIANG & NINFA, 2009).

As P_H podem ainda interagir com proteínas transportadoras de amônio, presentes em vários organismos e codificadas por genes *amt* (VON WIREN e MERRICK, 2004). GlnB e GlnZ de *A. brasiliense* são capazes de ligar à membrana celular após choque de amônio, de maneira dependente de AmtB (HUERGO *et al.*, 2006). Nesse organismo, GlnZ atua como um regulador negativo de AmtB, pois a taxa de captação de metilamônio em mutantes *glnZ* é duas vezes maior em relação à estirpe selvagem (COUTTS *et al.*, 2002). Em *E. coli*, GlnB e GlnK também se associam à membrana interna de forma dependente de amônio e AmtB (COUTTS *et al.*, 2002). Em excesso de nitrogênio, GlnK se encontra desuridililada e pode se ligar à membrana através de AmtB, bloqueando o canal de amônio (COUTTS *et al.*, 2002; GRUSWITZ *et al.*, 2007). A ligação GlnK-AmtB ocorre rapidamente após exposição a amônio e é reversível (JAVELLE *et al.*, 2004), sugerindo uma regulação fina do transporte de nitrogênio para o interior da célula, sensível a pequenas flutuações nos níveis de amônio (JAVELLE *et al.*, 2004, COUTTS *et al.*, 2002). Em *A. brasiliense*, o gene *glnZ* é monocistrônico e localizado distante de *amtB* (DE ZAMAROCZY, 1998), porém, na maioria dos organismos, os genes *glnK* e *amtB* são coexpressos e estão localizados no operón *glnKamtB*, que é ativado por NtrC, o que sugere que a função primária de GlnK seja regular a atividade de AmtB (VON WIREN & MERRICK, 2004).

Em *A. brasiliense*, a expressão do gene *glnB* é regulada por amônio e pelo ativador transcricional NtrC. Em altas concentrações de amônio, *glnB* é expresso a partir de um promotor dependente do fator σ 70. Por outro lado, em baixos níveis de amônio, *glnB* é expresso por um promotor alternativo dependente do fator σ 54, ativado por NtrC (DE ZAMAROCZY *et al.*, 1993). Nesta condição, observa-se uma expressão até cinco vezes maior de GlnB em relação à quantidade expressa em

excesso de amônio (HUERGO *et al.*, 2003). Sendo assim, GlnB é capaz de modular sua própria expressão, uma vez que está envolvida na regulação da atividade de NtrB e, consequentemente, de NtrC (HUERGO *et al.*, 2003). O mutante *glnB* de *A. brasiliense* apresentou redução da taxa de captação de íons metilamônio e foi capaz de utilizar nitrato como fonte de nitrogênio (DE ZAMAROCZY, 1998). Além disso, o mutante *glnB* é incapaz de fixar nitrogênio, uma vez que GlnB uridililada é indispensável para a atividade de NifA, ativadora dos genes *nif* (VAN DOMMELEN *et al.*, 2002). Essa regulação ocorre de forma independente de NtrC, pois mutantes *ntrC* são capazes de fixar nitrogênio e a expressão de NifA não é alterada em mutantes *glnB* (LIANG *et al.*, 1992), sugerindo a presença de outra via regulatória do gene *nifA* em *A. brasiliense* (MACHADO *et al.*, 1995).

O gene *glnZ* tem sua expressão regulada por NtrC e aumentada em baixos níveis de nitrogênio (DE ZAMAROCZY, 1998). Em *A. brasiliense*, GlnZ não participa no controle da atividade de NtrB-NtrC, ao contrário do que se observa em *E. coli* (DE ZAMAROCZY, 1998). O mutante *glnZ* de *A. brasiliense* é capaz de fixar nitrogênio da mesma forma que a estirpe selvagem, levando à conclusão que GlnZ não tem a mesma função de GlnB na regulação de NifA. Além disso, apresentou aumento de duas vezes no transporte de metilamônio, sugerindo que GlnZ pode atuar na regulação de AmtB (DE ZAMAROCZY, 1998).

O mutante duplo *glnBglnZ* apresenta deficiência de crescimento mesmo em meio rico em nutrientes, mas que pode ser reestabelecido tanto por *glnB* ou *glnZ*, indicando que a presença de, pelo menos, uma das PII é necessária para o crescimento de *A. brasiliense* (DE ZAMAROCZY, 1998).

A atividade da nitrogenase sofre regulação pós-traducional em *A. brasiliense* na qual a enzima é inativada reversivelmente (*switch on/off*) em resposta a estímulos ambientais. A adição de íons amônio causa sua rápida inativação devido à ADP-ribosilação de uma subunidade da dinitrogenase redutase (NifH) da nitrogenase, catalisada pela enzima ADP-ribosiltransferase (DraT) (ZHANG *et al.*, 1993). Por outro lado, quando a concentração de íons amônio diminui, o grupo ADP-ribosil é removido pela glicohidrolase (DraG) e a dinitrogenase redutase é reativada (HALBLEID & LUDDEN, 2000). Outros fatores ambientais, como mudanças no estado energético (ZHANG *et al.*, 1993) e anaerobiose também podem levar ao

desligamento/ligamento da nitrogenase mediado por DraT/DraG (MARTIN & REINHOLD-HUREK, 2002). GlnB e GlnZ de *A. brasiliense* participam do controle pós-traducional da nitrogenase interagindo diretamente com DraT e DraG, respectivamente (HUERGO *et al.*, 2006). O mutante *glnB* dessa espécie é deficiente no desligamento da nitrogenase, sugerindo que GlnB atua no controle da atividade de DraT (KLASSEN *et al.*, 2005). Por outro lado, o mutante *glnZ* apresentou deficiência no religamento da nitrogenase após consumo dos íons amônio, levando à hipótese de que GlnZ poderia atuar controlando a atividade de DraG (KLASSEN *et al.*, 2001). Em *A. brasiliense*, após um choque de amônio ocorre um sequestro de GlnZ e DraG pelo transportador AmtB, formando um complexo que se desfaz após o consumo dos íons amônio (HUERGO *et al.*, 2009). Em condições de baixo nitrogênio, GlnB e GlnZ estão uridililadas, DraT encontra-se inativa e DraG ativa, portanto, a nitrogenase não está modificada e permanece ligada. Nesse caso, as P_{II} apresentam fraca interação com DraT e DraG. Após adição de amônio, as P_{II} são desuridililadas e a formação dos complexos DraT-GlnB, DraG-GlnZ e AmtB-GlnZ-DraG é favorecida. Nestas condições, DraT está ativa e pode promover o desligamento da nitrogenase pela adição do grupo ADP-ribosil, enquanto que DraG está inativa (HUERGO *et al.*, 2009).

1.1.4 Sistema *ntr* e NtrC

Os mecanismos regulatórios que coordenam a assimilação de nitrogênio variam de acordo com a fonte de nitrogênio e o organismo. Em *E. coli*, a amônia é a fonte de nitrogênio preferencial e que melhor suporta o crescimento bacteriano, além disso, a presença de amônia reprime o sistema *ntr* (REITZER, 2003). Os produtos primários da assimilação da amônia são glutamato e glutamina. O controle transcracional realizado por NtrC depende da sua abundância e conformação. NtrB fosforila NtrC em condições de limitação de nitrogênio e também o desfosforila quando complexado com as P_{II} não uridililadas. O nível de fosforilação de NtrC depende da concentração de glutamina, que determina o estado de uridililação das P_{II} e também os níveis de ATP, ADP e 2-oxoglutarato, que são efetores alostéricos que atuam sobre as P_{II} e sua capacidade de regular atividade de NtrB (JIANG & NINFA, 2009).

NtrC é uma proteína regulatória e pode ser fosforilada em limitação de nitrogênio por NtrB e ativar genes de maneira dependente do fator alternativo sigma 54 da RNA polimerase (ROMBEL et al., 1998). NtrC pode também atuar como repressor transcrional, mas o papel da fosforilação sobre os promotores reprimidos ainda não está claro (SCHUMACHER et al., 2013). O mecanismo de ativação da transcrição envolve a fosforilação inicial do dímero de NtrC e subsequente oligomerização e ligação de NtrC fosforilado a uma sequência específica de DNA, que pode estar localizada distante do promotor (HERVÁS et al., 2009). Em seguida, NtrC interage com o fator sigma 54 da RNA polimerase e liga-se ao promotor através da formação de um loop de DNA, formando o complexo aberto e iniciando a transcrição (ZHANG et al., 2002). Os produtos dos genes ativados por NtrC incluem o transportador de amônio (AmtB), a glutamina sintetase (GlnA), transportadores de aminoácidos, as proteínas regulatórias NtrB e o próprio NtrC, entre outras enzimas não totalmente conhecidas (ZIMMER et al., 2000).

Análises de sítios sigma 54, microarray e outros estudos em *E. coli* sugerem que aproximadamente 100 genes sejam afetados pela limitação de nitrogênio de forma dependente do sistema *ntr* (REITZER, 2003). Uma das respostas fisiológicas desencadeadas pelo sistema *ntr* é o controle da assimilação de amônia, a fim de manter os níveis intracelulares de glutamina. De acordo com Zimmer et al. (2000), diversos sistemas de transporte de compostos nitrogenados também são induzidos por esse sistema, principalmente de aminoácidos, peptídeos, poliaminas e nucleosídeos. Em *E. coli*, enzimas de catabolismo também estão sob controle do sistema *ntr*, sendo pelo menos 19 delas relacionadas à degradação e transporte de poliaminas (ZIMMER, 2000; REITZER, 2003). Os níveis de poliaminas são correlacionados com a taxa de crescimento, portanto, a regulação desses genes pelo sistema *ntr* pode explicar a relação entre o baixo crescimento em limitação de nitrogênio e o conteúdo de poliaminas (TWEEDDALE et al., 1998; REITZER, 2003).

Em *E. coli* e *Klebsiella*, existem promotores regulados indiretamente por nitrogênio de maneira dependente do fator sigma 70 da RNA polimerase, através da proteína Nac, de controle e assimilação de nitrogênio (BENDER, 1991; REITZER, 2003). Genes ativados por Nac em *E. coli* estão envolvidos em transporte de moléculas nitrogenadas que podem servir como fontes de nitrogênio (ZIMMER et al.,

2000). Em *Klebsiella pneumoniae*, a utilização de uréia e alguns aminoácidos é também ativada por Nac (COLLINS *et al.*, 1993). Nac não responde diretamente à disponibilidade de nitrogênio, mas sua transcrição é regulada por NtrC (BENDER, 1991). Portanto, Nac atua como uma conexão entre NtrC e genes ativados por sigma 70.

Em *Pseudomonas*, estudos indicaram que NtrC é necessário para ativar a expressão de genes envolvidos na captação e metabolismo de nitrogênio (HERVÁS *et al.*, 2008). Mutantes que não expressam o fator sigma 54 são prejudicados na utilização de diversas fontes de nitrogênio (TOTTEN *et al.*, 1990). A análise do transcriptoma global de *P. putida* sugere que GlnK e AmtB são regulados por NtrC de maneira dependente de nitrogênio (HERVÁS *et al.*, 2008). Além disso, o transcriptoma revelou que genes que codificam para transportadores de aminoácidos em geral e envolvidos com assimilação de uréia são regulados por NtrC. Análises de RT-PCR confirmaram a expressão aumentada de *amtB* e *glnA* na estirpe selvagem em relação ao mutante que não expressa NtrC. Diferentemente de *E. coli*, *Pseudomonas* possui apenas uma proteína PII (GlnK) e não apresenta Nac (HERVÁS *et al.*, 2008).

Em *Burkholderia cenocepacia*, a análise fenotípica do mutante *ntrC* confirmou os dados de transcriptoma e mostrou que NtrC controla a utilização de diversas fontes de nitrogênio, produção de exopolissacarídeos e mobilidade, enquanto que a formação de biofilme foi parcialmente afetada no mutante (LIU *et al.*, 2017). Neste organismo, o mutante *ntrC* não foi afetado na resistência a antibióticos e nem a estresse oxidativo (LIU *et al.*, 2017 dados não mostrados). Genes que codificam enzimas do ciclo do ácido cítrico tiveram a transcrição aumentada no mutante *ntrC* em limitação de nitrogênio, reforçando a hipótese observada em *Pseudomonas putida*, de que NtrC reprime o metabolismo de carbono (HERVAS *et al.*, 2008).

Em *A. brasiliense*, o controle de captação de fontes alternativas de nitrogênio, transporte e assimilação de íons amônio, além de controle transcricional e pós-traducional da nitrogenase estão sob influência do sistema *ntr*. Dessa forma, o estudo do mutante que não expressa o ativador transcricional desse sistema, NtrC, pode levar a uma melhor compreensão dos fatores ainda não elucidados envolvidos

na regulação do metabolismo de nitrogênio, além de novos possíveis alvos desse ativador.

1.1.5 Proteômica

Proteômica é o conceito dado à análise sistemática que visa caracterizar o perfil proteico expresso em uma determinada condição biológica, seja pela abundância, atividade, modificações pós-traducionais ou pela interação entre as proteínas (WRIGHT *et al.*, 2012). Por meio dessa abordagem, o perfil global de expressão de proteínas pode ser investigado e comparado entre amostras, permitindo a identificação de proteínas diferencialmente expressas e o entendimento de mecanismos moleculares que norteiam as respostas à condição estudada. O proteoma apresenta maior número de variáveis em relação ao genoma e ao transcriptoma, devido a grande diversidade química das proteínas e capacidade dessas de interagir em complexos e redes de sinalização que podem variar muito em espaço e tempo (ALTELAAR *et al.*, 2013).

Para estudos proteômicos são necessárias ferramentas analíticas que apresentem seletividade, resolução e sensibilidade (POMASTOWSKI & BUSZEWSKI, 2014). De maneira geral, na abordagem mais utilizada as proteínas são fracionadas, digeridas e identificadas. Na estratégia *shotgun* do tipo “bottom-up”, proteínas purificadas ou misturas complexas de proteínas são digeridas em peptídeos por clivagem proteolítica, separadas por cromatografia líquida e analisadas por um espectrômetro de massas. Na proteômica “top-down”, um eletrospray (ESI) gera íons de proteínas intactas que são introduzidos em um analisador de massas, permitindo a análise de proteínas sem que haja clivagem. Dessa forma, características estruturais, que são perdidas na proteômica “bottom-up”, podem ser analisadas na estratégia “top-down”. Apesar das vantagens da proteômica “top-down” sobre a “bottom-up”, seu desenvolvimento técnico ainda apresenta alguns desafios e limitações. Como por exemplo podemos citar a dificuldade em lidar com proteínas inteiras ao invés de peptídeos, devido ao tamanho e solubilidade, além da sensitividade e limite de detecção dos espectrômetros de massas serem muito menores para proteínas em relação a peptídeos. Também, a capacidade de gerar dados na proteômica “top-down” ainda está muito abaixo da “bottom-up”, embora esteja evoluindo rapidamente. A

combinação entre proteômica “bottom-up” e “top-down” resulta em um arranjo otimizado para estudos proteômicos, sendo conhecida como análise proteômica “middle-down/up”. Nessa, a proteína é clivada em poucos fragmentos de tamanho grande antes de ser introduzida no espectrômetro de massas. A análise é denominada “middle-up” se o fragmento for analisado diretamente, e “middle-down” se mais uma fragmentação ocorrer dentro do espectrometro de massas previamente à análise.

Entre os métodos de separação de proteínas, que constituem a etapa de fracionamento da amostra, estão a eletroforese bidimensional (2D) e a cromatografia líquida. A eletroforese 2D consiste na aplicação de um campo elétrico para separação das proteínas de acordo com o ponto isoelétrico e massa molecular, na primeira e segunda dimensão, respectivamente. Na primeira etapa, as proteínas migram até que sua carga líquida seja igual a zero em um gel com gradiente de pH immobilizado. A segunda etapa é um gel SDS-PAGE (*polyacrylamide gel electrophoresis*) em que as proteínas são separadas pela massa molecular. Os géis são analisados com auxílio de softwares que detectam variações na expressão das proteínas entre as amostras, de acordo com intensidade e posição das bandas (O’FARRELL, 1975). As bandas podem ser excisadas do gel e analisadas por espectrômetro de massas para identificação. A tendência é a separação de proteínas e peptídeos por cromatografia líquida, que se baseia na adsorção do analito em colunas, de acordo com o tamanho da cadeia polipeptídica. As colunas mais empregadas nessa análise possuem fase estacionária apolar, permitindo que compostos mais apolares fiquem retidos e sejam eluídos com gradientes de solventes orgânicos (CATHERMAN *et al.*, 2014). Após a separação e previamente à digestão, as pontes dissulfeto entre os resíduos de cisteína devem ser reduzidos, normalmente com oditiotreitol (DTT). Em seguida, para impedir a reestruturação das pontes dissulfeto, realiza-se a alquilação dos enxofres com iodoacetamida (ZHANG *et al.*, 2013).

Após a eliminação da estrutura terciária das proteínas, elas são digeridas por processo enzimático, normalmente utilizando tripsina, que cliva resíduos de lisina e arginina pelo lado C-terminal, quando o próximo resíduo não for uma prolina. Com a sequência da proteína inferida a partir do sequencimento do genoma do organismo,

é possível prever o perfil peptídico gerado pela digestão e compará-lo com o obtido experimentalmente na espectrometria de massas.

A espectrometria de massas se baseia na formação de íons na fase gasosa, carregados positivamente ou negativamente, que podem ser detectados de acordo com sua massa/carga (m/z) (EL-ANEED et al., 2009). As técnicas de ionização, como eletrospray (ESI) e dessorção a laser assistida por matriz (MALDI), permitem que macromoléculas sejam transformadas em íons (TANAKA et al., 1988). A ionização por eletrospray foi desenvolvida por Fenn (FENN et al., 1989), e a técnica consiste em dissolver a amostra em um tampão ou solvente e bombeá-la a um fluxo de microlitros por minuto através de uma agulha sob alta voltagem, gerando um eletrospray que é evaporado e transmite sua carga pra o analito. Esse processo é brando, não ocorre a fragmentação dos íons na fase gasosa e o único requisito é que a molécula possa ser solubilizada em um solvente polar para permitir a incorporação da carga (MANN et al., 2001). Íons grandes podem apresentar mais de uma carga, levando à formação de envelopes isotópicos multicarregados, já que o espectrômetro de massas responde a razão massa/carga (HO et al., 2003). A abundância dos íons gerados é relativa, portanto, um padrão interno deve ser utilizado para propósitos de quantificação.

Na ionização por dessorção a laser assistida por matriz (MALDI), os íons gasosos são formados através da co-cristalização de uma matriz com o analito. De forma geral, a matriz é uma pequena molécula orgânica capaz de absorver o comprimento de onda emitido pelo laser, que transfere sua energia ao atingir a amostra co-cristalizada, causando dessorção e ionização dos analitos. Nesta técnica os íons são normalmente monocarregados e a intensidade do pico no cromatograma não pode ser correlacionada com a quantidade de analito na amostra, como ocorre na ESI, pois a heterogeneidade do cristal formado impossibilita o uso dessa técnica para quantificação e a qualidade do espectro de massas é influenciada pela posição do laser (KNOCHENMUSS & ZENOBI, 2003; EL-ANEED et al., 2009).

Existem várias opções de analisadores de massa para a separação dos íons gerados (EL-ANEED et al., 2009). O analisador por tempo de voo (*time of fly* – TOF) separa os íons pela velocidade com que atingem o detector no tubo de voo. Os íons são acelerados por um potencial fixo para dentro do tubo de voo, uma vez que todos

apresentam mesma carga e mesma energia potencial elétrica quando expostos ao campo e que essa energia é convertida em energia cinética, que é uma função da massa da molécula, é possível inferir a razão massa/carga. Íons com menor m/z alcançarão maior velocidade em relação aos com maior m/z. Os íons viajam por uma distância fixa dentro do tubo antes de atingirem o detector, e através da medida do tempo gasto pelo íon para chegar o detector é possível determinar a razão m/z (GLISH & VACHET, 2003).

Outro exemplo de analisador de massa é resultante da mobilidade do íon em um campo elétrico dinâmico, que está diretamente relacionada à razão m/z dos íons. Analisadores do tipo quadrupolo apresentam quatro hastes metálicas que emitem campos elétricos oscilantes, dessa forma apenas alguns valores de m/z conseguem atingir o detector. Um íon positivo se moverá em direção à haste carregada negativamente, porém, quando a polaridade da haste for trocada, o íon mudará sua trajetória antes de colidir com a haste. Assim, trajetórias oscilantes e complexas serão traçadas pelos íons e dependendo dos valores apropriados de potencial e frequência aplicados, somente uma estreita faixa de íons chegará ao detector. Íons com trajetórias instáveis colidirão com as hastes e não serão detectados. O espectro de massas é formado pelos íons detectados de acordo com a variação do campo elétrico.

Instrumentos de aprisionamento de íons (*Ion trapping*) estão relacionados aos analisadores do tipo quadrupolo. Enquanto que o quadrupolo apresenta campos elétricos em duas dimensões (x e y) e os íons se movem perpendicularmente ao campo, o analisador do tipo “ion trap” possui campos elétricos em todas as três dimensões, que permite o aprisionamento dos íons no campo (GLISH & VACHET, 2003). Os íons são capturados continuamente até atingir o número máximo de íons que podem ser atingidos sem que haja distorção do campo aplicado. Então, pacotes de íons com m/z próximos são ejetados e detectados para gerar o espectro de massas. Para experimentos em tandem, todos os íons são ejetados, exceto o de interesse, este é então fragmentado em íons produto que são analisados. Uma segunda versão do aprisionamento de íons é baseada na ressonância ciclotrônica de íons por transformada de Fourier (FT-ICR). Nesse tipo de analisador, o movimento circular de íons sob fortes campos magnéticos registra correntes

induzidas pela passagem desses pacotes de íons próximos à placa de detecção, em função do tempo. O domínio de tempo é convertido para o domínio de frequência através de um algoritmo matemático, a Transformada de Fourier, e em seguida convertido em m/z por meio de uma equação simples, resultando em um espectro de massas (MARSHALL *et al.*, 1998; ZUBAREV & MAKAROV, 2013).

Analisadores de massas conectados em série permitem o isolamento de um íon precursor de interesse, para que este possa sofrer fragmentação no primeiro analisador, e análise da m/z dos seus íons produto no segundo (GLISH & VACHET, 2003). A partir do espectro gerado pela fragmentação de um precursor, é possível reconstruir o peptídeo fragmentado pela análise da distância entre os picos, por sequenciamento *de novo*.

A aplicação de algoritmos é essencial na análise dos dados proteômicos (HEIN *et al.*, 2013). A maior parte dos softwares compara os espectros de fragmentação teórica de bancos de dados com os dados experimentais e retorna uma provável identificação das proteínas da amostra com um grau de confiança de acordo com o número de peptídeos identificados e outros parâmetros (ZHANG *et al.*, 2013). No caso de organismos que não tenham o genoma sequenciado, e portanto, não estão em bancos de dados, as ferramentas de bioinformática são necessárias para que seja feito o sequenciamento *de novo* juntamente com o alinhamento contra bancos de dados contendo sequências de organismos homólogos.

A análise proteômica é uma ferramenta importante no campo da biologia sistêmica, sendo um complemento às técnicas tradicionalmente utilizadas na pesquisa bioquímica e biologia molecular (ZHANG *et al.*, 2013). Essa técnica apresenta uma abordagem mais ampla, podendo levar ao entendimento de processos biológicos e fornecer um panorama geral sobre as respostas induzidas por NtrC nas vias metabólicas de *A. brasiliense*, bem como sua influência na cascata regulatória do metabolismo de nitrogênio neste organismo.

1.1.6 Metabolômica

A metabolômica é definida como o estudo de todos os compostos químicos de baixa massa molecular presente em um organismo e que são os produtos finais

das funções celulares, cujos níveis podem ser vistos como respostas dos sistemas biológicos a alterações ambientais ou genéticas (FIEHN, 2002). Por meio da análise metabolômica é possível descrever os metabólitos presentes em um organismo e suas concentrações relativas e absolutas, de acordo com o estado fisiológico do organismo, de forma a obter informações sobre os processos metabólicos ativos.

O conjunto de metabólitos é dinâmico e pode adquirir diversos arranjos atômicos quando comparados ao proteoma e transcriptoma, por isso proporciona uma grande variação nas propriedades físicas e químicas dos compostos. Podem ser analisados metabólitos de alto e baixo peso molecular, polares e apolares, de acordo com os compostos e vias metabólicas de interesse ou a questão biológica a ser respondida. Para isso, é necessária a utilização de metodologias e equipamentos específicos de acordo com as características de cada classe. Diferentemente do transcriptoma e do proteoma, o metaboloma não pode ser inferida a partir da informação genômica (LEI et al., 2011). Portanto, a identificação e quantificação dos metabólitos necessitam de técnicas sofisticadas, como espectrometria de massas, espectroscopia de ressonância magnética e fluorescência induzida por laser. A melhor técnica depende dos objetivos do estudo e é o ajuste entre sensibilidade, seletividade e rapidez. A ressonância magnética é altamente seletiva, porém apresenta baixa sensibilidade (LINDON & NICHOLSON, 2008). A fluorescência induzida por laser é a mais sensível das técnicas, mas não possui seletividade química. Enquanto que a espectrometria de massas apresenta uma combinação de seletividade e sensibilidade (LEI et al., 2011). A espectrometria de massas basicamente detecta a razão massa sobre a carga (m/z) de íons provenientes de uma fonte de ionização. Inicialmente, apenas compostos pequenos, voláteis e estáveis em temperatura ambiente podiam ser analisados em um espectrômetro de massas. O avanço dos métodos de ionização permitiu que uma ampla faixa de compostos químicos pudesse ser analisada por essa técnica, desde pequenas moléculas polares até macromoléculas. Esse desenvolvimento também possibilitou o acoplamento da espectrometria de massas à técnicas de separação, como cromatografia e eletroforese capilar, para análises de metabolomas complexos (LEI, 2011). Análises que requerem pré-separação são realizadas por GC-MS (gas chromatography – mass spectrometry), LC-MS (liquid chromatography – mass spectrometry) e CE-MS (capillary electrophoresis – mass spectrometry).

Existem duas categorias de análise metabolômica: “targeted” (DUDLEY et al., 2010) e “untargeted” (DE VOS et al., 2007). A análise “targeted” é direcionada a uma molécula alvo, voltada a identificar e quantificar determinado metabólito. Enquanto que na análise “untargeted” é gerado um perfil metabólico total das moléculas presentes no sistema, normalmente de forma qualitativa. A estratégia a ser utilizada em um experimento deve ser escolhida previamente de acordo com o objetivo do estudo.

Após a definição da estratégia, deve-se definir o tipo de amostra e método de extração dos compostos. Um passo importante é o “quenching” metabólico, que refere-se à interrupção imediata da atividade enzimática e é normalmente realizado através da adição de solventes orgânicos resfriados ou do congelamento imediato da amostra em nitrogênio líquido. As amostras devem ser estocadas a baixas temperaturas para evitar degradação de compostos ou ativação de enzimas.

O preparo da amostra para a análise metabolômica é uma das etapas mais importantes e depende da abordagem escolhida, tipo de amostra e técnica de análise. Isso é devido à complexidade das amostras biológicas, heterogeneidade e diferença na concentração dos metabólitos (ÁLVAREZ-SÁCHEZ et al., 2010). Para metabolômica “untargeted” o preparo é não seletivo e resume-se na remoção de sais pela adição de solventes orgânicos, seguidos de métodos mecânicos para romper e eliminar parede celular ou tecidos e extrair o metabólito eficientemente (ÁLVAREZ-SÁCHEZ et al., 2010). Nas análises “targeted”, o procedimento é seletivo e deve ser escolhido de acordo com o metabólito de interesse, com o objetivo de concentrar o analito, remover interferentes e selecionar a espécie de interesse (RATERINK et al., 2014).

Nas análises por eletroforese capilar (CE) é necessária a evaporação dos solventes orgânicos e ressuspenção do resíduo em água (KUEHNBAUM et al., 2015). Para cromatografia gasosa (GC) os analitos devem ser convertidos em espécies voláteis por derivatização para que possam ser analisados (GARCIA & BARBAS, 2011). Na ressonância magnética nuclear (NMR) os extratos precisam ser diluídos em solventes deuterados.

Devido à grande diversidade química dos metabólitos, até o momento não existe uma única técnica analítica capaz de cobrir o metaboloma completo de um organismo. Por isso, o uso de várias plataformas de análise proporciona maior cobertura de substâncias químicas detectadas e, consequentemente, maior entendimento biológico do organismo estudado (VILLAS-BÔAS & BRUHEIM, 2007).

A espectrometria de massas é a técnica mais usada na análise metabolômica devido a sua alta sensibilidade e seletividade (KUEHNBAUM & BRITZ-MCKIBBIN, 2013). Pode ser por infusão direta dos extratos (DIMS) ou por ionização assistida por matriz (MALDI-MS). O acoplamento de técnicas de separação (GC, LC ou CE) permite resolver problemas de supressão de ionização nos sinais das análises por infusão direta, além disso, a informação do tempo de retenção ou migração do metabólito separado previamente aumenta a confiabilidade da identificação com uso de padrões (KUEHNBAUM & BRITZ-MCKIBBIN, 2013).

A análise metabolômica gera dados complexos que requerem processamentos e ferramentas adequadas para garantir a integridade das variações biológicas detectadas. Etapas de alinhamento, agrupamento, correção do tempo de retenção e de linha de base, deconvolução espectral e normalização são necessárias na análise metabolômica “untargeted” e podem ser feitas com auxílio de diversos softwares para tratamento de dados metabolômicos (SUGIMOTO *et al.*, 2012). Para as análises “targeted” é feita a quantificação dos metabólitos selecionados através de padrões internos (GUO *et al.*, 2012). São aplicadas análises estatísticas para discriminar os metabólitos responsáveis por diferenciar grupos de amostras e também para avaliá-los separadamente, desprezando as relações entre eles. Testes t de Student, ANOVA e Mann-Whitney são utilizados com frequência (SUGIMOTO *et al.*, 2012).

Bibliotecas de espectros são utilizadas para identificação dos metabólitos em estudos “untargeted”. Essas bibliotecas podem ser comerciais, como a NIST (*National Institute of Standards and Technology*) ou particulares, construídas no próprio laboratório da análise. Também podem ser inferidas identificações putativas aos compostos utilizando bases de dados públicas online, como Metlin (TAUTENHAHN *et al.*, 2012) e HMDB (*Human Metabolome Database*) (ZHANG *et*

al., 2012). Identificações putativas devem ser confirmadas por outros métodos como metabolômica em fluxo, utilizando compostos marcados.

A interpretação biológica dos dados é feita correlacionando os metabólitos alterados com vias metabólicas (KARP & CASPI, 2011) através de ferramentas como KEGG (*Kyoto Encyclopedia of Genes and Genomes*) (KANEHISA et al., 2006) e MetaCyc (CASPI et al., 2012). É recomendada uma validação biológica dos resultados elaborando novos experimentos para confirmação e interpretação dos efeitos bioquímicos (MADSEN et al., 2010).

Neste trabalho foi realizada análise proteômica e metabolômica da estirpe selvagem de *Azospirillum brasilense* FP2 e seu mutante que não expressa o ativador transcrecional NtrC, em condições de alto e baixo nitrogênio. A combinação de dados abrangentes na expressão e regulação do proteoma, bem como de vias metabólicas ativas, permitem uma visão integrada e sistemática que proporciona uma compreensão da organização e funcionamento do sistema biológico. O objetivo foi gerar um panorama das proteínas e metabólitos encontrados nessas estirpes a fim de investigar mais detalhadamente aspectos ainda não elucidados do metabolismo de nitrogênio neste organismo, especialmente relacionados a NtrC. A escolha desse mutante levou em consideração o importante papel dessa proteína no processo de regulação do metabolismo de nitrogênio e sua capacidade de responder a diferentes estímulos através das proteínas PII. Além disso, a conservação e distribuição de NtrC em procariotos permite que seja feita uma correlação com os sistemas regulatórios de outras espécies.

2. MANUSCRITO

Proteomic and metabolomic analysis of *Azospirillum brasilense* *ntrC* mutant under high and low nitrogen conditions

Caroline Kukolj¹, Fábio O. Pedrosa¹, Gustavo A. de Souza^{2,3}, Lloyd W. Sumner⁴, Fernanda P. do Amaral⁵, Luciano F. Huergo^{1,6}, Glaucio Valdameri^{1,7}, Gary Stacey⁵,
 *Emanuel M. Souza¹

1-Departamento de Bioquímica e Biologia Molecular, UFPR, P.O Box 19046, 81531980, Curitiba, PR, Brazil.

2- Department of Immunology, University of Oslo and Oslo University Hospital, The Proteomics Core Facility, Rikshospitalet, Oslo, Norway.

3- Instituto do Cérebro, UFRN, Natal, RN, Brazil.

4- Department of Biochemistry, University of Missouri, Bond Life Sciences Center, 1201 Rollins Street, Columbia, Missouri 65211, United States

5- Divisions of Plant Science and Biochemistry, C.S. Bond Life Science Center, University of Missouri, Columbia, MO, USA.

6- Setor Litoral, UFPR, Matinhos, PR, Brazil.

7- Departamento de Análises Clínicas, UFPR, Curitiba, PR, Brazil.

*Correspondent author: Emanuel Maltempi de Souza.

Key words: *Azospirillum brasilense*. NtrC. Nitrogen metabolism. Proteomic. Metabolomic. Oxidative stress. *Setaria viridis*.

2.1 ABSTRACT

Azospirillum brasilense is a free-living diazotrophic bacterium that associates with important grasses and cereals, promoting plant growth and increasing crop productivity. The nitrogen metabolism in this organism is tightly regulated by the availability of nitrogen and by the Ntr regulatory system. This system comprises the GlnD protein, which is capable of adding uridylyl groups to the PII proteins, GlnB and GlnZ, under limiting nitrogen levels. Under such conditions, the histidine kinase NtrB cannot interact with GlnB and phosphorylate NtrC. When phosphorylated, NtrC is a transcriptional activator of genes involved in metabolism of alternative nitrogen sources. Considering the key role of NtrC in nitrogen metabolism in *Azospirillum brasilense*, in this work we evaluated the proteomic and metabolomic profiles of the

wild type FP2 strain and its mutant *ntrC* grown under high and low nitrogen conditions. Through the integrated data, we proposed a list of novel NtrC targets, including proteins involved in the response against oxidative stress, like glutathione S-transferase and hydroperoxide resistance protein, and showed that the presence of NtrC is important to bacterial survival under oxidative stress conditions.

2.2 INTRODUCTION

The *Azospirillum* genus includes free-living microorganisms able to colonize and promote the growth of important cereals and grasses, such as maize, sorghum, wheat, rice and oat, as well as bioenergy grasses such as *Setaria viridis* and *Brachypodium distachyon*^{1, 2, 3}. *Azospirillum* is able to fix nitrogen in association with plant roots and transfer to plant part of the N fixed (about 10% of the plant needs)². Among 16 *Azospirillum* species described, *Azospirillum brasilense* is the most studied⁴. The *ntr* system regulates nitrogen metabolism in *A. brasilense*, including nitrogen fixation. This system is composed of the proteins encoded by the genes *glnD*, *glnB*, *glnZ*, *ntrB* and *ntrC*. The GlnD protein is able to sense intracellular glutamine and acts as an uridylyltransferase/uridylyl-removing enzyme (UTase/UR) in response to nitrogen levels⁵. Under limiting nitrogen conditions, GlnD adds uridylyl groups (UMP) to the PII proteins, GlnB and GlnZ, in the presence of ATP and α-ketoglutarate^{6, 7}. Uridylylated GlnB cannot interact with the histidine kinase NtrB, which, in its free form, is able to phosphorylate NtrC⁸. NtrC is an enhancer binding protein that controls the transcription of nitrogen regulated promoters, in a sigma 54 (RpoN) factor dependent manner. NtrB and NtrC compose a two-component system in which NtrB is capable of phosphorylating NtrC when nitrogen levels are low⁹. On the other hand, the presence of nitrogen results in dephosphorylation and subsequent inactivation of NtrC. Previous studies defined the NtrC regulon for a number of organisms, including *Escherichia coli*¹⁰, *Sinorhizobium meliloti*¹¹ and *Pseudomonas putida*^{12, 13}. These studies showed the global regulatory function of NtrC in these organisms and suggested that NtrC is involved in the expression of genes related to transport and catabolism of nitrogen compounds, as well as regulation of central metabolic networks. In *Klebsiella pneumonia*, phosphorylated NtrC activates the transcription of *glnA* (encoding glutamine synthetase), *amtB* (encoding an ammonium transporter), *glnK* (homologue of *glnZ* in *A. brasilense*) and *nifA*¹⁴. The transcriptome analysis of *P. putida* suggests that *glnK* and *amtB* are also

regulated by nitrogen availability via NtrC¹⁵. In *Azospirillum brasilense*, NtrC acts as a transcriptional activator of *glnB*/*glnA*, *glnZ*, *amtB* and other operons involved in nitrogen assimilation¹⁶. In a nitrogen limiting condition, transcription of *glnB* increased five-fold mediated by the action of phosphorylated NtrC acting at the *glnB* sigma 54 factor dependent promoter^{16, 17}, thus GlnB is able to regulate its own expression, since it controls the activity of NtrB and, consequently, NtrC¹⁶. Uridylylated GlnB is essential for the activity of NifA, the transcriptional activator of *nif* genes. This regulation is independent of NtrC, as evidenced by the fact that *ntrC* mutants are able to fix nitrogen^{18, 19}. NtrC also regulates *glnZ* and its expression is increased under limiting nitrogen²⁰. Interestingly, in *A. brasilense*, GlnZ was not found to be involved in the activity of NtrB-NtrC, in contrast to what occurs in *E. coli*²⁰. The general nitrogen metabolism in *A. brasilense* comprises a complex and yet not fully elucidated regulatory cascade. The aim of this work was to contrast the proteomic and metabolomic responses in *A. brasilense* FP2 and an *ntrC* mutant when grown in high and low nitrogen. The goal was to better understand the nitrogen metabolism regulation in this organism and to also find new targets for the transcriptional activator NtrC. Basic knowledge about the physiological properties of *A. brasilense* is crucial for understanding aspects related to transfer of fixed N to plants and successful interactions.

2.3 EXPERIMENTAL SECTION

2.3.1 Bacterial strains and growth conditions

In this work we used *Azospirillum brasilense* FP2 (*wild type*)²¹ and isogenic LHNTRC5 (FP2 *ntrC::km*)¹⁶. The strains were grown in NFbHPN-lactate medium (HP = high phosphate)¹⁹ supplemented with ammonium chloride 20 mM and 1% LB medium and incubated at 30 °C, 120 rpm in an orbital shaker until an optical density (OD₆₀₀) of 0.5. The cultures were centrifuged for 10 min at 2000 xg and resuspended either in NFbHPN-lactate supplemented with 20 mM ammonium chloride (high N) or in NFbHP-lactate without added ammonium (low N). After four hours of incubation (at 30 °C, 120 rpm), the cells were centrifuged for 10 min at 2000 xg at 4°C. The pellets were frozen in liquid nitrogen and transferred to -80 °C until the protein extraction.

2.3.2 Protein extraction

The pelleted cells were suspended in 50 mM Tris-HCl pH 7.5 containing 100 mM of KCl. The cells were disrupted by sonication on ice and centrifuged at 20,000 xg at 4 °C for 45 minutes. The soluble fraction was collected and the protein content was determined by the Bradford assay²² using bovine serum albumin as a standard. Aliquots containing 100 µg of protein were frozen, lyophilized and sent to the Proteomics Core Facility, Rikshospitalet, Oslo, Norway for LC/MS/MS analysis. Four independent cultures were used for each condition, generating four independent protein samples that were subjected to four independent LC/MS/MS runs.

2.3.3 Western blot analysis

In order to confirm if the bacteria responded to the high and low nitrogen conditions western blots were performed using antibodies against *A. brasiliense* GlnB and GlnZ as described previously²³.

2.3.4 Label free quantitative LC-MS/MS analysis

For LC-MS/MS analysis, 15 µg of each sample were independently suspended in 50 µL of ammonium bicarbonate 100 mM pH 8.0 and reduced using 1 µl of DTT 1 mM for 45 min. The samples were incubated overnight at 37°C in a wet chamber with modified trypsin (Promega) in a ratio of 1:50. Protein digestion was quenched with TFA 3% (v/v). The sample was cleaned using C18 STAGE-TIPs as described²⁴ and suspended in 10 µL of 0.1% formic acid. Each protein sample was run in 3 µL injections. Peptide separation was performed on a nano-HPLC (EASY nLC1000, Thermo) using a reverse phase column of 25 cm, 75 µm of internal diameter and 2 µm particles. Peptides were eluted in 120 minutes runs using a linear gradient of 2 to 30% of organic solvent (100% acetonitrile and 0.1% formic acid) at 300 nL·min⁻¹. The analysis was performed in a QExactive Orbitrap (Thermo Scientific) and the sample acquisition parameters for MS scans were: microscans 1; resolution 70,000 at m/z 200; AGC target 3e6; maximum injection time 20 ms; scan range: 400-1200 m/z. The parameters for data dependent MS/MS acquisition were: microscans 1; resolution 17,500; AGC target 1e5; maximum injection time 100 ms; loop count 10; isolation width 2.0 m/z; collision energy 25.0%; single charged ions were excluded; and dynamic exclusion of 30 s. QExactive Orbitrap data was processed using MaxQuant v1.5.2.8, using the following parameters: variable modifications methionine oxidation;

N-acetylation of N-terminal; and conversion of glutamine and glutamate to pyro-glutamate. The first search was performed using 20 ppm error and the main search 6 ppm; maximum of two missed cleavages were allowed. Protein and peptide FDR threshold of 0.01; Min Unique Peptides: 1; Min Peptide Length: 7; Second peptides option ON; Match between runs ON, with Time Window of 2 min; Label-free quantitation ON, with minimal ratio count 2; iBAQ ON with log fit ON. Proteins were identified using NCBI *Azospirillum brasilense* Sp. 245 database. Additional searches including tyrosine uridylylation and adenylylation as variable modifications were performed. Statistical analysis was performed using MaxQuant – Perseus package version 1.5.0.30. Briefly, output with identified proteins from MaxQuant (proteingroups.txt) was loaded and normalized area under curve values were assigned for each protein. Proteins identified from contaminants and reversed sequences (from FDR calculations) were removed. Quantitative values were logarithmized at base 10, and non-assigned values (i.e., quantitation equal zero before log calculation) were replaced by normal distribution of the data (Width 0.3, Down shift 1.8). Statistically significant differences were assigned using two-way t-test and permutation-based FDR correction allowing 250 permutations. Proteins were considered to be differentially expressed between each treatment when the fold change was >2 and the p value was <0.05.

2.3.5 Determination of intracellular metabolites by GC-MS and data analysis

For metabolomic analysis, bacterial cells were grown in the same conditions as described for proteomic analysis. Cells were collected by centrifugation (20 min, 20000 xg at 4 °C), cells were washed twice with NFbHP-Lactate and water (1:1) plus twice with NFbHP-Lactate and water (1:3). The intracellular metabolites were extracted from the polar phase for GC-MS analysis. One mL methanol-water solution 80% (v/v), containing 25 µg ribitol, was added to the final pellet as an internal standard. The samples were sonicated for one hour and centrifuged at 20000 xg for 30 minutes at 4 °C. An aliquot of 800 µL of the supernatant was transferred to a glass vial and dried in a SpeedVac. The dried polar samples were subjected to derivatization with 50 µL methoxyamine hydrochloride (15 mg/mL in pyridine), briefly sonicated and incubated at 50 °C until the residue was resuspended. Subsequently, 50 µL of N-methyl-N-trimethylsilyl trifluoroacetamide (MSTFA) w/1% trimethylchlorosilane (TMCS) was added to the samples, vortexed and kept at 50 °C

for one hour for trimethylsilylation. After cooling to the room temperature, the sample was transferred to a 150 µL glass vial and the metabolites analyzed by GC-MS using an Agilent 6892 GC-MS Single Quad coupled to a 5973 MSD, scanning from m/z 50-650. The injection split ratio was set to 15:1 for polar samples. Separation was achieved with a temperature program beginning at 80 °C, ramped at 8 °C/min to 315 °C and held for 12 minutes, then ramped at 10 °C/min to 325 °C and held for 5 minutes, using a 60 m DB-5MS column (J & W Scientific, 0.25 mm ID, 0.25 um film thickness) and a constant flow of 1.0 mL/min. Sample components were identified by comparison of retention times and mass spectra with reference compounds, and matching to the library database. Metabolite peak areas representing the abundance of metabolites were normalized to the internal standard (ribitol) and cell biomass. The GC-MS analyses were conducted with three replicates for each treatment. Mass spectra deconvolution and metabolite identification were performed using *Automated Mass Spectral Deconvolution and Identification system* (AMDIS) from the National Institute of Standards and Technology (<http://chemdata.nist.gov/dokuwiki/doku.php?id=chemdata:start>) and a custom electron-ionization mass spectrometry metabolite library generated by combining libraries from the Noble Foundation²⁵, Max Planck Institute-Golm (<http://gmd.mpimp-golm.mpg.de>) and the Adams library (<http://essentialoilcomponentsbygcms.com>). Peak picking, alignment and quantification were achieved using Metabolomics Ion based Data Extraction Algorithm software (MET-IDEA) to generate an aligned data matrix suitable for statistical analysis. Analyte features were labeled by their retention time and mass, and exported to Metaboanalyst²⁶ (<http://www.metaboanalyst.ca/>) for multivariate analysis. Normalization by sum within the triplicates was performed after log transformation. Relative abundances of all the metabolites were analyzed using a Student's t test and the differences between the samples were considered to be significant at *p-value* < 0.05 and a fold change > 2. Principal component analysis (PCA) and cluster analysis were performed for all treatments using the Ward method.

2.3.6 Pathways analysis

Detailed analyses of metabolic pathways using Cluster of Orthologous Groups (COG)²⁷ and the Kyoto Encyclopedia of Genes and Genomes (KEGG)²⁸ were performed for the differential proteins and metabolites. According to KEGG,

there are 124 pathways in *A. brasiliense* Sp. 245 and all features were checked individually whether belongs to any of these pathways.

2.3.7 Plant colonization assay: Seed sterilization, germination conditions, plant inoculation, and plant growth conditions

In order to check the effect of inoculation with *Azospirillum brasiliense* FP2 wild type and its *ntrC* mutant on plant growth, we used the grass model system *Setaria viridis* A10.1. Seeds were sterilized with 5% (v/v) commercial bleach solution containing 0.1% (v/v) of Tween 20 for 3 minutes and, subsequently, washed three times with sterile distilled water for one minute. After sterilization, seeds were placed onto the surface of 1% phytigel made with Hoagland's nutrient solution³². Plates were placed vertically in the dark for 24 hours at 30 °C and transferred to a growth chamber for 2 days at 16 hours light and 8 hours dark at 23 °C. After germination, seedlings were transferred to a sterile soil mixture (vermiculite 1:3 turface). The seedlings were inoculated with 10⁷ bacterial cells inoculum diluted in 1mL Hoagland's solution with no nitrogen addition. Control plants were mock inoculated using 1 mL of Hoagland's solution. The suspensions used for inoculation were diluted and plated to confirm the inoculated bacterial numbers by counting CFU. Plants were grown for 20 days in the greenhouse with a photoperiod of 16 hours at and 8 hours dark, and watered everyday with ultrapure water and every 5 days with sterile Hoagland's nutrient solution without N source. Three independent experiments were performed.

2.3.8 Plant growth promotion measurements, statistical analysis and bacterial quantification

To assess the effect of bacterial inoculation on *S. viridis* growth, plants were harvested 20 days after inoculation and growth parameters were analyzed. Root area and lateral root number were measured using the WinRHIZO pro software (Regent Instruments, <http://www.regentinstruments.com/>) and shoot length, root and shoot dry weight were measured manually. The mean, standard deviation and error were calculated for all parameters and statistical significance was calculated using Student's T-test with a *p-value* threshold ≤ 0.05. In order to evaluate the ability of the studied strains to colonize *S. viridis*, bacteria from the root surface were counted. Roots of four plants for each treatment were vortexed in 1 mL of 0.9% (w/v) NaCl for 1 minute. The solution was serially diluted and plated in NFbHP-lactate medium

containing specifics antibiotics for each strain (Sm^R , Km^R). Colony forming units were counted after 3 days of incubation at 30°C.

2.3.9 Oxidative stress response analysis

For the growth rate analysis, previous saturated cultures of *A. brasiliense* FP2 and the *ntrC* mutant were diluted to an OD_{600} of 0.05 and grown under in high and low nitrogen (20 mM and 1 mM ammonium, respectively) conditions. Once the cultures reached exponential phase ($\text{OD}_{600} = 0.5$), H_2O_2 was added to the cultures in concentrations of 0.5, 2 and 4 mM and the OD_{600} was monitored every 30 minutes. For the relative survival rate analysis, the cultures were grown in the same conditions, with different H_2O_2 concentrations 0, 1, 2 and 4 mM. The viable bacterial cell number was determined by colony-forming-units (CFU), counting on plates from the moment of the stress induction, 2, 4 and 24 hours after H_2O_2 addition. The relative survival rate was calculated based on the control without H_2O_2 .

2.3.10 Analysis of the promoter region for putative genes regulated by NtrC

For 112 proteins likely regulated by NtrC we scanned the 300 bp upstream sequences in the correspondent genes for occurrences of sigma 54 binding site (TGGCACG-N₄-TTGC), as NtrC activates transcription in a sigma 54 dependent manner. Each of these genes was extracted from *A. brasiliense* sp245 reference genome and FIMO²⁹ was used to computationally find this motif in the upstream regions. Only motif occurrences with a *p-value* less than 0.0001 were accepted confidently.

2.3.11 RNA isolation, cDNA synthesis and quantitative RT-PCR

For total RNA isolation, *A. brasiliense* FP2 and *ntrC* mutant cultures were grown in high and low nitrogen, as previously described. Bacterial cells from 1.5 mL of culture were collected by centrifugation and were lysed in 300 μL of suspension buffer (Tris-HCl pH 8, 50 mM, EDTA pH 8 2 mM and SDS 0.2%) and 1 mL of TRIzol reagent (Invitrogen). After 5 minutes of incubation at room temperature, 200 μL of chloroform was added. The samples were homogenized and centrifuged for 15 minutes at 4°C and 20000 xg. 500 μL of isopropanol was added to the upper phase, followed by 10 minutes of incubation. After centrifugation, the pellet was washed twice with ethanol and resuspended in RNase free water. RNA samples were treated using the TurboTM DNA free kit, according to the manufacturer's instructions. Total

RNA integrity was analyzed by native agarose gel electrophoresis, and quantified using a NanoDrop spectrophotometer (Thermo Scientific). After quantification, reverse transcription was performed using 1 µg of RNA with a random primer and M-MLV reverse transcriptase kit (Sigma) to synthesized single strand cDNA. DNA contamination was checked with reactions that lacked reverse transcriptase as negative controls. Specific primers were designed using the Primer3Input interface³⁰ and are listed in table 3 (Supplementary material). The reactions were performed using *Power Up* SYBR Green PCR master mix 2x (Thermo Fisher Scientific) and 8 ng of cDNA in a final volume of 20 µL. Detection was carried out in triplicate on the ABI Prism 7500 detection system (Applied Biosystems) 50 °C for 2 min, 95 °C for 10 min followed by 40 cycles of 95 °C for 15 seconds and 60 °C for 1 min. Immediately after each run a dissociation curve was carried out 15 seconds at 95 °C, 1 minute at 60 °C increased to 95 °C for 15 seconds and 60°C for 15 seconds. Reaction specificity was confirmed by dissociation curves after the amplification was completed. All biological samples and reactions were assayed in three technical replicates. Fold change (n-fold) in gene expression was calculated using the relative quantitation method ($2^{-\Delta\Delta Ct}$)³¹. The average of the delta Ct (calculated using the *rpoC* and *rpoD* as housekeeping genes) in the control samples (wild type low N) was used to calculate the delta delta Ct (ddCt) and then the fold change. Statistical analyses were conducted using SAS (SAS version 9.4 for Windows, SAS Institute Inc., Cary, NC) and ddCt values were analyzed by ANOVA using the GLM procedure. All models included the effect of treatment and replicate as independent variables. Results are presented as fold change and represent the least square means (LS-means) of fold change in the three biological replicates.

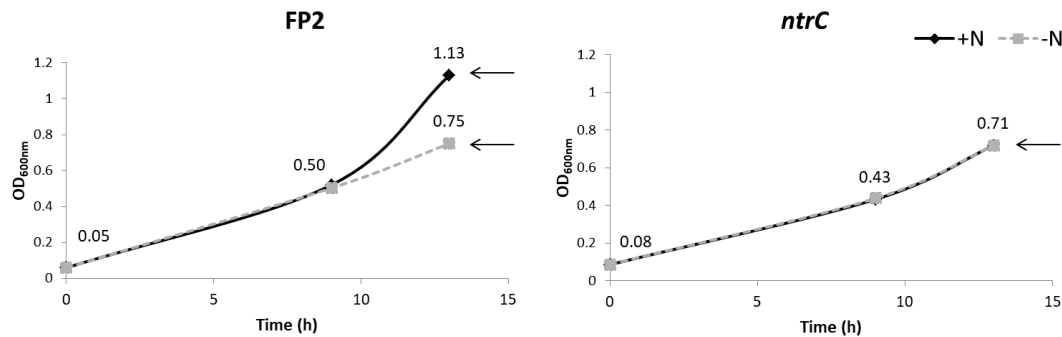
2.4 RESULTS AND DISCUSSION

2.4.1 Bacterial growth under limiting nitrogen

Azospirillum brasilense FP2 and its isogenic *ntrC* mutant were cultured in the presence or absence of ammonium chloride as nitrogen source. The growth profiles indicated that the *ntrC* mutant strain grew slower than the wild-type in the presence of nitrogen (figure 1). This effect is expected and can be attributable to the lack of an efficient nitrogen assimilation pathway in the mutant strain. On the other hand, both FP2 and *ntrC* strain showed similar growth rates in media without fixed nitrogen

(Figure 1). This data indicates that NtrC is required for fitness during growth in the presence of ammonium.

FIGURE 1 - GROWTH CURVE OF *Azospirillum brasiliense* FP2 AND *ntrC* UNDER HIGH AND LOW NITROGEN. The arrows indicate the time points where samples were collected for lc/ms/ms and metabolomic analysis. Values represent the mean of four independent experiments.

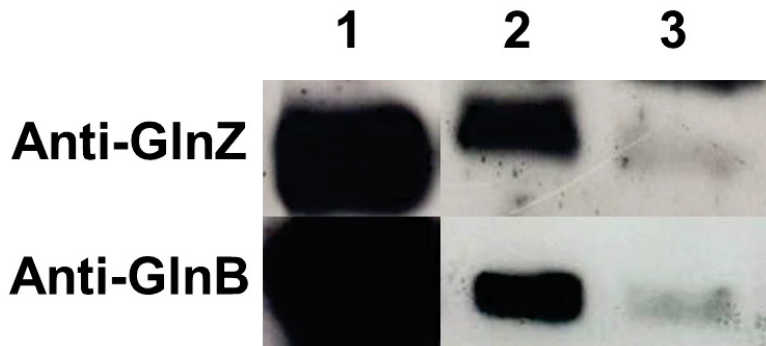


FONTE: a autora (2018).

2.4.2 Western blot analysis of GlnB and GlnZ abundance in *A. brasiliense* as a function of nitrogen availability

In order to determine if the growth conditions used were physiologically relevant for measuring NtrC activity, we probed the accumulation of the GlnB and GlnZ protein by Western-blot. These proteins play important roles in nitrogen metabolism and are predicted to be more abundant when the bacteria experience nitrogen starvation²³. The results in the wild-type strain showed that GlnB is poorly expressed under high N and its accumulation is induced upon N-limitation (Figure 2). These results are in agreement with previous analysis of the regulation of *glnB* transcription by NtrC^{16, 33, 20} therefore confirming that the conditions used reflect nitrogen sufficiency and limitation.

FIGURE 2 - WESTERN BLOTH ANALYSIS OF GlnB AND GlnZ EXPRESSION IN *Azospirillum brasiliense* FP2 GROWN IN HIGH AND LOW NITROGEN. 1. INDICATES THE PURIFIED PROTEIN, 2 & 3. INDICATE TREATMENT WITH LOW AND HIGH NITROGEN IN THE WILD TYPE FP2, RESPECTIVELY.



FONTE: a autora (2018).

2.4.3 Proteomic data overview

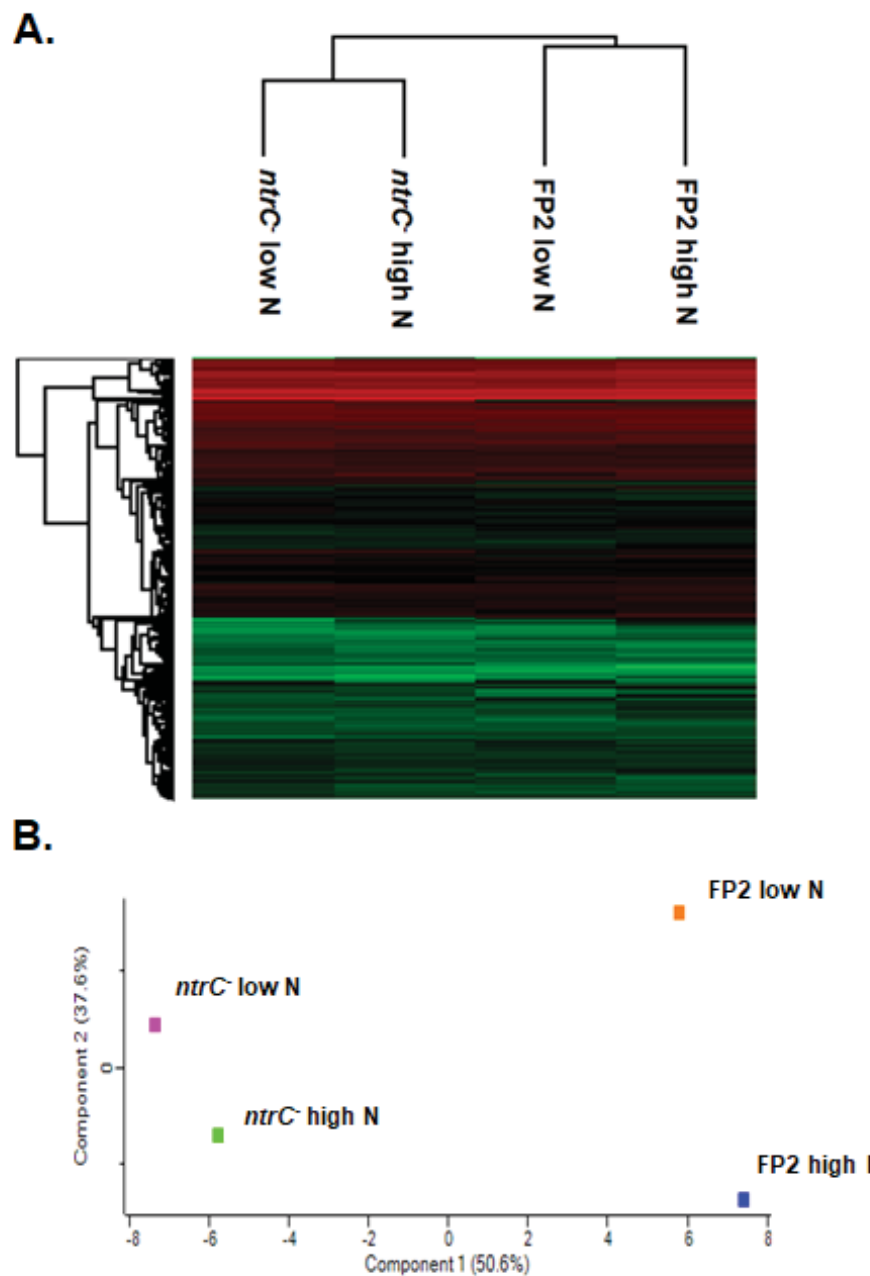
In order to determine how NtrC affects global gene expression, protein extracts of the wild-type and the *ntrC* strains cultured under high and low N were subjected to comparative proteomics analysis. Proteins were considered to be differentially expressed when the relative fold change was > 2 and the *p*-value was < 0.05 . A total of 2254 proteins were identified (1721 were differentially expressed) and quantified out of the 7541 estimated open reading frames encoded by the *Azospirillum brasiliense* Sp. 245 genome, a FP2 close strain for which a genome sequence is available so far³⁴. The number of differentially expressed proteins and the comparisons performed are described in table 1. Hierarchical clustering analysis showed that protein accumulation was different in the *ntrC* strain in comparison to wild-type despite the N source in the culture medium (Figure 3A), leading us to the conclusion that the nitrogen limitation response is different between the studied strains. Principal component analysis (Figure 3B) revealed that the proteome datasets were separated by both the lack of *ntrC* (X axis) and nitrogen condition used for growth (Y axis).

TABLE 1 - NUMBER OF DIFFERENTIALLY EXPRESSED PROTEINS FOR EACH COMPARISON.

	Upregulated	Downregulated	Total
FP2 low N x FP2 high N	180	306	486
<i>ntrC</i> low N x <i>ntrC</i> high N	154	122	276
FP2 low N x <i>ntrC</i> low N	205	261	466
FP2 high N x <i>ntrC</i> high N	299	194	493

FONTE: a autora (2018).

FIGURE 3 - (A) HIERARCHICAL CLUSTERING ANALYSIS DISPLAYED AS A HEAT MAP OF PROTEINS FROM *A. brasiliense* FP2 AND ITS ISOGENIC MUTANT *ntrC* UNDER HIGH AND LOW NITROGEN. The rows represent individual proteins and the columns are the samples. Proteins that changed in abundance are indicated in red and green, respectively. The proteins that were not changed are indicated in black. The intensity of the colors increased as the difference in abundance increased. (B) PCA of the protein samples showing separation between bacterial strains and treatments.



FONTE: a autora (2018).

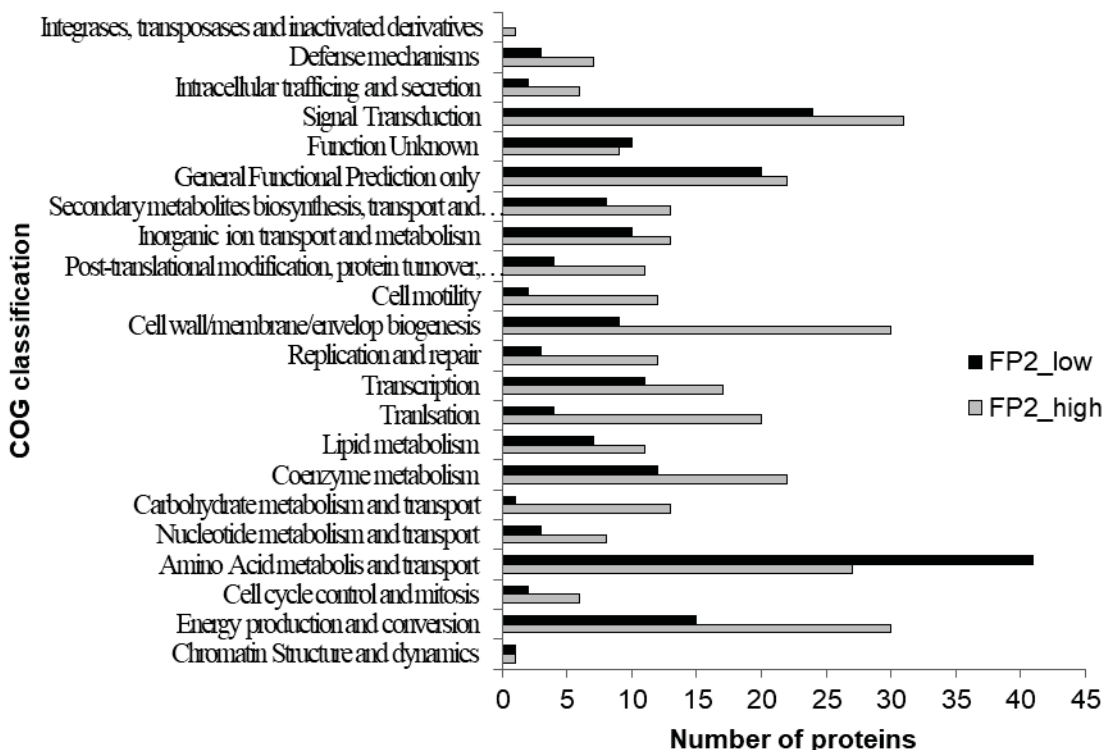
2.4.4 Proteomic profile of *A. brasiliense* FP2 in response to nitrogen limitation

The comparison analysis between *A. brasiliense* in low and high nitrogen identified 486 differentially expressed proteins. Among them, 180 were upregulated and 306 downregulated under low nitrogen (supplementary material table 4). We

categorized the protein expression profile by cluster of orthologous groups (COG). The upregulated proteins were grouped into 22 functional categories (figure 4). The majority of upregulated proteins in low nitrogen was classified in amino acid metabolism and transport (22.7%) and signal transduction (13.3%) categories. Followed by energy production and conversion (8.3%), coenzyme metabolism (6.7%) and transcription (6.1%). Similarly, part of the upregulated proteins in high nitrogen also belong to those categories (8.8 and 10.1%, respectively), as well as energy metabolism (9.8%), cell wall/membrane/envelop biogenesis (9.8%) and coenzyme metabolism (7.1%). As expected, the proteomic adaptation to nitrogen limitation involves a range of proteins known to be regulated by NtrC in response to nitrogen limitation. For example GlnZ (gi|392381004), the channel ammonium transporter AmtB (gi|392380681) and the NtrC itself (gi|392377167), with fold changes of 7.9, 128.6 and 3.3 respectively. Detailed analysis of metabolic pathways using the Kyoto Encyclopedia of Genes and Genomes (KEGG) database are in the supplementary material (table 5 and figure 15).

FIGURE 4 - FUNCTIONAL CLASSIFICATIONS OF DIFFERENTIALLY EXPRESSED PROTEINS UNDER LOW AND HIGH NITROGEN IN *A. brasiliense* FP2.

Upregulated proteins in *A. brasiliense* FP2 high vs low N

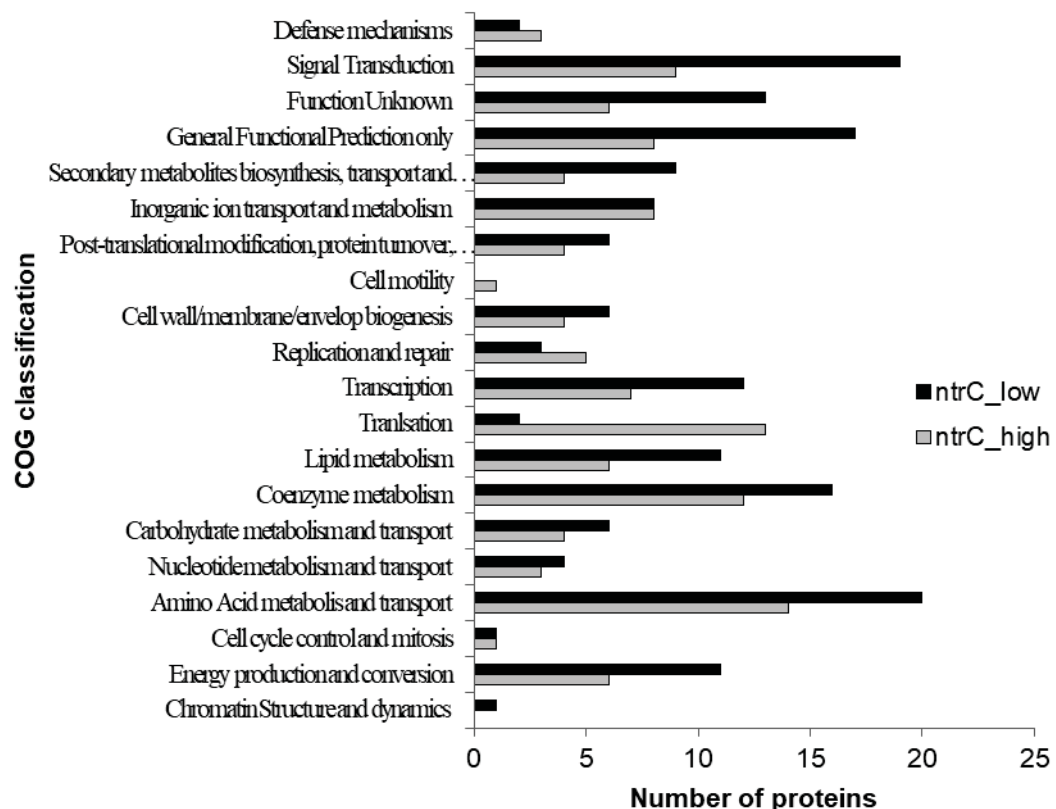


2.4.5 Proteins regulated by nitrogen availability in *A. brasiliense ntrC*

We next compared the proteomes of *A. brasiliense ntrC* in high and low nitrogen. This analysis indicated 276 differentially expressed proteins between the N-treatments. Among them, 154 proteins are induced and 122 are repressed in the mutant in response to nitrogen limitation (supplementary material table 6). Similarly to the wild type, the comparison between *A. brasiliense ntrC* low and high nitrogen proteomes showed that proteins related to signal transduction (12.3%) and amino acid metabolism and transport (13%) were the most affected by nitrogen limitation (Figure 5). Other categories induced by N limitation in the mutant were coenzyme metabolism (10.4%), transcription (7.8%), energy production and conversion (7.1%) and lipid metabolism (7.1%). On the other side, the most induced categories in the mutant under high N compared to low N are amino acid metabolism and transport (11.5%), translation (10.7%), coenzyme metabolism (9.8%), signal transduction (7.3%) and inorganic ion transport and metabolism (6.5%).

FIGURE 5 - FUNCTIONAL CLASSIFICATION OF DIFFERENTIALLY EXPRESSED PROTEINS IN *A. brasiliense ntrC* UNDER HIGH AND LOW NITROGEN.

Upregulated proteins in *A. brasiliense ntrC* high vs low N

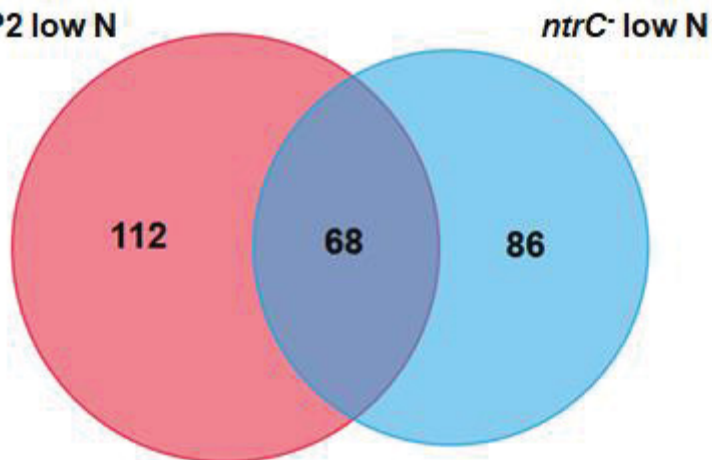


FONTE: a autora (2018).

2.4.6 Identification of proteins likely to belong to the NtrC regulon

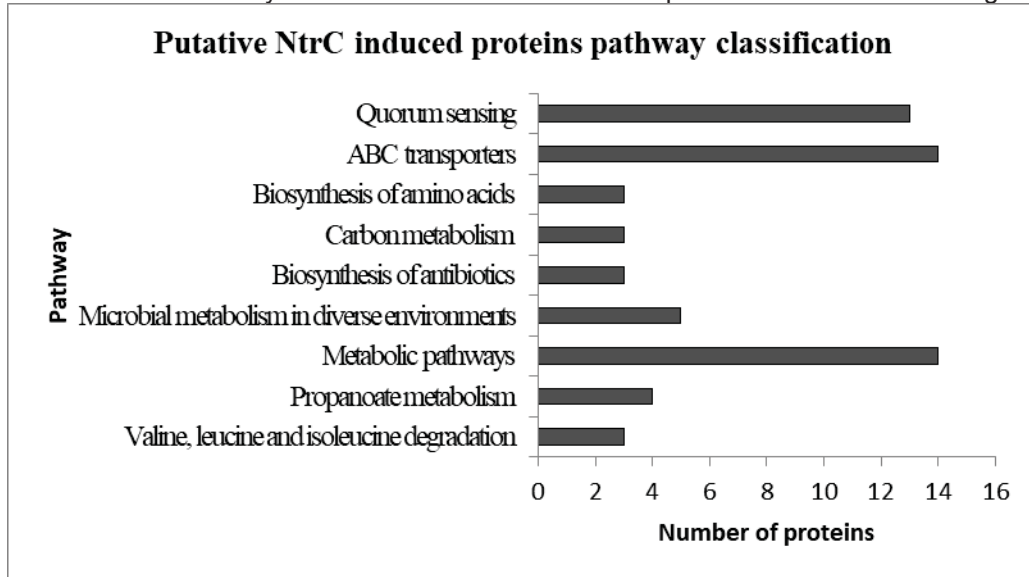
In order to determine which proteins were likely induced by NtrC we compared the protein expression profiles between wild type and the *ntrC* mutant grown under low nitrogen. 112 proteins were found to be exclusively upregulated in the wild type under low N; these proteins are likely to be directly or indirectly upregulated by NtrC (Figure 6) (Supplementary material table 7). These proteins were categorized using COG (supplementary material figure 16) and KEGG (Figure 7) which revealed that a significant portion (27%) of the total of these putative NtrC-regulated proteins belong to ABC transporter and other N-related transport system. Interestingly, this group has the highest fold changes, reaching up to 1050 for the urea ABC transporter (gi|392383070). 13 of these transporters (supplementary material table 8) are classified in the quorum sensing pathway and 2 of them (gi|392384046, FC 39.9; gi|392377481, FC 5.0) show putative sigma 54 binding sites in the promoter region of the correspondent gene, suggesting that NtrC may be involved in their regulation. The data is in accordance with previous reports which showed that NtrC is a major transcription factor involved in transport and assimilation of alternative N sources³⁵.

FIGURE 6 - VENN DIAGRAM OF DIFFERENTIALLY ABUNDANT PROTEINS THAT ARE UPREGULATED UNDER LOW NITROGEN TREATMENT IN *A. brasiliense* FP2 AND THE MUTANT *ntrC*.



FONTE: a autora (2018).

FIGURE 7 - KEGG CLASSIFICATION FOR THE CANDIDATE PROTEINS LIKELY INDUCED BY NTRC. Pathways that showed at least 3 induced proteins are shown in the figure.



FONTE: a autora (2018).

Enzymes involved in metabolic pathways are the most representative group, including the anthranilate synthase TrpE(G) (gi|392381934, FC 3.7), which catalyzes the first step of the tryptophan synthesis from chorismate. *Azospirillum brasilense* releases auxin indole-3-acetic acid (IAA) into the culture medium when growing in the presence of tryptophan³⁶. Previous studies demonstrated that IAA levels produced by *trpE(G)* mutant were much lower than that of the *A. brasilense* Yu62 wild-type strain³⁷. This suggests that NtrC may be involved in IAA synthesis. Among the induced proteins are those related to cofactor synthesis; such as, phosphomethylpyrimidine synthase ThiC (gi|392382255, FC 2.5), the thiamine biosynthesis protein ThiS (gi|392380014, FC 3.2) and the glycine oxidase ThiO (gi|392380015, FC 2.5), that participate in the synthesis of thiamin, and molybdopterin molybdenum transferase MoeA (gi|392382462, FC 50.3), involved in the molybdopterin biosynthesis process. The synthesis of both cofactors may be activated by NtrC. These cofactors are essentials for carbohydrate metabolism, providing functionality to enzymes such as carbon monoxide dehydrogenases (gi|392382384, FC 3.2; gi|392379727, FC 5.9; gi|392379728, FC 10.5) and glutamine-fructose-6-phosphate aminotransferase GlnS (gi|392382621, FC 2.8), which were also induced under low nitrogen.

Several upregulated proteins found in the wild type under low nitrogen are involved in amino acid metabolism, such as amidases (gi|392384043, FC 28.5;

gi|392384044, FC 18.5; gi|392384045, FC 36.8) that catalyze the hydrolysis of amides, releasing ammonium, and also the dihydroorotase PyrC (gi|392379716), with a fold change of 372. In *E. coli*, this latter enzyme catalyzes the third step of *de novo* pyrimidine biosynthesis, through reversible cyclization of carbamyl aspartate to form dihydroorotate. Interestingly, this enzyme is also upregulated (FC 273) when comparing FP2 low N against the mutant low N, indicating that NtrC might be involved in its regulation and in the *de novo* biosynthesis of pyrimidines. Enzymes related to lipid metabolism were found among those putatively induced by NtrC. Four of these are involved in lipid biosynthesis: long-chain fatty acid CoA ligase (LuxE) (gi|392378151, FC 2.9), prolipoprotein diacylglycerol (Lgt) (gi|392380055, FC 6.6) and acyl-CoA dehydrogenase CaiA (gi|392379744, FC 3.5; gi|392381791, FC 2.8). Previous studies showed that nitrogen starvation induced the accumulation of lipids in microalgae, like *Desmodesmus sp.* and *Chlorella sp.*^{38, 39, 40}. Furthermore, recent data showed that the PII proteins, which are regulated by NtrC and part of the Ntr system, affect lipid metabolism at posttranslational level⁴¹. Our data support the hypothesis that the NtrC-PII system may play a role in the regulation of not only nitrogen but also in carbon related metabolic pathways.

Proteins involved in signal transduction, such as two-component histidines kinases, transcriptional activators and methyl-accepting chemotaxis receptors were found among those putative induced by NtrC under low N. Most are involved the bacterial response to stress (HupB, HrcA, Crp/Fnr family, LysR family). The stress regulator HupB (gi|392382089, FC 3.1) is the beta subunit of HU protein, which is a nucleoid-associated protein that regulates gene expression by modulating the accessibility of DNA supercoils to transcriptional machinery^{42, 43}. In *Mycobacterium spp.*, the deletion of *hupB* affects growth under stress conditions⁴⁴. Among the members of LuxR/FixJ family (FlcA and gi|392383224), the transcriptional regulator FlcA (gi|392382764) that controls the morphological transformation of *A. brasiliense* cells from vegetative to cyst form, is upregulated in the wild type low N compared to high N (FC 18) and also when compared to the mutant under low N (FC 8.7), leading us to the hypothesis that it can be activated in an NtrC-dependent manner. *flcA* knock-out mutants are impaired in flocculation and colonization of plant root surfaces relative to the wild type Sp⁴⁵. It was shown that *A. brasiliense ntrC* has decrease in clumping and flocculation phenotype when grown under flocculation conditions

(elevated aeration and nitrogen starvation), compared to the wild-type⁴⁶. Furthermore, previous studies suggested that FlcA might control nitrogen assimilation and fixation by down regulating glutamine synthetase in *A. brasilense*⁴⁷.

Phosphate regulatory proteins were also found among the differentially expressed proteins. The two-component histidine kinase PhoR (gi|392380620, FC 2.3) is among those proteins likely induced by NtrC, although its partner PhoB was not detected in the proteome. PhoR-PhoB control the expression of proteins related to the phosphate acquisition, including the phosphate starvation protein PhoH (gi|392381702) whose abundance also increased under low nitrogen with a fold change of 9.0. On the other hand, both strains showed an upregulation of PhoU protein (gi|392382309) under high N. PhoU is the inhibitor of Pho regulon, required for PhoR dephosphorylation under phosphate rich conditions and is also involved in avoiding uncontrolled Pi uptake⁴⁸. A previous study showed that, in *Sinorhizobium meliloti*, the PII proteins were involved in the phosphate response, suggesting that the response to nitrogen limitation is co-regulated by nitrogen and phosphate levels⁴⁹. Our results also suggest a cross regulation between nitrogen and phosphate metabolisms, that might be mediated by NtrC.

Two components of the type II and VI secretion systems were also induced in the wild type low N, are them TamB and TssK (gi|392382683, FC 2.4; gi|392378699, FC 2.9). The type II secretion system is conserved in most gram-negative bacteria and transports folded proteins and a diverse array of substrates into the extracellular environment⁵⁰. The type VI secretion system translocates proteins into a variety of recipient cells and is capable of transporting effector proteins from one bacterial cell to another, playing a role in bacterial communication and interaction⁵¹.

Nitrogen starvation is known to cause oxidative stress in many organisms like *Chlorella* and *Acutodesmus*^{52, 53}. Eleven proteins (supplementary material table 9), related to the oxidative stress response, were upregulated in the wild type under low N and are likely regulated by NtrC. Among them, 3 are described as YhaK protein (gi|392381197, FC 2.1; gi|392381217, FC 4.7; gi|392378378, FC 4.8) which is a member of the pirin family. Members of this family are associated with diverse functions and, although their biological function is still not clearly understood, it was reported that YhaK may be involved in cellular redox regulation and sensing of

oxidative stresses in *E. coli*⁵⁴. The enzyme glutathione S-transferase (GstA) (gi|392382138, FC 8.5) is among the putative induced by NtrC and is best studied in eukaryotes. It catalyzes the conjugation of electrophilic compounds to reduced glutathione (GSH)⁵⁵, which is believed to function in defense against oxidative stress⁵⁶. Another upregulated protein involved in the response against oxidative stress is methionine sulfoxide reductase (MsrA, gi|392383323, FC 7.8), that repairs oxidized proteins through the reduction of methionine-S-sulfoxide to methionine⁵⁷. The organic hydroperoxide resistance protein Ohr (gi|392383934) is upregulated in the FP2 low N with a fold change of 2.9 and has been identified in numerous bacteria. It is included in the OsmC superfamily and acts in the detoxification of organic hydroperoxides, but not hydrogen peroxide⁵⁸. The enzyme azoreductase AzoR (gi|392381762) is upregulated in the wild type under low N when compared to the high N (FC 46) and also when compared to the mutant strain under low N (FC 27), suggesting that NtrC may regulate the abundance of this enzyme. AzoR is essential in *E. coli* for the maintenance of cellular GSH levels after addition of electrophilic quinones. Thus, AzoR seems related to resistance to thiol-specific stress⁵⁹.

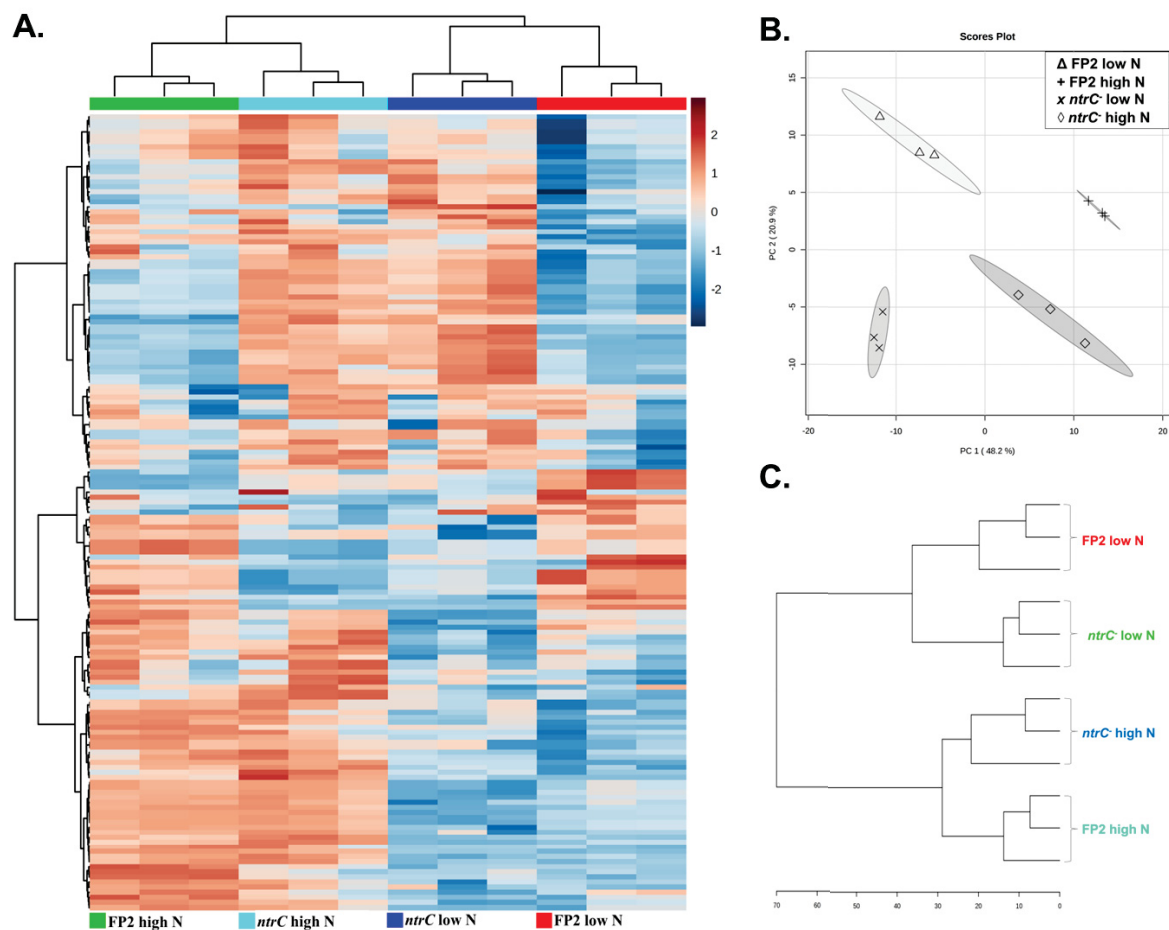
A group of non-characterized or hypothetical is among the proteins likely induced by NtrC, was not possible to attribute any function to these proteins; NtrC may activate these proteins in response to nitrogen starvation but their role needs to be further investigated.

2.4.7 Metabolomic profiling of *A. brasiliense*

In order to compare the metabolic response to nitrogen limitation between the *A. brasiliense* FP2 and *ntrC* strains, polar metabolites were extracted and subjected to untargeted metabolomic profiling using GC/MS. Metabolites were compared between the samples using Metaboanalyst and considered differentially abundant when the fold change was > 2 and $p\text{-value} < 0.05$. In total, we observed 167 putative compounds in the samples. Among those, 75 could be identified by matching with metabolite databases whereas 92 had no match (Supplementary material table 10). The identified metabolites include amino acids, sugars and fatty acids. The heat map indicates the relative abundance of all metabolites in all samples and the dendrogram shows the clustering of the samples according to the nitrogen levels and also the

separation between the strains (Figure 8A). We carried out a multivariate statistical analysis to evaluate whether the nitrogen starvation and the lack of the NtrC protein had a significant effect on the metabolite profile. As shown in figure 8B, a principal component analysis (PCA) resulted in clear separation of the metabolite fractions between the samples. This indicates that the nitrogen levels lead to a clear alteration of the metabolic profile between the two studied *Azospirillum* strains. Hierarchical clustering analysis was performed based on the degree of similarity of metabolite abundance profiles to show the global overview of all metabolites detected in all samples (Figure 8C). Metabolites with similar abundance patterns were positioned closer together.

FIGURE 8 - (A) HEAT MAP SHOWING ABUNDANCES OF ALL METABOLITES IN ALL SAMPLES. Each bar represents a metabolite colored by its abundance intensities on normalized scale from blue (decreased level) to red (increased level). The samples are showed in triplicates. (B) PCA ANALYSIS FOR ALL METABOLITE SAMPLES. (C) HIERARCHICAL CLUSTERING ANALYSIS BASED ON THE METABOLITE ABUNDANCE PROFILES FOR ALL SAMPLES.

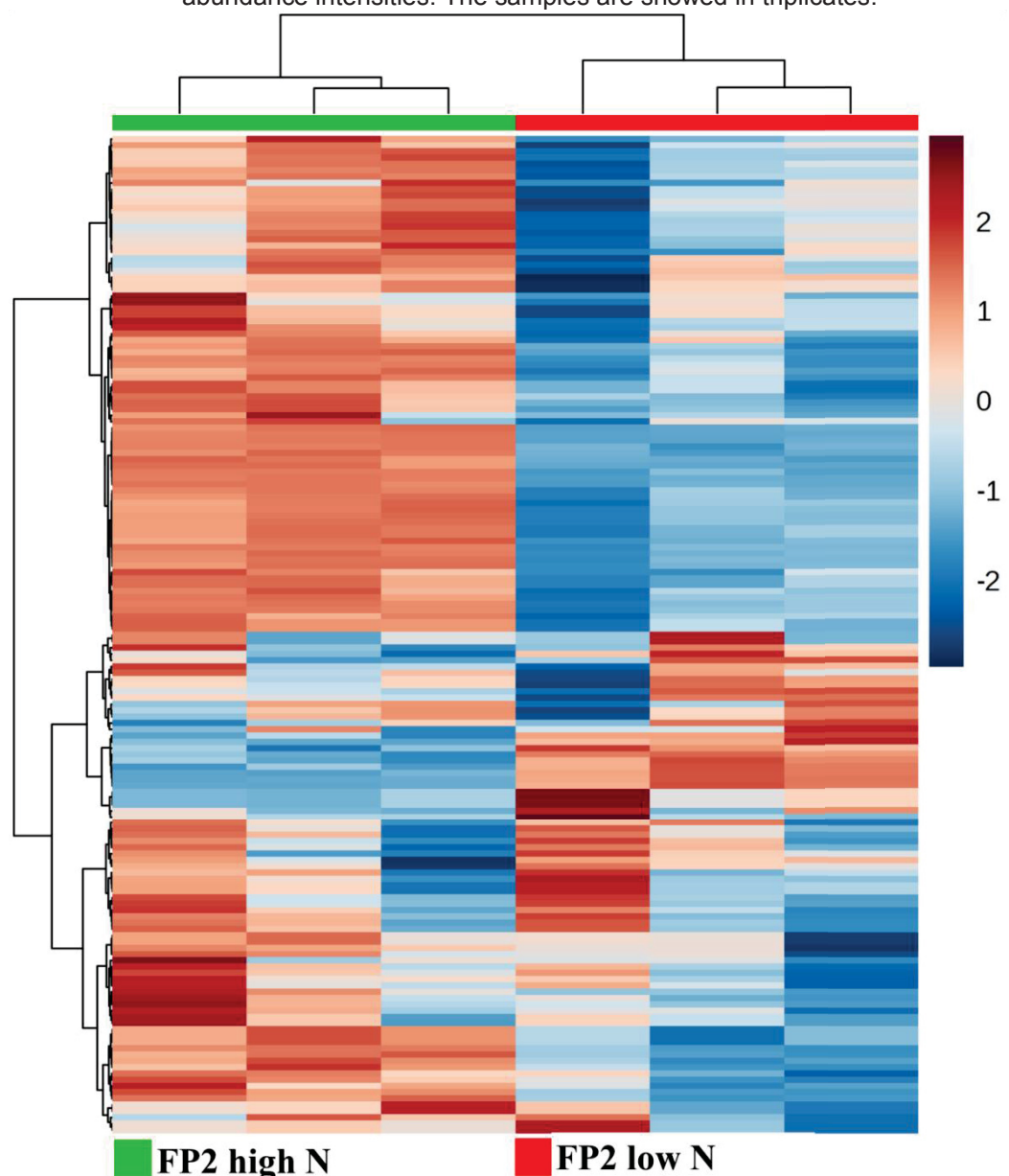


FONTE: a autora (2018).

2.4.8 Metabolomic changes in *A. brasiliense* FP2 in response to nitrogen limitation

Comparison of the metabolites identified in *A. brasiliense* FP2 cell extracts from the high and low nitrogen cultures revealed 60 differentially abundant compounds (Supplementary material table 11). Among these, 5 were more abundant under low nitrogen levels and 55 in high nitrogen. Figure 9 shows the heat map and hierarchical clustering of all metabolites found in this condition based on their abundances.

FIGURE 9 - HEAT MAP SHOWING ABUNDANCES OF ALL METABOLITES IN *A. brasiliense* FP2 HIGH AND LOW NITROGEN. Each bar represents a metabolite colored by its abundance intensities. The samples are showed in triplicates.



FONTE: a autora (2018).

In low nitrogen, the wild type strain showed more abundance of 2 sugars: two compounds identified as D-mannose (*m/z* 319.2) that are slightly different in their retention times (23.3 and 23.6 minutes) and an isomaltose (*m/z* 204.2). The KEGG database indicates that D-mannose and isomaltose belong to fructose, mannose, galactose, starch, sucrose, amino sugar and nucleotide metabolism pathways, indicating a high activity of the carbohydrate and energy metabolism under low nitrogen. This result is in agreement with our findings in the proteomic analysis, that showed an upregulation of four proteins from these pathways in the FP2 under low N, are them glutathione S-transferase (gi|392382138; FC 8.5) and gamma-glutamyltransferase (gi|392379721; FC 25.6), belonging to the starch and sucrose metabolism, glutamine-fructose-6-phosphate aminotransferase (gi|392382621; FC 2.8) from the amino sugar and nucleotide metabolism pathway and pyridoxal 4-dehydrogenase (gi|392383963; FC 2.6), involved in fructose and mannose metabolism. With regard to the 55 metabolites found more abundant in the high nitrogen condition, most are amino acids (30.9%) and 8 (14.5%) are organic compounds belonging to the carboxylic acid class. The high content of amino acids present in this condition, especially the branched chain amino acids, L-valine (*m/z* 218.1) and L-isoleucine (*m/z* 158.2), with fold changes of 13.6 and 5.8 respectively, reflects the nutritional status of the bacterial cells, which are in a nitrogen sufficient environment. Uric acid (*m/z* 456.2), with a fold change of 134.4, is the most abundant metabolite present in *A. brasiliense* FP2 when grown with high nitrogen. Uric acid is a nitrogen compound derived from the catabolism of purine. Bacteria have the ability to utilize purines as nitrogen and carbon sources when experiencing starvation conditions. The final products of purine degradation are glyoxylate and ammonia, which are recycled to synthesized organic molecules utilized to support growth. In the same pathway, xanthine (*m/z* 368.2), which is the first common intermediate of purine degradation, is more abundant in *A. brasiliense* FP2 under high nitrogen with a fold change of 27.2. Interestingly, our study showed uric acid and xanthine more abundant in both strains under high N condition than the low N. This is in accordance with our proteome analysis, which showed 9 and 7 upregulated proteins involved in purine metabolism for the wild type and the mutant, respectively, under high N, indicating a high activity of this pathway in this condition. It is expected as the ammonium is incorporated primarily in glutamate and glutamine, which subsequently function as nitrogen donors for the biosynthesis of other amino acids and the

precursors of purines and pyrimidines⁶². Aspartate (*m/z* 232.1) is more abundant in the FP2 high N than low N (FC 7.4) and, in *E. coli*, purines can stimulate growth in the presence of aspartate⁶³. Putrescine (*m/z* 174.1) is more abundant in high N in the wild type and in the mutant (FC 26.8 and 8.6, respectively). The concentration of intracellular polyamines is positively correlated with the growth rate and can affect the expression of hundreds genes in *E. coli*^{64, 65}. An additional 26 compounds whose abundance clearly changed based on nitrogen available could not be identified in the available databases.

2.4.9 Metabolomic changes in the *A. brasiliense ntrC* mutant in response to nitrogen limitation

A total of 54 metabolites were differentially regulated comparing extracts of the *A. brasiliense ntrC* mutant strain grown under high or low nitrogen conditions (Supplementary material table 12). Among these, fifty-two metabolites were more abundant in the mutant strain under high nitrogen. Seventeen (32.7%) were identified as amino acids and 8 (15.4%) as organic compounds. As observed for the wild type, uric acid (*m/z* 456.2) and xanthine (*m/z* 368.2) were also more abundant in the mutant under high N (FC 12.3 and 48.3, respectively) than in low N. We also observed one sugar (D-mannitol *m/z* 319.2) and one inorganic acid (phosphoric acid *m/z* 299.1) that are more abundant in the mutant strain under high N (FC 2.0 and 5.8, respectively). The polyamines L-putrescine (*m/z* 174.1) and spermidine (*m/z* 174.1) were increased in the mutant under high nitrogen (FC 8.6 and 2.0, respectively) and ornithine (*m/z* 174.2, FC 2.2), a precursor of polyamine synthesis⁶⁶, was also more abundant in this condition. These results are in agreement with our proteomic analysis, as two proteins involved in the ornithine and polyamine synthesis, agmatinase (gi|392379713; FC 5.9) and ornithine decarboxylase (gi|392380526; FC 8.6) were increased in the mutant under high nitrogen conditions.

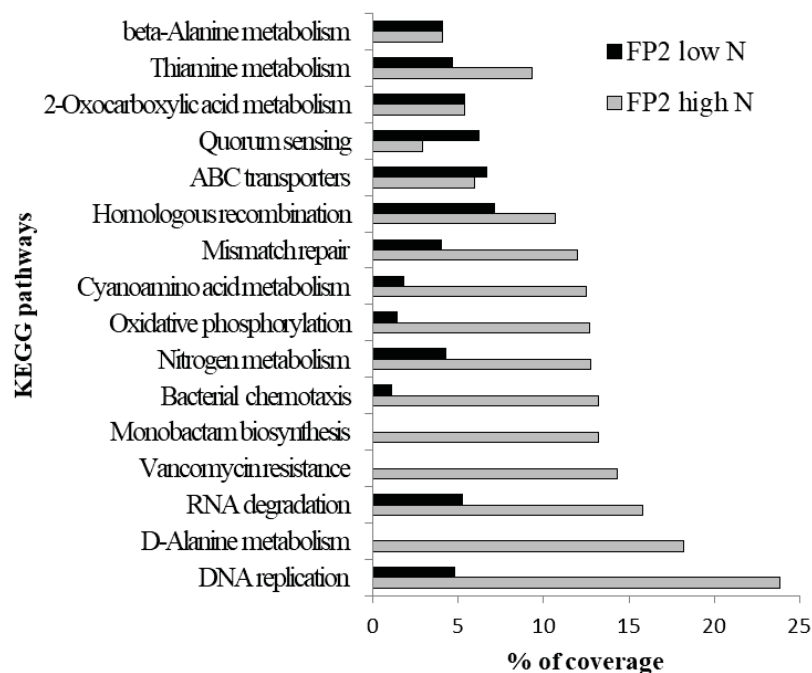
2.4.10 Proteome and metabolomics integration using pathway analysis

Proteomic and metabolomics analysis of *A. brasiliense* enabled the identification of important metabolic pathways that may be regulated by NtrC under nitrogen starvation. In order to better define these pathways, the list of differentially regulated proteins and metabolites was submitted to the KEGG server for pathway mapping analysis (Supplementary material table 13 and 14). Figure 10 (A, B) was constructed based on percentage of coverage for each pathway, integrating

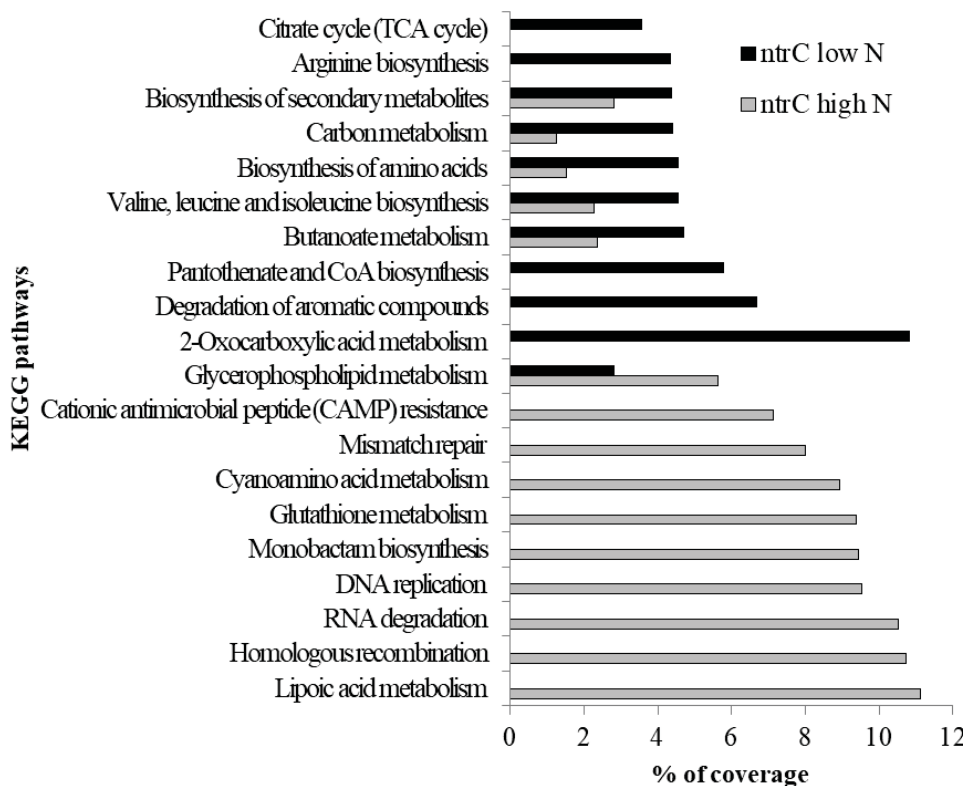
proteomics and metabolomics results, and shows the top ten most affected KEGG pathways by nitrogen levels for each studied strain. In the wild type, nitrogen limitation induced mostly the homologous recombination, quorum sensing and ABC transporters pathways, while in the mutant strain, the same condition activated mainly the degradation of aromatic compounds, 2-oxocarboxylic acid metabolism and phantothenate and CoA biosynthesis pathways. Interestingly, the most induced pathways in the wild type and also in the mutant strain under high nitrogen are DNA replication and RNA degradation, indicating that the high activity of these pathways are in response to N levels and independent of NtrC.

FIGURE 10 - INTEGRATED PROTEOMICS AND METABOLOMICS DATA IN PERCENTAGE OF COVERAGE FOR *A. brasiliense* BIOLOGICAL PATHWAYS. (A) COVERAGE OF THE TEN MOST AFFECTED PATHWAYS IN THE WILD TYPE LOW AND HIGH N. (B) COVERAGE OF THE TEN MOST AFFECTED PATHWAYS IN THE MUTANT UNDER LOW AND HIGH NITROGEN.

A. Coverage of affected pathways in FP2 low and high N



B. Coverage of affected pathways in *ntrC* low and high N



FONTE: a autora (2018).

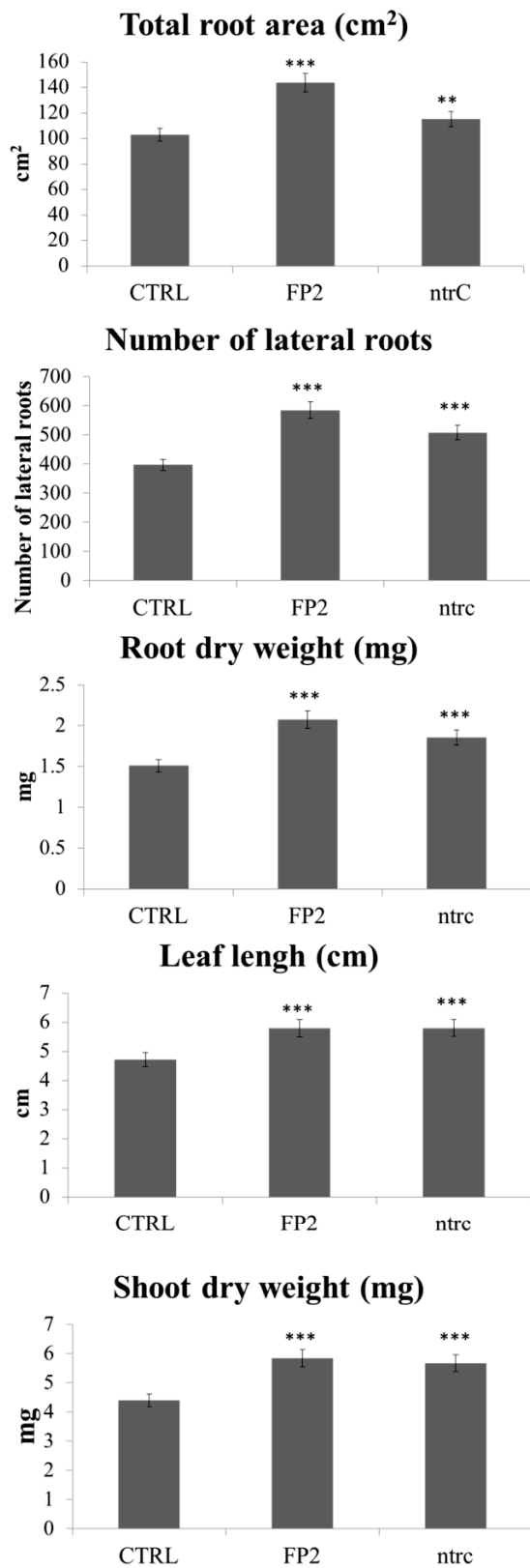
Considering that the transcriptional activator NtrC is active under low nitrogen, the pathways that are upregulated by nitrogen limitation in the wild type are potentially induced by NtrC. Consistent with our hypothesis that NtrC is involved in the oxidative stress response, the glutathione metabolism pathway is upregulated under low nitrogen in *A. brasiliense* FP2 (3.1% of pathway coverage), what is not observed in the mutant strain under the same condition. Another pathway that is potentially activated by NtrC is quorum sensing, with 6.2% of coverage in the wild type under low nitrogen against 1.5% in the mutant. The pathways upregulated in the wild type under high nitrogen are mainly related to TCA cycle (8.9% pathway coverage), oxidative phosphorylation (12.7%), arginine biosynthesis (8.7%), purine metabolism (6.5%) and amino acids metabolism. Pathways related to amino acid and lipoic acid metabolism are induced in both strains under high nitrogen, although this induction is more prominent in the wild type. The pathways that were most induced in the mutant under low N are those related to degradation of aromatic compounds and carboxylic acid metabolism.

2.4.11 Effects of *A. brasiliense* FP2 and *ntrC* mutant strains on *S. viridis* growth

The ability of *A. brasiliense* FP2 to promote plant growth is well established and demonstrated using a variety of plants; such as *Setaria viridis*, *Brachypodium distachyon* and maize^{67, 2, 3}. In our study, we used *Setaria viridis*, a grass model system, inoculated with *A. brasiliense* FP2 and its *ntrC* mutant strain. The effect of inoculation of *S. viridis* with *A. brasiliense* FP2 or the *ntrC* mutant was evaluated 20 days after inoculation. Both strains showed significant enhancement in all growth parameters analyzed compared to the non-inoculated control (Figure 11 and supplementary material table 15). The comparison between the wild type and mutant strain revealed a significant increase of root parameters in plants inoculated with FP2 strain. Our results also showed that aboveground parameters were not affected for either wild type or the *ntrC* mutant. These findings showed that both strains are capable of promoting plant growth and suggest that nitrogen regulation mediated by NtrC is not a major determinant of bacterial plant growth promotion under the conditions tested. In order to evaluate the ability of the *ntrC* mutant strain to colonize *S. viridis* roots, we performed a colonization assay. Four individual plants 20 days after inoculation were carefully removed from soil and used for counting the number of bacteria cells attached to the root surface by serial dilutions. Student's t-test was

performed with the whole set of data. No significant difference in the ability to colonize plant root was detected in the mutant compared to the wild type, and both strains reached 10^5 CFU mL⁻¹ (Supplementary material figure 19). These data suggest that NtrC does not play a significant role in the ability of the bacteria to colonize the host plant roots.

FIGURE 11 - *S. viridis* GROWTH PROMOTION FOR EACH *A. brasiliense* STRAIN COMPARED TO THE UN-INOCULATED CONTROL. BARS ARE MEAN OF N = X +- SE. Asterisk represents p-value = 0.01** and 0.001***.

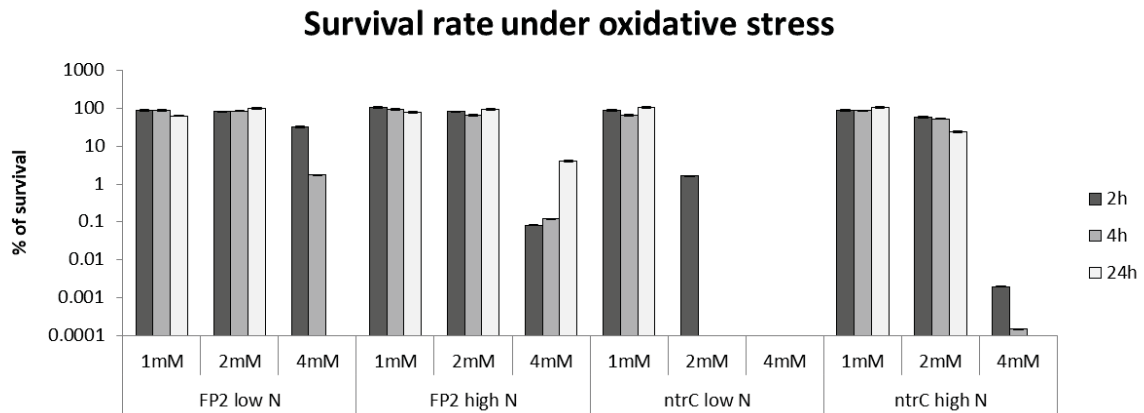


FONTE: a autora (2018).

2.4.12 Oxidative stress response

Our results showed that several proteins related to the oxidative stress response are likely to be induced by NtrC in *A. brasilense*. This result leads to the hypothesis that NtrC may be involved in this process. In order to investigate this further, we examined the effect of adding 0.5, 2 and 4 mM of H₂O₂ to bacterial cultures while measuring DO₆₀₀ to monitor the growth rate. We observed that the growth of the wild type strain was not affected by 0.5 mM of H₂O₂ in both nitrogen conditions. However, there was a difference in growth rate upon the addition of 2 and 4 mM H₂O₂ under both nitrogen conditions, suggesting that N-limited cells are more sensitive to oxidative stress. Moreover, for the *ntrC* mutant strain, 0.5 mM of H₂O₂ was enough to impair the growth, while 2 and 4 mM completely halted cell growth in the presence of both high and low ammonium (Supplementary material figure 17). We also evaluated the number of viable cells by plating 2, 4 and 24 hours after the addition of H₂O₂. Under low nitrogen conditions with 2 mM of H₂O₂, the number of viable cells in the wild type was similar to the control without H₂O₂, while no viable cells of the *ntrC* mutant could be recovered after 4 hours of treatment. Under high nitrogen conditions with 4 mM of H₂O₂, the viability of the wild type initially decreased but then recovered within 4 h. These same conditions, however, were lethal to the *ntrC* mutant, with no viable cells recovered even after 24 hours (Supplementary material figure 18). The survival rate was calculated based on the number of viable cells in the control without H₂O₂ and is shown in the figure 12. Under low N both strains showed a lower survival rate when compared to high N conditions, this is due to the sum of oxidative stresses caused by the low N level and the addition of H₂O₂. When comparing between strains under low N, the FP2 is able to survive in 2mM of H₂O₂, while the mutant dies after 4 hours. With increasing concentration of H₂O₂ to 4mM, the wild type still show a high survival rate after 4 hours. Contrary, the mutant does not show any viable cell 2 hours after the addition of H₂O₂. These results suggest that, in *A. brasilense*, NtrC is important for the bacterial survival under oxidative stress and the nitrogen status of the cells strongly impacts the ability to withstand this stress.

FIGURE 12 - CELL SURVIVAL RATE OF THE *A. brasiliense* FP2 AND *ntrC*, IN HIGH AND LOW NITROGEN, UNDER DIFFERENT CONCENTRATIONS OF H₂O₂.



FONTE: a autora (2018).

In *P. putida* under low N, the deletion of the *ntrC* gene also reduced the growth rate, but, on the other hand, rendered cells more resistance to oxidative stress⁶⁰. The transcriptome analysis showed that resistance in the mutant was due to derepression of several genes related to oxidative stress response⁶⁰. In this organism, different sets of genes were involved in the oxidative stress response depending on high or low nitrogen levels and NtrC sensed nitrogen availability was required for cellular defense against oxidative stress. Contrary of our findings, it was demonstrated that in *Herbaspirillum seropedicae* the *ntrC* mutant appeared to possess a more efficient defense response against oxidative stress⁶¹, indicating that in different organisms, NtrC might have distinct functions related to this response.

2.4.13 Analysis of the promoter region for putative genes regulated by NtrC

NtrC activates transcription of sigma 54 dependent promoters of genes involved in the use of alternative nitrogen sources. For the 112 putative proteins regulated by NtrC we analyzed 300 bp upstream the correspondent genes seeking for sigma 54 binding sites. Twenty one genes showed a putative sigma 54 binding site in their promoter region (table 2) with good match to the consensus sequence, including the GlnZ and the NtrC itself. Although these 19 remaining genes are stronger candidates to be induced by NtrC, further investigation is needed to evaluate the activity of these promoters.

TABLE 2 - PROTEINS WITH A SIGMA 54 MOTIF IN THE PROMOTER REGION OF THEIR CORRESPONDENT GENES.

Sequence Name	p-value	Matched Sequence	Protein name
gi 392383241	1.9E-06	TTGCACGGGGATTGC	hybrid sensor histidine kinase/response regulator, partial
gi 392384046	3.4E-06	TGGCACGATTCTGC	ABC transporter substrate-binding protein
gi 392377481	3.9E-06	TGGCATGGAACTTGC	spermidine/putrescine ABC transporter
	9.2E-06	TGGCACGGCGCTGT	ATPase
gi 392381749	6.2E-06	CGGCACGCGCCATGC	putative Methyl-accepting chemotaxis protein
	1.7E-05	TGGCACACCTCCTGC	
gi 392377639	7.4E-06	TGGCCCGACGGTAGC	NUDIX hydrolase
gi 392379403	9.8E-05	CGGCACGCCGCCGC	copper ABC transporter, permease component
gi 392377167	9.3E-06	TGGCCTGGGGCTTGC	nitrogen regulation protein NR(I) (NtrC)
gi 392378148	9.4E-06	TGGCCTGCCCGTTGC	succinyl-diaminopimelate desuccinylase
gi 392383934	1.3E-05	TGGCACGCAACACGC	organic hydroperoxide resistance protein, OsmC superfamily
gi 392379744	1.4E-05	AGGCACCCAGGTTGC	acyl-CoA dehydrogenase
gi 392383137	1.5E-05	TGGCACGCTGGCTGA	hypothetical protein
gi 392384143	1.5E-05	CGGAACGCGCATTGC	adenosylcobalamin-dependent methylmalonyl-CoA mutase (MutA)
gi 392381633	9.8E-05	CGGCGCGGCGGTGGC	protein of unknown function
gi 392381341	2.0E-05	CCGCACGCGGTTGC	hypothetical protein
gi 392379924	2.3E-05	AGGCGCGGTAAATTGC	exported protein of unknown function
gi 392381713	2.8E-05	TGGCACAGCGTTGA	chemotaxis sensory transducer
gi 392380826	3.1E-05	TGGCCCAAGGATTGC	16S rRNA maturation RNase (YbeY)
gi 392378005	3.6E-05	CGGCACGCTGTTGG	amino acid ABC transporter substrate-binding protein (GlnH)
gi 392381052	3.8E-05	TGGCACGAACGGTTC	hypothetical protein
gi 392382255	7.2E-05	TGGCCCGTTGTTCC	phosphomethylpyrimidine synthase (ThiC)
gi 392381004	8.2E-05	CGGCACGATTTTGA	nitrogen regulatory protein P-II 1 (GlnZ)

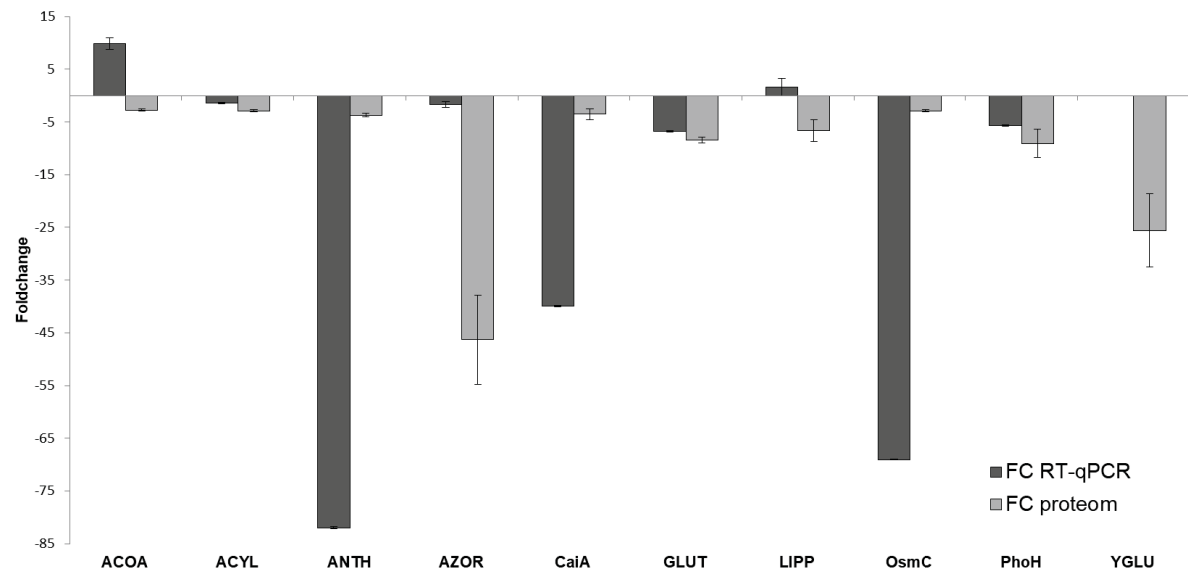
FONTE: a autora (2018).

2.4.14 mRNA levels of selected genes using RT-qPCR

We selected 10 genes whose protein products showed increased accumulation in *A. brasiliense* FP2 low N against high N, for further validation using qRT-PCR. From 10 selected genes, 7 were in general agreement with their corresponding changes in the protein levels, thereby confirming the transcription regulation (Figure 13). The consistency between the transcription level and protein expression was confirmed for long chain fatty acid Coa Ligase (ACYL) and acyl-CoA dehydrogenase (CaiA), related to lipid metabolism; azoreductase (AzoR), glutathione S-transferase (GLUT) and organic hydroperoxide resistance protein (OsmC), involved in response against oxidative stress; anthranilate synthase (ANTH), that

catalyzes the first step of the tryptophan synthesis; and for the phosphate starvation protein (PhoH). The mRNA expression of acyl-CoA dehydrogenase (ACOA) and the lipoprotein diacylglycerol transferase (LIPP) did not correlate with protein data, suggesting post-transcriptional regulatory events, while expression of gamma-glutamyltransferase (YGLU) was not detected in the qRT-PCR. All of the melting curves showed a single peak in the tested range of standard curves, suggesting good specificity. A non-detectable fluorescence signal in negative and blank controls indicated that the reaction system was not contaminated during the experimental procedures.

FIGURE 13 - TRANSCRIPTIONAL VALIDATION OF PROTEOMIC DATA USING RT-qPCR ASSAYS. THE VALUE OF FOLD CHANGE ON THE Y-AXIS INDICATES THE RATIO OF EITHER PROTEIN OR mRNA LEVEL IN THE *A. brasiliense* FP2 HIGH N WHEN COMPARED TO THE LOW N.



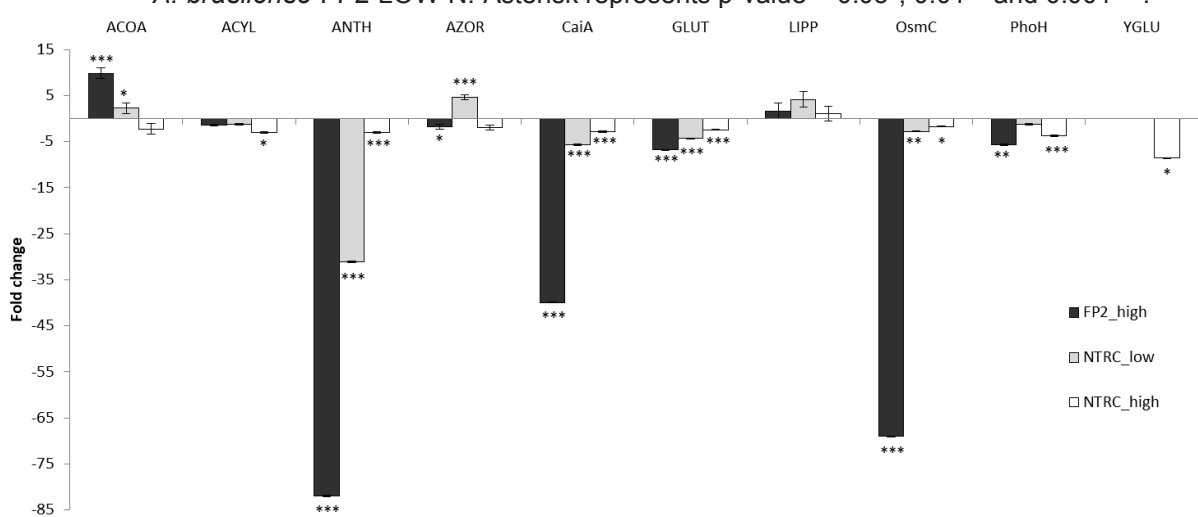
FONTE: a autora (2018).

2.4.15 qRT-PCR analyses of the differentially expressed genes

The mRNA transcription levels of expressed proteins detected by qRT-PCR relative to the control *A. brasiliense* wild-type low N are shown in figure 14. Only three mRNA expression levels showed upregulation, for Azoreductase (AzoR), lipoprotein diacylglycerol transferase (LIPP) and Acyl-CoA dehydrogenase (ACOA), including in the mutant strain, indicating that these genes are probably not induced by NtrC. On the other side, the downregulated genes are the most likely to be induced by NtrC. Notably, we observed a greater downregulation in all samples for anthranilate synthase (ANTH), acyl-CoA dehydrogenase (CaiA) and organic hydroperoxide resistance protein (OsmC), especially in the wild-type high N. The transcription levels

of glutathione S-transferase (GLUT), phosphate starvation protein (PhoH) and long chain fatty acid Coa Ligase (ACYL) were also downregulated in all samples compared to the wild type low N. These results are in agreement with our hypothesis that these genes are induced by NtrC. The expression of gamma-glutamyltransferase (YGLU) in the wild type high N and in the mutant low N was not detected by RT-qPCR.

FIGURE 14 - RELATIVE EXPRESSION OF SELECTED GENES COMPARED TO THE CONTROL *A. brasiliense* FP2 LOW N. Asterisk represents p-value = 0.05*; 0.01 and 0.001***.**



FONTE: a autora (2018).

2.5 CONCLUSION

Proteomic and metabolomics analyses showed the biological changes in protein and metabolite profiles of *A. brasiliense* FP2 and its mutant *ntrC*, under high and low nitrogen. The integrated data led us to a list of proteins likely induced by NtrC, since its targets are not fully determined. Further analyses are necessary to confirm these targets and elucidate how they are activated through NtrC. These studies can lead to a better understanding of the relationship between the candidate proteins and the transcriptional activator NtrC, as well as their role in nitrogen metabolism in *Azospirillum brasiliense*.

2.6 ACKNOWLEDGMENTS

This work was supported by CNPq, CAPES, the National Institute of Science and Technology of Biological Nitrogen Fixation – INCT-FBN. The Proteomics Core Facility at Rikshospitalet is supported by the South-East Health Authority of Norway (Helse Sør-Øst), the Research Council of Norway and by the Oslo University Hospital (OUS).

2.7 REFERENCES

- (1) Bashan, Y.; Holguin G.; de-Bashan L.E. Azospirillum-plant relationships: Physiological, molecular, agricultural and environmental advances (1997-2003). *Can. J. Microbiol.* 2004, 50, 521-577.
- (2) Pankiewicz, V. C.; Amaral, F. P.; Santos, K. F.; Agtuca, B. ; Xu, Y.; Schueler, M. J.; Arisi, A. C.; Steffens, M. B.; Souza, E. M.; Pedrosa, F. O.; Stacey, G.; Ferrieri, R. A. Robust biological nitrogen fixation in a model grass–bacterial association. *Plant J.* 2015, 81, 907-919.
- (3) Do Amaral F.P.; Pankiewicz V.C.; Arisi A.C.; De Souza E.M.; Pedrosa F.; Stacey G. Differential growth responses of Brachypodium distachyon genotypes to inoculation with plant growth promoting rhizobacteria. *Plant Mol Biol.* 2016, 90, 689-697.
- (4) Baldani, J.I.; Baldani, V.L.D. History on the biological nitrogen fixation research in graminaceous plants: special emphasis on the Brazilian experience. *Anais da Academia Brasileira de Ciências.* 2005, 77, 549-579.
- (5) Zhang, Y.; Burris, R. H.; Ludden, P.W.; Roberts, G. P. Regulation of nitrogen fixation in *Azospirillum brasiliense*. *FEMS Microbiology Letters.* 1997, 152, 195-204.
- (6) Jiang, P.; Peliska, J. A.; Ninfa, A. J. The regulation of *Escherichia coli* glutamine synthetase revisited: role of 2-ketoglutarate in the regulation of adenylylation state. *Biochemistry.* 1998, 37, 12802-12810.
- (7) Araújo, L.M.; Huergo, L.F.; Invitti, A.L.; Gimenes, C.I.; Bonatto, A.C.; Monteiro, R.A.; Souza, E.M.; Pedrosa, F.O.; Chubatsu, L.S. Different responses of the GlnB and GlnZ proteins upon in vitro uridylylation by the *Azospirillum brasiliense* GlnD protein. *Brazilian Journal of Medical and Biological Research.* 2008, 41(4), 289-294.
- (8) Jiang P.; Ninfa A.J.; Regulation of Autophosphorylation of *Escherichia coli* Nitrogen Regulator II by the PII Signal Transduction Protein. *Journal of Bacteriology.* 1999, 181(6), 1906-1911.
- (9) Ninfa, E.G.; Atkinson, M.R.; Kamberov, E.S.; Ninfa, A.J. Mechanism of autophosphorylation of *Escherichia coli* nitrogen regulator II (NRII or NtrB): trans-phosphorylation between subunits. *Journal of Bacteriology.* 1993, 175(21), 7024-7032.

- (10) Zimmer, D.P.; Soupene, E.; Lee, H.L.; Wendisch, V.F.; Khodursky, A.B.; Peter, B.J.; Bender, R.A.; Kustu, S. 2000. Nitrogen regulatory protein C-controlled genes of *Escherichia coli*: scavenging as a defense against nitrogen limitation. *Proc Natl Acad Sci U S A*. 2000, 97, 14674–14679.
- (11) Davalos, M.; Fourment, J.; Lucas, A.; Berges, H.; Kahn, D. 2004. Nitrogen regulation in *Sinorhizobium meliloti* probed with whole genome arrays. *FEMS Microbiol Lett*. 2004, 241, 33–40.
- (12) Hervas, A.B.; Canosa, I.; Santero, E. Transcriptome analysis of *Pseudomonas putida* in response to nitrogen availability. *J Bacteriol*. 2008, 190, 416–420.
- (13) Franck, W.L.; Qiu, J.; Lee, H.I.; Chang, W.S.; Stacey, G. DNA microarray-based identification of genes regulated by the two-component NtrBC system in *Bradyrhizobium japonicum*. *Appl. Environ. Microbiol.* 2015, 81(16), 5299-308.
- (14) Zhang, Y.; Pohlmann, E.L.; Roberts, G.P. GlnD is essential for NifA activation, NtrB/NtrC-regulated gene expression, and posttranslational regulation of nitrogenase activity in the photosynthetic, nitrogen-fixing bacterium *Rhodospirillum rubrum*. *J. Bacteriol.* 2005, 187, 4, 1254-1265.
- (15) Hervas, A.B.; Canosa, I.; Santero, E. Transcriptome analysis of *Pseudomonas putida* in response to nitrogen availability. *J Bacteriol*. 2008, 190, 416–420.
- (16) Huergo, L.F.; Souza, E.M.; Steffens, M.B.; Yates, M.G.; Pedrosa, F.O.; Chubatsu, L.S. Regulation of *glnB* gene promoter expression in *Azospirillum brasilense* by the NtrC protein. *FEMS Microbiology Letters*. 2003, 223, 33-40.
- (17) De Zamaroczy, M.; Paquelin, A.; Elmerich, C. Function organization of the *glnB-glnA* cluster of *Azospirillum brasilense*. *J. Bacteriol*. 1993, 175, 2507-2515.
- (18) Liang, Y. Y.; De Zamaroczy, M.; Arsene, F.; Paquelin, A.; Elmerich, C. Regulation of nitrogen fixation in *Azospirillum brasilense* Sp7: involvement of *nifA*, *glnA* and *glnB* gene products. *FEMS Microbiol. Lett*. 1992, 79, 113 – 119.
- (19) Machado, H. B.; Yates, M. G.; Funayama, S.; Rigo, L. U.; Steffens, M. B. R.; Souza, E. M., Pedrosa, F. O. The *ntrBC* genes of *Azospirillum brasilense* are part of a *nifR3-like-ntrB-ntrC* operon and are negatively regulated. *Can. J. Microbiol.* 1995, 41, 674-684.

- (20) De Zamaroczy, M. Structural homologues P(II) and P(z) of *Azospirillum brasilense* provide intracellular signaling for selective regulation of various nitrogen-dependent functions. *Mol. Microbiol.* 1998, 29, 449-463.
- (21) Pedrosa, F.O.; Yates, M.G. Regulation of nitrogen fixation (*nif*) genes of *Azospirillum brasilense* by *nifA* and *ntrC* (*glnG*) type genes. *FEMS Microbiol. Lett.* 1984, 23, 1, 95-101.
- (22) Bradford, M.M. A rapid and sensitive method for the quantitation of microgram quantities of protein utilizing the principle of protein-dye binding. *Analytical Biochemistry*. 1976, 72, 1, 248-254.
- (23) Huergo, L.F.; Souza, E.M.; Araujo, M.S.; Pedrosa, F.O.; Chubatsu, L.S.; Steffens, M.B.; Merrick, M. ADP-ribosylation of dinitrogenase reductase in *Azospirillum brasilense* is regulated by AmtB-dependent membrane sequestration of DraG. *Mol. Microbiol.* 2006, 59, 326-337.
- (24) Rappaport, J.; Ishihama, Y.; Mann, M. Stop and Go Extraction Tips for Matrix-Assisted Laser Desorption/Ionization, Nanoelectrospray, and LC/MS Sample Pretreatment in Proteomics. *Analytical Chemistry*. 2003, 75, 3, 663-670.
- (25) Sumner, L.W.; Amberg, A.; Barrett, D.; Beale, M.H.; Beger, R.; Daykin, C.A.; Fan, T.W.-M.; Fiehn, O.; Goodacre, R.; Griffin, J.L.; Hankemeier, T.; Hardy, N.; Harnly, J.; Higashi, R.; Kopka, J.; Lane, A.N.; Lindon, J.C.; Marriott, P.; Nicholls, A.W.; Reily, M.D.; Thaden, J.J.; Viant, M.R. Proposed minimum reporting standards for chemical analysis. *Metabolomics*. 2007, 3, 211-221.
- (26) Xia, J.; Psychogios, N.; Young, N.; Wishart, D.S. MetaboAnalyst: a web server for metabolomic data analysis and interpretation. *Nucleic Acids Res.* 2009, 37, 652-660.
- (27) Tatusov, R.L.; Galperin, M.Y.; Natale, D.A.; Koonin, E.V. The COG database: a tool for genome-scale analysis of protein functions and evolution. *Nucleic Acids Res.* 2000, 28 (1), 33-36.
- (28) Ogata, H.; Goto, S.; Sato, K.; Fujibuchi, W.; Bono, H.; Kanehisa, M. KEGG: Kyoto Encyclopedia of Genes and Genomes. *Nucleic Acids Res.* 1999, 27 (1), 29-34.
- (29) Grant, C.E.; Bailey, T.L.; Noble, W.S. FIMO: Scanning for occurrences of a given motif. *Bioinformatics*. 2011, 27(7), 1017-1018.

- (30) Untergasser, A.; Nijveen, H.; Rao, X.; Bisseling, T.; Geurts, R.; Leunissen, J.A.M. Primer3Plus, an enhanced web interface to Primer3. *Nucleic Acids Research*. 2007, 35(Web Server issue), W71–W74.
- (31) Livak, K.J.; Schmittgen, T.D. Analysis of relative gene expression data using real-time quantitative PCR and the 2(-Delta Delta C(T)) method. *Methods*. 2001, 25, 402–408.
- (32) Hoagland, D.R.; Arnon, D.I. The water-culture method for growing plants without soil. *J. Circ. Calif. Agric. Experiment Stn*. 1950, 347, 32.
- (33) Huergo, L.F.; Assumpcao, M.C.; Souza, E.M.; Steffens, M.B.; Yates, M.G.; Chubatsu, L.S.; Pedrosa, F.O. Repressor mutant forms of the *Azospirillum brasilense* NtrC protein. *Appl Environ Microbiol*. 2004, 70, 6320–6323.
- (34) Wisniewski-Dyé, F.; Borziak, K.; Khalsa-Moyers, G.; Alexandre, G.; Sukharnikov, L.O.; Wuichet, K.; Hurst, G.B.; McDonald, W.H.; Robertson, J.S.; Barbe, V.; Calteau, A.; Rouy, Z.; Mangenot, S.; Prigent-Combaret, C.; Normand, P.; Boyer, M.; Siguier, P.; Dessaix, Y.; Elmerich, C.; Condemine, G.; Krishnen, G.; Kennedy, I.; Paterson, A.H.; González, V.; Mavingui, P.; Zhulin, I.B. *Azospirillum* genomes reveal transition of bacteria from aquatic to terrestrial environments. *PLoS Genet*. 2011, 7: e1002430.
- (35) Zimmer, D. P.; Soupene, E.; Lee, H. L.; Wendisch, V. F.; Khodursky, A. B.; Peter, B. J.; Bender, R.A.; Kustu, S. Nitrogen regulatory protein C-controlled genes of *Escherichia coli*: Scavenging as a defense against nitrogen limitation. *Proceedings of the National Academy of Sciences of the United States of America*. 2000, 97(26), 14674–14679.
- (36) Carreno-Lopez, R.; Campos-Reales, N.; Elmerich, C.; Baca, B.E. Physiological evidence for differently regulated tryptophan-dependent pathways for indole-3-acetic acid synthesis in *Azospirillum brasilense*. *Mol. Gen. Genet.* 2000, 264, 521–530.
- (37) Ge, S.M.; Xie, B.E.; Chen, S.F. Characterization of two trpE genes encoding anthranilate synthase α-subunit in *Azospirillum brasilense*. *Biochem. Biophys. Res. Commun.* 2006, 341, 494–499.
- (38) Ruiz-Marin, A.; Mendoza-Espinosa, L.G.; Stephenson, T. Growth and nutrient removal in free and immobilized green algae in batch and semi-

- continuous cultures treating real wastewater. *Bioresource Technology*. 2010, 101, 58-64.
- (39) Rios, L.F.; Klein, B.C.; Luz Jr., L.F.; Maciel Filho, R.; Wolf Maciel, M.R. Nitrogen starvation for lipid accumulation in the microalga species *Desmodesmus sp.* *Appl. Biochem. Biotechnol.* 2015, 175, 469-47.
- (40) Zhu, S.; Wang, Y.; Huang, W.; Xu, J.; Wang, Z.; Xu, J.; Yuan, Z. Enhanced accumulation of carbohydrate and starch in *Chlorella zofingiensis* induced by nitrogen starvation. *Appl. Biochem. Biotechnol.* 2014, 174, 2435-2445.
- (41) Gerhardt, E.C.; Rodrigues, T.E.; Muller-Santos, M.; Pedrosa, F.O.; Souza, E.M.; Forchhammer, K.; Huergo, L.F. The Bacterial signal transduction protein GlnB regulates the committed step in fatty acid biosynthesis by acting as a dissociable regulatory subunit of acetyl-CoA carboxylase. *Mol Microbiol.* 2015, 95, 1025-1035.
- (42) Oberto, J., Nabti, S., Jooste, V., Mignot, H., & Rouviere-Yaniv, J. The HU Regulon Is Composed of Genes Responding to Anaerobiosis, Acid Stress, High Osmolarity and SOS Induction. *PLoS ONE*. 2009, 4(2), e4367.
- (43) Travers, A.; Muskhelishvili, G. Bacterial chromatin. *Curr Opin Genet Dev.* 2005, 15, 507–514.
- (44) Whiteford, D.C.; Klingelhoeft, J.J.; Bambenek, M.H.; Dahl, J.L. Deletion of the histone-like protein (Hlp) from *Mycobacterium smegmatis* results in increased sensitivity to UV exposure, freezing and isoniazid. *Microbiology*. 2011, 157, 327–335.
- (45) Pereg-Gerk, L.; Paquelin, A.; Gounon, P.; Kennedy, I.R. A transcriptional regulator of the LuxR-UhpA family, FlcA, controls flocculation and wheat root surface colonization by *Azospirillum brasilense* Sp7. *Elmerich C Mol Plant Microbe Interact.* 1998, 11(3), 177-87.
- (46) Bible, A.N.; Khalsa-Moyers, G.K.; Mukherjee, T.; Green, C.S.; Mishra, P.; Purcell, A.; Alexandre, G. Metabolic Adaptations of *Azospirillum brasilense* to Oxygen Stress by Cell-to-Cell Clumping and Flocculation. *Applied and Environmental Microbiology*. 2015, 81(24), 8346–8357.
- (47) Hou, X.; McMillan, M.; Coumans, J.V.F.; Poljak, A.; Raftery, M.J.; Pereg, L. Cellular responses during morphological transformation in

- Azospirillum brasiliense* and its *fIC*A knockout mutant. *PLoS ONE*. 2014, 9(12), e114435.
- (48) Gardner, S.G.; Johns, K.D.; Tanner, R.; McCleary, W.R. The PhoU protein from *Escherichia coli* interacts with PhoR, PstB, and metals to form a phosphate-signaling complex at the membrane. *J. Bacteriol.* 2014, 196, 1741–1752.
- (49) Hagberg, K.L.; Yurgel, S.N.; Mulder, M.; Kahn, M.L. Interaction between Nitrogen and Phosphate Stress Responses in *Sinorhizobium meliloti*. *Frontiers in Microbiology*. 2016, 7, 1928.
- (50) Green, E. R., & Mecsas, J. Bacterial Secretion Systems – An overview. *Microbiology Spectrum*. 2016, 4(1), 10.1128/microbiolspec.VMBF-0012-2015.
- (51) Russell, A.B.; Peterson, S.B.; Mougous, J.D. Type VI secretion effectors: poisons with a purpose. *Nature Reviews. Microbiology*. 2014, 12(2), 137–148.
- (52) Zhang, Y.M.; Chen, H.; He, C.L.; Wang, Q. Nitrogen Starvation Induced Oxidative Stress in an Oil-Producing Green Alga *Chlorella sorokiniana* C3. *PLoS ONE*. 2013, 8(7): e69225.
- (53) Chokshi, K.; Pancha, I.; Ghosh, A.; Mishra, S. Nitrogen starvation-induced cellular crosstalk of ROS-scavenging antioxidants and phytohormone enhanced the biofuel potential of green microalga *Acutodesmus dimorphus*. *Biotechnol. Biofuels*. 2017, 10(1), 60.
- (54) Gurmu, D.; Lu, J.; Johnson, K.A.; Nordlund, P.; Holmgren, A.; Erlandsen, H. The crystal structure of the protein YhaK from *Escherichia coli* reveals a new subclass of redox sensitive enterobacterial bicupins. *Proteins*. 2009, 74, 18–31.
- (55) Hayes, J.D.; Flanagan, J.U.; Jowsey, I.R. Glutathione transferases. *Annu Rev Pharmacol Toxicol*. 2005, 45, 51–88.
- (56) Kanai, T.; Takahashi, K.; Inoue, H. Three Distinct-Type Glutathione S-Transferases from *Escherichia coli* important for defense against oxidative stress. *The Journal of Biochemistry*. 2006, 140 (5), 703–711.
- (57) Oien, D.B.; Moskovitz, J. Substrates of the methionine sulfoxide reductase system and their physiological relevance. *Curr Top Dev Biol*. 2008, 80, 93–133.

- (58) Cussiol, J.R.; Alves, S.V.; De Oliveira, M.A.; Netto, L.E. Organic hydroperoxide resistance gene encodes a thiol-dependent peroxidase. *J. Biol. Chem.* 2003, 278, 11570–11578.
- (59) Liu, G.; Zhou, J.; Fu, Q.S.; Wang, J. The *Escherichia coli* azoreductase AzoR is involved in resistance to thiol-specific stress caused by electrophilic quinones. *J Bacteriol.* 2009, 191, 6394–6400.
- (60) Yeom, S.; Yeom, J.; Park, W. NtrC-sensed nitrogen availability is important for oxidative stress defense in *Pseudomonas putida* KT2440. *J. Microbiol.* 2010, 48, 153–159.
- (61) Sacomboio, E.N.M.; Kim, E.Y.S.; Correa, H.L.R.; Bonato, P.; Pedrosa, F.O.; de Souza, E.M.; Chubatsu, L.S.; Muller-Santos, M. The transcriptional regulator NtrC controls glucose-6-phosphate dehydrogenase expression and polyhydroxybutyrate synthesis through NADPH availability in *Herbaspirillum seropedicae*. *Sci. Rep.* 2017, 7:13546.
- (62) Zalkin, H.; Smith, J.L. Enzymes utilizing glutamine as an amide donor. *Adv. Enzymol. Relat. Areas Mol. Biol.* 1998, 72, 87–144.
- (63) Xi, H.; Schneider, B. L.; Reitzer, L. Purine Catabolism in *Escherichia coli* and Function of Xanthine Dehydrogenase in Purine Salvage. *Journal of Bacteriology*. 2000, 182(19), 5332–5341.
- (64) Tweeddale, H.; Notley-McRobb, L.; Ferenci, T. Effect of slow growth on metabolism of *Escherichia coli*, as revealed by global metabolite pool (“metabolome”) analysis. *Journal of Bacteriology*. 1998, 180(19), 5109–5116.
- (65) Yoshida, M.; Kashiwagi, K.; Shigemasa, A.; Taniguchi, S.; Yamamoto, K.; Makinoshima, H.; Ishihama, A.; Igarashi, K. A unifying model for the role of polyamines in bacterial cell growth, the polyamine modulon. *J Biol Chem.* 2004, 279(44), 46008–13.
- (66) Tabor, C.W., & Tabor, H. Polyamines in microorganisms. *Microbiological Reviews*. 1985, 49(1), 81–99.
- (67) Okon Y. *Azospirillum* as a potential inoculant for agriculture. *Trends Biotechnol.* 1985, 3, 223–228.

2.8 MATERIAL SUPPLEMENTAR

TABLE 3 - PRIMERS USED FOR RT-qPCR ANALYSIS.

Primer name:	Protein:	ID	Forward sequence:	Reverse sequence:
PHOH	Phosphate starvation protein (PhoH)	gi 392381702	GACATGCACGAGAAGATGG	TCAGCAGCATCTTGATCTG
AZOR	Azoreductase (AzorR)	gi 392381762	CACAGTTCTCGTCCTTACC	AACGAGATTGCCGGAAAGTG
ACOA	Acyl-CoA dehydrogenase	gi 392381791	CATCAGCCCTGTTCATCGTG	GTGAACATGTATTCGATGCC
ANTH	Anthranilate synthase	gi 392381934	CTGTACTCCCGTCTGATCC	ATTGCTCCGTATCCTCCAG
GLUT	Glutathione S-transferase	gi 392382138	ATTGCCTATGAACCGGATCG	TGAAAGAACATCCATTGCAG
PHBC	Poly-beta-hydroxybutyrate polymerase	gi 392382223	GTCCTCCCAAACCGGATCTGAT	AACATGTAGTCTTCGAAGGCC
ACYL	Long chain fatty acid Coa Ligase	gi 392382223	ATCAGCGTCTTCAGGGATT	GCGAAAATTGACGGTCATC
PHAA	Acetyl-CoA acetyltransferase (PhaA)	gi 392378463	CCACGATCAACCGCTACTG	CAGTAGGCTCCGGATAATG
OSMC	Organic hydroperoxide resistance protein (OsmC)	gi 392383934	ATTCTCTACACGACCAAAGC	CGGGAACACAGTGATCTTGTG
PHBB	Acetoacyl-CoA reductase (PhbB)	gi 392384431	GGACATCCCTGGTGAACAAC	ACGAGATGTTGATGATGCG
CAIA	Acy-CoA dehydrogenase (fatty acid beta oxidation I) (CaiaI)	gi 392379744	GTCGGACCTGATGACTCTG	GATCTCGTACTCCTTCATGC
LIPP	Lipoprotein diacylglycerol transferase	gi 392380055	TTCTACAAACCTGCCCTCTA	GTTGATGAAGTTGGCGATG
PHAR	Polydihydroxyalkanoate synthesis repressor (PhaR)	gi 392379928	CTGTCAGATGGTCAAGGAC	GAGAAGGGACTGCATCGAATA
YGLU	Gamma-glutamyltransferase	gi 392379721	CACCGTGACGTTCTGTTG	GAGTTGATGAAGGAAATGGC
RPOC	RpoC RNA polymerase subunit beta - Housekeeping 1	gi 1333324433	TCCCCAGAGCTTCGATCAGA	GGTTTCCGGCTTCTTGATCTC
RPOD	RpoD - RNA polymerase sigma factor - Housekeeping 2	gi 356877854	TTCCGGAGCAGATCGAAGACA	CGAGTCCTGCTCTTCCGGATT

FONTE: a autora (2018).

TABLE 4 - DIFFERENTIAL PROTEINS BETWEEN *A. brasiliense* FP2 LOW AND HIGH N.

t-test p-value	Fold change	Protein IDs	Protein name
Upregulated:			
0.0000006244	1050.53	gi 392383070	urea ABC transporter substrate-binding protein
0.000000684	371.82	gi 392379716	Dihydroorotate
0.000011633	314.07	gi 392378005	amino acid ABC transporter substrate-binding protein
0.000021683	252.95	gi 392377482	ABC transporter substrate-binding protein
0.000027057	218.62	gi 392381052	hypothetical protein
0.000000452	203.49	gi 392379722	ABC-type branched-chain amino acid transport systems, periplasmic component
0.000000002	200.21	gi 392383795	ABC transporter substrate-binding protein
0.0000006418	194.91	gi 392380217	hypothetical protein
0.0000002610	151.33	gi 392380023	putative oligopeptide ABC transporter (substrate-binding protein)
0.0000253530	129.56	gi 392380681	ammonia channel protein
0.0000009614	127.65	gi 392382401	amino acid ABC transporter substrate-binding protein
0.0000006775	83.73	gi 392383066	ABC transporter ATP-binding protein
0.000000649	71.42	gi 392382300	transcriptional regulator
0.0000003826	57.60	gi 392383067	ABC transporter ATP-binding protein
0.0000002815	53.73	gi 392383069	urea ABC transporter permease subunit UrtB
0.0006369320	50.34	gi 392382462	molybdopterin molybdenumtransferase MoeA
0.0000069952	50.20	gi 392380332	amino acid ABC transporter substrate-binding protein
0.0000002097	48.41	gi 392378105	nitrate ABC transporter substrate-binding protein
0.000000063	46.31	gi 392380304	branched-chain amino acid ABC transporter substrate-binding protein
0.000002223	46.30	gi 392381762	Azoreductase
0.000091062	39.96	gi 392384046	ABC transporter substrate-binding protein
0.000609629	37.51	gi 392380220	uracil phosphoribosyltransferase (fragment), partial
0.000000489	36.85	gi 392384045	N-carbamoylsarcosine amidase
0.000002718	28.54	gi 392384043	amidase (fragment), partial
0.000001701	25.56	gi 392379721	gamma-glutamyltransferase (fragment), partial
0.0000044189	24.46	gi 392381440	methyl-accepting chemotaxis protein

0.0000001080	23.87	gi 392378830	NAD(P)H:quinone oxidoreductase
0.015128100	18.96	gi 392380219	protein of unknown function
0.0000207576	18.50	gi 392384044	putative Glutamyl-tRNA(Gln) amidotransferase subunit A (Glu-ADT subunit A)
0.000159649	17.52	gi 392382764	DNA-binding response regulator
0.0000000074	15.92	gi 392383277	putative serine protein kinase
0.0000304346	15.77	gi 392381692	Dioxygenase
0.0000008002	15.37	gi 392378468	histidine kinase
0.0000003631	15.35	gi 392377401	phytoene dehydrogenase
0.0000182887	14.46	gi 392381713	conserved protein of unknown function
0.0000064031	14.45	gi 392379742	putative Oxoglutarate dehydrogenase (succinyl-transferring)
0.0000000277	14.21	gi 392379894	peptide ABC transporter substrate-binding protein
0.0000768467	13.80	gi 392379730	hypothetical protein
0.0000207710	12.68	gi 392379972	ABC transporter substrate-binding protein
0.023523000	11.30	gi 392381633	protein of unknown function
0.0200097200	10.75	gi 392377569	peptidase S41
0.0000208807	10.59	gi 392378731	X-Pro dipeptidyl-peptidase
0.0000004794	10.48	gi 392379728	carbon monoxide dehydrogenase
0.0000000817	10.00	gi 392378831	glutathione-dependent reductase
0.015106500	9.86	gi 392383348	2-dehydropanoate 2-reductase
0.000401030	9.62	gi 392377642	hypothetical protein
0.001097790	9.53	gi 392377487	N-acetyltransferase GCN5
0.015009000	9.52	gi 392380541	3-phosphoglycerate dehydrogenase
0.058880200	9.26	gi 392384143	adenosylcobalamin-dependent methylmalonyl-CoA mutase small subunit (MCM-beta)(N-terminal fragment), partial
0.0000016380	9.20	gi 392380932	hypothetical protein
0.0000007723	9.10	gi 392377298	hypothetical protein
0.0000047655	9.07	gi 392381702	phosphate starvation protein PhoH
0.002624170	8.80	gi 392377486	Asp/Glu/hydantoin racemase
0.0000017820	8.80	gi 392379968	Agmatinase
0.0000009321	8.54	gi 392381931	histidine kinase

0.0000000219	8.47	gi 392382138	glutathione S-transferase
0.000000065	8.06	gi 392383841	peptide ABC transporter substrate-binding protein
0.002077630	7.95	gi 392379394	hypothetical protein
0.000000245	7.92	gi 392381004	nitrogen regulatory protein P-II 1
0.011927300	7.85	gi 392383323	peptide methionine sulfoxide reductase
0.021653200	7.39	gi 392380333	hypothetical protein
0.0000169459	7.13	gi 392380218	conserved hypothetical protein
0.0000462504	6.76	gi 392378644	hypothetical protein
0.0000021131	6.71	gi 392383276	conserved protein of unknown function; putative coiled-coil domain
0.006843890	6.66	gi 392380055	prolipoprotein diacylglyceryl transferase
0.032970000	6.63	gi 392381384	trans-aconitate 2-methyltransferase
0.004553720	6.56	gi 392383857	Crp/Fnr family transcriptional regulator
0.006838200	6.52	gi 392383840	putative acetylornithine deacetylase or succinyl-diaminopimelate desuccinylase
0.018787300	6.52	gi 392382745	cobalamin biosynthesis protein CobD
0.0000097475	6.26	gi 392379726	ABC transporter ATP-binding protein
0.0000027411	6.23	gi 392383275	SpoVR family protein
0.033596600	6.16	gi 392381341	hypothetical protein
0.040832100	6.00	gi 392383137	hypothetical protein
0.002089930	5.94	gi 392379121	regulatory lipoprotein
0.000656394	5.92	gi 392379727	carbon monoxide dehydrogenase
0.000010976	5.72	gi 392383848	putative acetolactate synthase large subunit
0.000145688	5.22	gi 392379136	branched-chain amino acid ABC transporter substrate-binding protein
0.000259523	4.99	gi 392377481	spermidine/putrescine ABC transporter ATPase
0.0000491876	4.84	gi 392381659	septum formation initiator
0.031265500	4.82	gi 392383672	Glyoxalase
0.000469853	4.80	gi 392378378	quercetin 2,3-dioxygenase
0.000108830	4.74	gi 392381217	hypothetical protein
0.000300399	4.62	gi 392379403	copper ABC transporter, permease component (modular protein)
0.002083180	4.57	gi 392379740	ABC transporter substrate-binding protein
0.014850500	4.54	gi 392383727	aspartate aminotransferase family protein

0.0000963894	4.44	gi 392380240	haloacid dehalogenase
0.0000015684	4.43	gi 392377615	hybrid sensor histidine kinase/response regulator
0.0000004872	4.26	gi 392378815	hypothetical protein
0.000046632	4.23	gi 392384279	3-isopropylmalate dehydrogenase
0.0000025837	4.11	gi 392377227	putative Allophanate hydrolase, subunit 2 (modular protein)
0.005847440	4.09	gi 392381501	glycosyl transferase family 51
0.011902200	4.02	gi 392382711	sodium-translocating pyrophosphatase
0.040182700	4.00	gi 392380777	spermidine/putrescine ABC transporter, substrate-binding component
0.028890200	3.94	gi 392381749	putative Methyl-accepting chemotaxis protein with multiple PAS domains
0.0000002497	3.92	gi 392378456	putative transcriptional regulator, HTTH-XRE family
0.001486520	3.84	gi 392382271	D-amino acid dehydrogenase small subunit
0.034551600	3.79	gi 392381228	CBS domain-containing protein
0.0000076012	3.71	gi 392381934	anthranilate synthase
0.004550320	3.60	gi 392378104	nitrate ABC transporter permease
0.004271350	3.53	gi 392379744	acyl-CoA dehydrogenase
0.040504500	3.51	gi 392381471	transcriptional regulator
0.029619500	3.38	gi 392379387	transcriptional regulator
0.036026000	3.36	gi 392382481	crossover junction endodeoxyribonuclease
0.0000016855	3.34	gi 392377167	nitrogen regulation protein NR(I)
0.035518400	3.32	gi 392383224	transcriptional activator, LuxR/FixJ family
0.023407500	3.27	gi 392380209	hypothetical protein
0.000554616	3.25	gi 392380011	hypothetical protein
0.0000010635	3.21	gi 392382988	N-formylglutamate amidohydrolase
0.010302300	3.18	gi 392382384	carbon monoxide dehydrogenase
0.0000192568	3.17	gi 392380014	thiamine biosynthesis protein ThIS
0.033507200	3.14	gi 392382089	transcriptional regulator
0.005746320	3.13	gi 392380245	conserved exported protein of unknown function
0.000235680	3.08	gi 392383995	pyrroline-5-carboxylate reductase
0.000102209	3.07	gi 392378246	2-methylisocitrate lyase
0.0000003190	3.07	gi 392383726	methylmalonate-semialdehyde dehydrogenase (acylating)

0.0002785570	3.06	gi 392383241	hybrid sensor histidine kinase/response regulator, partial
0.051125000	3.02	gi 392381386	histidine kinase
0.001036760	3.02	gi 392383243	putative histidine kinase
0.000845249	2.95	gi 392378699	type VI secretion protein
0.000466139	2.93	gi 392379971	putative spermidine/putrescine transport protein (ABC superfamily, atp_bind)
0.036655300	2.90	gi 392383954	polar amino acid ABC transporter ATP-binding protein
0.000069344	2.87	gi 392378151	long-chain-fatty-acid--CoA ligase
0.000013582	2.87	gi 392383934	organic hydroperoxide resistance protein, OsmC superfamily
0.000247681	2.86	gi 392383349	elongation factor G
0.008167360	2.80	gi 392382621	glutamine--fructose-6-phosphate aminotransferase
0.002245490	2.78	gi 392379843	2-deoxy-D-gluconate 3-dehydrogenase
0.000012201	2.78	gi 392381791	acyl-CoA dehydrogenase
0.010354000	2.77	gi 392378148	succinyl-diaminopimelate desuccinylase
0.050366000	2.75	gi 392379195	LysR family transcriptional regulator
0.000059946	2.74	gi 392383844	ABC transporter ATP-binding protein
0.000056722	2.74	gi 392384245	ABC transporter substrate-binding protein
0.0000179907	2.71	gi 392378303	hypothetical protein
0.006598880	2.71	gi 392380988	heat-inducible transcriptional repressor HrcA
0.030663800	2.66	gi 392380533	peptidase S16
0.004130670	2.65	gi 392380229	formyl-CoA transferase
0.000025719	2.63	gi 392383963	pyridoxal 4-dehydrogenase
0.000017291	2.61	gi 392382708	transcription antitermination factor NusB
0.002583420	2.57	gi 392378001	lipolytic protein G-D-S-L family
0.000535505	2.56	gi 392377877	Imidazolonepropionase
0.047387900	2.54	gi 392377219	multidrug efflux system, subunit A (AcrB family) (fragment), partial
0.000259588	2.51	gi 392382255	phosphomethylpyrimidine synthase ThiC
0.003776440	2.48	gi 392380015	glycine oxidase
0.006116720	2.47	gi 392379802	Heptosyltransferase
0.001010240	2.44	gi 392377447	ABC transporter substrate-binding protein
0.000952554	2.42	gi 392382325	branched chain amino acid ABC transporter substrate-binding protein

0.047319200	2.41	gi 392379924	exported protein of unknown function
0.009355210	2.40	gi 392381410	RNA pyrophosphohydrolase
0.000060580	2.40	gi 392382329	membrane protein
0.002355080	2.39	gi 392377740	TIGR02302 family protein
0.000094434	2.39	gi 392384473	Acetyltransferase
0.014514000	2.38	gi 392382531	conserved hypothetical protein; beta-Ig-H3/Fasciclin domain
0.003230780	2.38	gi 392380620	two-component sensor histidine kinase
0.002981730	2.37	gi 392382683	membrane protein
0.010185100	2.34	gi 392378036	hypothetical protein
0.000499148	2.30	gi 392382040	hypothetical protein
0.0000693348	2.28	gi 392379049	protein of unknown function
0.036896700	2.26	gi 392383849	3-keto-5-aminohexanoate cleavage protein
0.002838270	2.25	gi 392381709	conserved protein of unknown function
0.001036990	2.23	gi 392380717	histidine kinase
0.0000340603	2.19	gi 392383847	acetylpolyamine amidohydrolase
0.0000131985	2.17	gi 392383998	putative Metallo-hydrolase/oxidoreductase superfamily protein; Beta-lactamase-like
0.0003214790	2.17	gi 392377639	NUDIX hydrolase
0.000043580	2.16	gi 392378882	IMP dehydrogenase
0.0248442100	2.16	gi 392381310	putative trypsin-like serine protease
0.000065445	2.14	gi 392382791	alcohol dehydrogenase
0.003936420	2.14	gi 392380646	amino acid ABC transporter substrate-binding protein
0.004590540	2.13	gi 392377389	single-stranded DNA-binding protein
0.016933600	2.12	gi 392383018	dimethylglycine dehydrogenase
0.014209400	2.12	gi 392377791	two-component response regulator
0.011116000	2.10	gi 392381197	hypothetical protein
0.004181820	2.10	gi 392380602	Co2+/Mg2+ efflux protein ApaG
0.001221770	2.10	gi 392381091	peptide-methionine (R)-S-oxide reductase
0.049896500	2.09	gi 392384281	hypothetical protein
0.044822100	2.07	gi 392381670	hypothetical protein
0.0000958846	2.05	gi 392379107	response regulator

0.015416100	2.05	gi 392383382	ABC transporter permease
0.021401200	2.04	gi 392377809	membrane protein
0.006198470	2.04	gi 392384087	ABC transporter permease
0.010023900	2.01	gi 392380826	16S rRNA maturation RNase YbeY
0.042083700	2.00	gi 392377612	LPS export ABC transporter permease LptG
Downregulated:			
0.000000333	280.78	gi 392382728	ATP-sulfurylase, subunit 2
0.000197195	175.28	gi 392380947	S-adenosylmethionine decarboxylase related
0.000031092	135.29	gi 392378123	hypothetical protein
0.000000031	80.92	gi 392381155	putative ATP-dependent RNA helicase with P-loop hydrolase domain (rhIE gene)
0.001583120	62.09	gi 392382435	agmatine deiminase
0.001249290	61.55	gi 392378810	hypothetical protein
0.0000001281	46.62	gi 392379397	U32 family peptidase
0.0000002801	46.11	gi 392383807	MBL fold hydrolase
0.000004665	42.20	gi 392382729	adenylyl-sulfate kinase
0.0000014392	31.37	gi 392380705	CardD family transcriptional regulator
0.003558820	26.47	gi 392381657	hypothetical protein
0.000000600	25.07	gi 392377600	phospholipid N-methyltransferase
0.0000395915	24.32	gi 392377166	PAS domain-containing sensor histidine kinase
0.0000042043	23.77	gi 392382045	GreA/GreB family elongation factor
0.0000090957	23.42	gi 392379391	hypothetical protein
0.0000018883	20.72	gi 392378114	protein of unknown function
0.001515120	20.23	gi 392379974	serine acetyltransferase
0.000030439	20.14	gi 392378480	dihydronoopterin aldolase
0.0000390647	19.89	gi 392378504	Uptake hydrogenase small subunit precursor (Hydrogenlyase) (Membrane-bound hydrogenase small subunit)
0.0003014880	17.75	gi 392382103	NADH-quinone oxidoreductase subunit M
0.0000374509	17.55	gi 392383591	homoserine O-succinyltransferase
0.000016675	17.39	gi 392382727	phosphoadenosine phosphosulfate reductase
0.0000003583	17.33	gi 392383668	DEAD/DEAH box helicase

0.0003261050	16.85	gi 392382972	flagellar basal body rod modification protein FlgD
0.0002080160	15.64	gi 392383487	Hydrolase
0.004371870	15.33	gi 392378135	quinolinate synthase, B subunit (L-aspartate oxidase)
0.004930370	14.93	gi 392379840	phosphate acetyltransferase
0.0000004597	14.79	gi 392382223	class I poly(R)-hydroxyalkanoic acid synthase
0.0000015153	14.49	gi 392378879	acriflavin resistance protein
0.0000007585	13.54	gi 392378501	Uptake hydrogenase large subunit precursor
0.0000266018	13.11	gi 392381198	hypothetical protein
0.008665380	12.83	gi 392383051	MarR family transcriptional regulator
0.0000006817	12.62	gi 392379914	peptidase M23
0.000059578	12.34	gi 392380526	ornithine decarboxylase
0.001801330	12.13	gi 392383746	exported protein of unknown function
0.0000383610	12.03	gi 392378492	hydrogenase accessory protein HyPB
0.0000359781	11.84	gi 392381074	ATP-binding protein
0.001282220	11.75	gi 392378172	arabinose 5-phosphate isomerase
0.0000007086	11.62	gi 392380737	cysteine synthase A
0.000000448	11.24	gi 392377861	tyrosine-tRNA ligase
0.001108800	10.71	gi 392380755	integral membrane protein linked to a cation pump
0.0000131298	10.54	gi 392382019	cytochrome c oxidase accessory protein CcoG
0.058199200	10.33	gi 392378520	cyclohexadienyl dehydrogenase
0.001448870	10.30	gi 392382073	Isomerase
0.018308400	10.07	gi 392380632	phosphotyrosine protein phosphatase
0.045253300	9.69	gi 392380782	conserved exported protein of unknown function
0.011917800	8.13	gi 392381680	molecular chaperone Tard
0.0006075570	7.93	gi 392380859	oxidoreductase subunit with NAD(P)-binding domain and ferredoxin-like domain
0.004931650	7.70	gi 392381219	hypothetical protein
0.000115090	7.46	gi 392377659	murein L,D-transpeptidase
0.000229543	7.39	gi 392381314	5-aminolevulinate synthase
0.002424620	7.29	gi 392381882	hypothetical protein
0.0000175252	7.28	gi 392383932	hypothetical protein

0.0000010294	6.92	gi 392380396	hypothetical protein
0.0000000581	6.72	gi 392382119	DNA polymerase III subunit alpha
0.002462960	6.68	gi 392378411	multidrug resistance efflux pump (EmrB-like) (fragment), partial
0.045655800	6.63	gi 392379656	cytochrome c
0.0000053252	6.55	gi 392377563	C4-dicarboxylate ABC transporter
0.000006192	6.52	gi 392379928	polyhydroxyalkanoate synthesis repressor
0.0000069422	6.25	gi 392381025	2-oxoglutarate synthase
0.0000263609	6.19	gi 392384345	L-lactate permease
0.0000029256	6.19	gi 392380302	hypothetical protein
0.011233400	5.99	gi 392384484	Tlp1
0.0000610427	5.98	gi 392384449	branched-chain amino acids ABC transporter; ATP-binding component
0.038876800	5.86	gi 392377421	segregation/condensation protein A
0.001063890	5.85	gi 392383636	chitin deacetylase
0.02020208900	5.82	gi 392381172	conserved protein of unknown function; putative CBS domain
0.009079980	5.73	gi 392381842	protein of unknown function, partial
0.0000155148	5.28	gi 392381288	hypothetical protein
0.0000575452	5.28	gi 392380438	NAD-dependent epimerase
0.054997700	5.21	gi 392378730	cell filamentation protein Fic
0.048792800	5.21	gi 392381270	two component sensor histidine kinase; membrane protein
0.009334970	5.17	gi 392378153	putative ABC transporter; ATP-binding protein
0.0000139016	5.06	gi 392377796	GGDEF domain-containing protein
0.0000145821	5.05	gi 392382461	molybdopterin synthase sulfur carrier subunit
0.0000016034	5.04	gi 392380671	23S rRNA (adenine(2503)-C(2))-methyltransferase RlmN
0.0000777834	5.02	gi 392384271	hypothetical protein
0.0000147633	4.98	gi 392381337	oxygen-independent coproporphyrinogen III oxidase
0.043479300	4.96	gi 392380661	cytochrome c biogenesis protein
0.029979600	4.95	gi 392382337	colicin V production protein
0.008587210	4.95	gi 392383653	conserved protein of unknown function
0.0000332752	4.92	gi 392377425	hypothetical protein
0.019249100	4.90	gi 392382224	hypothetical protein

0.000334523	4.89	gi 392378442	ATP synthase
0.032594500	4.80	gi 392377674	3-hydroxybutyrate dehydrogenase
0.011926300	4.79	gi 392381402	methyl-accepting chemotaxis protein (fragment), partial
0.000033417	4.70	gi 392380182	hypothetical protein
0.026319900	4.67	gi 392380574	hypothetical protein
0.004476540	4.66	gi 392378093	plasmid replication protein
0.001832870	4.66	gi 392382998	30S ribosomal protein S14
0.044266200	4.63	gi 392383368	exported protein of unknown function
0.001124000	4.61	gi 392378529	hypothetical protein
0.000452848	4.56	gi 392382957	flagellar motor switch protein FlIM
0.004990500	4.53	gi 392382360	4-hydroxy-tetrahydropicolinate synthase
0.031869800	4.52	gi 392383369	exported protein of unknown function
0.000245656	4.41	gi 392381917	propionyl-CoA synthetase
0.002147920	4.41	gi 392382369	MarR family transcriptional regulator
0.000550045	4.32	gi 392378215	conserved protein of unknown function
0.032029400	4.25	gi 392379146	hypothetical protein
0.000001386	4.23	gi 392381896	hypothetical protein
0.017296100	4.21	gi 392378406	cell division ATP-binding protein FtsE
0.033170300	4.16	gi 392382599	Dehydrogenase
0.011450700	4.06	gi 392377625	transcriptional regulator, MarR family
0.003099480	4.00	gi 392382427	DNA polymerase III subunit delta'
0.0000035605	3.92	gi 392382680	GTP-binding protein
0.020133300	3.91	gi 392378488	hydrogenase expression/formation protein HypE
0.0000002030	3.87	gi 392381026	2-oxoglutarate synthase
0.004523990	3.87	gi 392378113	conserved protein of unknown function
0.006403850	3.83	gi 392380392	dTDP-glucose 4,6-dehydratase
0.000207970	3.82	gi 392381029	peptidase C56
0.000013124	3.80	gi 392379159	hypothetical protein
0.000388121	3.75	gi 392380707	4Fe-4S ferredoxin
0.014273500	3.68	gi 392378514	hypothetical protein

0.055475900	3.66	gi 392379285	hypothetical protein
0.000280339	3.59	gi 392383941	glycine/betaine ABC transporter permease
0.034964500	3.56	gi 392382956	hypothetical protein
0.001109250	3.55	gi 392383630	tRNA (N(6)-L-threonylcarbamoyladenosine(37)-C(2))-methylthiotransferase MtaB
0.012531200	3.55	gi 392381354	flagellar motor switch protein FliG
0.034812300	3.55	gi 392380085	putative transcriptional regulator, TetR family
0.000000491	3.54	gi 392381516	3,4-dihydroxy-2-butanone 4-phosphate synthase
0.0008775040	3.53	gi 392378482	ribonuclease HII
0.0000582151	3.53	gi 392378413	hypothetical protein
0.048352500	3.53	gi 392382856	hypothetical protein
0.014345900	3.52	gi 392380420	UDP-glucose 4-epimerase GalE
0.024031000	3.49	gi 392382967	flagellar assembly protein FlfX
0.002334750	3.47	gi 392379743	2-oxoglutarate decarboxylase, component of the 2-oxoglutarate dehydrogenase complex, thiamin-binding (fragment), partial
0.000072706	3.47	gi 392382164	3-deoxy-8-phosphooctulonate synthase
0.0000204469	3.46	gi 392381674	conserved exported protein of unknown function
0.000533824	3.45	gi 392379395	hypothetical protein
0.001652660	3.44	gi 392382491	polysaccharide biosynthesis protein CapD
0.033792500	3.43	gi 392378373	ABC transporter ATP-binding protein
0.007115310	3.41	gi 392383058	trehalose-phosphatase
0.0000155942	3.40	gi 392380895	DNA polymerase III subunit epsilon
0.0000440652	3.39	gi 392377707	hypothetical protein
0.0001279170	3.39	gi 392378580	Hemolysin
0.001000190	3.37	gi 392377670	response regulator
0.0000566623	3.36	gi 392380911	major outer membrane protein OmaA
0.0000219961	3.36	gi 392377160	lipoyl synthase
0.014801100	3.36	gi 392383594	methyl-accepting chemotaxis protein
0.012496900	3.34	gi 392380573	glycerol-3-phosphate dehydrogenase
0.035280500	3.32	gi 392382309	phosphate transport system regulatory protein PhoU
0.0006443720	3.30	gi 392377420	putative chromosome segregation and condensation protein ScpB

0.0000644385	3.28	gi 392384266	protein of unknown function
0.017010000	3.28	gi 392383891	conserved exported protein of unknown function
0.001293510	3.26	gi 392381007	cell envelope biogenesis protein LolA
0.000481674	3.25	gi 392383631	cell division protein
0.002373180	3.24	gi 392381185	hypothetical protein
0.000567421	3.22	gi 392380047	biotin synthase BioB
0.013865400	3.17	gi 392377205	ABC transporter substrate-binding protein
0.000456120	3.17	gi 392381424	50S ribosomal protein L27
0.023686100	3.14	gi 392380345	aldehyde dehydrogenase
0.038828100	3.13	gi 392379404	ABC transporter ATP-binding protein
0.021700700	3.12	gi 392379179	lipopolysaccharide biosynthesis (fragment), partial
0.019548200	3.10	gi 392382343	ABC transporter permease
0.037197400	3.10	gi 392381721	trehalose-6-phosphate synthase
0.005791190	3.05	gi 392382477	5-formyltetrahydrofolate cyclo-ligase
0.0000228887	3.04	gi 392380684	glycogen synthase
0.014669900	3.03	gi 392380738	hypothetical protein
0.035542600	3.03	gi 392383613	diguanylate cyclase
0.031705900	3.02	gi 392382655	cobyric acid synthase CobbQ
0.0000090819	3.02	gi 392377297	Phasin
0.000075862	3.02	gi 392377613	leucyl aminopeptidase
0.008635960	3.01	gi 392382676	conserved protein of unknown function; putative histidine triad hydrolase domain
0.016241300	3.00	gi 392380924	hypothetical protein
0.003316630	3.00	gi 392383793	Peptidase
0.001851660	2.99	gi 392381227	hypothetical protein
0.0000037227	2.99	gi 392378673	formate acetyltransferase
0.013652200	2.97	gi 392382796	hypothetical protein
0.000202739	2.96	gi 392383170	Farnesyltransferase
0.007888560	2.95	gi 392377409	protein of unknown function
0.000408506	2.95	gi 392383942	proline/glycine betaine ABC transporter ATP-binding protein
0.000302363	2.93	gi 392380904	chromosome partitioning protein

0.0003917940	2.92	gi 392382322	ABC transporter ATP-binding protein
0.014229200	2.91	gi 392378481	adenine DNA methyltransferase
0.002847200	2.88	gi 392382675	cellulose synthase
0.019667000	2.88	gi 392383948	IclR family transcriptional regulator
0.001289110	2.87	gi 392382074	acyl hydratase
0.006738100	2.86	gi 392383135	hypothetical protein
0.052096800	2.85	gi 392381047	heme A synthase
0.015448200	2.83	gi 392378198	exported protein of unknown function
0.007374910	2.81	gi 392377857	TPR repeat-containing protein (fragment), partial
0.001444860	2.80	gi 392383946	conserved protein of unknown function
0.000136233	2.80	gi 392378598	glyoxalase
0.026963500	2.79	gi 392382319	hypothetical protein
0.023596700	2.79	gi 392381577	pyruvate dehydrogenase subunit beta
0.005569600	2.75	gi 392382335	Oxidoreductase
0.000923820	2.75	gi 392377689	precorrin-4 C(11)-methyltransferase
0.000267876	2.74	gi 392378578	1-deoxy-D-xylulose-5-phosphate synthase
0.003500520	2.71	gi 392380790	inorganic pyrophosphatase
0.007900090	2.71	gi 392382712	hypothetical protein
0.019359000	2.70	gi 392380180	conserved exported protein of unknown function
0.004204070	2.70	gi 392381707	cell division topological specificity factor MinE
0.041412800	2.69	gi 392383826	NAD-dependent dehydratase
0.042851300	2.69	gi 392382486	protein TolR
0.005714050	2.69	gi 392383693	3-hydroxyisobutyrate dehydrogenase
0.036263800	2.69	gi 392383200	D-alanine--D-alanine ligase
0.009396690	2.69	gi 392379365	two-component system sensor histidine kinase/response regulator
0.007803200	2.66	gi 392380992	hypothetical protein
0.001644430	2.64	gi 392383652	anti-sigma factor antagonist
0.055567300	2.64	gi 392381308	DNA polymerase V
0.028868600	2.63	gi 392377628	two-component response transcriptional regulator (OmpR family)
0.001172850	2.62	gi 392378500	hydrogenase 2 maturation endopeptidase

0.0000181446	2.60	gi 392382890	DNA primase
0.0000212165	2.60	gi 392380133	hypothetical protein
0.0000486408	2.60	gi 392382612	dienelactone hydrolase
0.0000072973	2.59	gi 392382887	conserved exported protein of unknown function
0.006455470	2.59	gi 392382095	NADH-quinone oxidoreductase subunit E
0.0000246735	2.58	gi 392384251	conserved exported protein of unknown function
0.0000214105	2.58	gi 392378674	sigma-54-dependent Fis family transcriptional regulator
0.014061400	2.55	gi 392381389	bifunctional heptose 7-phosphate kinase/heptose 1-phosphate adenylyltransferase
0.0001309060	2.55	gi 392378749	Nucleotidyltransferase
0.0000508213	2.54	gi 392380269	periplasmic nitrate reductase electron transfer subunit
0.012688300	2.53	gi 392377657	putative Serine-type D-Ala-D-Ala carboxypeptidase
0.0000079536	2.53	gi 392378668	hypothetical protein
0.0000614318	2.53	gi 392381409	hypothetical protein
0.0000012978	2.52	gi 392382912	Oxidoreductase
0.0000467186	2.51	gi 392377581	RNA degradosome polyphosphate kinase
0.018064500	2.51	gi 392377282	hypothetical protein
0.0000018446	2.49	gi 392383752	glutamate dehydrogenase
0.002337300	2.49	gi 392382179	Peroxiredoxin
0.0000588348	2.47	gi 392381575	acetoin catabolism protein X
0.0000275426	2.47	gi 392380760	cytochrome c oxidase, cbb3-type subunit I
0.041576200	2.47	gi 392382279	urease subunit gamma
0.013029200	2.45	gi 392379393	cyclic nucleotide-binding protein
0.0000034428	2.45	gi 392382354	acyl carrier protein
0.00000338477	2.45	gi 392380905	chromosome partitioning protein
0.042095000	2.43	gi 392383617	Rossman fold protein, TIGR00730 family
0.014379500	2.43	gi 392383875	cytochrome ubiquinol oxidase subunit I
0.0000001568	2.42	gi 392380759	cytochrome c oxidase, cbb3-type subunit II
0.0000005514	2.42	gi 392381656	ribonucleotide-diphosphate reductase subunit alpha
0.0000356044	2.42	gi 392381344	DTW domain-containing protein
0.005197870	2.41	gi 392381484	phosphoribosylformylglycinaimidine synthase

0.0000121271	2.41	gi 392381453	indolepyruvate/phenylpyruvate decarboxylase
0.0007758980	2.40	gi 392379297	serine/threonine-protein kinase PknK, partial
0.005893300	2.40	gi 392377603	Guanylate kinase (GMP kinase)
0.000018168	2.38	gi 392380184	methylamine utilization protein MauG
0.001344850	2.37	gi 392381441	protein of unknown function
0.0000315650	2.36	gi 392380757	cytochrome c oxidase, cbb3-type subunit III
0.045154800	2.35	gi 392379293	hypothetical protein
0.008700430	2.35	gi 392380100	mannonate dehydratase
0.001605940	2.35	gi 392383005	30S ribosomal protein S3
0.0000033777	2.35	gi 392383001	MULTISPECIES: 50S ribosomal protein L14
0.014776200	2.34	gi 392382862	hybrid sensor histidine kinase/response regulator
0.010168200	2.33	gi 392381400	fructose-6-phosphate aldolase
0.057832500	2.33	gi 392379184	hypothetical protein
0.005599090	2.32	gi 392384040	multidrug ABC transporter ATP-binding protein
0.0000015865	2.32	gi 392383203	cell division protein FtsZ
0.0002481750	2.32	gi 392377888	conserved exported protein of unknown function
0.043434200	2.32	gi 392382408	GNAT family acetyltransferase
0.0000472745	2.32	gi 392382348	50S ribosomal protein L9
0.0000123500	2.31	gi 392380821	methionine adenosyltransferase
0.026121200	2.31	gi 392381579	shikimate 5-dehydrogenase
0.002687610	2.30	gi 392378842	protein phosphatase
0.034859900	2.30	gi 392377680	ABC transporter ATP-binding protein
0.036095600	2.27	gi 392383643	chemotaxis response regulator CheY
0.0000620454	2.27	gi 392383006	50S ribosomal protein L22
0.009891110	2.27	gi 392380237	oxalyl-CoA decarboxylase
0.026914300	2.25	gi 392382263	GntR family transcriptional regulator
0.002863150	2.25	gi 392383191	UDP-N-acetylmuramoyl-L-alanyl-D-glutamate-2,6-diaminopimelate ligase
0.012002100	2.24	gi 392382000	protein of unknown function
0.007378820	2.24	gi 392380667	methyl-accepting chemotaxis protein
0.053706500	2.23	gi 392377208	methyltransferase type 11

0.0000573927	2.23	gi 392380270	nitrate reductase catalytic subunit
0.0008729290	2.22	gi 392382589	VacJ-like lipoprotein
0.001647930	2.21	gi 392379818	protein of unknown function, partial
0.044394900	2.18	gi 392380647	histidine/lysine/arginine/ornithine ABC transporter ATP-binding protein HisP
0.017756600	2.18	gi 392378454	flagellar assembly protein FliH
0.011909000	2.18	gi 392380565	hypothetical protein
0.007515340	2.18	gi 392381994	polyphosphate kinase 2
0.059777400	2.17	gi 392379303	ABC transporter substrate-binding protein
0.038102800	2.17	gi 392379677	ABC transporter substrate-binding protein
0.0000958196	2.17	gi 392378778	formyltetrahydrofolate deformylase
0.0000898233	2.17	gi 392378409	multidrug transporter
0.003514330	2.16	gi 392383940	glycine/betaine ABC transporter substrate-binding protein
0.0006722860	2.16	gi 392383162	2-isopropylmalate synthase
0.0000055904	2.16	gi 392382725	sulfite reductase
0.0006334790	2.15	gi 392382875	hypothetical protein
0.0001027240	2.12	gi 392381035	ferredoxin--NADP(+) reductase
0.0002076440	2.12	gi 392377825	molybdenum cofactor biosynthesis protein
0.001462070	2.11	gi 392380516	sn-glycerol-3-phosphate ABC transporter ATP-binding protein
0.0033533680	2.11	gi 392378204	hypothetical protein
0.010261700	2.11	gi 392381232	malate synthase A
0.058035200	2.10	gi 392383017	MULTISPECIES: 30S ribosomal protein S12
0.0000536558	2.10	gi 392381284	diguanylate cyclase
0.005692760	2.10	gi 392382162	CTP synthetase
0.025971600	2.09	gi 392378575	acetoin utilization protein
0.0000865918	2.08	gi 392382489	peptidoglycan-associated lipoprotein
0.039665100	2.08	gi 392383734	GCN5-related N-acetyltransferase
0.049252800	2.07	gi 392382111	quinolinolate synthetase
0.036014100	2.07	gi 392382140	citrate synthase (fragment), partial
0.0000083744	2.07	gi 392381924	conserved protein of unknown function

0.004929290	2.07	gi 392377778	Ribonuclease
0.000994305	2.06	gi 392381024	Rubrerythrin
0.006311620	2.05	gi 392383750	DNA-binding response regulator
0.013166700	2.05	gi 392381796	cobyric acid a,c-diamide synthase
0.036651000	2.05	gi 392381292	16S rRNA processing protein RimM
0.009727000	2.05	gi 392379032	mandelate racemase
0.025150700	2.04	gi 392384531	chemotaxis protein X
0.012553100	2.03	gi 392380456	Phosphomannomutase
0.002909120	2.02	gi 392380938	colanic acid biosynthesis glycosyltransferase WcaL
0.002031190	2.02	gi 392380902	tRNA uridine(34) 5-carboxymethylaminomethyl synthesis enzyme MnmG
0.003226310	2.02	gi 392382439	ABC transporter ATP-binding protein
0.014001300	2.02	gi 392378453	flagellar motor switch protein FlN
0.004370470	2.01	gi 392381368	hypothetical protein
0.000330154	2.00	gi 392382122	30S ribosomal subunit protein S2

FONTE: a autora (2018).

TABLE 5 - KEGG PATHWAY CLASSIFICATION FOR DIFFERENTIAL PROTEINS IN *A. brasiliense* FP2 IN RESPONSE TO NITROGEN LIMITATION.

Pathway Codes	Azospirillum Sp245 Pathways	Number of Proteins:		Total Number in Pathway:	% of coverage FP2 high N	% of coverage FP2 low N
		FP2 high N	FP2 low N			
abs00010	Glycolysis / Gluconeogenesis	2	0	47	4.26	0.00
abs00020	Citrate cycle (TCA cycle)	4	1	36	11.11	2.78
abs00030	Pentose phosphate pathway	1	0	22	4.55	0.00
abs00040	Pentose and glucuronate interconversions	1	1	25	4.00	4.00
abs00051	Fructose and mannose metabolism	2	1	26	7.69	3.85
abs00052	Galactose metabolism	1	0	20	5.00	0.00
abs00053	Ascorbate and aldarate metabolism	1	1	11	9.09	9.09
abs00061	Fatty acid biosynthesis	0	0	28	0.00	0.00
abs00071	Fatty acid degradation	0	0	24	0.00	0.00
abs00072	Synthesis and degradation of ketone bodies	1	0	7	14.29	0.00
abs00130	Ubiquinone and other terpenoid-quinone biosynthesis	0	1	12	0.00	8.33
abs00190	Oxidative phosphorylation	9	1	55	16.36	1.82
abs00220	Arginine biosynthesis	2	1	23	8.70	4.35
abs00230	Purine metabolism	9	1	94	9.57	1.06
abs00240	Pyrimidine metabolism	5	3	53	9.43	5.66
abs00250	Alanine, aspartate and glutamate metabolism	2	1	26	7.69	3.85
abs00260	Glycine, serine and threonine metabolism	1	0	33	3.03	0.00
abs00261	Monobactam biosynthesis	3	0	14	21.43	0.00
abs00270	Cysteine and methionine metabolism	6	0	41	14.63	0.00
abs00280	Valine, leucine and isoleucine degradation	1	3	40	2.50	7.50
abs00281	Geraniol degradation	0	0	5	0.00	0.00
abs00290	Valine, leucine and isoleucine biosynthesis	1	1	21	4.76	4.76
abs00300	Lysine biosynthesis	2	1	17	11.76	5.88
abs00310	Lysine degradation	1	1	19	5.26	5.26
abs00311	Penicillin and cephalosporin biosynthesis	0	0	2	0.00	0.00

abs00330	Arginine and proline metabolism	3	2	37	8.11	5.41
abs00332	Carbapenem biosynthesis	0	0	2	0.00	0.00
abs00340	Histidine metabolism	0	1	18	0.00	5.56
abs00350	Tyrosine metabolism	0	0	11	0.00	0.00
abs00360	Phenylalanine metabolism	0	1	14	0.00	7.14
abs00361	Chlorocyclohexane and chlorobenzene degradation	0	0	5	0.00	0.00
abs00362	Benzoate degradation	0	0	28	0.00	0.00
abs00364	Fluorobenzoate degradation	0	0	5	0.00	0.00
abs00380	Tryptophan metabolism	1	1	23	4.35	4.35
abs00400	Phenylalanine, tyrosine and tryptophan biosynthesis	1	1	18	5.56	5.56
abs00401	Novobiocin biosynthesis	1	0	4	25.00	0.00
abs00410	beta-Alanine metabolism	0	2	17	0.00	11.76
abs00430	Taurine and hypotaurine metabolism	0	1	17	0.00	5.88
abs00440	Phosphonate and phosphinate metabolism	0	0	4	0.00	0.00
abs00450	Selenocompound metabolism	2	0	14	14.29	0.00
abs00460	Cyanoamino acid metabolism	0	1	11	0.00	9.09
abs00471	D-Glutamine and D-glutamate metabolism	0	0	3	0.00	0.00
abs00472	D-Arginine and D-ornithine metabolism	0	0	1	0.00	0.00
abs00473	D-Alanine metabolism	1	0	5	20.00	0.00
abs00480	Glutathione metabolism	2	2	26	7.69	7.69
abs00500	Starch and sucrose metabolism	3	0	33	9.09	0.00
abs00520	Amino sugar and nucleotide sugar metabolism	7	1	49	14.29	2.04
abs00521	Streptomycin biosynthesis	1	0	8	12.50	0.00
abs00523	Polyketide sugar unit biosynthesis	1	0	5	20.00	0.00
abs00525	Acarbose and validamycin biosynthesis	1	0	2	50.00	0.00
abs00540	Lipopolysaccharide biosynthesis	3	0	16	18.75	0.00
abs00550	Peptidoglycan biosynthesis	2	0	21	9.52	0.00
abs00561	Glycerolipid metabolism	0	0	12	0.00	0.00
abs00562	Inositol phosphate metabolism	0	1	4	0.00	25.00

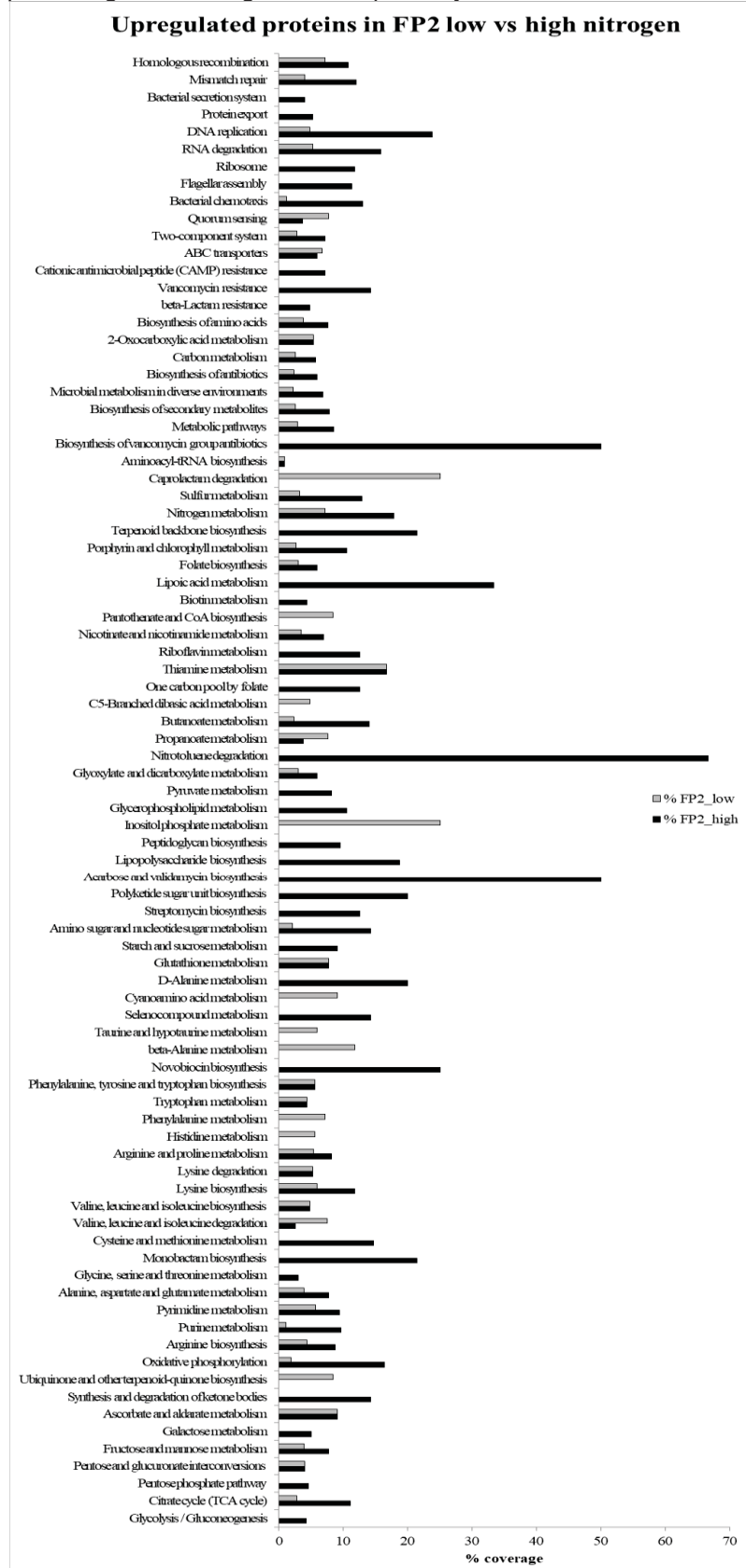
abs00564	Glycerophospholipid metabolism	2	0	19	19	10.53	0.00
abs00590	Arachidonic acid metabolism	0	0	1	1	0.00	0.00
abs00592	alpha-Linolenic acid metabolism	0	0	1	1	0.00	0.00
abs00600	Sphingolipid metabolism	0	0	3	3	0.00	0.00
abs00620	Pyruvate metabolism	5	0	61	8.20	0.00	0.00
abs00621	Dioxin degradation	0	0	2	0.00	0.00	0.00
abs00623	Toluene degradation	0	0	3	0.00	0.00	0.00
abs00624	Polycyclic aromatic hydrocarbon degradation	0	0	3	0.00	0.00	0.00
abs00625	Chloroalkane and chloroalkene degradation	0	0	17	0.00	0.00	0.00
abs00626	Naphthalene degradation	0	0	5	0.00	0.00	0.00
abs00627	Aminobenzoate degradation	0	0	15	0.00	0.00	0.00
abs00630	Glyoxylate and dicarboxylate metabolism	4	2	67	5.97	2.99	0.00
abs00633	Nitrotoluene degradation	2	0	3	66.67	0.00	0.00
abs00640	Propanoate metabolism	2	4	53	3.77	7.55	0.00
abs00643	Styrene degradation	0	0	6	0.00	0.00	0.00
abs00650	Butanoate metabolism	6	1	43	13.95	2.33	0.00
abs00660	C5-Branched dibasic acid metabolism	0	1	21	0.00	4.76	0.00
abs00670	One carbon pool by folate	2	0	16	12.50	0.00	0.00
abs00680	Methane metabolism	0	0	47	0.00	0.00	0.00
abs00710	Carbon fixation in photosynthetic organisms	0	0	20	0.00	0.00	0.00
abs00730	Thiamine metabolism	2	2	12	16.67	16.67	0.00
abs00740	Riboflavin metabolism	1	0	8	12.50	0.00	0.00
abs00750	Vitamin B6 metabolism	0	0	7	0.00	0.00	0.00
abs00760	Nicotinate and nicotinamide metabolism	2	1	29	6.90	3.45	0.00
abs00770	Pantothenate and CoA biosynthesis	0	2	24	0.00	8.33	0.00
abs00780	Biotin metabolism	1	0	23	4.35	0.00	0.00
abs00785	Lipoic acid metabolism	1	0	3	33.33	0.00	0.00
abs00790	Folate biosynthesis	2	1	34	5.88	2.94	0.00
abs00860	Porphyrin and chlorophyll metabolism	4	1	38	10.53	2.63	0.00
abs00900	Terpenoid backbone biosynthesis	3	0	14	21.43	0.00	0.00

abs00903	Limonene and pinene degradation	0	0	6	0.00	0.00
abs00906	Carotenoid biosynthesis	0	0	2	0.00	0.00
abs00909	Sesquiterpenoid and triterpenoid biosynthesis	0	0	1	0.00	0.00
abs00910	Nitrogen metabolism	5	2	28	17.86	7.14
abs00920	Sulfur metabolism	8	2	62	12.90	3.23
abs00930	Capro lactam degradation	0	1	4	0.00	25.00
abs00970	Aminoacyl-tRNA biosynthesis	1	1	111	0.90	0.90
abs01040	Biosynthesis of unsaturated fatty acids	0	0	13	0.00	0.00
abs01053	Biosynthesis of siderophore group nonribosomal peptides	0	0	4	0.00	0.00
abs01054	Nonribosomal peptide structures	0	0	1	0.00	0.00
abs01055	Biosynthesis of vancomycin group antibiotics	1	0	2	50.00	0.00
abs01100	Metabolic pathways	70	24	826	8.47	2.91
abs01110	Biosynthesis of secondary metabolites	25	8	321	7.79	2.49
abs01120	Microbial metabolism in diverse environments	22	7	324	6.79	2.16
abs01130	Biosynthesis of antibiotics	15	6	255	5.88	2.35
abs01200	Carbon metabolism	9	4	159	5.66	2.52
abs01210	2-Oxocarboxylic acid metabolism	2	2	37	5.41	5.41
abs01212	Fatty acid metabolism	0	0	40	0.00	0.00
abs01220	Degradation of aromatic compounds	0	0	15	0.00	0.00
abs01230	Biosynthesis of amino acids	10	5	132	7.58	3.79
abs01501	beta-Lactam resistance	1	0	21	4.76	0.00
abs01502	Vancomycin resistance	1	0	7	14.29	0.00
abs01503	Cationic antimicrobial peptide (CAMP) resistance	1	0	14	7.14	0.00
abs02010	ABC transporters	17	19	285	5.96	6.67
abs02020	Two-component system	13	5	182	7.14	2.75
abs02024	Quorum sensing	8	17	219	3.65	7.76
abs02030	Bacterial chemotaxis	11	1	85	12.94	1.18
abs02040	Flagellar assembly	7	0	62	11.29	0.00
abs02060	Phosphotransferase system (PTS)	0	0	10	0.00	0.00

abs03010	Ribosome	8	0	68	68	11.76	0.00
abs03018	RNA degradation	3	1	19	19	15.79	5.26
abs03020	RNA polymerase	0	0	4	4	0.00	0.00
abs03030	DNA replication	5	1	21	21	23.81	4.76
abs03060	Protein export	1	0	19	19	5.26	0.00
abs03070	Bacterial secretion system	1	0	25	25	4.00	0.00
abs03410	Base excision repair	0	0	17	17	0.00	0.00
abs03420	Nucleotide excision repair	0	0	12	12	0.00	0.00
abs03430	Mismatch repair	3	1	25	25	12.00	4.00
abs03440	Homologous recombination	3	2	28	28	10.71	7.14

FONTE: a autora (2018).

FIGURE 15 - KEGG PATHWAY CLASSIFICATION FOR UPREGULATED PROTEINS IN *A. brasiliense* FP2 IN RESPONSE TO NITROGEN LIMITATION. Bars indicate the percentage of coverage for each pathway.



FONTE: a autora (2018).

TABLE 6 - DIFFERENTIAL PROTEINS BETWEEN *A. brasilense* *ntrC* LOW AND HIGH NITROGEN.

t-test p-value	Fold change	Protein IDs	Protein
Upregulated:			
4.81969E-06	45.68	gi 392380219	protein of unknown function
0.000309716	40.86	gi 392382300	transcriptional regulator
0.000267749	39.21	gi 392382401	amino acid ABC transporter substrate-binding protein
0.0087887	25.40	gi 392382711	sodium-translocating pyrophosphatase
2.11682E-05	24.72	gi 392381648	putative short chain dehydrogenase
0.0311138	22.98	gi 392381231	site-specific tyrosine recombinase
0.000495456	20.12	gi 392382419	putative thiosulfate sulfurtransferase
3.96225E-05	19.64	gi 392382531	conserved hypothetical protein; beta-Ig-H3/Fasciclin domain
0.000103853	17.46	gi 392381931	histidine kinase
0.0261707	13.48	gi 392380541	3-phosphoglycerate dehydrogenase
7.09958E-06	13.19	gi 392383847	acetylpolyamine amidohydrolase
1.04943E-06	12.47	gi 392380217	hypothetical protein
3.01953E-05	12.00	gi 392380220	uracil phosphoribosyltransferase (fragment), partial
2.89003E-06	11.68	gi 392380023	putative oligopeptide ABC transporter (substrate-binding protein)
0.000427061	10.50	gi 392379840	phosphate acetyltransferase
1.29797E-05	9.29	gi 392383277	putative serine protein kinase
0.000318639	8.54	gi 392382271	D-amino acid dehydrogenase small subunit
0.0156242	7.30	gi 392383950	N-formylglutamate deformylase
0.000502584	7.23	gi 392383275	SpoVR family protein
0.00066395	7.08	gi 392383259	Aldolase
1.27264E-06	7.00	gi 392383276	conserved protein of unknown function; putative coiled-coil domain
0.000189407	6.77	gi 392382167	pyrroloquinoline quinone biosynthesis protein PqqD
0.00241479	6.14	gi 392380218	conserved hypothetical protein
0.00839657	5.98	gi 392381379	methyltransferase UbiE
0.00177683	5.68	gi 392383848	putative acetolactate synthase large subunit
0.00568224	5.60	gi 392380240	haloacid dehalogenase
0.0384281	5.56	gi 392378783	2-aminobenzoate-CoA ligase
0.00595984	5.52	gi 392377487	N-acetyltransferase GCN5
0.0430085	5.50	gi 392380178	hypothetical protein
0.00316317	5.30	gi 392378303	hypothetical protein
6.98549E-06	5.29	gi 392383841	peptide ABC transporter substrate-binding protein
0.0135412	5.13	gi 392378729	putative hemerythrin-like, metal-binding (MHR) protein (bacteriohemerythrin)
0.0149885	4.97	gi 392377642	hypothetical protein
0.0124711	4.81	gi 392381044	putative endonuclease/exonuclease/phosphatase
2.79733E-06	4.71	gi 392381440	methyl-accepting chemotaxis protein
0.0025993	4.64	gi 392383212	Lipoprotein
0.00208524	4.64	gi 392381995	hypothetical protein
0.0182822	4.59	gi 392377838	CoA transferase
0.0357966	4.56	gi 392378851	hypothetical protein
0.0574603	4.55	gi 392380095	glucose dehydrogenase precursor
0.00860715	4.45	gi 392377401	phytoene dehydrogenase

0.0160929	4.23	gi 392379394	hypothetical protein
0.00122834	4.22	gi 392382168	pyrroloquinoline quinone biosynthesis protein C
0.000299132	4.18	gi 392383844	ABC transporter ATP-binding protein
0.00414384	4.14	gi 392383067	ABC transporter ATP-binding protein
0.00033178	4.11	gi 392378882	IMP dehydrogenase
0.000746744	4.06	gi 392377868	conserved protein of unknown function
0.0134024	4.04	gi 392379742	putative Oxoglutarate dehydrogenase (succinyl-transferring)
0.00222764	3.95	gi 392381384	trans-aconitate 2-methyltransferase
0.00117266	3.75	gi 392379121	regulatory lipoprotein
0.00847676	3.64	gi 392384245	ABC transporter substrate-binding protein
0.000110281	3.62	gi 392378830	NAD(P)H:quinone oxidoreductase
0.00792277	3.62	gi 392380533	peptidase S16
0.00183057	3.34	gi 392378875	glycosyl transferase
0.0070573	3.30	gi 392381310	putative trypsin-like serine protease
0.000635092	3.24	gi 392380011	hypothetical protein
0.000237859	3.22	gi 392383349	elongation factor G
0.0424222	3.21	gi 392382649	hypothetical protein
0.00198606	3.15	gi 392383243	putative histidine kinase
0.0241494	3.12	gi 392382509	histidine kinase
0.00257558	3.07	gi 392381670	hypothetical protein
0.0548794	2.99	gi 392382663	protein of unknown function
0.000665472	2.97	gi 392379758	mononuclear molybdenum enzyme YedY
7.00709E-05	2.92	gi 392381718	4-alpha-hydroxy-tetrahydropterin dehydratase (fragment), partial
0.0426814	2.90	gi 392380688	LysR family transcriptional regulator
0.0302654	2.88	gi 392381380	inorganic triphosphatase
0.000585338	2.88	gi 392377806	methyl-accepting chemotaxis protein
0.0309575	2.86	gi 392380102	putative transcriptional regulator, GntR Family
0.0598386	2.85	gi 392382452	RNA polymerase factor sigma-32
0.0478035	2.81	gi 392380889	uroporphyrinogen decarboxylase
0.0210017	2.80	gi 392377227	putative Allophanate hydrolase, subunit 2 (modular protein)
0.000786186	2.80	gi 392381091	peptide-methionine (R)-S-oxide reductase
0.00947536	2.78	gi 392382325	branched chain amino acid ABC transporter substrate-binding protein
0.0117917	2.77	gi 392379968	Agmatinase
0.0518124	2.74	gi 392383364	serine/threonine protein kinase
0.000119249	2.70	gi 392378246	2-methylisocitrate lyase
0.0312023	2.69	gi 392377162	competence damage-inducible protein A
0.00127905	2.68	gi 392380040	putative ABC transporter (substrate-binding protein)
0.00453486	2.67	gi 392380245	conserved exported protein of unknown function
0.0213428	2.66	gi 392377887	ferrous iron transporter B
0.0477669	2.64	gi 392378884	hypothetical protein
0.0126753	2.64	gi 392384445	FMN reductase
0.00531627	2.63	gi 392381709	conserved protein of unknown function
0.00642602	2.62	gi 392382776	phytoene desaturase
0.0048505	2.59	gi 392378001	lipolytic protein G-D-S-L family

0.014354	2.56	gi 392380026	acetylornithine deacetylase
0.059087	2.54	gi 392380013	thiazole synthase
0.000469964	2.50	gi 392383348	2-dehydropantoate 2-reductase
0.00450328	2.49	gi 392380623	DNA-binding response regulator
0.0408984	2.48	gi 392382133	hypothetical protein
0.00133935	2.48	gi 392381651	Lysophospholipase
4.47562E-05	2.48	gi 392384279	3-isopropylmalate dehydrogenase
1.23954E-05	2.48	gi 392379843	2-deoxy-D-gluconate 3-dehydrogenase
0.016511	2.47	gi 392382082	malonyl-CoA decarboxylase
0.0212773	2.46	gi 392381691	two-component sensor histidine kinase
0.00662116	2.45	gi 392378424	conserved protein of unknown function; putative coiled-coil and glutathione domains
0.0115464	2.44	gi 392382571	alpha-amylase
0.0024471	2.37	gi 392377219	multidrug efflux system, subunit A (AcrB family) (fragment), partial
0.0480553	2.36	gi 392379319	aspartate aminotransferase family protein
0.000360245	2.36	gi 392382537	hypothetical protein
0.0483422	2.31	gi 392380602	Co2+/Mg2+ efflux protein ApaG
0.0556723	2.31	gi 392378329	Arginase
0.00767297	2.31	gi 392382745	cobalamin biosynthesis protein CobD
0.0105799	2.30	gi 392384019	2-keto-4-methylthiobutyrate aminotransferase
0.000606798	2.30	gi 392379938	Phosphohydrolase
0.0336078	2.30	gi 392377791	two-component response regulator
0.0200966	2.28	gi 392382605	C4-dicarboxylate ABC transporter
0.00311037	2.26	gi 392382568	3'(2'),5'-bisphosphate nucleotidase CysQ
0.0448238	2.25	gi 392378831	glutathione-dependent reductase
0.0119328	2.24	gi 392383846	Zn-dependent hydrolase
0.0543218	2.24	gi 392383292	putative Ubiquinone biosynthesis protein COQ7
0.00121741	2.23	gi 392379933	beta-ketoacyl-ACP reductase
0.033168	2.23	gi 392380609	putative Sensor protein/two-component sensor histidine kinase
0.00148568	2.22	gi 392380717	histidine kinase
0.00749542	2.22	gi 392383018	dimethylglycine dehydrogenase
0.0248805	2.21	gi 392377298	hypothetical protein
0.000824017	2.21	gi 392380646	amino acid ABC transporter substrate-binding protein
0.0156284	2.19	gi 392381659	septum formation initiator
0.00727991	2.19	gi 392382533	putative ATP-dependent DNA helicase
0.000127458	2.19	gi 392378128	OHCU decarboxylase
0.0239793	2.18	gi 392383604	hypothetical protein
0.0133653	2.18	gi 392379065	hypothetical protein
0.000759565	2.18	gi 392381311	Oxidoreductase
0.04271	2.17	gi 392383963	pyridoxal 4-dehydrogenase
0.0215087	2.17	gi 392383176	hypothetical protein
0.00984977	2.16	gi 392378999	enoyl-CoA hydratase
0.0189193	2.16	gi 392382329	membrane protein
0.000778356	2.15	gi 392380229	formyl-CoA transferase
0.00814614	2.15	gi 392383346	DNA-binding ferritin-like protein
0.00910048	2.14	gi 392380713	putative ATP-dependent DNA/RNA helicase

0.00448392	2.13	gi 392380932	hypothetical protein
0.0535427	2.11	gi 392382592	hypothetical protein
0.000979893	2.11	gi 392383643	chemotaxis response regulator CheY
0.00444812	2.10	gi 392381647	(R)-hydratase
0.000952586	2.09	gi 392378668	hypothetical protein
0.00290873	2.08	gi 392381213	diguanylate cyclase
0.000486239	2.07	gi 392380221	ABC transporter substrate-binding protein
0.0573744	2.07	gi 392381269	two-component system response regulator
0.0126951	2.07	gi 392377644	S-(hydroxymethyl)glutathione dehydrogenase/class III alcohol dehydrogenase
0.0457976	2.07	gi 392382126	phosphatidate cytidylyltransferase
0.00401497	2.07	gi 392382239	oxidoreductase (fragment), partial
0.0192623	2.06	gi 392378787	Imidazolonepropionase
0.000281909	2.06	gi 392383995	pyrroline-5-carboxylate reductase
0.000809258	2.04	gi 392380559	protease HtpX
0.0152716	2.04	gi 392383990	hypothetical protein
0.0019209	2.04	gi 392382988	N-formylglutamate amidohydrolase
0.0101589	2.03	gi 392384516	citrate (Si)-synthase
0.0249357	2.03	gi 392381754	nitrogenase iron protein
0.00556599	2.01	gi 392382040	hypothetical protein
0.00409236	2.01	gi 392380237	oxalyl-CoA decarboxylase
0.000347418	2.01	gi 392381058	cytochrome c biogenesis protein CcsA
0.0416275	2.01	gi 392379762	Ketodeoxygluconokinase
0.011406	2.00	gi 392378782	putative transcriptional regulator, MarR family
0.0549244	2.00	gi 392377746	response regulator

Downregulated:

0.00319798	95.26	gi 392382728	ATP-sulfurylase, subunit 2
3.39987E-06	80.86	gi 392378123	hypothetical protein
8.36677E-07	74.35	gi 392380705	CarD family transcriptional regulator
0.000151472	40.05	gi 392382045	GreA/GreB family elongation factor
0.000285778	32.31	gi 392377600	phospholipid N-methyltransferase
4.57193E-06	29.95	gi 392381155	putative ATP-dependent RNA helicase with P-loop hydrolase domain (rhIE gene)
6.82445E-05	20.36	gi 392381198	hypothetical protein
0.0427876	16.00	gi 392380596	ABC transporter ATP-binding protein
8.29522E-05	13.68	gi 392382887	conserved exported protein of unknown function
6.8958E-07	13.52	gi 392381576	acetoin:2,6-dichlorophenolindophenol oxidoreductase subunit alpha
6.61606E-05	12.13	gi 392380085	putative transcriptional regulator, TetR family
8.29228E-05	11.40	gi 392378135	quinolinate synthase, B subunit (L-aspartate oxidase)
0.00796798	10.27	gi 392384149	ribonucleotide-diphosphate reductase subunit alpha
6.72375E-06	10.24	gi 392381577	pyruvate dehydrogenase subunit beta
0.0261891	9.31	gi 392378480	dihydronoopterin aldolase
0.000282965	9.18	gi 392383807	MBL fold hydrolase
1.38853E-05	8.64	gi 392380526	ornithine decarboxylase
0.0418081	7.87	gi 392382135	lactoylglutathione lyase
0.000120835	7.76	gi 392379914	peptidase M23

0.012921	6.87	gi 392378138	quinolinate synthetase
0.00370522	6.86	gi 392381292	16S rRNA processing protein RimM
0.0227558	6.77	gi 392377710	putative branched-chain amino acid ABC transporter, ATP-binding component (livG-like)
0.000862933	6.65	gi 392380521	two-component sensor histidine kinase, partial
0.000180677	6.10	gi 392378114	protein of unknown function
0.0548117	5.89	gi 392377569	peptidase S41
0.0198878	5.88	gi 392383320	putative 23S rRNA (guanosine-2'-O)-methyltransferase (RlmB-like)
0.000259952	5.74	gi 392378093	plasmid replication protein
0.000400635	5.58	gi 392383668	DEAD/DEAH box helicase
0.00946577	5.58	gi 392382617	AsnC family transcriptional regulator
0.0001801	5.40	gi 392382729	adenylyl-sulfate kinase
0.000882266	5.34	gi 392377861	tyrosine-tRNA ligase
0.0257211	5.32	gi 392382074	acyl dehydratase
0.00596045	5.19	gi 392381633	protein of unknown function
0.0386275	5.10	gi 392379713	Agmatinase
0.00251796	5.09	gi 392380737	cysteine synthase A
0.000487222	4.97	gi 392383754	putative Regulator of nucleoside diphosphate kinase
0.0255617	4.97	gi 392380606	aminoacyl-tRNA deacylase
0.0100634	4.76	gi 392378201	heme oxygenase
0.0142988	4.49	gi 392382343	ABC transporter permease
0.017887	4.40	gi 392378413	hypothetical protein
0.00796275	4.39	gi 392384473	Acetyltransferase
0.00593128	4.35	gi 392379184	hypothetical protein
0.000725826	4.33	gi 392380573	glycerol-3-phosphate dehydrogenase
1.08087E-05	4.28	gi 392381516	3,4-dihydroxy-2-butanone 4-phosphate synthase
0.00299016	4.28	gi 392382998	30S ribosomal protein S14
0.0143256	4.01	gi 392377599	hypothetical protein
0.000431709	3.97	gi 392382810	ATP-dependent acyl-CoA ligase
0.00942575	3.84	gi 392383875	cytochrome ubiquinol oxidase subunit I
0.000518505	3.77	gi 392382427	DNA polymerase III subunit delta'
0.000019957	3.77	gi 392380358	hypothetical protein
0.0432993	3.72	gi 392384040	multidrug ABC transporter ATP-binding protein
0.00703208	3.72	gi 392379397	U32 family peptidase
0.010845	3.68	gi 392378520	cyclohexadienyl dehydrogenase
0.0365579	3.62	gi 392378373	ABC transporter ATP-binding protein
0.0102165	3.54	gi 392382727	phosphoadenosine phosphosulfate reductase
0.0036489	3.52	gi 392383932	hypothetical protein
0.000078301	3.39	gi 392380671	23S rRNA (adenine(2503)-C(2))-methyltransferase RlmN
0.0350921	3.36	gi 392377678	ABC transporter permease
0.00373921	3.25	gi 392383733	asparagine synthetase B
0.0299682	3.23	gi 392377888	conserved exported protein of unknown function
0.01724	3.19	gi 392383734	GCN5-related N-acetyltransferase
0.00093197	3.16	gi 392381579	shikimate 5-dehydrogenase
0.00351099	3.11	gi 392378879	acriflavin resistance protein
0.00131571	3.11	gi 392380992	hypothetical protein

0.00398691	3.10	gi 392381882	hypothetical protein
0.00624624	3.10	gi 392377165	tRNA-dihydrouridine synthase
0.0091136	3.08	gi 392382712	hypothetical protein
0.053506	3.04	gi 392377625	transcriptional regulator, MarR family
0.00441321	3.03	gi 392381896	hypothetical protein
0.0492137	3.02	gi 392382956	hypothetical protein
0.0183001	3.01	gi 392377498	conserved protein of unknown function
0.0365516	3.01	gi 392381971	rod shape-determining protein MreC
0.000924562	2.99	gi 392379303	ABC transporter substrate-binding protein
0.00205392	2.99	gi 392381424	50S ribosomal protein L27
0.0521031	2.97	gi 392383630	tRNA (N(6)-L-threonylcarbamoyladenosine(37)-C(2))-methylthiotransferase MtaB
0.00360297	2.94	gi 392384345	L-lactate permease
0.0143002	2.94	gi 392381402	methyl-accepting chemotaxis protein (fragment), partial
0.0050996	2.92	gi 392378401	ribonucleoside-diphosphate reductase, adenosylcobalamin-dependent
0.00713496	2.88	gi 392382482	Holliday junction ATP-dependent DNA helicase RuvA
0.0323783	2.84	gi 392382875	hypothetical protein
0.0187246	2.79	gi 392382119	DNA polymerase III subunit alpha
0.00442816	2.74	gi 392379926	putative Glutathionylspermidine synthase
0.00151704	2.73	gi 392377166	PAS domain-containing sensor histidine kinase
0.0112616	2.71	gi 392380182	hypothetical protein
0.00262664	2.66	gi 392382223	class I poly(R)-hydroxyalkanoic acid synthase
0.0561385	2.65	gi 392383087	protein of unknown function
0.0195818	2.65	gi 392383058	trehalose-phosphatase
0.00653029	2.65	gi 392379928	polyhydroxyalkanoate synthesis repressor
0.0135896	2.58	gi 392382477	5-formyltetrahydrofolate cyclo-ligase
0.0548526	2.53	gi 392379827	pyruvate formate-lyase 1-activating enzyme
0.0464794	2.50	gi 392382919	antibiotic biosynthesis monooxygenase
0.000912371	2.45	gi 392380396	hypothetical protein
0.0152991	2.43	gi 392378215	conserved protein of unknown function
0.00278163	2.42	gi 392377786	conserved protein of unknown function; TfuA core domain
0.0130006	2.42	gi 392378178	PTS IIA-like nitrogen-regulatory protein PtsN
0.00342379	2.36	gi 392383170	Farnesyltransferase
0.0252014	2.36	gi 392381558	RND superfamily drug exporter
0.024483	2.36	gi 392381441	protein of unknown function
0.00973137	2.35	gi 392379912	hypothetical protein
0.00117421	2.34	gi 392382797	flagellar motor protein MotA
0.00145764	2.34	gi 392382612	dienelactone hydrolase
0.00120961	2.33	gi 392377402	superoxide dismutase
0.000517165	2.33	gi 392377160	lipoyl synthase
0.0349333	2.33	gi 392378353	protein of unknown function
0.045928	2.32	gi 392382866	MFS transporter
0.00552336	2.29	gi 392381656	ribonucleotide-diphosphate reductase subunit alpha
0.047012	2.29	gi 392381288	hypothetical protein
0.0100238	2.24	gi 392383942	proline/glycine betaine ABC transporter ATP-binding protein

0.000476243	2.21	gi 392378437	chemotaxis protein CheR
0.0273302	2.21	gi 392381207	ornithine cyclodeaminase
0.0487361	2.20	gi 392379323	glutathione S-transferase
0.000831748	2.19	gi 392381859	alcohol dehydrogenase
0.0151998	2.16	gi 392381498	Bacterioferritin
0.0123123	2.11	gi 392383940	glycine/betaine ABC transporter substrate-binding protein
0.000310419	2.07	gi 392381546	hypothetical protein
0.0153187	2.07	gi 392377295	conserved protein of unknown function; putative Radical SAM domain
0.0459123	2.05	gi 392377297	Phasin
0.0354822	2.05	gi 392378794	S-adenosyl-L-methionine (SAM)-dependent methyltransferase PhcB
0.000160625	2.05	gi 392377628	two-component response transcriptional regulator (OmpR family)
0.0455761	2.04	gi 392380047	biotin synthase BioB
0.00090184	2.02	gi 392382309	phosphate transport system regulatory protein PhoU
0.0420938	2.01	gi 392378812	GGDEF domain-containing protein

FONTE: a autora (2018).

TABLE 7 - CANDIDATE PROTEINS TO BE INDUCED BY NtrC.

t-test p-value	Fold change	Protein IDs	Protein name
6.24384E-06	1050.53	gi 392383070	urea ABC transporter substrate-binding protein
6.84436E-07	371.82	gi 392379716	dihydroorotate
1.16334E-05	314.07	gi 392378005	amino acid ABC transporter substrate-binding protein
2.16826E-05	252.95	gi 392377482	ABC transporter substrate-binding protein
2.70573E-05	218.62	gi 392381052	hypothetical protein
4.51513E-07	203.49	gi 392379722	ABC-type branched-chain amino acid transport systems, periplasmic component
2.21816E-09	200.21	gi 392383795	ABC transporter substrate-binding protein
0.00025353	129.56	gi 392380681	ammonia channel protein AmtB
6.7752E-06	83.73	gi 392383066	ABC transporter ATP-binding protein
2.81529E-06	53.73	gi 392383069	branched-chain amino acid ABC transporter permease
0.00636932	50.34	gi 392382462	molybdopterin molybdenumtransferase MoeA
6.99517E-05	50.20	gi 392380332	amino acid ABC transporter substrate-binding protein
2.09728E-06	48.41	gi 392378105	nitrate ABC transporter substrate-binding protein
6.30232E-08	46.31	gi 392380304	branched-chain amino acid ABC transporter substrate-binding protein
2.22341E-06	46.30	gi 392381762	azoreductase
9.10616E-05	39.96	gi 392384046	ABC transporter substrate-binding protein
4.88648E-07	36.85	gi 392384045	N-carbamoylsarcosine amidase
2.71765E-06	28.54	gi 392384043	amidase (fragment), partial
1.70096E-06	25.56	gi 392379721	gamma-glutamyltransferase (fragment), partial
0.000207576	18.50	gi 392384044	putative Glutamyl-tRNA(Gln) amidotransferase subunit A (Glu-ADT subunit A)
0.000159649	17.52	gi 392382764	transcriptional regulator, LuxR/FixJ family
0.000304346	15.77	gi 392381692	dioxygenase
8.00219E-06	15.37	gi 392378468	histidine kinase
0.000182887	14.46	gi 392381713	conserved protein of unknown function

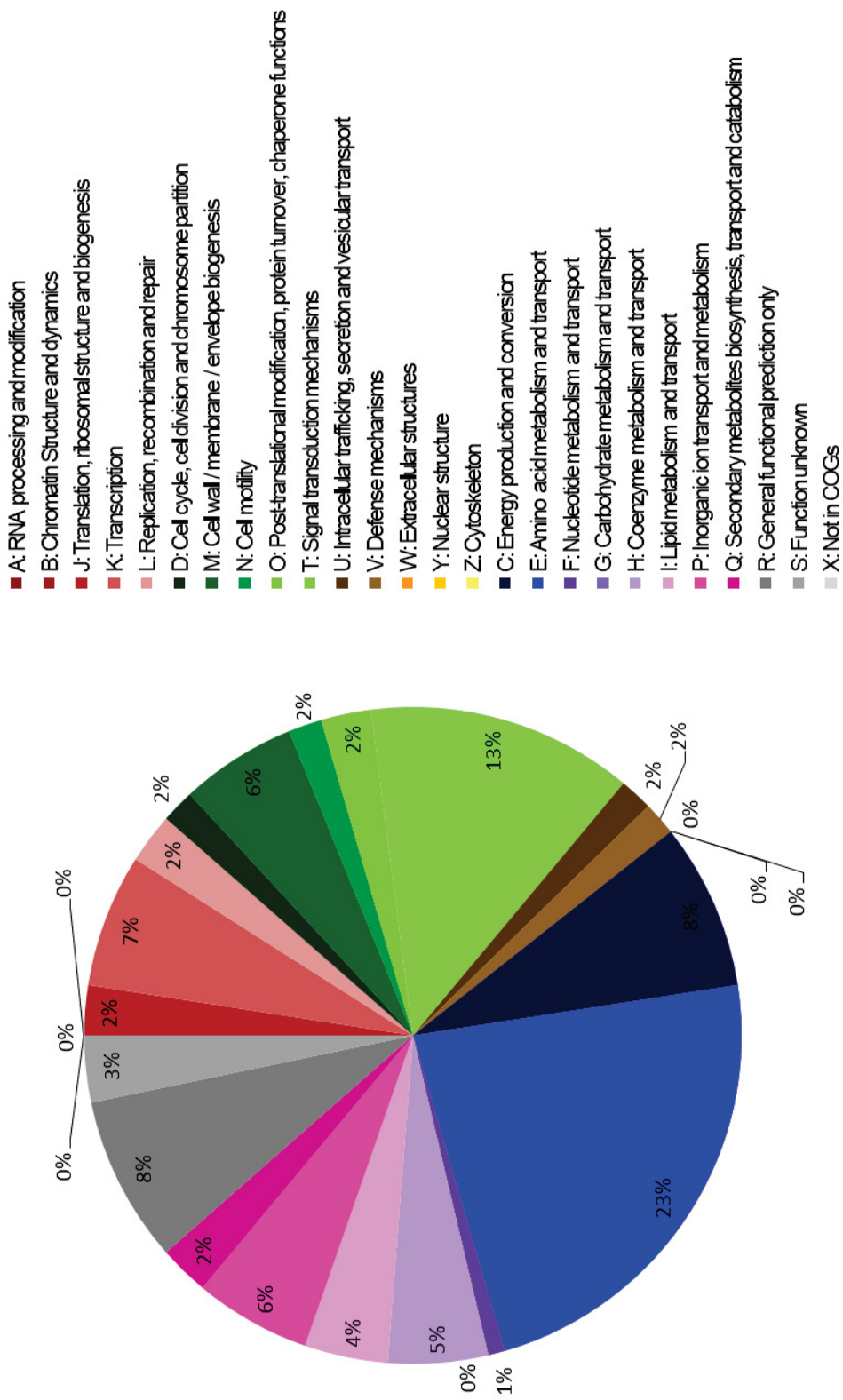
2.77071E-07	14.21	gi 392379894	peptide ABC transporter substrate-binding protein
0.000768467	13.80	gi 392379730	hypothetical protein
0.00020771	12.68	gi 392379972	ABC transporter substrate-binding protein
0.023523	11.30	gi 392381633	protein of unknown function
0.0200972	10.75	gi 392377569	peptidase S41
0.000208807	10.59	gi 392378731	X-Pro dipeptidyl-peptidase
4.79385E-06	10.48	gi 392379728	carbon monoxide dehydrogenase - medium chain adenosylcobalamin-dependent methylmalonyl-CoA mutase small subunit (MCM-beta)(N-terminal fragment), partial
0.0588802	9.26	gi 392384143	
4.76545E-05	9.07	gi 392381702	phosphate starvation protein PhoH
0.00262417	8.80	gi 392377486	Asp/Glu/hydantoin racemase
2.18787E-07	8.47	gi 392382138	glutathione S-transferase
2.44582E-07	7.92	gi 392381004	nitrogen regulatory protein P-II 1 (GlnZ)
0.0119273	7.85	gi 392383323	peptide methionine sulfoxide reductase
0.0216532	7.39	gi 392380333	hypothetical protein
0.000462504	6.76	gi 392378644	NMT1/THI5 like domain protein
0.00684389	6.66	gi 392380055	prolipoprotein diacylglycerol transferase
0.00455372	6.56	gi 392383857	Crp/Fnr family transcriptional regulator
0.0068382	6.52	gi 392383840	putative acetylornithine deacetylase or succinyl-diaminopimelate desuccinylase
9.74746E-05	6.26	gi 392379726	ABC transporter ATP-binding protein
0.0335966	6.16	gi 392381341	hypothetical protein
0.0408321	6.00	gi 392383137	hypothetical protein
0.000656394	5.92	gi 392379727	carbon monoxide dehydrogenase - large chain
0.000145688	5.22	gi 392379136	branched-chain amino acid ABC transporter substrate-binding protein
0.000259523	4.99	gi 392377481	spermidine/putrescine ABC transporter ATPase
0.0312655	4.82	gi 392383672	glyoxalase
0.000469853	4.80	gi 392378378	quercetin 2,3-dioxygenase
0.00010883	4.74	gi 392381217	hypothetical protein
0.000300399	4.62	gi 392379403	copper ABC transporter, permease component (modular protein)
0.00208318	4.57	gi 392379740	putative periplasmic mannitol-binding protein; putative TRAP-T transport system, dctP subunit (plasmid)
0.0148505	4.54	gi 392383727	aspartate aminotransferase family protein
0.000015684	4.43	gi 392377615	hybrid sensor histidine kinase/response regulator
4.87214E-06	4.26	gi 392378815	hypothetical protein
0.00584744	4.09	gi 392381501	glycosyl transferase family 51
0.0401827	4.00	gi 392380777	spermidine/putrescine ABC transporter, substrate-binding component
0.0288902	3.94	gi 392381749	putative Methyl-accepting chemotaxis protein with multiple PAS domains
2.49693E-06	3.92	gi 392378456	putative transcriptional regulator, HTH-XRE family
0.0345516	3.79	gi 392381228	CBS domain-containing protein
7.60116E-05	3.71	gi 392381934	anthranilate synthase
0.00455032	3.60	gi 392378104	nitrate ABC transporter permease
0.00427135	3.53	gi 392379744	acyl-CoA dehydrogenase
0.0405045	3.51	gi 392381471	transcriptional regulator
0.0296195	3.38	gi 392379387	transcriptional regulator

0.036026	3.36	gi 392382481	crossover junction endodeoxyribonuclease
1.68548E-05	3.34	gi 392377167	nitrogen regulation protein NR(I) (NtrC)
0.0355184	3.32	gi 392383224	transcriptional activator, LuxR/FixJ family
0.0234075	3.27	gi 392380209	hypothetical protein
0.0103023	3.18	gi 392382384	carbon monoxide dehydrogenase
0.000192568	3.17	gi 392380014	thiamine biosynthesis protein ThiS
0.0335072	3.14	gi 392382089	transcriptional regulator
3.19003E-06	3.07	gi 392383726	methylmalonate-semialdehyde dehydrogenase (acylating)
0.00278557	3.06	gi 392383241	hybrid sensor histidine kinase/response regulator, partial
0.051125	3.02	gi 392381386	histidine kinase
0.000845249	2.95	gi 392378699	type VI secretion protein
0.000466139	2.93	gi 392379971	putative sperimidine/putrescine transport protein (ABC superfamily, atp_bind)
0.0366553	2.90	gi 392383954	polar amino acid ABC transporter ATP-binding protein
6.93437E-05	2.87	gi 392378151	long-chain-fatty-acid--CoA ligase
1.35816E-05	2.87	gi 392383934	organic hydroperoxide resistance protein, OsmC superfamily
0.00816736	2.80	gi 392382621	glutamine--fructose-6-phosphate aminotransferase
1.22005E-05	2.78	gi 392381791	acyl-CoA dehydrogenase
0.010354	2.77	gi 392378148	succinyl-diaminopimelate desuccinylase
0.050366	2.75	gi 392379195	LysR family transcriptional regulator
0.00659888	2.71	gi 392380988	heat-inducible transcriptional repressor HrcA
0.000017291	2.61	gi 392382708	transcription antitermination factor NusB
0.000259588	2.51	gi 392382255	phosphomethylpyrimidine synthase ThiC
0.00377644	2.48	gi 392380015	glycine oxidase
0.00611672	2.47	gi 392379802	heptosyltransferase
0.00101024	2.44	gi 392377447	ABC transporter substrate-binding protein
0.0473192	2.41	gi 392379924	exported protein of unknown function
0.00935521	2.40	gi 392381410	RNA pyrophosphohydrolase - NUDIX
0.00235508	2.39	gi 392377740	TIGR02302 family protein
9.44335E-05	2.39	gi 392384473	acetyltransferase
0.00323078	2.38	gi 392380620	two-component sensor histidine kinase
0.00298173	2.37	gi 392382683	membrane protein/Type II secretion system (T2SS), protein N
0.0101851	2.34	gi 392378036	hypothetical protein
0.000693348	2.28	gi 392379049	protein of unknown function
0.0368967	2.26	gi 392383849	3-keto-5-aminohexanoate cleavage protein
0.000131985	2.17	gi 392383998	putative Metallo-hydrolase/oxidoreductase superfamily protein; Beta-lactamase-like
0.00321479	2.17	gi 392377639	NUDIX hydrolase
6.54447E-05	2.14	gi 392382791	alcohol dehydrogenase
0.00459054	2.13	gi 392377389	single-stranded DNA-binding protein
0.0111116	2.10	gi 392381197	hypothetical protein
0.0498965	2.09	gi 392384281	hypothetical protein
0.000958846	2.05	gi 392379107	response regulator
0.0154161	2.05	gi 392383382	ABC transporter permease
0.0214012	2.04	gi 392377809	membrane protein omp
0.00619847	2.04	gi 392384087	ABC transporter permease

0.0100239	2.01	gi 392380826	16S rRNA maturation RNase YbeY
0.0420837	2.00	gi 392377612	LPS export ABC transporter permease LptG

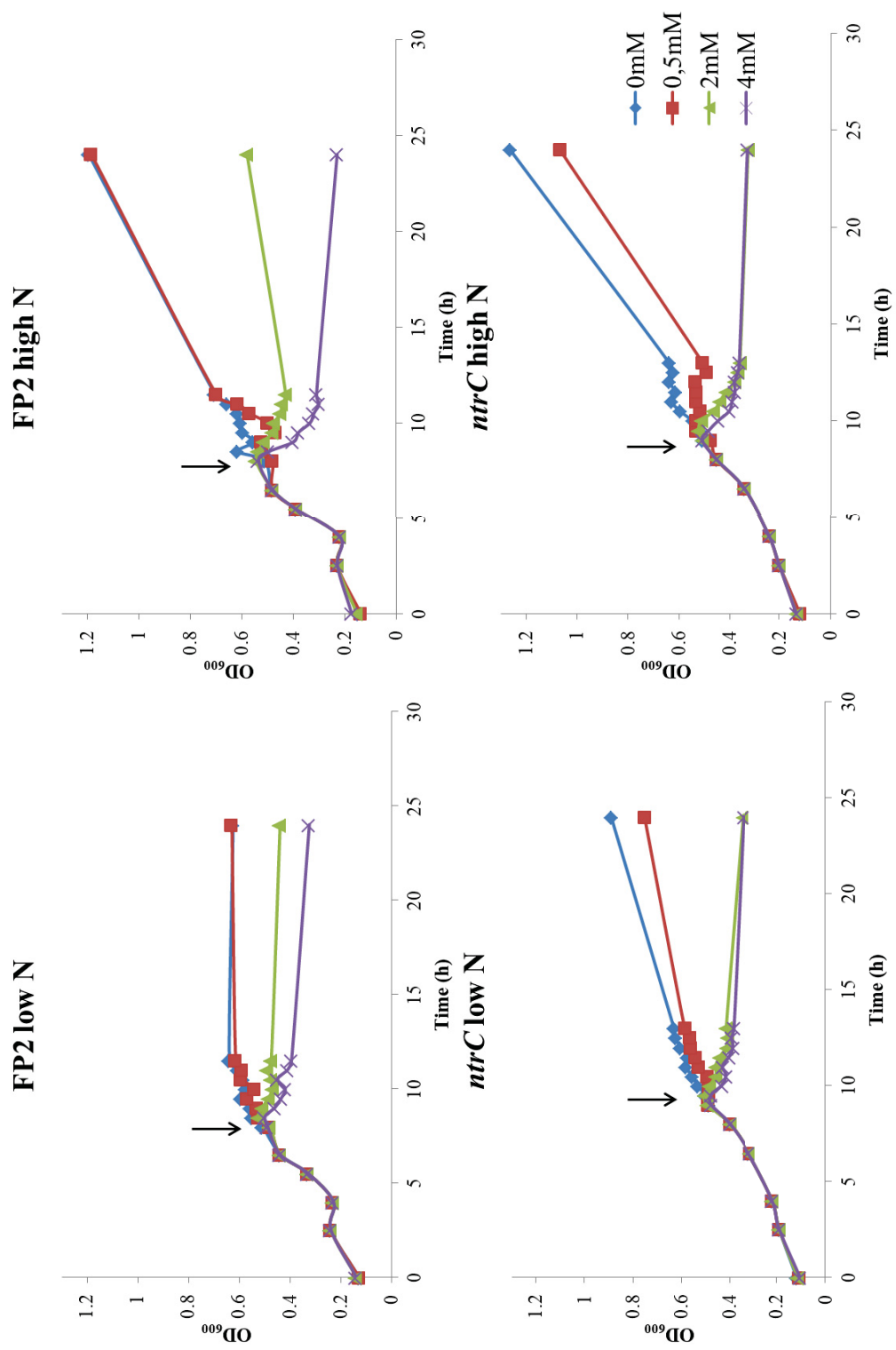
FONTE: a autora (2018).

FIGURE 16 - COG CLASSIFICATION FOR PUTATIVE PROTEINS REGULATED BY NtrC.



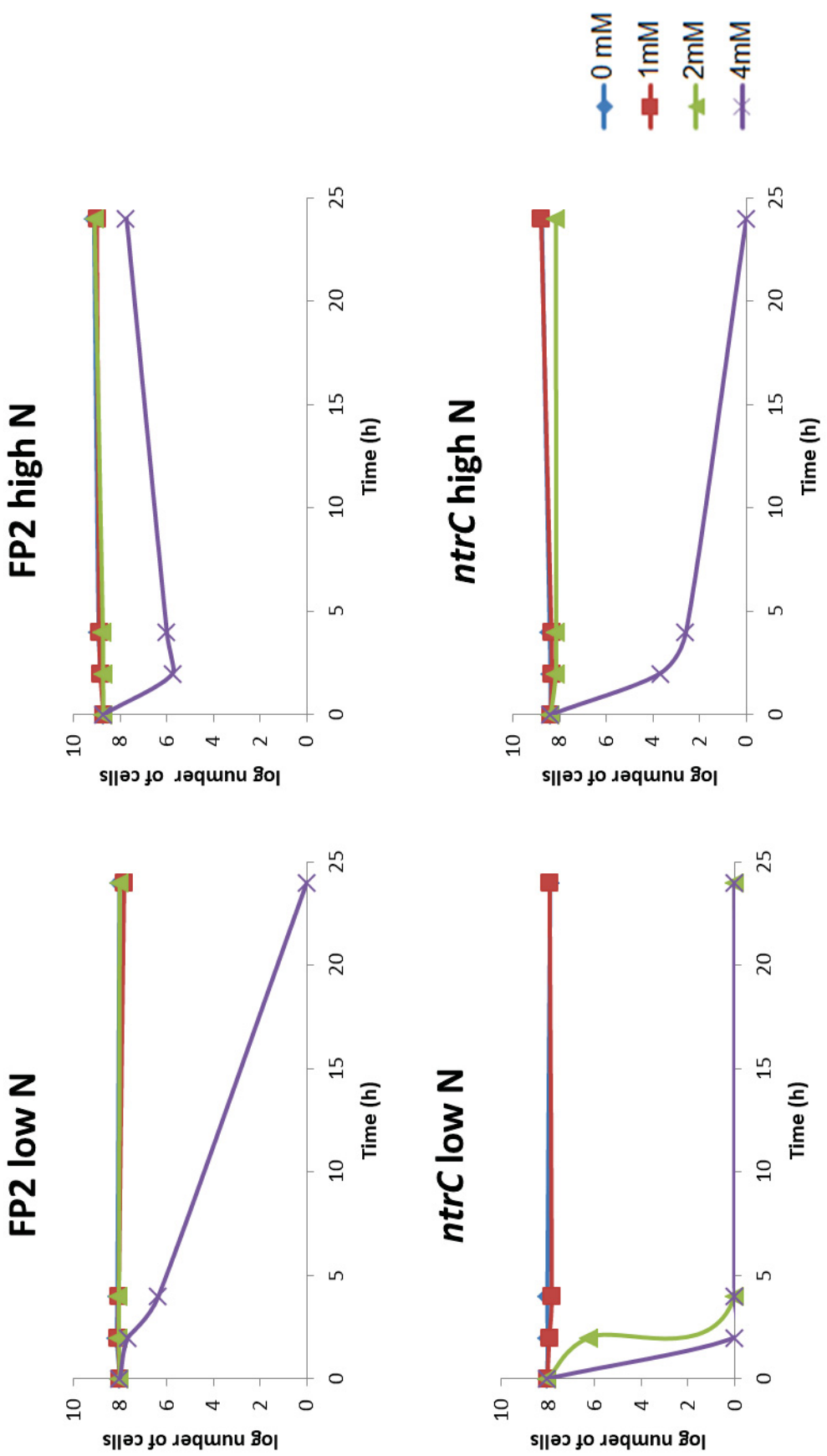
FONTE: a autora (2018).

FIGURE 17 - GROWTH CURVE UNDER DIFFERENT CONCENTRATIONS OF H_2O_2 BASED ON OD₆₀₀. The arrows indicate the point when H_2O_2 was added.



FONTE: a autora (2018).

FIGURE 18 - GROWTH CURVE UNDER DIFFERENT CONCENTRATIONS OF H_2O_2 BASED ON CFU COUNT.



FONTE: a autora (2018).

TABLE 8 - NtrC REGULATION CANDIDATES INVOLVED IN THE QUORUM SENSING PATHWAY .

FC	ID	Protein
2.44	gi 392377447	ABC transporter substrate-binding protein
4.99	gi 392377481	spermidine/putrescine ABC transporter ATPase
252.95	gi 392377482	ABC transporter substrate-binding protein
200.21	gi 392383795	ABC transporter substrate-binding protein
39.96	gi 392384046	ABC transporter substrate-binding protein
5.22	gi 392379136	branched-chain amino acid ABC transporter substrate-binding protein
203.49	gi 392379722	ABC-type branched-chain amino acid transport systems, periplasmic component
6.26	gi 392379726	ABC transporter ATP-binding protein
14.21	gi 392379894	peptide ABC transporter substrate-binding protein
2.93	gi 392379971	putative spermidine/putrescine transport protein (ABC superfamily, atp_bind)
12.68	gi 392379972	ABC transporter substrate-binding protein
46.31	gi 392380304	branched-chain amino acid ABC transporter substrate-binding protein
50.20	gi 392380332	amino acid ABC transporter substrate-binding protein

FONTE: a autora (2018).

TABLE 9 - NtrC REGULATION CANDIDATES INVOLVED IN THE OXIDATIVE STRESS RESPONSE .

t-test p value	FC	Protein IDs	Proteína
2.19E-07	8.47	gi 392382138	glutathione S-transferase (GstA)
0.0119273	7.85	gi 392383323	peptide methionine sulfoxide reductase (Msra)
0.011116	2.10	gi 392381197	hypothetical protein - Redox-sensitive bicupin YhaK, pirin superfamily
0.00010883	4.74	gi 392381217	hypothetical protein -pirin family (YhaK)
0.00935521	2.40	gi 392381410	RNA pyrophosphohydrolase - NUDIX (NudH)
0.000304346	15.77	gi 392381692	dioxygenase
2.22E-06	46.30	gi 392381762	azoreductase (AzoR)
0.000469853	4.80	gi 392378378	queretin 2,3-dioxogenase - pirin family (YhaK)
0.00321479	2.17	gi 392377639	NUDIX hydrolase
1.36E-05	2.87	gi 392383934	organic hydroperoxide resistance protein, OsmC superfamily (Ohr)
1.70E-06	25.56	gi 392379721	gamma-glutamyltransferase (fragment), partial

FONTE: a autora (2018).

TABLE 10 - TOTAL METABOLITES, RETENTION TIMES AND ABUNDANCES IN EACH TREATMENT AND TRIPPLICATES.

Compound	Retention time(min)	<i>m/z</i>	Abundances											
			FP2 high N (1)	FP2 high N (2)	FP2 high N (3)	FP2 low N (1)	FP2 low N (2)	FP2 low N (3)	ntrC high N (1)	ntrC high N (2)	ntrC high N (3)	ntrC low N (1)	ntrC low N (2)	ntrC low N (3)
Unknown	9.1335	156.2	1.56	1.41	1.39	2.25	1.46	1.69	2.38	2.04	1.99	2.13	3.13	3.16
Unknown	9.1559	158.2	16.96	13.12	10.77	32.22	15.16	16.75	19.93	21.04	22.50	21.85	30.34	31.67
Boric Acid, O,O,O-TMS	9.204	221.1	37.89	23.28	21.25	61.83	28.74	29.01	50.85	49.40	37.95	39.98	77.72	70.81
Unknown	9.3044	191.1	2.04	1.24	1.14	3.26	1.50	1.56	2.63	2.56	2.00	2.05	3.93	3.64
Unknown	9.3993	155.1	0.31	0.25	0.21	0.56	0.30	0.34	0.36	0.38	0.45	0.39	0.58	0.60
Unknown	9.4068	155.2	0.31	0.25	0.21	0.56	0.30	0.34	0.36	0.39	0.45	0.39	0.58	0.60
Unknown	9.8666	243.9	0.05	0.01	0.00	0.08	0.04	0.05	0.00	0.09	0.12	0.08	0.10	0.05
Unknown	9.9969	172.1	0.51	0.32	0.23	0.32	0.23	0.22	0.00	0.00	0.00	0.00	0.00	0.00
Unknown	10.0525	244	0.16	0.06	0.00	0.50	0.10	0.07	0.00	0.21	0.24	0.10	0.30	0.23
Propanoic Acid, 2-(methoxyimino)- trimethylsilyl ester	10.2763	174.1	0.38	0.38	0.25	0.47	0.32	0.15	0.48	0.19	0.26	0.05	0.62	0.59
Unknown	10.2858	174.1	0.38	0.38	0.25	0.47	0.32	0.15	0.48	0.19	0.26	0.05	0.62	0.59
4-HYDROXYPYRIDI NE,O-TMS	10.2966	152.1	0.65	0.62	0.81	0.65	0.57	0.83	0.98	0.75	0.58	1.09	0.97	0.92
Lactic Acid, O,O- TMS	10.4648	191.1	110.06	107.72	103.37	199.80	119.35	126.41	126.62	125.77	119.96	128.06	186.43	166.64
Unknown	10.7476	186.2	0.03	0.02	0.02	0.06	0.03	0.04	0.07	0.06	0.03	0.07	0.10	0.11
Unknown	10.7788	173.1	0.94	0.68	0.49	0.09	0.06	0.10	0.15	0.07	0.02	0.05	0.05	0.00
Norvaline, O-TMS	11.1098	156.1	0.09	0.09	0.08	0.00	0.00	0.00	0.06	0.03	0.04	0.00	0.00	0.00
L-Alanine, N,O- TMS	11.2238	190.1	1.12	0.74	0.81	0.76	0.42	0.46	1.04	1.15	0.95	0.25	0.30	0.31
Disiloxane, Hexamethyl	11.2706	204.1	0.52	0.48	0.44	1.47	0.44	0.36	0.61	0.73	0.77	0.93	0.66	1.10
Unknown	11.276	204.1	0.52	0.48	0.44	1.47	0.44	0.36	0.61	0.73	0.77	0.93	0.66	1.10

Tris(trimethylsilyl) hydroxylamine	11.6117	249.1	0.72	0.65	0.66	0.76	0.58	0.53	1.04	0.93	0.98	0.72	1.37	1.35
Unknown	11.807	232.1	0.11	0.09	0.08	0.18	0.11	0.13	0.12	0.13	0.10	0.09	0.17	0.18
Unknown	11.8789	220.1	1.10	0.79	1.06	1.21	0.85	1.20	0.81	0.75	0.57	0.84	0.97	0.90
Unknown	12.1909	191.1	171.88	201.38	215.73	165.40	166.15	218.67	307.50	271.04	326.92	274.08	207.71	246.74
Pentasioxane Dodecamethyl	12.214	369.1	1.63	1.75	1.53	2.00	1.49	1.81	1.80	1.97	2.04	2.20	1.76	1.53
Oxalic Acid TMS	12.2696	219.2	0.37	0.42	0.44	0.36	0.32	0.44	0.60	0.53	0.64	0.57	0.43	0.51
Ethylbis(trimethylsilyl)amine	12.3835	174.1	0.32	0.35	0.45	0.12	0.28	0.34	0.47	0.35	0.22	0.29	0.33	0.28
Heptanoic Acid TMS	12.4256	187.1	0.61	0.38	0.39	0.76	0.43	0.38	0.46	0.57	0.50	0.28	0.55	0.65
Unknown	12.5334	188.2	0.68	0.65	0.52	0.39	0.51	0.63	0.85	0.69	0.46	1.11	0.95	0.93
Unknown	12.5626	218.1	0.39	0.32	0.21	0.40	0.14	0.10	0.09	0.26	0.38	0.06	0.12	0.05
Unknown	12.8162	205.1	1.79	1.29	1.07	1.66	0.71	0.75	0.89	1.06	1.72	0.42	0.63	0.35
Ethanol Amine, N,O,O-TMS	12.8725	174.1	4.74	5.04	3.32	5.52	4.10	4.17	2.09	4.24	6.06	1.24	2.20	0.90
L-Valine, N-(trimethylsilyl)-, trimethylsilyl ester	13.1994	218.1	1.68	1.56	1.73	0.21	0.15	0.17	1.66	1.26	0.81	0.03	0.02	0.03
Unknown	13.3127	158	0.12	0.12	0.06	0.03	0.03	0.02	0.01	0.03	0.05	0.00	0.00	0.00
Unknown	13.3181	158	0.12	0.12	0.06	0.03	0.03	0.02	0.01	0.03	0.04	0.00	0.00	0.00
Unknown	13.4449	159.2	0.37	0.31	0.31	0.06	0.07	0.05	0.08	0.05	0.03	0.04	0.04	0.07
Unknown	13.5012	233.2	0.27	0.27	0.30	0.09	0.11	0.11	0.25	0.24	0.29	0.25	0.16	0.23
Unknown	13.5311	159.1	0.61	0.51	0.59	0.06	0.03	0.05	0.10	0.08	0.04	0.04	0.04	0.06
Unknown	13.5589	336.1	0.94	0.95	1.08	0.20	0.37	0.46	0.94	0.53	0.27	0.29	0.34	0.29
Unknown	13.9353	155.1	0.34	0.06	0.01	0.61	0.08	0.03	0.03	0.20	0.24	0.05	0.13	0.08
Benzoic Acid, O-TMS	13.997	179.1	0.39	0.18	0.16	0.44	0.22	0.14	0.25	0.39	0.33	0.20	0.42	0.30
Glycerol, 3 TMS	14.0493	205.1	4.13	2.57	1.80	5.77	2.74	2.34	2.50	2.91	2.93	1.01	1.30	1.15
Phosphoric Acid, O,O-TMS	14.092	299.1	109.39	47.16	20.60	54.98	37.75	15.45	5.69	27.51	31.41	1.79	6.04	4.82
Ethanolamine	14.1388	174.2	10.91	9.70	8.22	12.02	7.77	7.63	7.00	10.11	9.53	3.54	4.96	3.64

(3TMS)										
L-Isoleucine, N,O-TMS	14.5321	158.2	2.00	1.81	1.88	0.55	0.40	0.48	1.66	1.79
Unknown	14.5755	219.1	0.19	0.17	0.09	0.01	0.03	0.10	0.08	0.05
Unknown	14.581	219.1	0.19	0.17	0.09	0.01	0.03	0.10	0.08	0.05
Unknown	14.6949	219.2	0.75	0.82	0.73	0.14	0.14	0.17	0.61	0.58
Proline (2TMS)	14.7315	216	0.04	0.03	0.03	0.00	0.00	0.03	0.01	0.01
Glycine (3TMS)	14.8394	174.1	3.15	2.79	2.76	1.84	1.84	1.78	2.90	2.63
Succinic Acid 2 TMS	14.8543	247.1	2.58	2.71	2.79	2.01	2.11	2.72	1.41	1.08
Uracil, O,O-TMS	15.3257	241.1	2.18	1.97	1.73	0.37	0.47	0.61	1.23	1.00
Unknown	15.3318	185	0.24	0.30	0.43	0.09	0.18	0.26	0.49	0.26
Unknown	15.3385	184.1	2.02	2.53	3.71	0.92	1.67	2.25	4.36	2.24
L-Serine, N,O,O-TMS	15.5569	204.1	0.52	0.61	0.65	0.27	0.24	0.19	0.74	0.58
Nonanoic Acid TMS	15.7272	215.1	0.23	0.05	0.06	0.04	0.06	0.05	0.08	0.10
L-Alanine, N,N,O-TMS	15.7767	188.1	0.30	0.38	0.52	0.05	0.18	0.23	1.13	0.78
Unknown	15.8743	306.1	0.20	0.14	0.18	0.18	0.28	0.29	0.05	0.08
Unknown	15.9113	306.2	0.20	0.15	0.18	0.18	0.28	0.29	0.05	0.08
L-Threonine, N,O,O-TMS	15.9903	218.1	0.57	0.63	0.72	0.26	0.22	0.27	0.67	0.59
Unknown	16.1497	175.1	0.08	0.08	0.09	0.01	0.10	0.12	0.12	0.06
Unknown	17.1535	350.2	0.21	0.14	0.13	0.17	0.15	0.17	0.15	0.11
Decanoic acid (1TMS)	17.3027	229.1	0.20	0.04	0.05	0.01	0.04	0.03	0.05	0.06
Citramalic Acid, O,O,O-TMS	17.4566	247.1	0.30	0.26	0.25	0.04	0.05	0.06	0.10	0.08
Malic Acid, O,O,O-TMS	17.5936	233.2	0.11	0.12	0.11	0.04	0.03	0.03	0.08	0.06
Niacin, O-TMS	17.8921	179.1	0.48	0.44	0.33	0.11	0.14	0.17	0.33	0.23
L-Aspartic acid, N,O,O-TMS	18.1342	232.1	0.28	0.29	0.30	0.05	0.06	0.06	0.40	0.38

L-Methionine, N,O-TMS	18.278	176.1	0.38	0.34	0.33	0.16	0.19	0.13	0.36	0.25	0.22	0.02	0.04	0.07
Pyroglutamic acid (2TMS)	18.36	156.1	1.33	1.77	1.97	0.65	0.82	0.95	5.22	3.86	2.57	0.86	0.78	1.01
Unknown	18.5906	288.2	0.05	0.06	0.10	0.01	0.04	0.05	0.10	0.06	0.02	0.04	0.07	0.04
Unknown	18.5954	288.2	0.05	0.06	0.10	0.01	0.04	0.05	0.10	0.06	0.02	0.04	0.07	0.04
Glutaric acid, 2- hydroxy- (3TMS)	18.9304	247.1	0.18	0.19	0.19	0.06	0.07	0.09	0.22	0.16	0.10	0.10	0.08	0.12
Unknown	18.9325	247.1	0.18	0.19	0.19	0.06	0.07	0.09	0.22	0.16	0.10	0.10	0.08	0.12
Unknown	19.2553	233.1	11.92	16.23	20.91	8.63	19.27	31.80	44.22	27.09	52.34	72.48	38.57	47.13
L-Glutamic Acid, N,O-O-TMS	19.627	246.1	0.67	0.74	0.87	0.17	0.25	0.28	1.93	1.67	1.31	0.07	0.07	0.06
L-Phenylalanine, N,O-TMS	19.9627	218.1	1.32	1.42	1.45	0.41	0.38	0.45	1.32	1.14	0.75	0.09	0.09	0.10
Unknown	20.0339	231.2	0.21	0.18	0.15	0.01	0.01	0.02	0.07	0.08	0.03	0.01	0.00	0.00
Dodecanoic Acid, O-TMS	20.2503	257.3	0.08	0.02	0.03	0.05	0.04	0.02	0.04	0.06	0.03	0.03	0.04	0.06
Arabinose	20.3391	307.1	0.11	0.11	0.09	0.31	0.22	0.31	0.26	0.32	0.24	0.28	0.25	0.24
methoxyamine (4TMS)	20.3459	217.1	0.16	0.13	0.13	0.34	0.25	0.34	0.29	0.34	0.30	0.31	0.26	0.24
Xylose, O,O,O-O- TMS, MEOX1	20.4768	306.1	0.02	0.01	0.00	0.04	0.01	0.01	0.01	0.00	0.02	0.00	0.01	0.00
Unknown	20.4849	306.2	0.02	0.01	0.00	0.04	0.01	0.01	0.01	0.00	0.02	0.00	0.01	0.00
Unknown	20.6172	218.1	0.25	0.18	0.16	0.43	0.36	0.34	0.24	0.16	0.14	0.16	0.21	0.23
Unknown	20.7922	205.1	0.26	0.19	0.18	0.30	0.24	0.24	0.22	0.16	0.14	0.17	0.22	0.24
L-Putrescine, N,N,N-N-TMS	21.5267	174.1	22.44	26.32	29.39	1.54	1.19	1.53	28.09	23.29	32.30	3.44	3.84	3.58
Unknown	21.6392	205.1	0.74	0.66	0.61	0.83	0.68	0.73	2.25	1.51	1.23	1.60	3.00	3.58
Unknown	21.6718	217.1	8.09	7.13	5.77	9.63	8.04	8.85	19.01	13.92	11.26	13.91	23.74	28.74
Unknown	21.724	316.1	0.12	0.05	0.02	0.13	0.12	0.03	0.01	0.18	0.11	0.00	0.17	0.09
Levulinic acid, 5- amino- (1MEOX) (3TMS) MP	21.7396	174.1	0.39	0.36	0.39	0.19	0.20	0.19	0.45	0.31	0.29	0.26	0.50	0.57
3-	22.2103	295.1	0.35	0.19	0.14	0.28	0.14	0.14	0.22	0.25	0.26	0.15	0.23	0.18

Hydroxyflavone, O-TMS									
Ornithine (4TMS)	22.4409	174.2	0.37	0.42	0.39	0.24	0.27	0.20	0.43
Unknown	22.544	217.2	0.46	0.39	0.37	0.45	0.31	0.35	0.54
Unknown	22.6722	217.1	0.34	0.27	0.25	0.42	0.29	0.18	0.27
Unknown	22.6783	204.1	0.18	0.14	0.13	0.24	0.17	0.14	0.13
Tetradecanoic Acid, O-TMS	22.9082	285.2	0.70	0.56	0.52	0.61	0.55	0.90	0.97
Unknown	23.0317	160.1	0.27	0.20	0.20	0.11	0.14	0.12	0.20
Unknown	23.0378	160.1	0.27	0.20	0.20	0.11	0.14	0.12	0.20
Unknown	23.0852	265.2	0.08	0.06	0.04	0.15	0.05	0.04	0.04
Adenine, N,N- TMS	23.2975	264.1	0.49	0.50	0.63	0.89	0.95	1.15	0.37
D-(+)-Mannose, O,O,O,O-O-TMS, MEOX1	23.3497	319.2	3.09	2.69	2.85	21.28	24.52	22.70	4.62
Unknown	23.4162	205.1	2.43	2.01	2.14	14.63	17.77	16.05	3.70
Unknown	23.5322	378.2	0.03	0.02	0.00	0.05	0.01	0.00	0.00
D-(+)-Mannose, O,O,O,O-O-TMS, o-methylloxime 2	23.6414	319.2	0.48	0.39	0.48	3.35	3.75	3.39	0.73
L-Lysine, N,N,N,O-TMS	23.777	174.1	3.43	3.34	3.78	1.72	1.75	1.90	3.66
L-Tyrosine, N,O- bis(trimethylsilyl) , trimethylsilyl ester	24.0246	218.1	1.57	1.74	1.82	0.40	0.50	0.54	1.61
Unknown	24.1453	299.3	0.36	0.33	0.39	0.25	0.40	0.43	0.46
Pentadecanoic Acid TMS	24.1494	299.3	0.36	0.33	0.39	0.25	0.40	0.43	0.46
Glucopyranose, D- (5TMS)	24.184	204.1	0.27	0.18	0.21	0.36	0.34	0.27	0.15
Unknown	24.188	204.1	0.27	0.18	0.21	0.36	0.34	0.27	0.15
Pimelic acid, 2,6- diamino- (4TMS)	24.46	272.2	2.87	4.00	5.41	1.35	2.12	2.66	5.59

Unknown	24.8873	159	0.16	0.33	0.41	0.11	0.35	0.64	0.91	0.48	0.97	2.67	0.74	1.08
Xanthine, N,O,O-TMS	24.9361	368.2	0.20	0.39	0.32	0.00	0.02	0.02	0.15	0.10	0.02	0.00	0.00	0.00
Hexadecenoic acid, 9-(Z)-(1TMS)	25.1247	311.3	13.52	15.99	15.52	16.78	17.65	16.19	29.81	27.75	24.63	19.48	27.58	34.79
Unknown	25.1674	241.2	0.21	0.24	0.23	0.22	0.27	0.24	0.42	0.41	0.37	0.30	0.42	0.53
Hexadecanoic Acid, O-TMS	25.3322	313.3	14.41	13.05	12.47	15.75	15.32	13.03	20.76	19.64	16.32	15.97	23.64	24.17
D-Mannitol, O,O,O,O,O-TMS	25.5404	319.2	2.43	2.14	2.90	4.16	2.16	2.23	3.01	3.29	3.54	2.08	1.93	1.42
Galactosamine, N-acetyl-(1MEOX)(4TMS)	25.6055	319.2	2.43	2.14	2.90	4.16	2.16	2.23	3.01	3.29	3.54	2.08	2.01	1.49
Uric Acid, N,N,O,O-TMS	25.7934	456.2	1.28	1.33	1.61	0.00	0.04	0.00	0.66	0.03	0.13	0.00	0.01	0.07
Unknown	25.8524	406.3	0.14	0.09	0.04	0.24	0.07	0.06	0.07	0.15	0.16	0.06	0.13	0.12
Unknown	25.9975	220.2	0.07	0.02	0.01	0.02	0.02	0.01	0.01	0.02	0.02	0.00	0.00	0.00
Unknown	26.0016	220.2	0.07	0.02	0.01	0.02	0.02	0.01	0.01	0.02	0.02	0.00	0.00	0.00
Methyl 9-(Z)-octadecenoate	26.1447	264.2	0.08	0.04	0.02	0.13	0.03	0.03	0.01	0.03	0.04	0.00	0.00	0.00
Unknown	26.2803	325.3	0.99	0.64	0.60	0.56	0.76	0.72	1.00	1.10	1.03	0.89	1.29	1.41
Unknown	26.3176	325.3	0.99	0.64	0.60	0.56	0.76	0.72	1.00	1.10	1.03	0.89	1.29	1.41
Unknown	26.3868	236.3	0.09	0.09	0.09	0.03	0.01	0.01	0.08	0.05	0.02	0.05	0.01	0.01
Unknown	26.5937	186.1	0.23	0.40	0.57	0.05	0.09	0.11	0.53	0.32	0.18	0.10	0.10	0.09
Unknown	26.9959	299.3	0.73	1.03	1.33	0.60	0.70	1.03	2.31	1.24	0.92	1.56	1.40	1.19
Unknown	27.1213	339.3	0.36	0.08	0.07	0.05	0.11	0.08	0.12	0.20	0.07	0.10	0.17	0.15
Unknown	27.1953	340.4	0.08	0.02	0.02	14.00	0.02	0.01	32.45	0.06	0.01	0.01	0.02	0.01
Octadecenoic acid, 9-(Z)-(1TMS)	27.3818	339.3	48.77	62.97	62.31	52.34	67.00	66.54	119.92	99.81	93.19	87.03	116.25	138.26
Unknown	27.5493	342.3	0.32	0.25	0.24	0.34	0.27	0.24	0.38	0.32	0.31	0.32	0.44	0.49
Stearic Acid, O-TMS	27.5527	342.3	0.32	0.25	0.24	0.34	0.27	0.24	0.38	0.32	0.31	0.32	0.44	0.49

Spermidine, N,N,N,N-TMS	27.7318	174.1	0.14	0.18	0.19	0.18	0.17	0.31	0.20	0.24	0.19	0.15	0.11	0.08
Unknown	28.1536	339.3	0.45	0.26	0.17	0.13	0.16	0.20	0.30	0.38	0.20	0.24	0.31	0.32
Unknown	28.6209	250.2	0.84	0.88	0.99	0.77	0.43	0.46	0.82	0.60	0.41	0.32	0.38	0.35
Unknown	28.8657	325.3	6.33	9.58	12.81	3.27	4.64	6.68	13.42	6.50	4.49	6.97	6.19	5.54
Unknown	29.0706	238	0.04	0.02	0.01	0.01	0.00	0.01	0.01	0.01	0.01	0.01	0.01	0.01
Unknown	29.3961	295.2	0.32	0.21	0.17	0.40	0.22	0.19	0.29	0.28	0.34	0.25	0.42	0.31
Unknown	29.3995	168.2	0.04	0.01	0.01	0.02	0.00	0.00	0.00	0.01	0.02	0.01	0.00	0.02
Unknown	29.4829	338.3	1.24	0.68	0.93	0.21	0.36	0.42	0.37	0.29	0.21	0.15	0.14	0.15
Unknown	29.9889	353.2	0.04	0.05	0.05	0.04	0.03	0.03	0.05	0.01	0.00	0.02	0.00	0.01
Unknown	30.836	369.3	0.39	0.28	0.36	0.32	0.17	0.20	0.38	0.34	0.33	0.26	0.25	0.31
Unknown	30.9865	371.2	0.51	0.29	0.34	0.48	0.23	0.29	0.51	0.41	0.38	0.38	0.41	0.33
ALPHA,BETA-TREHALOSE-TMS	31.129	217.1	2.60	1.29	1.23	4.80	2.51	2.52	1.01	0.88	0.89	0.82	1.32	1.35
Unknown	31.2578	257.1	5.37	2.71	2.85	3.67	4.90	5.28	0.21	0.21	0.32	0.99	1.17	0.86
Unknown	31.5698	230.1	0.19	0.14	0.16	0.24	0.21	0.22	0.13	0.10	0.13	0.30	0.39	0.40
Unknown	31.7943	174.2	1.28	0.67	0.46	0.93	0.54	0.53	0.50	0.94	1.06	0.46	0.70	0.41
Laminaribose Meox 2	31.8343	204.1	1.54	0.72	0.63	1.35	1.51	1.41	0.24	0.22	0.32	0.40	0.56	0.38
ISOMALTOSERIE MEOX1 TMS	32.3104	204.2	0.42	0.48	0.38	1.74	1.73	1.67	0.56	0.47	0.33	0.47	0.66	0.45
Isopropyl-beta-D-thiogalactopyranoside(IPTG), O,O,O-TMS	32.5173	361.2	3.33	2.62	2.47	8.36	6.02	6.19	1.76	1.62	1.74	1.65	2.93	2.73
Maltose Monohydrate MEOX1 TMS	32.6428	361.2	1570.4	1334.4	1379.5	2657.5	1775.5	2019.7	1022.9	1025.6	1083.5	1126.0	1327.7	1176.4
Unknown	32.7262	361.2	1570.4	1334.4	1379.5	2657.5	1775.5	2019.7	1022.9	1025.6	1083.5	1126.0	1327.7	1176.4
Unknown	32.7323	207.1	22.58	18.87	18.88	31.22	28.65	32.67	14.97	14.41	15.00	15.89	19.11	16.00
a,b-Trehalose (8TMS); alpha-D-Glc-(1,1)-beta-D-	32.7377	362.2	711.23	545.56	563.14	1075.8	862.18	977.23	306.38	311.43	328.72	342.86	397.25	348.93

Glc														
a,b-Trehalose (8TMS); alpha-D-Glc-(1,1)-beta-D-Glc	32.7404	361.3	1570.4	1334.4	1379.5	2657.5	1775.5	2019.7	1022.9	1025.6	1083.5	1126.0	1327.7	
Trehalose TMS	32.7431	175.1	6.89	5.64	5.64	8.56	8.39	9.54	3.75	3.68	3.83	4.08	4.77	4.29
Maltose Monohydrate MEOX2 TMS	32.9893	361.2	4.72	3.39	3.17	11.57	10.39	10.08	2.04	2.21	2.08	1.93	1.84	1.15
Unknown	33.1914	347.3	0.41	0.11	0.04	1.08	0.31	0.07	0.22	0.52	0.70	0.13	0.34	0.45
Unknown	33.2098	333.3	0.17	0.03	0.00	0.23	0.09	0.02	0.04	0.17	0.15	0.02	0.06	0.14
Unknown	33.534	236.1	0.51	0.49	0.46	0.67	0.38	0.50	0.17	0.17	0.17	0.21	0.29	0.25
Adenosine, 5-methylthio-(3TMS)	33.5353	236.1	0.51	0.49	0.46	0.67	0.38	0.50	0.17	0.17	0.17	0.21	0.29	0.25
Unknown	33.5489	236.1	0.51	0.49	0.46	0.67	0.38	0.50	0.17	0.17	0.17	0.21	0.29	0.25
Unknown	33.9151	33.9	0.02	0.03	0.01	0.04	0.03	0.07	0.02	0.01	0.01	0.02	0.04	0.01
Unknown	34.2183	34.2	4.10	2.15	1.32	3.92	2.19	1.91	1.46	2.88	3.29	1.34	2.02	1.19
Silanamine, 1,1,1-trimethyl-N-propyl-N-(trimethylsilyl)	34.2224	34.2	4.10	2.15	1.31	3.89	2.19	1.91	1.46	2.87	3.29	1.33	2.02	1.19
Melezitose TMS	34.6802	361.2	0.55	0.35	0.45	1.51	0.90	0.92	0.43	0.37	0.32	0.42	0.89	0.67
Unknown	46.5443	207.1	55.19	49.63	49.14	84.55	56.09	63.18	73.28	67.43	70.36	69.60	92.92	86.88
Unknown	46.5654	347.2	0.26	0.14	0.10	0.32	0.09	0.06	0.12	0.28	0.36	0.08	0.18	0.10

FONTE: a autora (2018).

TABLE 11 - DIFFERENTIAL METABOLITES IN *A. brasiliense* FP2 HIGH AND LOW NITROGEN.

FP2 high N vs FP2 low N	Retention time (min)	m/z	Fold Change	log2(FC)	Class
Uric Acid, N,N,O,O-TMS	25.7934	456.2	134.40	7.0704	Organic compound
Norvaline, O-TMS	11.1098	156.1	79.34	6.31	Amino acid
Proline 2TMS	14.7315	216	30.64	4.9373	Amino acid
Xanthine, N,O,O-TMS	24.9361	368.2	27.23	4.7669	Purine
L-Putrescine, N,N,N,N-TMS	21.5267	174.1	26.80	4.7441	Polyamine
Unknown	20.0339	231.2	19.02	4.2492	Unknown
Unknown	13.5311	159.1	18.16	4.1823	Unknown
Unknown	10.7788	173.1	14.72	3.8793	Unknown
L-Valine, N-trimethylsilyl-, trimethylsilyl ester	13.1994	218.1	13.63	3.7684	Amino acid
Unknown	14.5755	219.1	11.54	3.5288	Unknown
Unknown	14.581	219.1	11.54	3.5288	Unknown
Unknown	13.4449	159.2	7.65	2.9358	Unknown
Citramalic Acid, O,O,O-TMS	17.4566	247.1	7.65	2.9352	Organic compound
L-Aspartic acid, N,O,O-TMS	18.1342	232.1	7.44	2.8959	Amino acid
Unknown	14.6949	219.2	7.44	2.8945	Unknown
Unknown	26.5937	186.1	6.76	2.7563	Unknown
Unknown	26.3868	236.3	6.53	2.7081	Unknown
Unknown	13.3181	158	5.85	2.5484	Unknown
L-Isoleucine, N,O-TMS	14.5321	158.2	5.79	2.5345	Amino acid
Uracil, O,O-TMS	15.3257	241.1	5.67	2.5026	Pirimidine
Unknown	13.3127	158	5.41	2.4355	Unknown
L-Tyrosine, N,O-bistrimethylsilyl-, trimethylsilyl ester	24.0246	218.1	5.07	2.3423	Amino acid
Malic Acid, O,O,O-TMS	17.5936	233.2	4.92	2.2979	Organic compound
L-Phenylalanine, N,O-TMS	19.9627	218.1	4.87	2.2844	Amino acid
Unknown	29.0706	238	4.67	2.2242	Unknown
L-Glutamic Acid, N,O,O-TMS	19.627	246.1	4.57	2.1913	Amino acid
Niacin, O-TMS	17.8921	179.1	4.18	2.0639	Organic compound
Unknown	13.5589	336.1	3.98	1.9927	Unknown

	Retention time (min)	m/z	Fold Change	log2(FC)	Class
FP2 low N vs FP2 high N					
Unknown	27.1953	340.4	77.98	6.285	Unknown
D--Mannose, O,O,O,O-TMS, MEOX1	23.3497	319.2	5.60	2.486	Sugar
FP2 low N vs FP2 high N					
Unknown	29.4829	338.3	3.94	1.9767	Unknown
Unknown	13.5012	233.2	3.80	1.9274	Unknown
L-Serine, N,O,O-TMS	15.5569	204.1	3.73	1.9008	Amino acid
L-Threonine, N,O,O-TMS	15.9903	218.1	3.72	1.8972	Amino acid
Glutaric acid, 2-hydroxy- 3TMS	18.9304	247.1	3.61	1.8503	Organic compound
Unknown	18.9325	247.1	3.61	1.8503	Unknown
L-Alanine, N,N,O-TMS	15.7767	188.1	3.53	1.8178	Amino acid
L-Methionine, N,O-TMS	18.278	176.1	3.14	1.6492	Amino acid
Pyroglutamic acid 2TMS	18.36	156.1	2.99	1.5799	Amino acid
Pimelic acid, 2,6-diamino- 4TMS	24.46	272.2	2.83	1.5029	Organic compound
L-Lysine, N,N,N,O-TMS	23.777	174.1	2.82	1.4932	Amino acid
Unknown	28.8657	325.3	2.80	1.4867	Unknown
Levulinic acid, 5-amino- 1MEOX 3TMS MP	21.7396	174.1	2.78	1.477	Organic compound
Unknown	27.1213	339.3	2.67	1.4181	Unknown
Unknown	15.3318	185	2.58	1.3671	Unknown
Unknown	28.1536	339.3	2.52	1.3313	Unknown
Unknown	23.0317	160.1	2.47	1.3055	Unknown
Unknown	23.0378	160.1	2.47	1.3055	Unknown
Unknown	28.6209	250.2	2.44	1.2874	Unknown
Ornithine 4TMS	22.4409	174.2	2.41	1.2672	Amino acid
L-Alanine, N,O-TMS	11.2238	190.1	2.40	1.2657	Amino acid
Unknown	15.3385	184.1	2.40	1.2619	Unknown
Phosphoric Acid, O,O,O-TMS	14.092	299.1	2.34	1.227	Inorganic acid
Glycine 3TMS	14.8394	174.1	2.28	1.1882	Amino acid
Unknown	12.5626	218.1	2.25	1.1711	Unknown
Unknown	30.836	369.3	2.19	1.1303	Unknown
Ethylbistrimethylsilylamine	12.3835	174.1	2.12	1.0808	Organic compound

D-Mannose, O,O,O,O-TMS, o-methyloxime 2	23.6414	319.2	5.45	2.4465	Sugar
Unknown	23.4162	205.1	5.22	2.3838	Unknown
ISOMALTOSE MEOX1 TMS	32.3104	204.2	2.82	1.4931	Sugar

FONTE: a autora (2018).

TABLE 12 - DIFFERENTIAL METABOLITES IN *A. brasiliense ntrC* HIGH AND LOW NITROGEN.

<i>ntrC</i> high N vs <i>ntrC</i> low N	Retention time (min)	<i>m/z</i>	Fold Change	log ₂ (FC)	Class
Unknown	27.1953	340.4	1063.70	10.055	Unknown
L-Valine, N-trimethylsilyl-, trimethylsilyl ester	13.1994	218.1	49.47	5.6286	Amino acid
Xanthine, N,O-O-TMS	24.9361	368.2	48.33	5.5948	Amino acid
L-Glutamic Acid, N,O,O-TMS	19.627	246.1	27.40	4.7762	Amino acid
Norvaline, O-TMS	11.1098	156.1	22.20	4.4722	Amino acid
Unknown	14.6949	219.2	17.32	4.1146	Unknown
Unknown	13.3127	158	16.50	4.0443	Unknown
L-Isoleucine, N,O-TMS	14.5321	158.2	15.33	3.9381	Amino acid
Unknown	13.3181	158	14.94	3.9007	Unknown
Unknown	20.0339	231.2	14.78	3.8858	Unknown
Methyl 9-Z-octadecenoate	26.1447	264.2	14.55	3.8632	Organic compound
L-Phenylalanine, N,O-TMS	19.9627	218.1	13.10	3.7115	Amino acid
Uric Acid, N,N,O,O-TMS	25.7934	456.2	12.28	3.6182	Organic compound
L-Tyrosine, N,O-bistrimethylsilyl-, trimethylsilyl ester	24.0246	218.1	8.74	3.1275	Amino acid
L-Putrescine, N,N,N,N-TMS	21.5267	174.1	8.58	3.1003	Polyamine
Unknown	25.9975	220.2	8.44	3.0771	Unknown
Unknown	26.0016	220.2	8.44	3.0771	Unknown
L-Aspartic acid, N,O,O-TMS	18.1342	232.1	7.73	2.9496	Amino acid
L-Lysine, N,N,N,O-TMS	23.777	174.1	7.03	2.8128	Amino acid
L-Methionine, N,O-TMS	18.278	176.1	6.95	2.796	Amino acid
Glycine 3TMS	14.8394	174.1	6.87	2.78	Amino acid
L-Serine, N,O,O-TMS	15.5569	204.1	6.73	2.7496	Amino acid
Phosphoric Acid, O,O,O-TMS	14.092	299.1	5.81	2.5395	Inorganic acid

		Retention time	<i>m/z</i>	Fold Change	log ₂ (FC)	Class
Unknown		23.0317	160.1	5.46	2.4481	Unknown
Unknown		23.0378	160.1	5.46	2.4481	Unknown
Pyroglutamic acid 2TMS		18.36	156.1	4.88	2.2872	Amino acid
Unknown		15.8743	306.1	4.68	2.2258	Unknown
Unknown		15.913	306.2	4.68	2.2258	Unknown
L-Alanine, N,O-TMS		11.2238	190.1	4.11	2.0392	Amino acid
Unknown		26.5937	186.1	3.99	1.9981	Unknown
L-Alanine, N,N,O-TMS		15.7767	188.1	3.96	1.9872	Amino acid
L-Threonine, N,O,O-TMS		15.9903	218.1	3.84	1.9399	Amino acid
Unknown		12.5626	218.1	3.54	1.8255	Unknown
Malic Acid, O,O,O-TMS		17.5936	233.2	3.40	1.7645	Organic compound
Pimelic acid, 2,6-diamino- 4TMS		24.46	272.2	3.35	1.7447	Organic compound
Unknown		10.7788	173.1	3.23	1.6917	Unknown
Ethanol Amine, N,O,O-TMS		12.8725	174.1	3.22	1.6891	Organic compound
Unknown		12.8162	205.1	2.94	1.5551	Unknown
Unknown		23.5322	378.2	2.80	1.4847	Unknown
Glycerol, 3 TMS		14.0493	205.1	2.69	1.4293	Organic compound
Unknown		26.3868	236.3	2.52	1.3342	Unknown
Ethanolamine 3TMS		14.1388	174.2	2.46	1.3007	Organic compound
Unknown		46.5654	347.2	2.42	1.2748	Unknown
Niacin, O-TMS		17.8921	179.1	2.41	1.27	Organic compound
Unknown		14.5755	219.1	2.29	1.1942	Unknown
Unknown		14.581	219.1	2.29	1.1942	Unknown
Ornithine 4TMS		22.4409	174.2	2.24	1.1656	Amino acid
Unknown		29.4829	338.3	2.15	1.1012	Unknown
Unknown		13.5589	336.1	2.13	1.0875	Unknown
Unknown		13.9353	155.1	2.05	1.0391	Unknown
Spermidine, N,N,N,N-TMS		27.7318	174.1	2.03	1.0185	Polyamine
D-Mannitol, O,O,O,O,O-TMS		25.5404	319.2	2.01	1.0071	Sugar
<i>ntrc</i> low N vs <i>ntrc</i> high N						

		(min)				
Unknown		31.2578	257.1	3.71	1.8911	Unknown
Unknown		31.5698	230.1	2.72	1.4462	Unknown

FONTE: a autora (2018).

TABLE 13 - KEGG DISTRIBUTION OF PROTEOME AND METABOLOMICS DATA FOR *A. brasiliense ntrC HIGH AND LOW NITROGEN.*

Pathway Codes:	Annotation:	Number of proteins and metabolites:					
		ntrC high N	ntrC low N	Total Number in Pathway	% of coverage ntrC high N	% of coverage ntrC low N	
abs00010	Glycolysis / Gluconeogenesis	1	1	78	1.28	1.28	
abs00020	Citrate cycle (TCA cycle)	0	2	56	0.00	3.57	
abs00030	Pentose phosphate pathway	0	1	57	0.00	1.75	
abs00040	Pentose and glucuronate interconversions	1	1	80	1.25	1.25	
abs00051	Fructose and mannose metabolism	1	1	80	1.25	1.25	
abs00052	Galactose metabolism	1	0	66	1.52	0.00	
abs00053	Ascorbate and aldarate metabolism	0	1	58	0.00	1.72	
abs00061	Fatty acid biosynthesis	1	0	78	1.28	0.00	
abs00071	Fatty acid degradation	0	1	74	0.00	1.35	
abs00072	Synthesis and degradation of ketone bodies	0	0	13	0.00	0.00	
abs00130	Ubiquinone and other terpenoid-quinone biosynthesis	1	2	102	0.98	1.96	
abs00190	Oxidative phosphorylation	1	1	71	1.41	1.41	
abs00220	Arginine biosynthesis	0	2	46	0.00	4.35	
abs00230	Purine metabolism	9	0	186	4.84	0.00	
abs00240	Pyrimidine metabolism	5	3	119	4.20	2.52	
abs00250	Alanine, aspartate and glutamate metabolism	2	0	54	3.70	0.00	
abs00260	Glycine, serine and threonine metabolism	3	0	83	3.61	0.00	
abs00261	Monobactam biosynthesis	5	0	53	9.43	0.00	
abs00270	Cysteine and methionine metabolism	3	1	103	2.91	0.97	
abs00280	Valine, leucine and isoleucine degradation	0	1	82	0.00	1.22	
abs00281	Geraniol degradation	0	0	26	0.00	0.00	

abs00290	Valine, leucine and isoleucine biosynthesis	1	2	44	2.27	4.55
abs00300	Lysine biosynthesis	0	0	52	0.00	0.00
abs00310	Lysine degradation	1	1	71	1.41	1.41
abs00311	Penicillin and cephalosporin biosynthesis	0	0	20	0.00	0.00
abs00330	Arginine and proline metabolism	4	3	114	3.51	2.63
abs00332	Carbapenem biosynthesis	0	0	34	0.00	0.00
abs00340	Histidine metabolism	0	1	65	0.00	1.54
abs00350	Tyrosine metabolism	1	1	89	1.12	1.12
abs00360	Phenylalanine metabolism	1	1	86	1.16	1.16
abs00361	Chlorocyclohexane and chlorobenzene degradation	0	0	88	0.00	0.00
abs00362	Benzoate degradation	0	0	100	0.00	0.00
abs00364	Fluorobenzoate degradation	0	0	37	0.00	0.00
abs00380	Tryptophan metabolism	0	1	104	0.00	0.96
abs00400	Phenylalanine, tyrosine and tryptophan biosynthesis	2	0	53	3.77	0.00
abs00401	Novobiocin biosynthesis	2	0	36	5.56	0.00
abs00410	beta-Alanine metabolism	1	1	49	2.04	2.04
abs00430	Taurine and hypotaurine metabolism	0	0	39	0.00	0.00
abs00440	Phosphonate and phosphinate metabolism	1	0	61	1.64	0.00
abs00450	Selenocompound metabolism	2	0	41	4.88	0.00
abs00460	Cyanoamino acid metabolism	5	0	56	8.93	0.00
abs00471	D-Glutamine and D-glutamate metabolism	0	0	15	0.00	0.00
abs00472	D-Arginine and D-ornithine metabolism	0	0	11	0.00	0.00
abs00473	D-Alanine metabolism	0	0	11	0.00	0.00
abs00480	Glutathione metabolism	6	0	64	9.38	0.00
abs00500	Starch and sucrose metabolism	1	1	70	1.43	1.43
abs00520	Amino sugar and nucleotide sugar metabolism	0	0	157	0.00	0.00
abs00521	Streptomycin biosynthesis	0	0	32	0.00	0.00
abs00523	Polyketide sugar unit biosynthesis	0	0	63	0.00	0.00

abs00525	Acarbose and validamycin biosynthesis	0	0	38	0.00	0.00
abs00540	Lipopolysaccharide biosynthesis	0	0	46	0.00	0.00
abs00550	Peptidoglycan biosynthesis	0	0	46	0.00	0.00
abs00561	Glycerolipid metabolism	1	0	47	2.13	0.00
abs00562	Inositol phosphate metabolism	0	0	51	0.00	0.00
abs00564	Glycerophospholipid metabolism	4	2	71	5.63	2.82
abs00590	Arachidonic acid metabolism	0	0	76	0.00	0.00
abs00592	alpha-Linolenic acid metabolism	0	0	43	0.00	0.00
abs00600	Sphingolipid metabolism	1	0	28	3.57	0.00
abs00620	Pyruvate metabolism	2	0	92	2.17	0.00
abs00621	Dioxin degradation	0	0	60	0.00	0.00
abs00623	Toluene degradation	0	0	50	0.00	0.00
abs00624	Polycyclic aromatic hydrocarbon degradation	0	0	108	0.00	0.00
abs00625	Chloroalkane and chloroalkene degradation	0	2	60	0.00	3.33
abs00626	Naphthalene degradation	0	1	65	0.00	1.54
abs00627	Aminobenzoate degradation	0	1	100	0.00	1.00
abs00630	Glyoxylate and dicarboxylate metabolism	2	4	128	1.56	3.13
abs00633	Nitrotoluene degradation	0	0	30	0.00	0.00
abs00640	Propanoate metabolism	1	1	101	0.99	0.99
abs00643	Styrene degradation	0	0	30	0.00	0.00
abs00650	Butanoate metabolism	2	4	85	2.35	4.71
abs00660	C5-Branched dibasic acid metabolism	0	1	55	0.00	1.82
abs00670	One carbon pool by folate	1	0	25	4.00	0.00
abs00680	Methane metabolism	4	1	131	3.05	0.76
abs00710	Carbon fixation in photosynthetic organisms	0	0	43	0.00	0.00
abs00730	Thiamine metabolism	2	1	43	4.65	2.33
abs00740	Riboflavin metabolism	1	0	28	3.57	0.00
abs00750	Vitamin B6 metabolism	0	0	35	0.00	0.00
abs00760	Nicotinate and nicotinamide metabolism	3	1	84	3.57	1.19
abs00770	Pantothenate and CoA biosynthesis	0	3	52	0.00	5.77

abs00780	Biotin metabolism	2	0	51	3.92	0.00
abs00785	Lipoic acid metabolism	1	0	9	11.11	0.00
abs00790	Folate biosynthesis	1	1	91	1.10	1.10
abs00860	Porphyrin and chlorophyll metabolism	3	2	179	1.68	1.12
abs00900	Terpenoid backbone biosynthesis	1	0	59	1.69	0.00
abs00903	Limonene and pinene degradation	0	0	70	0.00	0.00
abs00906	Carotenoid biosynthesis	0	0	117	0.00	0.00
abs00909	Sesquiterpenoid and triterpenoid biosynthesis	0	0	89	0.00	0.00
abs00910	Nitrogen metabolism	0	1	47	0.00	2.13
abs00920	Sulfur metabolism	5	1	94	5.32	1.06
abs00930	Caprolactam degradation	0	1	30	0.00	3.33
abs00970	Aminoacyl-tRNA biosynthesis	6	0	163	3.68	0.00
abs01040	Biosynthesis of unsaturated fatty acids	1	0	67	1.49	0.00
abs01053	Biosynthesis of siderophore group nonribosomal peptides	0	0	17	0.00	0.00
abs01054	Nonribosomal peptide structures	0	0	15	0.00	0.00
abs01055	Biosynthesis of vancomycin group antibiotics	1	0	21	4.76	0.00
abs01100	Metabolic pathways	24	26	826	2.91	3.15
abs01110	Biosynthesis of secondary metabolites	9	14	321	2.80	4.36
abs01120	Microbial metabolism in diverse environments	5	10	324	1.54	3.09
abs01130	Biosynthesis of antibiotics	5	9	255	1.96	3.53
abs01200	Carbon metabolism	2	7	159	1.26	4.40
abs01210	2-Oxocarboxylic acid metabolism	0	4	37	0.00	10.81
abs01212	Fatty acid metabolism	0	0	40	0.00	0.00
abs01220	Degradation of aromatic compounds	0	1	15	0.00	6.67
abs01230	Biosynthesis of amino acids	2	6	132	1.52	4.55
abs01501	beta-Lactam resistance	1	0	21	4.76	0.00
abs01502	Vancomycin resistance	0	0	7	0.00	0.00
abs01503	Cationic antimicrobial peptide (CAMP) resistance	1	0	14	7.14	0.00

abs02010	ABC transporters	6	5	285	2.11	1.75
abs02020	Two-component system	3	8	238	1.26	3.36
abs02024	Quorum sensing	3	4	274	1.09	1.46
abs02030	Bacterial chemotaxis	1	3	91	1.10	3.30
abs02040	Flagellar assembly	0	0	62	0.00	0.00
abs02060	Phosphotransferase system (PTS)	2	0	66	3.03	0.00
abs03010	Ribosome	2	0	68	2.94	0.00
abs03018	RNA degradation	2	0	19	10.53	0.00
abs03020	RNA polymerase	0	0	4	0.00	0.00
abs03030	DNA replication	2	0	21	9.52	0.00
abs03060	Protein export	0	0	19	0.00	0.00
abs03070	Bacterial secretion system	0	0	26	0.00	0.00
abs03410	Base excision repair	0	0	17	0.00	0.00
abs03420	Nucleotide excision repair	0	0	12	0.00	0.00
abs03430	Mismatch repair	2	0	25	8.00	0.00
abs03440	Homologous recombination	3	0	28	10.71	0.00

FONTE: a autora (2018).

TABLE 14 - KEGG DISTRIBUTION OF PROTEOME AND METABOLOMICS DATA FOR *A. brasiliense* FP2 HIGH AND LOW NITROGEN.

Pathway Codes:	Annotation:	Number of proteins and metabolites:			
		FP2 high N	FP2 low N	Total Number in Pathway	% of coverage FP2 high N
abs00010	Glycolysis / Gluconeogenesis	2	0	78	2.56
abs00020	Citrate cycle (TCA cycle)	5	1	56	8.93
abs00030	Pentose phosphate pathway	1	0	57	1.75
abs00040	Pentose and glucuronate interconversions	1	1	80	1.25
abs00051	Fructose and mannose metabolism	4	3	80	5.00
abs00052	Galactose metabolism	3	2	66	4.55
abs00053	Ascorbate and aldarate metabolism	1	1	58	1.72
abs00061	Fatty acid biosynthesis	0	0	78	0.00
abs00071	Fatty acid degradation	1	0	74	1.35

abs00072	Synthesis and degradation of ketone bodies	1	0	13	7.69	0.00
abs00130	Ubiquinone and other terpenoid-quinone biosynthesis	1	1	102	0.98	0.98
abs00190	Oxidative phosphorylation	9	1	71	12.68	1.41
abs00220	Arginine biosynthesis	4	1	46	8.70	2.17
abs00230	Purine metabolism	12	1	186	6.45	0.54
abs00240	Pyrimidine metabolism	6	3	119	5.04	2.52
abs00250	Alanine, aspartate and glutamate metabolism	5	1	54	9.26	1.85
abs00260	Glycine, serine and threonine metabolism	5	0	83	6.02	0.00
abs00261	Monobactam biosynthesis	7	0	53	13.21	0.00
abs00270	Cysteine and methionine metabolism	10	0	103	9.71	0.00
abs00280	Valine, leucine and isoleucine degradation	3	3	82	3.66	3.66
abs00281	Geraniol degradation	0	0	26	0.00	0.00
abs00290	Valine, leucine and isoleucine biosynthesis	4	1	44	9.09	2.27
abs00300	Lysine biosynthesis	4	1	52	7.69	1.92
abs00310	Lysine degradation	4	1	71	5.63	1.41
abs00311	Penicillin and cephalosporin biosynthesis	1	0	20	5.00	0.00
abs00330	Arginine and proline metabolism	5	2	114	4.39	1.75
abs00332	Carbapenem biosynthesis	1	0	34	2.94	0.00
abs00340	Histidine metabolism	2	1	65	3.08	1.54
abs00350	Tyrosine metabolism	1	0	89	1.12	0.00
abs00360	Phenylalanine metabolism	2	1	86	2.33	1.16
abs00361	Chlorocyclohexane and chlorobenzene degradation	0	0	88	0.00	0.00
abs00362	Benzoate degradation	0	0	100	0.00	0.00
abs00364	Fluorobenzoate degradation	0	0	37	0.00	0.00
abs00380	Tryptophan metabolism	1	1	104	0.96	0.96
abs00400	Phenylalanine, tyrosine and tryptophan biosynthesis	3	1	53	5.66	1.89
abs00401	Novobiocin biosynthesis	2	0	36	5.56	0.00
abs00410	beta-Alanine metabolism	2	2	49	4.08	4.08

abs00430	Taurine and hypotaurine metabolism	2	1	39	5.13	2.56
abs00440	Phosphonate and phosphinate metabolism	1	0	61	1.64	0.00
abs00450	Selenocompound metabolism	3	0	41	7.32	0.00
abs00460	Cyanoamino acid metabolism	7	1	56	12.50	1.79
abs00471	D-Glutamine and D-glutamate metabolism	1	0	15	6.67	0.00
abs00472	D-Arginine and D-ornithine metabolism	0	0	11	0.00	0.00
abs00473	D-Alanine metabolism	2	0	11	18.18	0.00
abs00480	Glutathione metabolism	6	2	64	9.38	3.13
abs00500	Starch and sucrose metabolism	4	1	70	5.71	1.43
abs00520	Amino sugar and nucleotide sugar metabolism	9	3	157	5.73	1.91
abs00521	Streptomycin biosynthesis	1	0	32	3.13	0.00
abs00523	Polyketide sugar unit biosynthesis	1	0	63	1.59	0.00
abs00525	Acarbose and validamycin biosynthesis	1	0	38	2.63	0.00
abs00540	Lipopolysaccharide biosynthesis	3	0	46	6.52	0.00
abs00550	Peptidoglycan biosynthesis	2	0	46	4.35	0.00
abs00561	Glycerolipid metabolism	0	0	47	0.00	0.00
abs00562	Inositol phosphate metabolism	0	1	51	0.00	1.96
abs00564	Glycerophospholipid metabolism	2	0	71	2.82	0.00
abs00590	Arachidonic acid metabolism	0	0	76	0.00	0.00
abs00592	alpha-Linolenic acid metabolism	0	0	43	0.00	0.00
abs00600	Sphingolipid metabolism	1	0	28	3.57	0.00
abs00620	Pyruvate metabolism	6	0	92	6.52	0.00
abs00621	Dioxin degradation	0	0	60	0.00	0.00
abs00623	Toluene degradation	0	0	50	0.00	0.00
abs00624	Polycyclic aromatic hydrocarbon degradation	0	0	108	0.00	0.00
abs00625	Chloroalkane and chloroalkene degradation	0	0	60	0.00	0.00
abs00626	Naphthalene degradation	0	0	65	0.00	0.00
abs00627	Aminobenzoate degradation	0	0	100	0.00	0.00
abs00630	Glyoxylate and dicarboxylate metabolism	8	2	128	6.25	1.56
abs00633	Nitrotoluene degradation	2	0	30	6.67	0.00

abs00640	Propanoate metabolism	2	4	101	1.98	3.96
abs00643	Styrene degradation	0	0	30	0.00	0.00
abs00650	Butanoate metabolism	7	1	85	8.24	1.18
abs00660	C5-Branched dibasic acid metabolism	1	1	55	1.82	1.82
abs00670	One carbon pool by folate	2	0	25	8.00	0.00
abs00680	Methane metabolism	4	0	131	3.05	0.00
abs00710	Carbon fixation in photosynthetic organisms	3	0	43	6.98	0.00
abs00730	Thiamine metabolism	4	2	43	9.30	4.65
abs00740	Riboflavin metabolism	1	0	28	3.57	0.00
abs00750	Vitamin B6 metabolism	0	0	35	0.00	0.00
abs00760	Nicotinate and nicotinamide metabolism	4	1	84	4.76	1.19
abs00770	Pantothenate and CoA biosynthesis	3	2	52	5.77	3.85
abs00780	Biotin metabolism	3	0	51	5.88	0.00
abs00785	Lipoic acid metabolism	1	0	9	11.11	0.00
abs00790	Folate biosynthesis	2	1	91	2.20	1.10
abs00860	Porphyrin and chlorophyll metabolism	7	1	179	3.91	0.56
abs00900	Terpenoid backbone biosynthesis	3	0	59	5.08	0.00
abs00903	Limonene and pinene degradation	0	0	70	0.00	0.00
abs00906	Carotenoid biosynthesis	0	0	117	0.00	0.00
abs00909	Sesquiterpenoid and triterpenoid biosynthesis	0	0	89	0.00	0.00
abs00910	Nitrogen metabolism	6	2	47	12.77	4.26
abs00920	Sulfur metabolism	9	2	94	9.57	2.13
abs00930	Caprolactam degradation	0	1	30	0.00	3.33
abs00970	Aminoacyl-tRNA biosynthesis	13	1	163	7.98	0.61
abs01040	Biosynthesis of unsaturated fatty acids peptides	0	0	67	0.00	0.00
abs01053	Biosynthesis of siderophore group nonribosomal peptides	0	0	15	0.00	0.00
abs01055	Biosynthesis of vancomycin group antibiotics	2	0	21	9.52	0.00
abs01100	Metabolic pathways	70	24	826	8.47	2.91

abs01110	Biosynthesis of secondary metabolites	25	8	321	7.79	2.49
abs01120	Microbial metabolism in diverse environments	22	7	324	6.79	2.16
abs01130	Biosynthesis of antibiotics	15	6	255	5.88	2.35
abs01200	Carbon metabolism	9	4	159	5.66	2.52
abs01210	2-Oxocarboxylic acid metabolism	2	2	37	5.41	5.41
abs01212	Fatty acid metabolism	0	0	40	0.00	0.00
abs01220	Degradation of aromatic compounds	0	0	15	0.00	0.00
abs01230	Biosynthesis of amino acids	10	5	132	7.58	3.79
abs01501	beta-Lactam resistance	1	0	21	4.76	0.00
abs01502	Vancomycin resistance	1	0	7	14.29	0.00
abs01503	Cationic antimicrobial peptide (CAMP) resistance	1	0	14	7.14	0.00
abs02010	ABC transporters	17	19	285	5.96	6.67
abs02020	Two-component system	16	5	238	6.72	2.10
abs02024	Quorum sensing	8	17	274	2.92	6.20
abs02030	Bacterial chemotaxis	12	1	91	13.19	1.10
abs02040	Flagellar assembly	7	0	62	11.29	0.00
abs02060	Phosphotransferase system (PTS)	2	2	66	3.03	3.03
abs03010	Ribosome	8	0	68	11.76	0.00
abs03018	RNA degradation	3	1	19	15.79	5.26
abs03020	RNA polymerase	0	0	4	0.00	0.00
abs03030	DNA replication	5	1	21	23.81	4.76
abs03060	Protein export	1	0	19	5.26	0.00
abs03070	Bacterial secretion system	1	0	26	3.85	0.00
abs03410	Base excision repair	0	0	17	0.00	0.00
abs03420	Nucleotide excision repair	0	0	12	0.00	0.00
abs03430	Mismatch repair	3	1	25	12.00	4.00
abs03440	Homologous recombination	3	2	28	10.71	7.14

FONTE: a autora (2018).

TABLE 15 - PLANT ASSAY.

Non inoculated *S. viridis*

	Root area (cm²)	Number of lateral roots	Leaf length (cm)	Leaf dry weight (g)	Root dry weight (g)
1	152.316	642	5.5	5.8	1.1
2	159.232	768	4.3	6.8	2.3
3	139.379	670	5.4	3.7	2.5
4	104.616	410	6.6	6.4	2.3
5	171.213	621	6.1	6.7	2.3
6	90.786	390	4.1	6.8	2.2
7	165.574	628	5.2	4.6	1.5
8	125.096	432	5.9	4.3	1.4
9	129.696	615	6.3	6.3	2.1
10	140.427	637	5.7	7.1	2.5
11	162.515	620	6	6.5	2.7
12	129.485	552	5.2	7.5	2.4
13	148.316	724	5.3	5.1	2.2
14	119.094	451	5.3	5.3	0.9
15	145.601	721	4.7	7.8	2
16	154.556	650	5.4	3.8	2.8
17	106.004	453	5.9	6.5	2.3
18	100.679	615	6.2	5.5	1.5
19	112.896	543	5.7	7.7	2.2
20	119.137	537	6.1	7.6	1.7
21	99.935	601	3.9	4.3	1.8
22	118.325	661	6.1	4	1.5
23	142.096	643	5	4.4	1.3
24	143.284	736	5.7	8.3	1.9
25	132.384	825	5.8	8.7	1.4
26	124.406	656	6.3	3.7	2.5
27	92.461	475	5.5	4.1	1.8
28	90.473	357	4.6	5.9	1.9
29	90.713	364	3.7	4.3	1.6
30	96.546	444	4	4.6	2.7
31	114.747	506	4.9	7.8	2
32	116.774	572	4.9	6.9	2.1
33	92.107	370	6	6.2	1.8
34	76.914	230	7.2	6.8	1.5
35	96.614	406	3.5	5.7	1.4
36	93.33	393	3.8	7.1	1.1
37	42.37	115	5.6	4.7	0.9
38	86.315	332	6.7	4.6	1.6
39	82.789	339	5.1	6.5	1.9
40	44.299	132	4.8	3.7	1.1
41	77.34	359	3.8	6.5	1
42	81.561	326	4.2	5.9	0.8

43	75.142	351	6.1	3.3	1.6
44	82.562	292	4.2	4.3	0.9
45	25.602	52	4	3.6	1.1
46	86.037	297	6.5	3.4	2.1
47	88.827	323	5	5.5	1.8
48	121.629	419	5.4	3.7	1.1
49	71.709	237	5.4	3.3	1.2
50	84.193	365	4	3.7	1.1
51	66.467	292	4.8	4	0.7
52	91.303	269	4.6	5.3	1.9
53	102.691	317	5.1	4.2	1.2
54	91.318	450	3.8	3.6	1.3
55	64.103	232	4.4	5.2	2.2
56	96.125	490	5.4	3.7	1.5
57	81.696	318	5.5	3.2	1.1
58	74.059	336	4.2	3	1.2
59	97.636	587	3.6	4.1	1.1
60	96.805	318	3.8	5	1.5
61	62.496	232	2.5	6	1.1
62	73.682	362	5.5	3	2.2
63	103.851	337	3.9	4.6	0.8
64	127.963	604	5.6	3.1	1.3
65	90.585	243	3.7	3.3	1.1
66	55.177	210	4.1	4.4	1.3
67	102.78	209	4.4	5.6	0.6
68	99.176	256	4.5	4.2	1.4
69	127.918	258	5.9	4	0.9
70	75.065	193	4.8	6.2	1.5
71	87.145	384	5.1	3.7	1.2
72	106.312	323	5.2	3.6	0.9
73	94.592	295	3.9	2.7	1.2
74	124.086	279	4	2.6	1
75	138.233	458	4.4	3.5	1.2
76	81.145	256	3.6	1.9	1.4
77	86.738	312	3.8	3.6	1.6
78	102.609	275	4.1	2.5	1.4
79	133.61	450	4	2.4	1.2
80	69.891	255	3.9	3.8	1.1
81	111.846	295	3.8	3.4	0.7
82	94.187	334	4.4	3.1	1
83	91.693	203	4.1	4.5	1.1
84	135.557	341	3.9	2.9	0.8
85	104.143	219	4.5	2.2	1.1
86	85.764	331	4.2	2.9	0.8
87	95.856	331	4.8	2.5	1.1
88	159.184	333	3.7	3.1	1.3

89	79.909	192	4	2.6	1.6
90	105.394	286	4	2.8	0.9
91	116.094	325	4.3	3	-
92	80.592	229	4.4	2.4	-
93	93.603	148	3.9	2.6	-
94	85.409	212	4	3	-
95	74.307	288	3.7	2.9	-
96	98.918	252	3.9	2.7	-
97	-	-	3.7	3	-
98	-	-	4	2.1	-
99	-	-	3.9	2	-
100	-	-	4.1	1.8	-
101	-	-	3.7	3.6	-
102	-	-	4.2	2.6	-
103	-	-	3.7	2.8	-
104	-	-	4.2	2.4	-
105	-	-	3.8	2.5	-
106	-	-	4.3	3	-
107	-	-	4	-	-
108	-	-	-	-	-
Average	102.7689063	395.5833333	4.709345794	4.393396226	1.51
St. deviation	28.49651044	166.8887271	0.911046713	1.670513923	0.538939287
Error	0.29683865	1.73842424	0.008514455	0.015759565	0.005988214

S. viridis + A. brasiliense FP2

	Root area (cm ²)	Number of lateral roots	Leaf length (cm)	Leaf dry weight (g)	Root dry weight (g)
1	162.437	668	5.6	6	2.4
2	130.658	749	4.9	5.1	2.9
3	148.021	642	8.2	7.5	2.6
4	132.163	563	7.2	7.3	2.6
5	136.267	644	5.4	5	1.7
6	107.577	495	5.9	7.1	2.9
7	153.634	878	7.5	6.6	3.1
8	138.823	595	6.1	8.3	2.4
9	74.573	410	5.5	5.6	1.7
10	123.263	783	6.5	9.1	3.3
11	136.351	554	6.7	7.2	2.7
12	109.907	616	6.6	7.6	2
13	122.402	680	7	7.2	3
14	141.83	670	5.4	8.4	1.4
15	87.25	392	6.5	7.5	3.8
16	121.154	622	6.6	8.8	2
17	125.05	619	5.9	7.1	2
18	126.27	646	6.2	8.6	2.5
19	146.768	676	7.1	7	2.1
20	127.938	774	5.5	9.1	2.5

21	132.705	855	5.5	8	1.9
22	148.351	694	6.6	10.1	2.9
23	128.139	804	9	6.4	1.9
24	119.171	615	6.8	6.7	3.2
25	142.17	710	6.9	7.2	2.9
26	131.444	539	4.5	6.2	2.3
27	125.815	634	5.7	4.8	2.6
28	181.843	882	6	6.7	2.1
29	132.131	596	4.6	10.9	1.4
30	96.16	666	6	4.9	3
31	154.706	797	7.3	5.3	2.1
32	187.59	991	4.4	9.4	2.6
33	158.753	830	6.4	11.3	2.5
34	128.761	469	5.4	6.5	3.8
35	126.821	446	5.5	7.2	3.5
36	145.77	680	6.7	7.6	3.1
37	124.517	535	7.5	4	2.2
38	112.46	393	7.4	5.7	4.1
39	160.307	516	7.2	7.2	2.3
40	185.812	617	8.8	6.7	2.5
41	103.198	709	6	5.7	2
42	122.647	512	6.5	4.8	2.4
43	151.446	371	7.7	8	1.7
44	120.535	636	6.3	4	3.2
45	145.872	415	6.3	6.2	2.8
46	180.008	702	7.3	6.9	2.7
47	128.624	950	6.5	6.7	2.1
48	144.384	780	7.4	5.5	2.1
49	162.473	540	6.2	5.5	2
50	100.277	646	7	6.1	1.5
51	117.322	671	7	8.3	2.2
52	138.452	680	7.4	4.1	1.7
53	120.32	649	7.4	7.8	3
54	170.023	655	7.1	9.6	1.6
55	162.503	625	7.2	7.4	2
56	142.848	567	6.3	5.3	3.3
57	193.045	864	6.6	5.9	2.2
58	146.771	822	7.2	7.6	1.9
59	135.395	642	5.7	5.9	1.6
60	179.82	928	7.5	5.6	2
61	130.198	683	6.5	6.8	2.2
62	165.522	732	6.4	6	1.6
63	145.91	517	5.6	5.9	1.8
64	148.573	681	6.6	5.5	2.1
65	103.346	308	6.1	4.8	1
66	110.274	359	8.5	6.7	1.1

67	114.285	453	6.4	5.9	1.4
68	164.366	494	6.1	5.5	1.5
69	167.632	234	7.9	6	1.3
70	123.361	340	7	7.1	0.9
71	160.592	430	6.6	3.4	1.7
72	170.953	527	3.9	3.8	1
73	153.702	539	5.8	4	1.5
74	124.254	305	3.6	5.6	1.4
75	137.311	398	4.7	3.6	0.7
76	145.105	249	4.4	3.6	1.9
77	174.577	234	4.5	5	1.2
78	120.742	435	4.3	4.5	1.6
79	192.825	500	4	2.6	1.6
80	161.002	513	4.4	3.8	1.4
81	207.49	816	4.3	5.1	1.1
82	119.556	380	3.5	5.2	1.7
83	149.016	324	4.3	4.6	1.1
84	124.568	409	4.6	3.3	2.1
85	170.422	301	4	3.9	1.9
86	158.588	562	6.1	6.2	1.6
87	194.766	545	4.8	4.6	1.1
88	126.811	185	4.1	3.3	1.9
89	236.175	645	4.5	4.3	1.7
90	183.39	645	5.2	2.8	1.4
91	170.035	494	5	4.7	1.5
92	169.687	651	3.7	4.3	1.2
93	114.364	472	4.2	3.4	1.1
94	161.531	434	4.2	6	1.6
95	251.618	655	4.4	3.6	1.5
96	104.493	217	3.7	3.6	1.2
97	-	-	4.4	2.8	-
98	-	-	4.3	4.3	-
99	-	-	3.7	2.4	-
100	-	-	4.3	3.4	-
101	-	-	4.6	4.4	-
102	-	-	3.9	3.1	-
103	-	-	3.9	3.6	-
104	-	-	3.5	4.3	-
105	-	-	4.3	2.6	-
106	-	-	3.6	2.3	-
107	-	-	4	-	-
108	-	-	-	-	-
Average	143.7371354	583.0729167	5.789719626	5.830188679	2.073958333
St. deviation	29.56048616	174.2610736	1.343585284	1.919864864	0.715198806
Error	0.307921731	1.815219516	0.012556872	0.018111933	0.007449988

T-test (vs CTRL)	2.13373E-18	1.53928E-12	7.78092E-11	2.60442E-08	7.87449E-09
<i>S.viridis + A. brasiliense ntrC</i>					
	Root area (cm ²)	Number of lateral roots	Leaf length (cm)	Leaf dry weight (g)	Root dry weight (g)
1	108.324	445	7.3	7.7	2.2
2	133.474	568	5	9.3	1.5
3	82.592	234	6.9	4.3	2.8
4	100.935	454	6.8	7.4	2.8
5	127.62	595	4.7	6.4	2.4
6	172.879	471	5.9	7.7	2.2
7	135.693	686	5	5.9	3.4
8	120.461	536	5.2	6.3	1.9
9	126.599	452	6	6	1.6
10	130.344	628	6.8	4	2.4
11	130.158	615	4.8	6.8	2.6
12	124.047	576	5.5	6.2	2.3
13	126.031	576	6.2	7.9	2.5
14	153.606	606	6.6	5.4	1.5
15	161.823	654	5.5	8.8	1.7
16	151.861	854	5.9	7.3	2.5
17	144.067	574	6.9	5	2.7
18	108.007	582	5.5	5.4	3.1
19	154.652	776	5.5	4.6	2
20	172.327	694	6.8	8.9	1.6
21	119.01	603	6.8	6.1	1.8
22	135.206	509	6.9	8.8	2.6
23	152.736	604	7.1	7.5	2
24	141.131	606	5.9	6.4	2.3
25	129.551	665	5.7	7.5	1.8
26	186.343	892	6	6.7	1.4
27	122.701	514	6.2	5.5	2.1
28	143.352	674	5.7	6.7	2
29	137.113	509	6.2	5.7	1.8
30	139.374	619	5.9	4	1.9
31	164.195	742	5.5	5	2.6
32	124.719	841	5.7	6.6	1.8
33	96.57	531	6.7	7.8	1.5
34	120.264	780	8.6	8.9	1
35	95.045	437	4.5	5.9	1.5
36	104.921	567	6.6	8.8	2.6
37	102.391	477	5.8	6.9	2.1
38	81.538	522	7.9	4.9	1.8
39	67.709	392	5.6	6.5	2.2
40	97.9	529	8.1	5.6	1.6
41	86.31	477	7	6.6	2.2
42	101.186	654	6.3	5.2	1.6

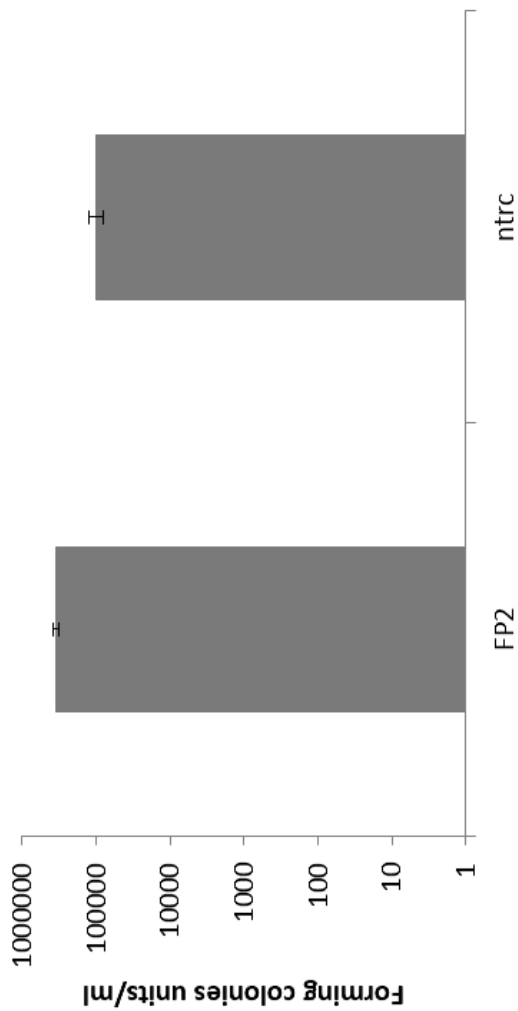
43	106.803	528	7.3	6.5	2.3
44	117.685	607	7.4	6.3	1.8
45	109.625	522	6.6	5.8	2.6
46	101.776	591	6.4	6.3	1.4
47	49.429	269	6.9	7.9	1.4
48	84.376	530	7	5.6	3.2
49	49.186	177	6.2	4.6	1.9
50	73.866	375	7.5	4.9	1.8
51	103.51	431	7.1	7.8	2
52	96.679	667	6.7	5.8	1.1
53	98.95	836	7.1	6.1	2.9
54	111.036	510	6	10.3	2.2
55	120.951	643	6.9	8.9	1.4
56	82.896	467	7	6.2	2.7
57	63.636	408	5.6	4.7	1.4
58	71.738	425	5.8	6.3	1.9
59	141.877	838	7.3	4.8	1.6
60	72.171	483	7.2	8.5	2.2
61	81.274	587	6.9	5.7	2.3
62	72.399	403	7.3	8.1	1.7
63	115.113	716	8.1	5.8	2.6
64	114.694	314	7	6.7	1.6
65	134.375	479	7	5.4	2
66	139.656	338	6.5	7	3
67	177.094	472	6.9	7.4	2.2
68	190.228	375	6.1	8.3	1.1
69	123.769	254	6.3	6.4	1.7
70	127.264	370	6.6	7.6	1.6
71	85.668	272	7.8	8.5	1.5
72	93.995	366	6.6	4.5	1.6
73	100.974	270	5	2.5	1.2
74	88.444	243	4.5	3.6	1.6
75	100.127	467	4	3.1	1.6
76	135.256	544	4.5	4.9	1.3
77	88.505	339	5.4	5.3	1.2
78	97.324	318	4.8	3.1	1.2
79	75.748	161	4.3	4	0.9
80	138.414	553	4.2	4.8	1.2
81	111.516	442	4.8	4.2	2.2
82	95.722	446	3.7	4.6	1.5
83	132.798	444	4.8	5.9	2
84	98.771	462	4.1	4.4	1.2
85	88.19	168	4.2	3.8	1.5
86	148.579	548	4.2	3.3	0.8
87	90.03	359	4.4	3.4	1.1
88	77.877	251	4.7	4.1	1.5

89	89.563	344	5	2.8	1.6
90	136.601	561	4.6	2.9	1.6
91	113.982	563	4.6	4.2	1
92	115.144	462	3.8	2.4	1.9
93	135.85	410	4.3	3.5	1.3
94	112.707	343	4.4	3	1.5
95	145.918	463	3.9	3.6	1.2
96	-	-	4.9	2.9	1.5
97	-	-	4	3.5	1.8
98	-	-	4.4	2.5	1
99	-	-	4.5	3	1.6
100	-	-	4.3	4.9	0.8
101	-	-	3.9	4.6	-
102	-	-	5	5	-
103	-	-	4.8	2.6	-
104	-	-	4.2	4.6	-
105	-	-	3.7	4.8	-
106	-	-	4	3.2	-
107	-	-	-	4	-
108	-	-	-	4.9	-
Average	115.2055158	506.6736842	5.797169811	5.662037037	1.854
St. deviation	29.47401828	157.6762467	1.200271789	1.805429958	0.562035586
Error	0.310252824	1.659749966	0.011323319	0.016716944	0.005620356
T-test (vs CTRL)	0.003595589	4.91517E-06	3.68851E-12	2.74353E-07	2.95734E-05
T-test (vs FP2)	3.16237E-10	0.001833417	0.966152468	0.512098834	0.018583701

FONTE: a autora (2018).

FIGURE 19 - ROOT COLONIZATION OF WILD TYPE AND MUTANT STRAIN. Twenty days after inoculation the number of CFU was determined.

Colonization assay



FONTE: a autora (2018).

3. CONSIDERAÇÕES FINAIS

A análise proteômica revelou a variação de enzimas importantes em função do nível de nitrogênio e da ausência do regulador transcricional NtrC. Um total de 2254 proteínas foram identificadas, sendo 1721 diferenciais nas comparações realizadas. Em ambas estirpes estudadas, a limitação de nitrogênio alterou principalmente vias relacionadas ao metabolismo de amino ácidos, transporte e transdução de sinais. Foi possível determinar uma lista de 112 proteínas candidatas à regulação por NtrC, considerando proteínas induzidas exclusivamente na estirpe selvagem em baixo nitrogênio. Para essas proteínas foi feita uma análise nas regiões promotoras de seus genes em busca de sítios sigma 54, considerando que NtrC ativa a transcrição de maneira dependente desse fator. Vinte e um genes apresentaram putativos sítios de ligação sigma 54, com boa sobreposição da sequência consenso. Grande parte das proteínas candidatas à regulação por NtrC, e coincidentemente também os mais altos “fold changes”, são transportadores ABC ou outros sistemas de transporte relacionados a nitrogênio. Esses dados estão em concordância com estudos prévios que demonstraram o envolvimento de NtrC na regulação do transporte e assimilação de fontes alternativas de nitrogênio em *E. coli* (Zimmer *et al.*, 2000). A proteína TrpE(G) está entre as possivelmente reguladas por NtrC. Essa enzima catalisa a primeira etapa da biossíntese de triptofano, que está relacionado à produção de IAA pela bactéria (Shi-Mei, 2006), sugerindo uma possível correlação entre NtrC e a produção desse hormônio. Também foram encontradas enzimas do metabolismo de carboidratos, de amino ácidos e lipídeos, suportando a hipótese de que NtrC está envolvido na regulação de diversas vias metabólicas. Proteínas envolvidas na transdução de sinais também estão entre as possíveis induzidas por NtrC, incluindo HupB, HrcA, FlcA, sendo a maioria delas relacionadas à resposta a estresse. Nossos resultados sugerem uma co-regulação entre o metabolismo de nitrogênio e fosfato, que pode ser mediada por NtrC, uma vez que PhoR (histidina quinase do sistema de dois componentes que controla a expressão de enzimas relacionadas à aquisição de fosfato) e PhoH (*phosphate starvation protein*) estão entre as possíveis proteínas induzidas por esse ativador. Essa co-regulação já foi relatada em estudos prévios em *Sinorhizobium meliloti* (Hagberg, 2016). Onze proteínas relacionadas à resposta a estresse oxidativo estão entre as candidatas à regulação por NtrC. Entre elas, YhaK, considerada marcador de estresse oxidativo em *E. coli* (Gurmu, 2008),

GstA, que cataliza a conjugação de glutationa reduzida com compostos eletrofílicos tóxico (Hayes, 2005). Além dessas, as enzimas MsrA, Ohr, AzoR, também relacionadas a estresse oxidativo, estão mais expressas exclusivamente na estirpe selvagem em baixo nitrogênio. Esse resultado nos levou à hipótese de que NtrC poderia estar envolvido na resposta a estresse oxidativo. Analisamos a taxa de crescimento das duas estirpes estudadas, em baixo e alto nitrogênio, na presença de diferentes concentrações de peróxido de hidrogênio e verificamos que ambas estirpes são mais sensíveis a estresse oxidativo quando em limitação de nitrogênio. Além disso, o crescimento da estirpe mutante foi prejudicado com 0,5 mM de peróxido de hidrogênio, e totalmente inibido em 2 e 4 mM, independente do nível de nitrogênio. Após quatro horas da adição de peróxido de hidrogênio e em baixo nitrogênio, o número de células viáveis da estirpe selvagem e do controle sem adição de peróxido foi muito próximo, enquanto que nenhuma célula viável foi recuperada na estirpe mutante. Em alto nitrogênio e em 4 mM de peróxido, a estirpe selvagem apresentou uma diminuição no número de células viáveis nas primeiras horas, mas que foi recuperado em 4 horas. Essa mesma condição foi letal para a estirpe mutante, indicando que NtrC é fundamental para sobrevivência de *A. brasiliense* sob estresse oxidativo.

Seguindo as mesmas condições da análise proteômica, foi realizada análise dos metabólitos presentes na fase polar do extrato através de GC/MS. Foram detectados 167 compostos, dos quais 75 foram identificados. Na estirpe selvagem em baixo nitrogênio, três açúcares estão mais abundantes em relação à condição de alto nitrogênio. Esse resultado está em concordância com a análise proteômica, que demonstrou alta atividade do metabolismo de carboidratos e energia nessa estirpe e condição. Por outro lado, em alto nitrogênio, a maior parte dos metabólitos identificados em ambas estirpes são amino ácidos, o que reflete o estado nutricional das células em uma condição de suficiência de nitrogênio. O metabólito que apresentou maior diferença de abundância na estirpe selvagem entre alto e baixo nitrogênio (FC 134,4) foi ácido úrico, resultante do catabolismo de purinas. No mutante esse metabólito também está mais abundante em alto nitrogênio. Ainda nessa via, a análise metabolômica revelou a presença de xantinas mais abundantes em ambas as estirpes em alto nitrogênio. Da mesma forma, o proteoma demonstrou proteínas diferenciais relacionadas ao metabolismo de purinas em ambas as

estirpes sob alto nitrogênio. Dentre os metabólitos mais abundantes no mutante em alto nitrogênio estão compostos orgânicos, um açúcar (D-mannitol), ácido fosfórico e poliaminas.

Para integrar dados de proteômica e metabolômica, proteínas e metabólitos diferenciais foram juntamente mapeados nas vias KEGG e os resultados demonstrados em porcentagem de cobertura da via, dessa forma foi possível avaliar o efeito geral da limitação de nitrogênio em cada estirpe. Dentre as vias reguladas na estirpe selvagem em baixo nitrogênio, a indução do metabolismo de glutationa é consistente com a hipótese de que NtrC estaria envolvido na resposta a estresse oxidativo. Para o mutante, a limitação de nitrogênio induziu principalmente vias de degradação de compostos aromáticos e do metabolismo de ácido cítrico.

O efeito da inoculação de *A. brasiliense* FP2 e seu mutante *ntrC* foi avaliado no modelo de gramíneas *Setaria viridis*. Ambas estirpes mostraram-se eficientes na promoção do crescimento vegetal quando comparadas ao controle não inoculado. Porém, foi constatado um aumento significativo nos parâmetros de crescimento de raiz das plantas inoculadas com a estirpe selvagem em relação à mutante. Os ensaios de colonização também não demonstraram diferenças entre as estirpes. Nossos resultados indicam que ambas estirpes são capazes de promover crescimento e colonizar igualmente *S. viridis*, portanto, NtrC não é um fator determinante nessas habilidades de *A. brasiliense*.

Dez genes cujos produtos proteicos estão induzidos na estirpe selvagem em baixo nitrogênio foram selecionados para validação por qRT-PCR. Dentre eles, 7 mostraram consistência entre expressão transcripcional e análise proteômica, confirmando a confiabilidade da análise. O nível de transcrição dos genes selecionados foi comparado entre as amostras utilizando FP2 sob baixo nitrogênio como controle. Os genes das enzimas azoreductase (AzoR), lipoprotein diacylglycerol transferase (LIPP) e acyl-CoA dehydrogenase (ACOA) estão mais expressos na estirpe mutante em baixo nitrogênio, portanto não são induzidos por NtrC. Por outro lado, os genes correspondentes às enzimas anthranilate synthase (ANTH), acyl-CoA dehydrogenase (CaiA), organic hydroperoxide resistance protein (OsmC), glutathione S-transferase (GLUT), phosphate starvation protein (PhoH) e long chain fatty acid Coa ligase (ACYL) estão menos expressos em FP2 alto

nitrogênio em relação ao controle, reforçando a hipótese de que são regulados por NtrC.

A limitação de nitrogênio levou a diferentes respostas proteômicas e metabolômicas entre as estirpes selvagem e mutante. A integração desses dados possibilitou a seleção de alvos candidatos à regulação por NtrC. Estudos mais detalhados serão necessários para compreender a relação entre NtrC e os alvos propostos neste trabalho. Estudos dos sítios de ligação de NtrC em *A. brasiliense* FP2 e a construção de estirpes mutantes para as proteínas candidatas constituem a continuação deste trabalho e podem levar a um esclarecimento mais detalhado da relação entre elas e o metabolismo de nitrogênio nesse microrganismo.

4. CONCLUSÕES

1. Os perfis proteômico e metabolômico mostraram que as mudanças biológicas de *A. brasiliense* FP2 e seu mutante *ntrC* em resposta à limitação de N são bastante distintos. Um total de 2254 proteínas foram identificadas, sendo que 1721 são diferenciais em pelo menos uma das comparações realizadas.
2. Os dados integrados levaram a vias metabólicas possivelmente reguladas por NtrC direta ou indiretamente, sendo que as vias de recombinação homóloga, quorum sensing e transportadores ABC são as mais induzidas no selvagem em baixo nitrogênio.
3. A análise dos conjuntos de proteínas diferenciais possibilitou a definição de 112 proteínas potencialmente induzidas por NtrC, no entanto mais estudos para confirmação são necessários.
4. Dentre os novos possíveis alvos de NtrC, a categoria mais induzida e com maiores “fold changes” é a de transportadores, corroborando a hipótese de que NtrC é um fator de transcrição envolvido no transporte e assimilação de fontes de nitrogênio.
5. A enzima antranilato sintase pertence ao grupo das potencialmente induzidas por NtrC e a expressão do seu mRNA está aumentada em baixo nitrogênio na estirpe selvagem, confirmando sua indução nessa condição. O envolvimento dessa enzima na síntese de ácido indolacético e sua potencial regulação por NtrC, levou à hipótese de que NtrC possa estar relacionado à promoção de crescimento em plantas.

6. Onze proteínas relacionadas a resposta contra estress oxidativo estão entre as potencialmente reguladas por NtrC. A indução do estresse oxidativo com peróxido de hidrogênio mostrou que a estirpe selvagem é mais resistente a esse tipo de estresse em relação à mutante, especialmente em alto nitrogênio. Levando à hipótese de que NtrC é importante para sobrevivência da bactéria sob estresse oxidativo e que a disponibilidade de nitrogênio interfere na habilidade da bactéria de sobreviver a esse estresse.
7. A proteína OsmC atua na resistência contra hidroperóxidos e está entre as candidatas à regulação por NtrC. Essa proteína apresentou sítio de ligação de NrtC e de sigma 54 na região promotora. Além disso, a análise do mRNA mostrou uma maior expressão em baixo nitrogênio na estirpe selvagem. Essas evidências tornam essa proteína uma forte candidata à indução por NtrC.
8. A análise da região promotora dos genes candidatos à regulação por NtrC mostrou que, dos 112 candidatos, 21 apresentam sítio de ligação sigma 54, incluindo *glnZ* e *ntrC*. Os demais genes estão relacionados a transportadores, quimiotaxia, síntese de cofatores e proteínas hipotéticas e são potencialmente regulados por NtrC.
9. A inoculação de *A. brasiliense* FP2 e seu mutante *ntrC* em *Setaria viridis* mostrou que ambas estirpes são capazes de promover crescimento vegetal em relação a plantas não inoculadas. Na comparação entre selvagem e mutante houve um aumento significativo dos parâmetros relacionados à raiz das plantas inoculadas com o selvagem em relação ao mutante, indicando que NtrC influencia, mas não inibe, a habilidade de promover crescimento vegetal.

REFERÊNCIAS

- ALTELAAR, A. F.; MUÑOZ, J.; HECK, A. J. Next-generation proteomics: towards an integrative view of proteome dynamics. **Nature Reviews Genetics.** v. 14 , p. 35-48, 2013.
- ÁLVAREZ-SÁCHEZ, B.; PRIEGO-CAPOTE, F.; LUQUE DE CASTRO, M. D.; Metabolomics analysis I. Selection of biological samples and practical aspects preceding sample preparation. **Trends Anal. Chem.** v. 29, p. 111-119, 2010.
- ARAÚJO, L.M.; HUERGO, L.F.; INVITTI, A.L.; GIMENES, C.I.; BONATTO, A.C.; MONTEIRO, R.A.; SOUZA, E.M.; PEDROSA, F.O.; CHUBATSU, L.S. Different responses of the GlnB and GlnZ proteins upon in vitro uridylylation by the *Azospirillum brasilense* GlnD protein. **Brazilian Journal of Medical and Biological Research.** v. 41(4), p. 289-294, 2008.
- ARCONDÉGUY, T.; JACK, R.; MERRICK, M. PII signal transduction proteins, pivotal players in microbial nitrogen control. **Microbiol. Mol. Biol. Rev.** v. 65, p. 80-105, 2001.
- ATKINSON, M. R.; NINFA, A. J. Role of the GlnK signal transduction protein in the regulation of nitrogen assimilation in *Escherichia coli*. **Molecular Microbiology**, v. 29, n. 2, p. 431-447, 1998.
- BALDANI, J.I.; BALDANI, V.L.D. History on the biological nitrogen fixation research in graminaceous plants: special emphasis on the Brazilian experience. **Anais da Academia Brasileira de Ciências.** v. 77, p. 549-579, 2005.
- BASHAN, Y.; HOLGUIN, G.; DE-BASHAN, L.E. *Azospirillum*-plant relationships physiological, molecular, agricultural, and environmental advances (1997-2003). **Can. J Microbiol.** v. 50, p. 521-577, 2004.
- BENDER, R. A. The role of the NAC protein in the nitrogen regulation of *Klebsiella aerogenes*. **Mol. Microbiology**. v. 5, p. 2575-2580, 1991.

BENNETT, B. D.; KIMBALL, E. H.; GAO, M.; OSTERHOUT, R.; VAN DIEN, S. J.; RABINOWITZ, J. D. Absolute metabolite concentrations and implied enzyme active site occupancy in *Escherichia coli*. **Nat Chem Biol.** p. 593-599, 2009.

BIBLE, A.N.; KHALSA-MOYERS, G.K.; MUKHERJEE, T.; GREEN, C.S.; MISHRA, P.; PURCELL, A.; ALEXANDRE, G. Metabolic Adaptations of *Azospirillum brasiliense* to Oxygen Stress by Cell-to-Cell Clumping and Flocculation. **Applied and Environmental Microbiology**. v. 81(24), p. 8346–8357, 2015.

BRADFORD, M.M. A rapid and sensitive method for the quantitation of microgram quantities of protein utilizing the principle of protein-dye binding. **Analytical Biochemistry**. v. 72(1), p. 248-254, 1976.

CARRENO-LOPEZ, R.; CAMPOS-REALES, N.; ELMERICH, C.; BACA, B.E. Physiological evidence for differently regulated tryptophan-dependent pathways for indole-3-acetic acid synthesis in *Azospirillum brasiliense*. **Mol. Gen. Genet.** v. 264, p. 521-530, 2000.

CASPI, R.; ALTMAN, T.; DREHER, K.; FULCHER, C. A.; SUBHRAVETI, P.; KESELER, I. M.; KOTHARI, A.; KRUMMENACKER, M.; LATENDRESSE, M.; MUELLER, L. A.; ONG, Q.; PALEY, S.; PUJAR, A.; SHEARER, A. G.; TRAVERS, M.; WEERASINGHE, D.; ZHANG, P.; KARP, P. D.; The MetaCyc database of metabolic pathways and enzymes and the BioCyc collection of pathway/genome databases. **Nucleic Acids Res.** v. 40, p. 742-53, 2012.

CATHERMAN, A. D.; SKINNER, O. S.; KELLEHER, N. L. Top Down proteomics: Facts and perspectives. **Biochemical and Biophysical Research Communications**. v. 445, p. 683-693, 2014.

CHOKSHI, K.; PANCHA, I.; GHOSH, A.; MISHRA, S. Nitrogen starvation-induced cellular crosstalk of ROS-scavenging antioxidants and phytohormone enhanced the biofuel potential of green microalga *Acutodesmus dimorphus*. **Biotechnol. Biofuels**. v. 10(1), p. 60, 2017.

CHUBATSU, L.; MONTEIRO, R.; DE SOUZA, EMANUEL; *et al.* Nitrogen fixation control in *Herbaspirillum seropedicae*. **Plant and Soil**, v. 356, n. 1, p. 197–207, 2012.

COLLINS, C. M.; GUTMAN, M. D.; LAMAN, H. Identification of a nitrogen-regulated promoter controlling expression of *Klebsiella pneumonia* urease genes. **Mol. Microbiology**. v. 8, p. 187-198, 1993.

COUTTS, C.; THOMAS, G.; BLKEY, D. MERRICK, M. Membrane sequestration of the signal transduction protein GlnK by the ammonium transporter AmtB. **EMBO J.** v. 21, p. 536-545, 2002

CUSSIOL, J.R.; ALVES, S.V.; DE OLIVEIRA, M.A.; NETTO, L.E. Organic hydroperoxide resistance gene encodes a thiol-dependent peroxidase. **J. Biol. Chem.** v. 278, p. 11570–11578, 2003.

DAVALOS, M.; FOURMENT, J.; LUCAS, A.; BERGES, H.; KAHN, D. 2004. Nitrogen regulation in *Sinorhizobium meliloti* probed with whole genome arrays. **FEMS Microbiol Lett.** v. 241, p. 33–40, 2004.

DE VOS, R. C. H.; MOCO, S.; LOMMEN, A.; KEURENTJES, J. J. B.; BINO, R. J.; HALL, R. D. Untargeted large-scale plant metabolomics using liquid chromatography coupled to mass spectrometry. **Nature Protocols**. v. 2, p. 778-791, 2007.

DE ZAMAROCZY, DELORM, F.; ELMERICH, C. Characterization of three different nitrogen-regulated promoter regions for the expression of *glnB* and *glnA* in *Azospirillum brasilense*. **Mol. Gen. Genet.** v. 224, p. 421-430, 1990.

DE ZAMAROCZY, M. Structural homologues P_{II} and P_z of *Azospirillum brasilense* provide intracellular signaling for selective regulation of various nitrogen-dependent functions. **Mol. Microbiol.** v. 29, p. 449-463, 1998.

DE ZAMAROCZY, M.; PAQUELIN, A.; ELMERICH, C. Function organization of the *glnB-glnA* cluster of *Azospirillum brasilense*. **J. Bacteriol.** v. 175, p. 2507-2515, 1993.

DE ZAMAROCZY, M.; PAQUELIN, A.; PELTRE, G.; FORCHHAMMER, K.; ELMERICH, C. Coexistence of two structurally similar but functionally different PII proteins in *Azospirillum brasilense*. **J. Bacteriol.** v. 178, p. 4143-4149, 1996.

DE ZAMAROCZY, PAQUELIN, A.; ELMERICH, C. Function organization of the *glnB-glnA* cluster of *Azospirillum brasilense*. **J. Bacteriol.** v. 175, p. 2507-2515, 1993.

DO AMARAL F.P.; PANKIEVICZ V.C.; ARISI A.C.; DE SOUZA E.M.; PEDROSA F.; STACEY G. Differential growth responses of *Brachypodium distachyon* genotypes to inoculation with plant growth promoting rhizobacteria. **Plant Mol Biol.** v. 90, p. 689-697, 2016.

DUDLEY, E.; YOUSEF, M.; WANG, Y.; GRIFFITHS, W. J. Targeted metabolomics and mass spectrometry. **Advances in Protein Chemistry and Structural Biology.** v. 80, p. 45 - 83, 2010.

EL-ANEED, A.; COHEN, A.; BANOUB, J. Mass Spectrometry, Review of the Basics: Electrospray, MALDI, and Commonly Used Mass Analyzers. **Applied Spectroscopy Reviews.** v. 44, p. 210-230, 2009.

FENN, J. B.; MANN, M.; MENG, C. K.; WONG, S. F.; WHITEHOUSE, C. M. Electrospray ionization for mass spectrometry of large biomolecules. **Science.** v. 246, p. 64-71, 1989.

FIEHN, O. Metabolomics - the link between genotypes and phenotypes. **Plant Molecular Biology.** v. 48, p. 155-171, 2002.

FOKINA, O.; CHELLAMUTHU, V.-R.; FORCHHAMMER, KARL; ZETH, K. Mechanism of 2-Oxoglutarate Signaling by the *Synechococcus elongatus* PII Signal Transduction Protein. **Proceedings of the National Academy of Sciences of the USA,** v. 107, n. 46, p. 19760–19765, 2010.

FRANCK, W.L.; QIU, J.; LEE, H.I.; CHANG, W.S.; STACEY, G. DNA microarray-based identification of genes regulated by the two-component NtrBC system in

Bradyrhizobium japonicum. **Appl. Environ. Microbiol.** v. 81(16), p. 5299-308, 2015.

GARCIA, A.; BARBAS, C.; Em Gas Chromatography-mass Spectrometry (GC-MS)-based metabolomics. **Methods Mol Biol.** v. 708, p. 191-204, 2011.

GARDNER, S.G.; JOHNS, K.D.; TANNER, R.; MCCLEARY, W.R. The PhoU protein from *Escherichia coli* interacts with PhoR, PstB, and metals to form a phosphate-signaling complex at the membrane. **J. Bacteriol.** v. 196, p. 1741–1752, 2014.

GE, S.M.; XIE, B.E.; CHEN, S.F. Characterization of two trpE genes encoding anthranilate synthase α-subunit in *Azospirillum brasilense*. **Biochem. Biophys. Res. Commun.** v. 341, p. 494–499, 2006.

GERHARDT, E.C.; RODRIGUES, T.E.; MULLER-SANTOS, M.; PEDROSA, F.O.; SOUZA, E.M.; FORCHHAMMER, K.; HUERGO, L.F. The Bacterial signal transduction protein GlnB regulates the committed step in fatty acid biosynthesis by acting as a dissociable regulatory subunit of acetyl-CoA carboxylase. **Mol Microbiol.** v. 95, p. 1025-1035, 2015.

GLISH, G. L.; VACHET, R. W. The basics of mass spectrometry in the twenty-first century. **Nature Reviews Drug Discovery.** v. 2, p. 140-150, 2003.

GRANT, C.E.; BAILEY, T.L.; NOBLE, W.S. FIMO: Scanning for occurrences of a given motif. **Bioinformatics.** v. 27(7), p. 1017-1018, 2011.

GREEN, E. R., & MECSAS, J. Bacterial Secretion Systems – An overview. **Microbiology Spectrum.** v. 4(1), 10.1128/microbiolspec.VMBF-0012-2015, 2016.

GRUSWITZ, F.; O'CONNELL, J., 3rd; STROUD, R. M. Inhibitory complex of the transmembrane ammonia channel, AmtB, and the cytosolic regulatory protein, GlnK, at 1.96 Å. **Proceedings of the National Academy of Sciences of the USA,** v. 104, n. 1, p. 42–47, 2007.

GUO, B.; CHEN, B.; LIU, A.; ZHU, W.; YAO, S.; Liquid chromatography-mass spectrometric multiple reaction monitoring-based strategies for expanding targeted profiling towards quantitative metabolomics. **Curr. Drug Metab.** v. 13, p. 1226-43, 2012.

GURMU, D.; LU, J.; JOHNSON, K.A.; NORDLUND, P.; HOLMGREN, A.; ERLANDSEN, H. The crystal structure of the protein YhaK from *Escherichia coli* reveals a new subclass of redox sensitive enterobacterial bicupins. **Proteins.** v. 74, p. 18–31, 2009.

HAGBERG, K.L.; YURGEL, S.N.; MULDER, M.; KAHN, M.L. Interaction between Nitrogen and Phosphate Stress Responses in *Sinorhizobium meliloti*. **Frontiers in Microbiology.** v. 7, p. 1928, 2016.

HALBLEID, C M; ZHANG, Y; LUDDEN, P W. Regulation of dinitrogenase reductase ADP-ribosyltransferase and dinitrogenase reductase-activating glycohydrolase by a redox-dependent conformational change of nitrogenase Fe protein. **The Journal of Biological Chemistry**, v. 275, n. 5, p. 3493–3500, 2000.

HAYES, J.D.; FLANAGAN, J.U.; JOWSEY, I.R. Glutathione transferases. **Annu Rev Pharmacol Toxicol.** v. 45, p. 51–88, 2005.

HERVAS, A.B.; CANOSA, I.; SANTERO, E. Transcriptome analysis of *Pseudomonas putida* in response to nitrogen availability. **J Bacteriol.** v. 190, p. 416–420, 2008.

HERVÁS, A. B.; CANOSA, I.; LITTLE, R.; DIXON, R.; SANTERO, E. NtrC-dependent regulatory network for nitrogen assimilation in *Pseudomonas putida*. **J Bacteriol.** v. 191, p. 6123–6135, 2009.

HEIN, M. Y. Proteomic Analysis of Cellular Systems. In: Walhout, A. J. M., Vidal, M., et al. **Handbook of Systems Biology**. Academic Press, p.3-25, 2013.

HO, C. S. Electrospray Ionisation Mass Spectrometry: Principles and Clinical Applications. **The Clinical Biochemist Reviews.** v. 24, p. 3-12, 2003.

HOAGLAND, D.R.; ARNON, D.I. The water culture method for growing plants without soil. **J. Circ. Calif. Agric. Experiment Stn.** v. 347, p. 32, 1950.

HOU, X.; MCMILLAN, M.; COUMANS, J.V.F.; POLJAK, A.; RAFTERY, M.J.; PEREG, L. Cellular responses during morphological transformation in *Azospirillum brasilense* and its *flcA* knockout mutant. **PLoS ONE.** v. 9(12), e114435, 2014.

HUANG, L. Y.; GUO, W.; JIA, L.; FU, Y.; GUI, S.; LU, F. Cloning, expression, and characterization of a thermostable and pH-stable laccase from *Klebsiella pneumoniae* and its application to dye decolorization. **Process Biochem.** v. 53, p.125–134, 2017.

HUERGO, L. F., SOUZA, E. M., STEFFENS, M. B., YATES, M. G., PEDROSA, F. O., CHUBATSU, L. S. Regulation of *glnB* gene promoter expression in *Azospirillum brasilense* by the NtrC protein. **FEMS Microbiol. Lett.**, v. 6, n. 223 (1), p. 33-40, 2003.

HUERGO, L. F.; CHANDRA, G.; MERRICK, M. PII signal transduction proteins: nitrogen regulation and beyond. **Fems Microbiology Reviews**, v. 37, n. 2, p. 251-283, 2013.

HUERGO, L. F.; CHUBATSU, L. S.; SOUZA, E. M.; PEDROSA, F. O.; STEFFENS,M. B.; MERRICK, M. Interactions between PII proteins and the nitrogenase regulatory enzymes DraT and DraG in *Azospirillum brasilense*. **FEBS Lett.** v.580(22), p. 5232-6, 2006.

HUERGO, L. F.; MERRICK, M.; MONTEIRO, R. A. *et al.* *In Vitro* Interactions between the PII Proteins and the Nitrogenase Regulatory Enzymes Dinitrogenase Reductase ADP-ribosyltransferase (DraT) and Dinitrogenase Reductase-activating Glycohydrolase (DraG) in *Azospirillum brasilense*. **Journal of Biological Chemistry**, v. 284, n. 11, p. 6674–6682, 2009.

HUERGO, L.F.; ASSUMPCAO, M.C.; SOUZA, E.M.; STEFFENS, M.B.; YATES, M.G.; CHUBATSU, L.S.; PEDROSA, F.O. Repressor mutant forms of the

Azospirillum brasilense NtrC protein. **Appl Environ Microbiol.** v. 70, p. 6320-6323, 2004.

HUERGO, L.F.; MONTEIRO, R.A.; BONATTO, A.C.; RIGO, L.U.; STEFFENS, M.B.R.; CRUZ, L.M.; CHUBATSU, L.S.; SOUZA, E.M.; PEDROSA, F.O. Regulation of nitrogen fixation in *Azospirillum brasilense*. In: CASSÁN, F.D.; GARCIA DE SALAMONE, I. ***Azospirillum* sp.**: cell physiology, plant interactions and agronomic research in Argentina. Asociación Argentina de Microbiología, Argentina, p.17-35, 2008.

HUERGO, L.F.; SOUZA, E.M.; ARAUJO, M.S.; PEDROSA, F.O.; CHUBATSU, L.S.; STEFFENS, M.B.; MERRICK, M. ADP-ribosylation of dinitrogenase reductase in *Azospirillum brasilense* is regulated by AmtB-dependent membrane sequestration of DraG. **Mol. Microbiol.** v. 59, p. 326-337, 2006.

JAVELLE, A.; SEVERI, E.; THORNTON, J.; MERRICK , M. Ammonium sensing in *Escherichia coli*. Role of the ammonium transporter AmtB and AmtB-GlnK complex formation. **J. Biol. Chem.** v. 279 (10), p. 8530-8538, 2004.

JIANG P.; NINFA A.J. Regulation of Autophosphorylation of *Escherichia coli* Nitrogen Regulator II by the PII Signal Transduction Protein. **Journal of Bacteriology.** v. 181(6), p. 1906-1911, 1999.

JIANG, P.; NINFA, A. J. Sensation and signaling of alpha-ketoglutarate and adenylylate energy charge by the *Escherichia coli* PII signal transduction protein require cooperation of the three ligand-binding sites within the PII trimer. **Biochemistry**, v. 48, n. 48, p. 11522-11531, 2009.

JIANG, P.; PELISKA, J. A.; NINFA, A. J. The regulation of *Escherichia coli* glutamine synthetase revisited: role of 2-ketoglutarate in the regulation of adenylylation state. **Biochemistry**. v. 37, p. 12802-12810, 1998.

KAMBEROV, E. S., ATKINSON, M. R., NINFA, A. J. The *Escherichia coli* PII signal transduction protein is activated upon binding 2-ketoglutarate and ATP. **J. Biol. Chem.**, v. 270, p. 17797 – 17807, 1995.

KANAI, T.; TAKAHASHI, K.; INOUE, H. Three Distinct-Type Glutathione S-Transferases from *Escherichia coli* important for defense against oxidative stress. **The Journal of Biochemistry.** v. 140 (5), p. 703–711, 2006.

KANEHISA, M.; GOTO, S.; HATTORI, M.; AOKI-KINOSHITA, K. F.; ITOH, M.; KAWASHIMA, S.; KATAYAMA, T.; ARAKI, M.; HIRAKAWA, M.; From genomics to chemical genomics: new developments in KEGG. **Nucleic Acids Res.** v. 34, p. 354-7, 2006.

KARP, P. D.; CASPI, R.; A survey of metabolic databases emphasizing the MetaCyc family. **Arch. Toxicol.** v. 85, p. 1015-33, 2011.

KLASSEN, G., DE SOUZA, E. M., YATES, M. G., RIGO, L. U., INABA, J., PEDROSA, F. DE O. Control of nitrogenase reactivation by the GlnZ protein in *Azospirillum brasilense*. **J. Bacteriol.**, v. 183, n.22, p. 6710-6713, 2001.

KLASSEN, G., SOUZA, E. M., YATES, M. G., RIGO, L. U., COSTA, R. M., INABA, J., PEDROSA, F. O. Nitrogenase switch-off by ammonium ions in *Azospirillum brasilense* requires the GlnB nitrogen signal transducing protein. **App. Env. Microbiol.** v. 71, p. 5637-5641, 2005.

KNOCHENMUSS, R.; ZENOBI, R. MALDI ionization: the role of in-plume processes. **Chemical Reviews.** v. 103, p. 441-452, 2003.

KUEHNBAUM, N. L.; BRITZ-MCKIBBIN, P.; New advances in separation science for metabolomics: resolving chemical diversity in a post-genomic era. **Chem. Ver.** v. 113, p. 2437-68, 2013.

KUEHNBAUM, N. L.; GILLEN, J. B.; KORMENDI, A.; LAM, K. P.; DIBATTISTA, A.; GIBALA, M. J.; BRITZ-MCKIBBIN, P.; Multiplexed separations for biomarker discovery in metabolomics: Elucidating adaptive responses to exercise training. **Electrophoresis.** v. 36, p. 2226-2236, 2015.

LEI, Z.; HUHMAN, D. V.; SUMMER, L. W. Mass spectrometry strategies in metabolomics. **J Biol Chem.** v. 286, p. 25435-42, 2011.

LI, H. et al. cDNA-AFLP analysis of differential gene expression related to cell chemotactic and encystment of *Azospirillum brasilense*. **Microbiol Res**, v. 166, n. 8, p. 595-605, 2011.

LIANG, Y. Y.; DE ZAMAROCZY, M.; ARSENE, F.; PAQUELIN, A.; ELMERICH, C. Regulation of nitrogen fixation in *Azospirillum brasilense* Sp7: involvement of *nifA*, *glnA* and *glnB* gene products. **FEMS Microbiol. Lett.** v. 79, p. 113 – 119, 1992.

LINDON, J. C.; NICHOLSON, J. K. Analytical technologies for metabonomics and metabolomics, and multi-omic information recovery. **Trends in Analytical Chemistry**. v. 27, p. 194-205, 2008.

LIU, G.; ZHOU, J.; FU, Q.S.; WANG, J. The *Escherichia coli* azoreductase AzoR is involved in resistance to thiol-specific stress caused by electrophilic quinones. **J Bacteriol**. v. 191, p. 6394–6400, 2009.

LIVAK, K.J.; SCHMITTGEN, T.D. Analysis of relative gene expression data using real time quantitative PCR and the 2(Delta Delta C(T)) method. **Methods**. v. 25, p. 402–408, 2001.

MACHADO, H. B.; YATES, M. G.; FUNAYAMA, S.; RIGO, L. U.; STEFFENS, M. B. R.; SOUZA, E. M., PEDROSA, F. O. The *ntrBC* genes of *Azospirillum brasilense* are part of a *nifR3-like-ntrB-ntrC* operon and are negatively regulated. **Can. J. Microbiol.** v. 41, p. 674-684, 1995.

MADSEN, R.; LUNDSTEDT, T.; TRYGG, J.; Chemometrics in metabolomics--a review in human disease diagnosis. **Anal. Chim. Acta**. v. 659, p. 23-33, 2010.

MANN, M.; HENDRICKSON, R. C.; PANDEY, A. Analysis of proteins and proteomes by mass spectrometry. **Annual Review of Biochemistry**. v. 70, p. 437-473, 2001.

MARSHALL, A. G.; HENDRICKSON, C. L.; JACKSON, G. S. Fourier transform ion cyclotron resonance mass spectrometry: A primer. **Mass Spectrometry Reviews**. v. 17, p. 1-35, 1998.

MARTIN, D. E.; REINHOLD-HUREK, B. Distinct roles of PII-like signal transmitter proteins and *amtB* in regulation of *nif* gene expression, nitrogenase activity, and posttranslational modification of NifH in *Azoarcus* sp. strain BH72. **J. Bacteriol.** v. 184, p. 2251-2259, 2002.

NINFA, A.J.; JIANG, P. PII signal transduction proteins: sensors of alpha-ketoglutarate that regulate nitrogen metabolism. **Current Opinion Microbiol.** v. 8, p. 168-173, 2005.

NINFA, E. G.; ATKINSON, M. R.; KAMBEROV, E. S.; NINFA, A. J. Mechanism of autophosphorylation of *Escherichia coli* nitrogen regulator II (NRII or NtrB): trans phosphorylation between subunits. **J. Bacteriol.** v. 175, p. 7024-7032, 1993.

NINFA, E.G.; ATKINSON, M.R.; KAMBEROV, E.S.; NINFA, A.J. Mechanism of autophosphorylation of *Escherichia coli* nitrogen regulator II (NRII or NtrB): transphosphorylation between subunits. **Journal of Bacteriology.** v. 175(21), p. 7024–7032, 1993.

OBERTO, J., NABTI, S., JOOSTE, V., MIGNOT, H., & ROUVIERE-YANIV, J. The HU Regulon Is Composed of Genes Responding to Anaerobiosis, Acid Stress, High Osmolarity and SOS Induction. **PLoS ONE.** v. 4(2), e4367, 2009.

O'FARRELL, P. H. High Resolution Two-Dimensional Electrophoresis of Proteins. **The Journal of biological chemistry.** v. 250, p. 4007-4021, 1975.

OGATA, H.; GOTO, S.; SATO, K.; FUJIBUCHI, W.; BONO, H.; KANEHISA, M. KEGG: Kyoto Encyclopedia of Genes and Genomes. **Nucleic Acids Res.** v. 27 (1), p. 29–34, 1999.

OJEN, D.B.; MOSKOVITZ; J. Substrates of the methionine sulfoxide reductase system and their physiological relevance. **Curr Top Dev Biol.** v. 80, p. 93–133, 1998.

OKON Y. Azospirillum as a potential inoculant for agriculture. **Trends Biotechnol.** v. 3, p. 223–228, 1985.

PANKIEVICZ, V. C.; AMARAL, F. P.; SANTOS, K. F.; AGTUCA, B. ; XU, Y.; SCHUELLER, M. J.; ARISI, A. C.; STEFFENS, M. B.; SOUZA, E. M.; PEDROSA, F. O.; STACEY, G.; FERRIERI, R. A. Robust biological nitrogen fixation in a model grass–bacterial association. **Plant J.** v. 81, p. 907-919, 2015.

PEDROSA, F.O.; YATES, M.G. Regulation of nitrogen fixation (*nif*) genes of *Azospirillum brasilense* by *nifA* and *ntrC* (*glnG*) type genes. **FEMS Microbiol. Lett.** v. 23(1), p. 95-101, 1984.

PEREG-GERK, L.; PAQUELIN, A.; GOUNON, P.; KENNEDY, I.R. A transcriptional regulator of the LuxR-UhpA family, FlcA, controls flocculation and wheat root surface colonization by *Azospirillum brasilense* Sp7. **Elmerich C Mol Plant Microbe Interact.** v. 11(3), p. 177-87, 1998.

POMASTOWSKI, P.; BUSZEWSKI, B. Two-dimensional gel electrophoresis in the light of new developments. **Trends in Analytical Chemistry.** v. 53, p. 167-177, 2014.

RAPPSILBER, J.; ISHIHAMA, Y.; MANN, M. Stop and Go Extraction Tips for Matrix-Assisted Laser Desorption/Ionization, Nanoelectrospray, and LC/MS Sample Pretreatment in Proteomics. **Analytical Chemistry.** v. 75(3), p. 663-670, 2003.

RATERINK, R. J.; LINDENBURG, P. W.; VREEKEN, R. J.; RAMAUTAR, R.; HANKEMEIER, T.; Recent developments in sample-pretreatment techniques for mass spectrometry-based metabolomics. **Trends Anal. Chem.** v. 61, p. 157-167, 2014.

REIS, V. M.; BALDANI, V. L. D.; BALDANI, J. I.; DÖBEREINER, J. Biological nitrogen fixation in gramineae and palm trees. **Critical Review in Plant Sciences,** v. 19, n. 3, p. 227-247, 2000.

REITZER, L. Nitrogen assimilation and gobal regulation in *Escherichia coli*. **Annual review in microbiology.** v. 57, p. 155-76, 2003.

RIOS, L.F.; KLEIN, B.C.; LUZ JR., L.F.; MACIEL FILHO, R.; WOLF MACIEL, M.R. Nitrogen starvation for lipid accumulation in the microalga species *Desmodesmus* sp. **Appl. Biochem. Biotechnol.** v. 175, p. 469-47, 2015.

RUIZ-MARIN, A.; MENDOZA-ESPINOSA, L.G.; STEPHENSON, T. Growth and nutrient removal in free and immobilized green algae in batch and semi-continuous cultures treating real wastewater. **Bioresource Technology**. v. 101, p. 58-64, 2010.

RUSSELL, A.B.; PETERSON, S.B.; MOUGOUS, J.D. Type VI secretion effectors: poisons with a purpose. **Nature Reviews. Microbiology**. v. 12(2), p. 137–148, 2014.

SACOMBOIO, E.N.M.; KIM, E.Y.S.; CORREA, H.L.R.; BONATO, P.; PEDROSA, F.O.; DE SOUZA, E.M.; CHUBATSU, L.S.; MULLER-SANTOS, M. The transcriptional regulator NtrC controls glucose-6-phosphate dehydrogenase expression and polyhydroxybutyrate synthesis through NADPH availability in *Herbaspirillum seropedicae*. **Sci. Rep.** v. 7, p. 13546, 2017.

SMITH, C. A. et al. METLIN: a metabolite mass spectral database. **Ther. Drug Monit.** v. 27, p. 747-751, 2005.

SMITH, C. A., WANT, E. J., O'MAILLE, G., ABAGYAN, R. & SIUZDAK, G. XCMS: processing mass spectrometry data for metabolite profiling using nonlinear peak alignment, matching and identification. **Anal. Chem.** v. 78, p. 779-787, 2006.

SUGIMOTO, M.; KAWAKAMI, M.; ROBERT, M.; SOGA, T.; TOMITA, M.; Bioinformatics Tools for Mass Spectroscopy-Based Metabolomic Data Processing and Analysis. **Curr. Bioinform.** v. 7, p. 96-108, 2012.

SUMNER, L.W.; AMBERG, A.; BARRETT, D.; BEALE, M.H.; BEGER, R.; DAYKIN, C.A.; FAN, T.W.-M; FIEHN, O.; GOODACRE, R.; GRIFFIN, J.L.; HANKEMEIER, T.; HARDY, N.; HARNLY, J.; HIGASHI, R.; KOPKA, J.; LANE, A.N.; LINDON, J.C.; MARRIOTT, P.; NICHOLLS, A.W.; REILY, M.D.;

- THADEN, J.J.; VIANT, M.R. Proposed minimum reporting standards for chemical analysis. **Metabolomics.** v. 3, p. 211–221, 2007.
- TABOR, C.W., & TABOR, H. Polyamines in microorganisms. **Microbiological Reviews.** v. 49(1), p. 81–99, 1985.
- TANAKA, K.; WAKI, H.; IDO, Y.; AKITA, S.; YOSHIDA, Y.; YOSHIDA, T.; MATSUO, T. Protein and polymer analyses up to m/z 100 000 by laser ionization time-of-flight mass spectrometry. **Rapid Communications in Mass Spectrometry.** v. 2, p. 151-153, 1988.
- TATUSOV, R.L.; GALPERIN, M.Y.; NATALE, D.A.; KOONIN, E.V. The COG database: a tool for genome-scale analysis of protein functions and evolution. **Nucleic Acids Res.** v. 28 (1), p. 33–36, 2000.
- TAUTENHAHN, R.; CHO, K.; URITBOONTHAI, W.; ZHU, Z. J.; PATTI, G. J.; SIUZDAK, G.; An accelerated workflow for untargeted metabolomics using the METLIN database. **Nat. Biotechnol.** v. 30, p. 826-8, 2012.
- TOTTEN, P. A.; LARA, J. C.; LORY, S. The *rpoN* gene product of *Pseudomonas aeruginosa* is required for expression of diverse genes, including the flagellin gene. **J. Bacteriol.** v. 172, p. 389-396, 1990.
- TRAVERS, A.; MUSKHELISHVILI, G. Bacterial chromatin. **Curr Opin Genet Dev.** v. 15, p. 507–514, 2005.
- TWEEDDALE, H.; NOTLEY-MCROBB, L.; FERENCI, T. Effect of slow growth on metabolism of *Escherichia coli*, as revealed by global metabolite pool (“metabolome”) analysis. **Journal of Bacteriology.** v. 180(19), p. 5109–5116, 1998.
- UNTERGASSER, A.; NIJVEEN, H.; RAO, X.; BISSELING, T.; GEURTS, R.; LEUNISSEN, J.A.M. Primer3Plus, an enhanced web interface to Primer3. **Nucleic Acids Research.** v. 35(Web Server issue), W71–W74, 2007.

VAN DOMMELEN, A.; KEIJERS, V.; SOMERS, E.; VANDERLEYDEN, J. Cloning and characterisation of the *Azospirillum brasilense* *glnD* gene and analysis of a *glnD* mutant. **Mol. Genet. Genomics**, v. 266, n. 5, p. 813-820, 2002.

VILLAS-BÔAS, S. G.; BRUHEIM, P.; The potential of metabolomics tools in bioremediation studies. **OMICS**. v. 11, p. 305-313, 2007.

VON WIRÉN, N.; MERRICK, M. Regulation and function of ammonium carriers in bacteria, fungi and plants. **Trends in Current Genetics**. v. 9, p. 95-120, 2004.

WHITEFORD, D.C.; KLINGELHOETS, J.J.; BAMBENEK, M.H.; DAHL, J.L. Deletion of the histone-like protein (Hlp) from *Mycobacterium smegmatis* results in increased sensitivity to UV exposure, freezing and isoniazid. **Microbiology**. v. 157, p. 327–335, 2011.

WISNIEWSKI-DYÉ, F.; BORZIAK, K.; KHALSA-MOYERS, G.; ALEXANDRE, G.; SUKHARNIKOV, L.O.; WUICHET, K.; HURST, G.B.; McDONALD, W.H.; ROBERTSON, J.S.; BARBE, V.; CALTEAU, A.; ROUY, Z.; MANGENOT, S.; PRIGENT-COMBARET, C.; NORMAND, P.; BOYER, M.; SIGUIER, P.; DESSAUX, Y.; ELMERICH, C.; CONDEMINE, G.; KRISHNEN, G.; KENNEDY, I.; PATERSON, A.H.; GONZÁLEZ, V.; MAVINGUI, P.; ZHULIN, I.B. *Azospirillum* genomes reveal transition of bacteria from aquatic to terrestrial environments. **PLoS Genet.** v. 7: e1002430, 2011.

XI, H.; SCHNEIDER, B. L.; REITZER, L. Purine Catabolism in *Escherichia coli* and function of xanthine dehydrogenase in purine Salvage. **Journal of Bacteriology**. v. 182(19), p. 5332–5341, 2000.

XIA, J.; PSYCHOGIOS, N.; YOUNG, N.; WISHART, D.S. MetaboAnalyst: a web server for metabolomic data analysis and interpretation. **Nucleic Acids Res.** v. 37, p. 652–660, 2009.

YEOM, S.; YEOM, J.; PARK, W. NtrC-sensed nitrogen availability is important for oxidative stress defense in *Pseudomonas putida* KT2440. **J. Microbiol.** v. 48, p. 153-159, 2010.

- YOSHIDA, M.; KASHIWAGI, K.; SHIGEMASA, A.; TANIGUCHI, S.; YAMAMOTO, K.; MAKINOSHIMA, H.; ISHIHAMA, A.; IGARASHI, K. A unifying model for the role of polyamines in bacterial cell growth, the polyamine modulon. **J Biol Chem.** v. 29; 279(44), p. 46008-13, 2004.
- ZALKIN, H.; SMITH, J.L. Enzymes utilizing glutamine as an amide donor. **Adv. Enzymol. Relat. Areas Mol. Biol.** v. 72, p. 87–144, 1998.
- ZHANG, Y., R. H. BURRIS, P. W. LUDDEN, G. P. ROBERTS. Posttranslational regulation of nitrogenase activity by anaerobiosis and ammonium in *Azospirillum brasilense*. **J Bacteriol.** v. 175, p.6781–6788, 1993.
- ZHANG, Y.; BURRIS, R. H.; LUDDEN, P.W.; ROBERTS, G. P. Regulation of nitrogen fixation in *Azospirillum brasilense*. **FEMS Microbiology Letters.** v. 152, p. 195-204, 1997.
- ZHANG, X.; CHANEY, M.; WIGNESHWERARAJ, S. R.; SCHUMACHER, J.; BORDES, P.; CANNON, W.; BUCK, M. Mechanochemical ATPases and transcriptional activation. **Mol. Microbiol.** v. 45, p. 895-903, 2002.
- ZHANG, Y.; POHLMANN, E.L.; ROBERTS, G.P. GlnD is essential for NifA activation, NtrB/NtrC-regulated gene expression, and posttranslational regulation of nitrogenase activity in the photosynthetic, nitrogen-fixing bacterium *Rhodospirillum rubrum*. **J. Bacteriol.**, v. 187, n. 4, 1254-1265, 2005.
- ZHANG, Y. M.; CHEN, H.; HE, C. L.; WANG, Q. Nitrogen Starvation Induced Oxidative Stress in an Oil-Producing Green Alga *Chlorella sorokiniana* C3. **PLoS ONE.** v. 8(7), p. 69225, 2013.
- ZHANG, Y.; FONSLOW, B. R.; SHAN, B.; BAEK, M. C.; YATES, J. R., 3RD. Protein analysis by shotgun/bottom-up proteomics. **Chemical Reviews.** v. 113, p. 2343-2394, 2013.
- ZHU, S.; WANG, Y.; HUANG, W.; XU, J.; WANG, Z.; XU, J.; YUAN, Z. Enhanced accumulation of carbohydrate and starch in *Chlorella zofingiensis* induced by nitrogen starvation. **Appl. Biochem. Biotechnol.** v. 174, p. 2435-2445, 2014.

ZIMMER, D. P.; SOUPENE, E.; LEE, H. L.; WENDISCH, V. F.; KHODURSKY, A. B.; PETER, B. J.; BENDER, R.A.; KUSTU, S. Nitrogen regulatory protein C-controlled genes of *Escherichia coli*: Scavenging as a defense against nitrogen limitation. **Proceedings of the National Academy of Sciences of the United States of America.** v. 97(26), p. 14674–14679, 2000.

ZUBAREV, R. A.; MAKAROV, A. Orbitrap Mass Spectrometry. **Analytical Chemistry.** v. 85, p. 5288-5296, 2013.

WISHART, D. S.; TZUR, D.; KNOX, C.; EISNER, R.; GUO, A. C.; YOUNG, N.; CHENG, D.; JEWELL, K.; ARNDT, D.; SAWHNEY, S.; FUNG, C.; NIKOLAI, L.; LEWIS, M.; COUTOULY, M. A.; FORSYTHE, I.; TANG, P.; SHRIVASTAVA, S.; JERONCIC, K.; STOTHARD, P.; AMEGBEY, G.; BLOCK, D.; HAU, D. D.; WAGNER, J.; MINIACI, J.; CLEMENTS, M.; GEBREMEDHIN, M.; GUO, N.; ZHANG, Y.; DUGGAN, G. E.; MACINNIS, G. D.; WELJIE, A. M.; DOWLATABADI, R.; BAMFORTH, F.; CLIVE, D.; GREINER, R.; LI, L.; MARRIE, T.; SYKES, B. D.; VOGEL, H. J.; QUERENGESSER, L.; HMDB: the Human Metabolome Database. **Nucleic Acids Res.** v. 35, p. 521, 2007.

WRIGHT, P. C.; NOIREL, J.; OW, S. Y; FAZELI, A. A review of current proteomics technologies with a survey on their widespread use in reproductive biology investigations. **Theriogenology.** v. 77, p. 738- 765, 2012.

APÊNDICE 1

Neste apêndice serão apresentados dados não incluídos no artigo, além dos principais experimentos que levaram à definição e modificação da estratégia de trabalho.

Linhagens bacterianas, meios de cultura e condições de crescimento

As estirpes de *A. brasiliense* utilizadas no início do projeto foram FP2 (*Nal^r Sm^r*, estirpe selvagem, SP7 *Nif⁺*) (PEDROSA E YATES, 1984), 7611 (*Nal^r Sm^r Nif⁺, glnZ::Ω*) (DE ZAMAROCZY, 1998), 2812 (*Nal^r Sm^r Km^r Nif⁻, glnB::km glnZ::Ω*) (DE ZAMAROCZY, 1998), LFH3 (*Nal^r Nif⁻* estirpe derivada de LFH2 *ΔglnB* (HUERGO et al., 2006)), 7628 (*Nal^r Km^r Nif⁻, glnB::km*) (DE ZAMAROCZY, 1996) e LHNTRC5 (*Nal^r Sm^r Km^r Nif⁺, ntrC::km*) (HUERGO et al., 2006). As bactérias foram cultivadas a 30 °C em meio NFb-lactato (MACHADO et al., 1995) contendo 50mM de mistura de fosfatos e 20mM de cloreto de amônio. Além disso, os antibióticos adequados para cada estirpe também foram adicionados nas concentrações: 10 µg/mL ácido nalidíxico, 80 µg/mL estreptomicina e 100 µg/mL canamicina.

Confirmação das estirpes estudadas

Foi feita uma confirmação das estirpes através de PCR's de colônia com os primers F/R (GGAAGATGCATGAAACTGGTTATGGC / TCCTCCACTAGTCCTCAGAGAGCTCGG), que flanqueiam *glnZ*, e F2/R2 (CCCTATCCGTTGGCAGTCGC / CGTTATGTCATGCCTTCCCAAGC), que flanqueiam o *glnB*. Com os primers para *glnZ*, os mutantes 2812 e 7611, negativos para esse gene, não amplificaram, uma vez que não possuem esse gene. As demais estirpes geraram um produto de 300 pares de base, referente à *glnZ*. Utilizando os primers F2/R2, o produto esperado possui cerca de 800 pb, dessa forma, o mutante LFH3, que possui uma deleção de *glnB*, gerou um produto de aproximadamente 500 pares de base e os demais não amplificaram. Esse resultado confirma que as estirpes estão corretas e pode ser observado na figura 20.

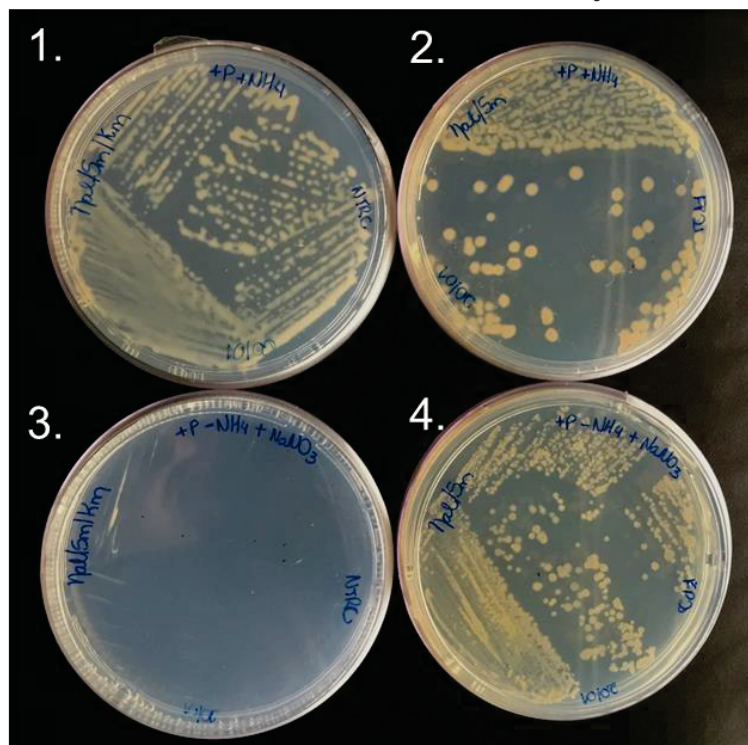
FIGURA 20 - ELETROFORESE EM GEL DE AGAROSE DOS FRAGMENTOS AMPLIFICADOS COM PRIMERS PARA *glnZ* (F/R) e *glnB* (F2/R2).



FONTE: a autora (2018).

A estirpe LHNTRC5 não é capaz de crescer em meio NFb-lactato sólido contendo NaNO_3 20Mm como fonte única de nitrogênio, uma vez que NtrC é indispensável para assimilação de nitrato. A confirmação dessa estirpe foi feita em placa e está na figura 21. As estirpes 2812 e LFH3 cresceram mais lentamente nesse meio, enquanto que as demais apresentaram crescimento normal (dados não mostrados).

FIGURA 21 - CONFIRMAÇÃO DA ESTIRPE LHNTRC5. 1. LHNTRC5 em 20mM de amônio. 2. FP2 em 20mM de amônio. 3. LHNTRC5 em 20mM de NaNO_3 . 4. FP2 em 20mM de NaNO_3 .

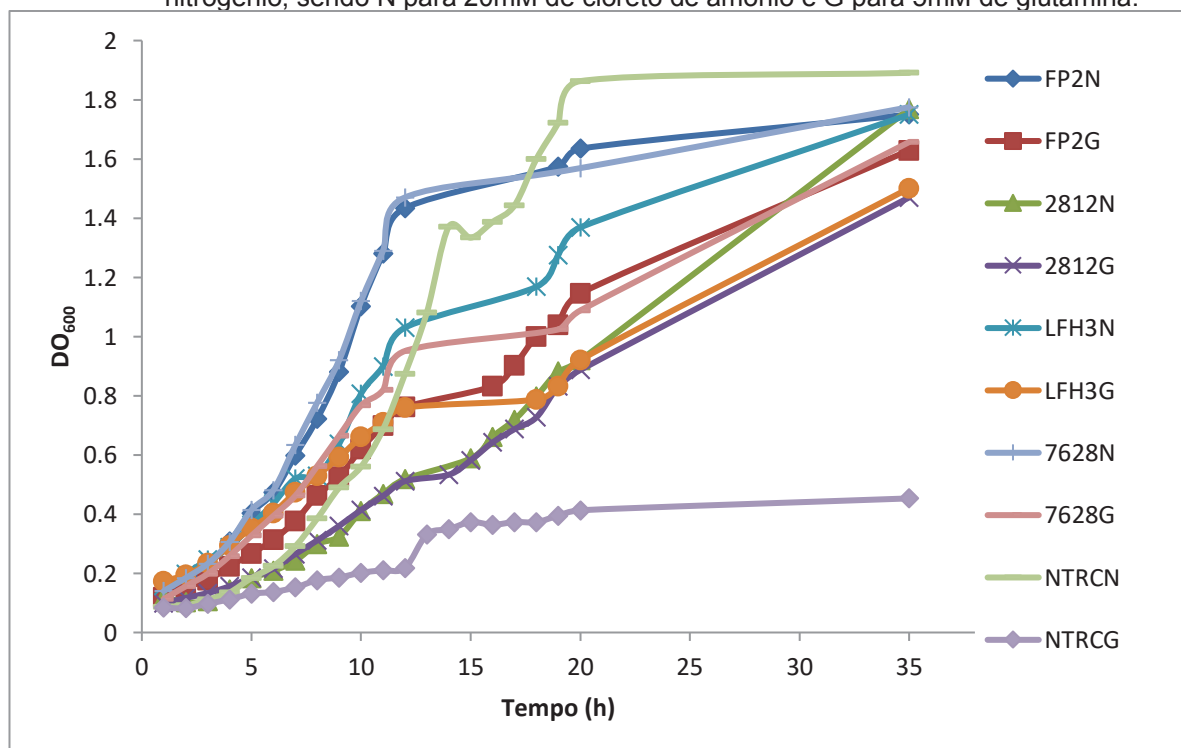


FONTE: a autora (2018).

Avaliação do perfil de crescimento das estirpes estudadas e definição das condições de baixo e alto nitrogênio

Foram produzidas curvas de crescimento das bactérias em várias condições, para verificar a resposta de cada estirpe e definir uma condição de baixo e alto nitrogênio. O objetivo era encontrar um ponto para coletar as células, no qual todas as estirpes estivessem na sua fase logarítmica de crescimento. As condições padrão para cultivo das bactérias são: 30°C em meio NFb-lactato (MACHADO *et al.*, 1995) contendo 50mM de mistura de fosfatos e 20mM de cloreto de amônio, acrescido dos antibióticos adequados para cada estirpe. Inicialmente, foram testadas duas condições de disponibilidade de nitrogênio: 20mM de cloreto de amônio e em 5mM de glutamina como fonte de nitrogênio, mantendo as demais condições de cultivo descritas. A estirpe 7611 não foi incluída nessa curva. A densidade ótica (DO_{600}) de cada cultura foi medida a cada uma hora, por 12 horas consecutivas partindo de um DO_{600} inicial de 0,05. A curva e os tempos de duplicação de cada estirpe em cada condição estão representados na figura 22 e na tabela 16.

FIGURA 22 - CURVA DE CRESCIMENTO DAS ESTIRPES ESTUDADAS EM 20mM DE CLORETO DE AMÔNIO E EM 5mM DE GLUTAMINA. O nome da estirpe é seguido da fonte de nitrogênio, sendo N para 20mM de cloreto de amônio e G para 5mM de glutamina.



FONTE: a autora (2018).

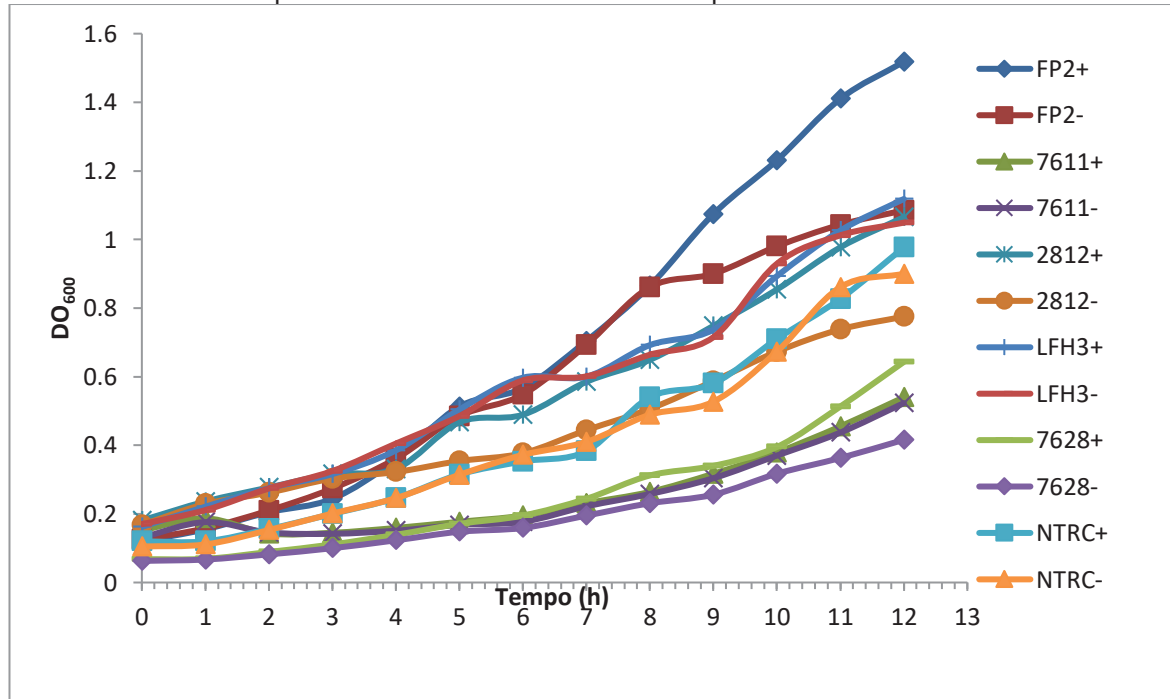
TABELA 16 - TEMPOS DE GERAÇÃO EM HORAS DAS ESTIRPES ESTUDADAS EM 20mM DE CLORETO DE AMÔNIO E EM 5mM DE GLUTAMINA.

Estirpe / Tempo de geração	20mM de cloreto de amônio	5mM de glutamina
FP2	3,019	4,030
2812	4,959	4,408
LFH3	3,436	5,524
7628	3,192	3,496
LHNTRC5	3,007	6,674

FONTE: a autora (2018).

Houve grande diferença no perfil de crescimento entre as estirpes, impossibilitando a escolha de um ponto comum a todas para realizar a análise. As próximas condições testadas foram 20mM e 2mM de cloreto de amônio, sendo considerado alto e baixo nitrogênio, respectivamente. As leituras foram realizadas de hora em hora por 12 horas consecutivas e a curva e tempos de geração de cada estirpe em cada condição estão descritos na figura 23 e tabela 17.

FIGURA 23 - CURVA DE CRESCIMENTO DAS ESTIRPES ESTUDADAS EM 20mM E 2mM DE CLORETO DE AMÔNIO. O nome da estirpe é seguido da concentração de nitrogênio, sendo + para 20mM de cloreto de amônio e - para 2mM.



FONTE: a autora (2018).

TABELA 17 - TEMPOS DE GERAÇÃO EM HORAS DAS ESTIRPES ESTUDADAS EM 20mM E 2mM DE CLORETO DE AMÔNIO.

Estirpe / Tempo de geração	20mM de cloreto de amônio	2mM de cloreto de amônio
FP2	2,714	2,687
2812	4,771	6,093
LFH3	3,472	3,356
7628	3,326	4,239
LHNTRC5	3,730	3,829
7611	4,561	4,603

FONTE: a autora (2018).

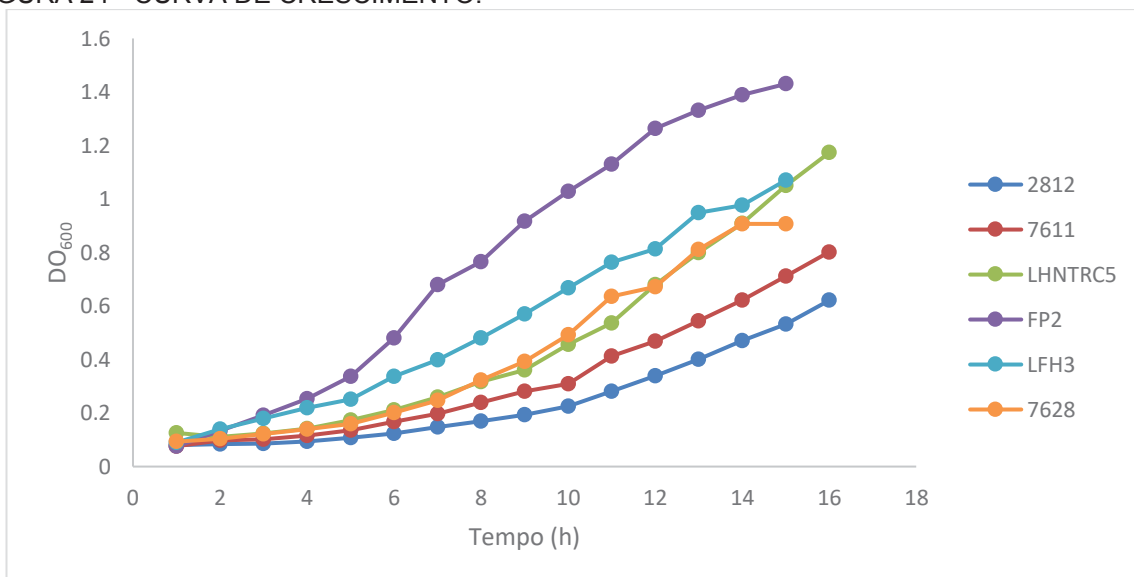
Os tempos de geração em baixo e alto amônio ficaram muito parecidos e novamente não foi possível determinar um ponto para coleta das amostras. Esse resultado sugere que 2mM de amônio ainda represente uma alta concentração de nitrogênio para o microrganismo, de forma a não impactar significativamente no seu tempo de duplicação. Além disso, entre as estirpes houve grande diferença no perfil de crescimento, de forma que, cada estirpe atinge uma determinada DO₆₀₀ em tempos muito diferentes. Isso impossibilitou a escolha de um ponto para coleta das amostras, pois poderia levar a resultados falso positivos, ou seja, proteínas diferencialmente expressas que seriam encontradas devido às diferentes tempos de crescimento em que as culturas se encontram, apesar de mesma DO₆₀₀, e não devido à disponibilidade de nitrogênio.

Considerando esse problema, a próxima estratégia testada para determinar o ponto de coleta das células foi utilizar o citômetro de fluxo para acompanhar o crescimento bacteriano. O objetivo era traçar um perfil de crescimento celular para cada estirpe em cada condição, baseando-se na quantidade de DNA por célula. Dessa forma, seria possível coletar as amostras de cada estirpe na mesma fase do crescimento. A coleta seria realizada no ponto de maior fluorescência, correspondente à maior quantidade de DNA por célula, ou seja, momento que supostamente antecede uma divisão. Dessa forma, todas as culturas seriam coletadas no mesmo estágio de crescimento, minimizando a variabilidade das proteínas em função disso.

A tentativa de sincronização das células foi feita com restrição de nutrientes (carbono e fosfato) e a hipótese era que, na ausência de nutrientes, as bactérias não se dividiriam após acumular certa quantidade de DNA. Dessa forma, após a readição do nutriente restrito, as células retomariam o crescimento de forma

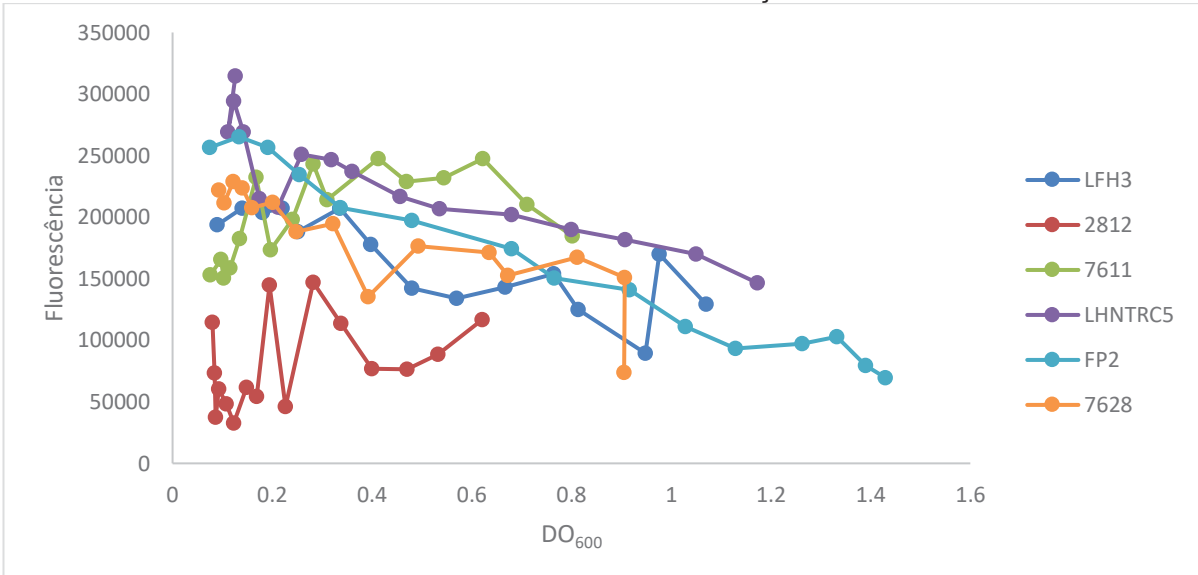
sincronizada, levando a um padrão semelhante a um ciclo celular, com fases bem definidas de duplicação de DNA e divisão celular. Porém, a retirada dos nutrientes impediu o desenvolvimento da cultura e diminuiu o tamanho da célula, além disso, o perfil apresentou um pico largo e indefinido. Concluiu-se que a restrição de nutrientes não é eficiente para sincronização das células bacterianas. A partir disso, as curvas de crescimento baseadas em DO₆₀₀ obtidas anteriormente foram utilizadas para escolha de um ponto ao meio da fase log de cada estirpe, no qual as células estariam aproximadamente sincronizadas. Foram realizados testes para definição do fluoróforo utilizando *Sybr Green I, II e Gold* em várias concentrações. Foi estabelecido que o *SYBR Green I*, na diluição 0,1x, seria o fluoróforo utilizado na análise. Foi realizado um teste inicial com a estirpe FP2 e posteriormente com todas as estirpes cultivadas em 20mM de amônio, no qual foi feito um inóculo com DO₆₀₀ ajustada para 0,05 e foi realizada contagem de células, análise de quantidade de DNA por fluorescência e leitura da DO₆₀₀ de hora em hora por 15 horas consecutivas. Os resultados obtidos nessa análise estão representados nas figuras 24, 25 e 26.

FIGURA 24 - CURVA DE CRESCIMENTO.



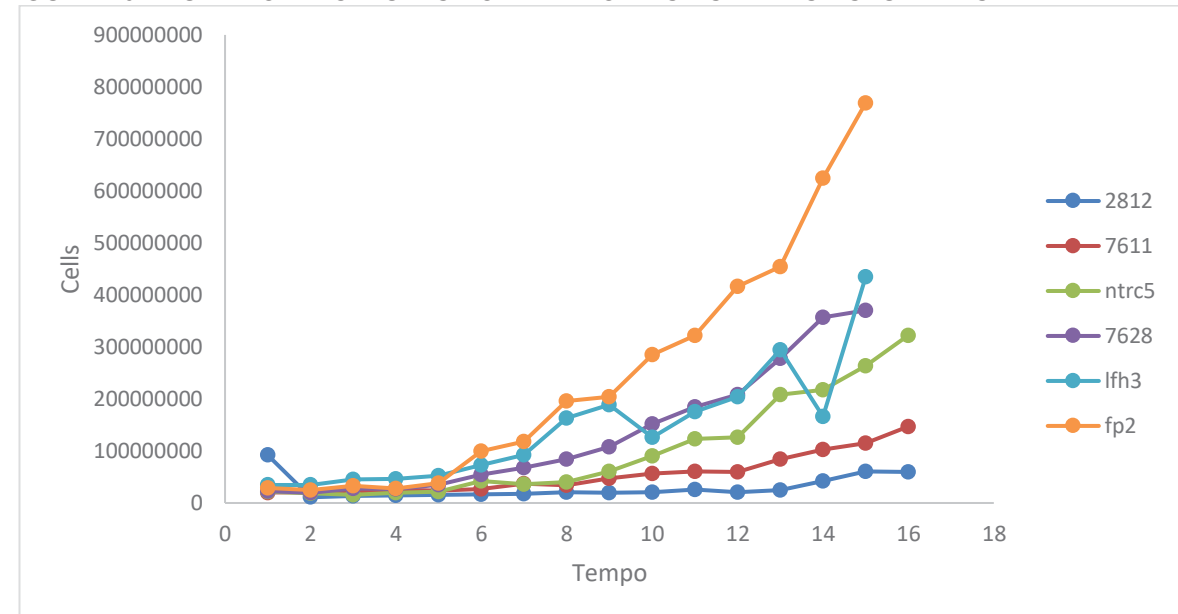
FONTE: a autora (2018).

FIGURA 25 - FLUORESCÊNCIA DE CADA CULTURA EM FUNÇÃO DE DO₆₀₀.



FONTE: a autora (2018).

FIGURA 26 - NÚMERO DE CÉLULAS POR TEMPO DAS ESTIRPES ESTUDADAS.



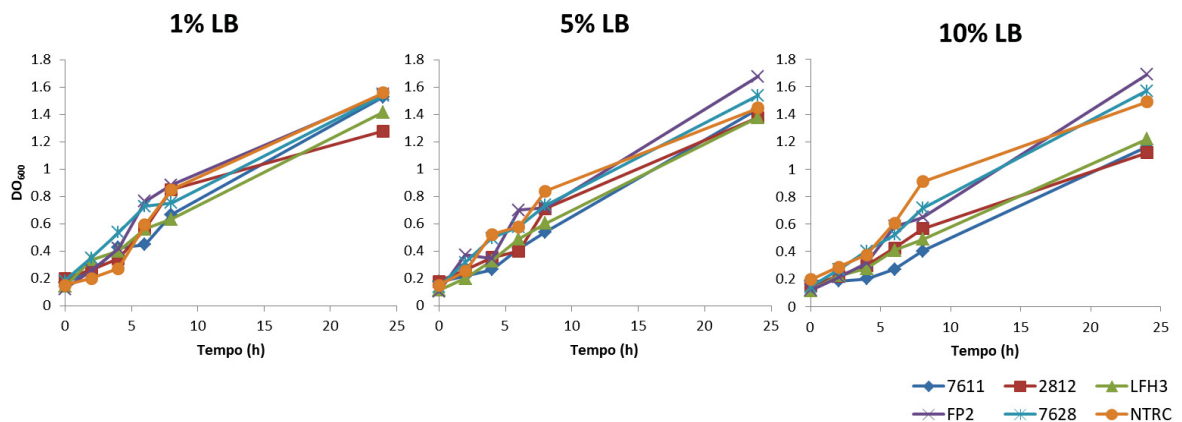
FONTE: a autora (2018).

Os perfis de fluorescência não seguiram um padrão de ciclo celular e são inconclusivos, apresentando fases e picos não definidos. Portanto, não foi possível determinar um ponto comum a todas as estirpes para coleta da amostra.

Uma nova estratégia foi traçada para definir as condições de baixo e alto nitrogênio do estudo. A fim de homogeneizar o crescimento entre as estirpes, as bactérias foram cultivadas nas condições padrão descritas, adicionando-se 10, 5 ou

1% de meio LB ao inóculo em DO₆₀₀ 0,05. A DO₆₀₀ foi monitorada de hora em hora e as curvas de crescimento obtidas estão representadas na figura 27.

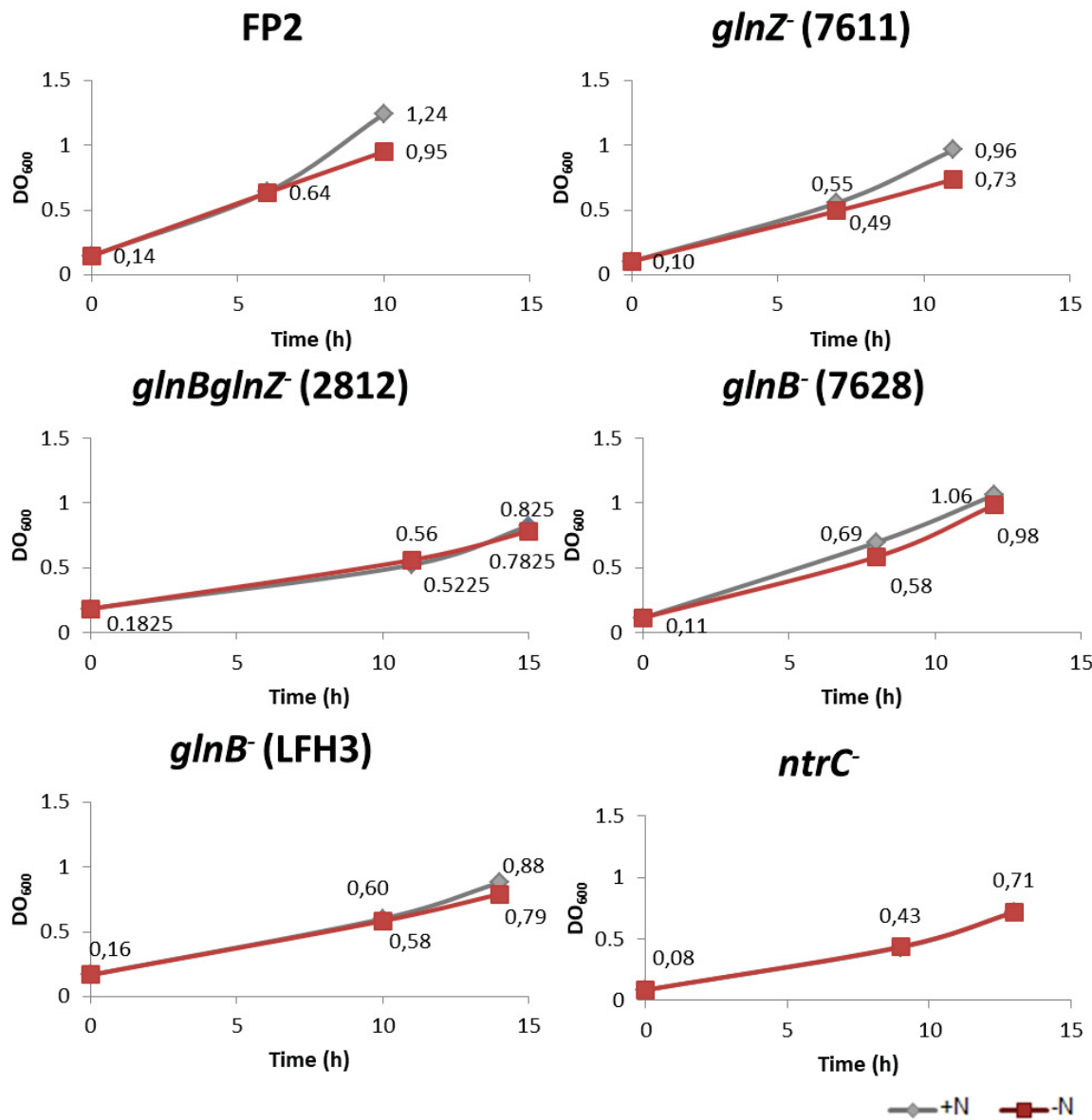
FIGURA 27 - PERFIL DE CRESCIMENTO DAS BACTÉRIAS INOCULADAS EM LACTATO ADICIONADO DE 1, 5 E 10% DE LB.



FONTE: a autora (2018).

Foi determinado que a adição de 1% de LB minimiza a variabilidade no crescimento entre as estirpes em relação as outras concentrações. A partir disso, a estratégia final para obtenção das amostras em baixo e alto nitrogênio foi estabelecida. As bactérias foram cultivadas em meio lactato adicionado de 20mM de cloreto de amônio, 50mM de mistura de fosfatos e 1% LB até atingirem DO₆₀₀ 0,5, que representa aproximadamente o meio da fase log para todas as estirpes. Nesse ponto, as culturas foram divididas em duas partes, centrifugadas e reinoculadas, sendo uma parte em 20mM de cloreto de amônio e a outra na ausência de fonte nitrogênio, ambas sem LB. Após 4 horas de incubação a 30°C e sob agitação de 120rpm, obtivemos as amostras em alto e baixo nitrogênio, respectivamente. As curvas de crescimento para cada estirpe nas condições estabelecidas são mostradas na figura 28.

FIGURA 28 - PERFIL DE CRESCIMENTO DE CADA ESTIRPE EM ALTO (+N) E BAIXO (-N) NITROGÊNIO.



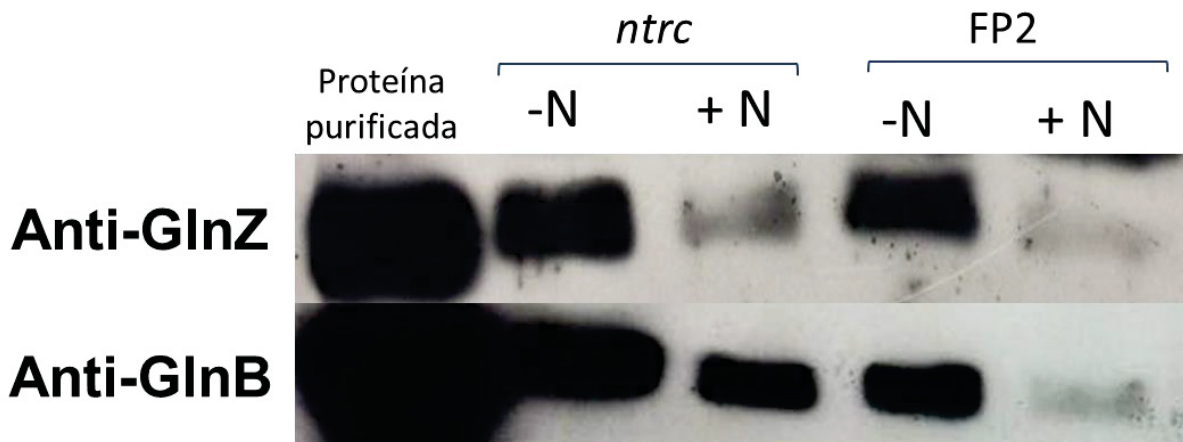
FONTE: a autora (2018).

Confirmação das condições de alto e baixo nitrogênio

Para confirmar se o sistema *ntr* das bactérias estava respondendo a essa condição estabelecida, foi feito um ensaio western blot utilizando os anticorpos para as proteínas GlnB e GlnZ. Foram utilizados extratos proteicos das estirpes FP2 e mutante *ntrC*, na concentração de 10 μ g de proteína, em baixo e alto nitrogênio, além de um controle com GlnB e GlnZ purificados. Ambas proteínas apresentaram expressão aumentada na estirpe FP2 (FIGURA 29) sob privação de nitrogênio, confirmando a resposta do sistema *ntr*, uma vez que nessa condição NtrC está

fosforilado e aumenta a transcrição de *glnB* e *glnZ*. Na estirpe que não expressa NtrC, GlnB e GlnZ apresentaram expressão constitutiva. Portanto, o sistema ntr está ativo e responde às condições de baixo e alto N estabelecidas.

FIGURA 29 - WESTERN BLOTH DE *A. brasiliense* FP2 E *ntrc* EM ALTO E BAIXO NITROGÊNIO.



FONTE: a autora (2018).

Neste trabalho, foram produzidas amostras de todas as estirpes estudadas para extração de proteínas e RNA, além de amostras de FP2 e do mutante *ntrC* para extração de metabólitos. Os dados de RNA e as proteínas diferencias das demais estirpes estão sob análise em outros trabalhos do departamento.

Padronização do protocolo de extração de proteínas

Considerando que a estratégia inicial do projeto era o uso de 2D-DIGE, foi necessário padronizar uma extração de proteínas compatível com a isoeletrofocalização, uma vez que essa técnica demanda um pH exato de 8,5, para que a marcação com CyDye ocorra, além de grande quantidade de proteínas por amostra. No primeiro teste de extração foram feitas duas alíquotas de 20 mL de cultura para a estirpe FP2, nas DO₆₀₀'s 0,5, 0,75 e 0,96. Essas alíquotas foram centrifugadas e o pellet lavado duas vezes com solução Tris-HCl 30 mM pH7,2, centrifugado a 12000g por 5 minutos a 4 °C e o sobrenadante descartado. Em seguida, foi ressuspandido em 1 mL de solução de lise (7M ureia, 2M toureia, 4% CHAPS, 30 mM Tris e pH 8,5), homogeneizado e incubado em temperatura ambiente por 30 minutos. Uma das alíquotas de cada DO foi sonicada em banho de gelo por 10 segundos, 5 vezes, com intervalos de um minuto e a outra alíquota não foi sonicada. As amostras foram centrifugadas por 30 minutos a 4 °C e 20000g, o sobrenadante transferido para um novo tubo e centrifugado por mais 15 minutos nas

mesmas condições. Esse sobrenadante foi armazenado a -20 °C e dosado pelo método de Bradford (BRADFORD,1976). As concentrações de proteína total obtidas estão descritas na tabela 18.

TABELA 18 - CONCENTRAÇÕES OBTIDAS NA DOSAGEM DE PROTEÍNAS.

Amostra	Concentração ($\mu\text{g}/\mu\text{L}$)
20mL de cultura DO ₆₀₀ 0,5	0,54
20mL de cultura DO ₆₀₀ 0,5 + sonicação	1,02
20mL de cultura DO ₆₀₀ 0,75	0,73
20mL de cultura DO ₆₀₀ 0,75 + sonicação	1,47
20mL de cultura DO ₆₀₀ 0,96	0,56
20mL de cultura DO ₆₀₀ 0,96 + sonicação	0,68

FONTE: a autora (2018).

O método testado apresentou baixo rendimento, as proteínas ficaram pouco concentradas, porém, a sonicação aumentou a quantidade de proteína total extraída. Novos testes foram feitos utilizando o mesmo protocolo com pequenas alterações e partindo de volumes maiores de cultura 50 e 100 mL. Além disso, o tempo de sonicação foi aumentado para 25 vezes de 5 segundos e o volume de tampão de lise no qual a amostra foi ressuspendida foi diminuído de 1 mL para 300 μL . Houve melhora no rendimento e o protocolo para extração de proteínas foi definido. Inicialmente, culturas bacterianas de 50 mL das estirpes nas condições de alto e baixo nitrogênio foram centrifugadas a 16100g por 10 minutos a 4° C e os pellets congelados em nitrogênio líquido armazenados a -80° C até o momento da extração. Os pellets foram ressuspensos em 400 μL de tampão de lise contendo 7M ureia, 2M tioureia, 4% CHAPS, 30mM Tris em pH 8,5, homogeneizados e incubados em temperatura ambiente por 30 minutos. Em seguida, as amostras foram sonicadas em banho de gelo 25 vezes por 5 segundos, com intervalos de 30 segundos e centrifugadas a 20000g por 45 minutos a 4°C. O sobrenadante foi transferido para um novo tubo e centrifugado por mais 30 minutos nas mesmas condições. O segundo sobrenadante foi armazenado a -20°C e dosado pelo método de Bradford (BRADFORD,1976). O rendimento obtido no teste utilizando esse protocolo está descrito na tabela 19.

TABELA 19 - RENDIMENTO OBTIDO NA DOSAGEM DE PROTEÍNAS.

Amostra	Concentração ($\mu\text{g}/\mu\text{L}$)
50 mL de cultura DO ₆₀₀ 0,68 – Replicata 1	6,8
50 mL de cultura DO ₆₀₀ 0,68 - Replicata 2	7,5
50 mL de cultura DO ₆₀₀ 0,68 - Replicata 3	6,8

FONTE: a autora (2018).

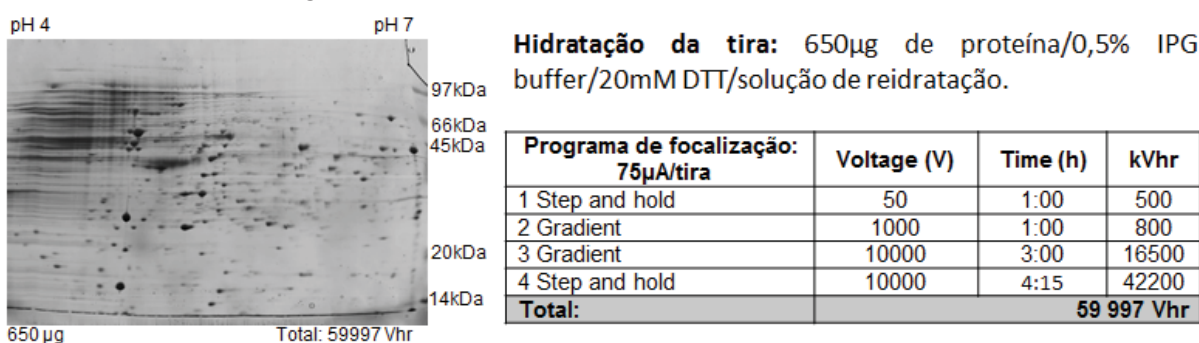
Houve melhora no rendimento da extração e aumento na concentração de proteínas, levando à definição do protocolo de extração de proteínas.

Padronização da isoeletrofocalização em tiras de 24cm e pH 4-7

A padronização do protocolo de isoeletrofocalização foi realizada em equipamento *IPGphor II* (*GE Healthcare*), seguindo inicialmente o protocolo recomendado pelo fabricante. Foram feitos testes utilizando kit *CleanUp* (*GE Healthcare*), alterando a concentração de proteínas, DTT e programa de focalização, além da produção de novos extratos proteicos. Foram utilizadas tiras de 24 cm e pH 4-7, hidratadas em suporte de acrílico por 16 horas com solução contendo proteínas, IPG buffer, DTT e solução de reidratação. Após a focalização, as proteínas foram reduzidas e alquiladas com DTT 1% e iodacetamida 2,5% em tampão de equilíbrio por 30 minutos cada, e submetidas à segunda dimensão em sistema de eletroforese vertical *Ettan DaltSix* (*GE Healthcare*), SDS-PAGE em gel de acrilamida 12%, limitando-se a corrente em 10 mA/gel na primeira hora de corrida, e 40 mA/gel até o azul de bromofenol atingir o limite inferior do gel. Após corrida, os géis permaneceram por uma hora em solução fixadora (1,3% ácido fosfórico e 20% metanol), seguido de coloração em Coomassie coloidal.

No primeiro teste foi utilizado o protocolo recomendado pelo fabricante, descrito na figura 30.

FIGURA 30 - GEL 2-D TESTE 1, UTILIZANDO PROTOCOLO RECOMENDADO PELO FABRICANTE.

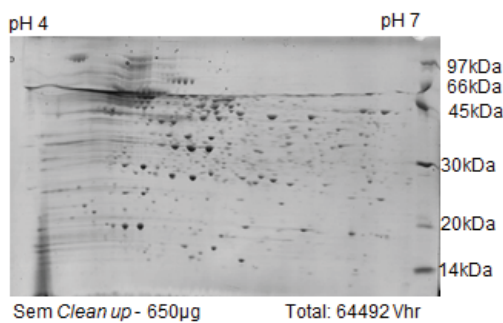


FONTE: a autora (2018).

Não ocorreu uma focalização adequada, sobretudo na parte ácida, que apresentou muitas bandas não resolvidas, denominadas *streaks*. De acordo com o manual do fabricante, esse problema ocorre devido à presença de interferentes e impurezas não proteicas na amostra. Portanto, foram feitos novos testes (FIGURA

31 e 32) utilizando kit *CleanUp*, que precipita as proteínas a fim de eliminar eventuais contaminantes e sal da amostra. Além disso, o programa de isoeletrofocalização foi otimizado e a concentração de IPG buffer na amostra aumentada.

FIGURA 31 - GEL 2-D TESTE 2. Amostra não tratada com CleanUp.

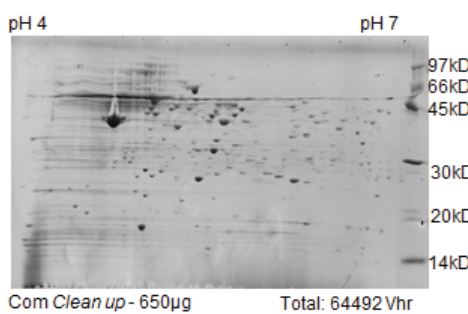


Hidratação da tira: 650µg de proteína/0,75% IPG buffer/50mM DTT/solução de reidratação.

Programa de focalização: 75µA/tira	Voltage (V)	Time (h)	Vhr
1 Step and hold	50	2:00	-
2 Step and hold	500	-	500
3 Gradient	1000	-	5200
4 Gradient	10000	-	16500
5 Step and hold	10000	-	42200
Total:			64 492 Vhr

FONTE: a autora (2018).

FIGURA 32 - GEL 2-D TESTE 3. Amostra tratada com CleanUp.



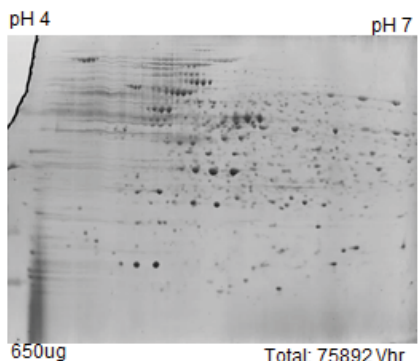
Hidratação da tira: 650µg de proteína utilizando *CleanUp*/0,75% IPG buffer/50mM DTT/solução de reidratação.

Programa de focalização: 75µA/tira	Voltage (V)	Time (h)	Vhr
1 Step and hold	50	2:00	-
2 Step and hold	500	-	500
3 Gradient	1000	-	5200
4 Gradient	10000	-	16500
5 Step and hold	10000	-	42200
Total:			64 492 Vhr

FONTE: a autora (2018).

Não houve melhora na focalização da parte ácida, apesar da precipitação das proteínas e consequente eliminação de impurezas. Além disso, com a utilização do *CleanUp* houve perda de algumas bandas. Para o próximo teste, descrito na figura 33, o protocolo de isoeletrofocalização foi alterado e a concentração de IPG buffer aumentada novamente.

FIGURA 33 - GEL 2-D TESTE 4.



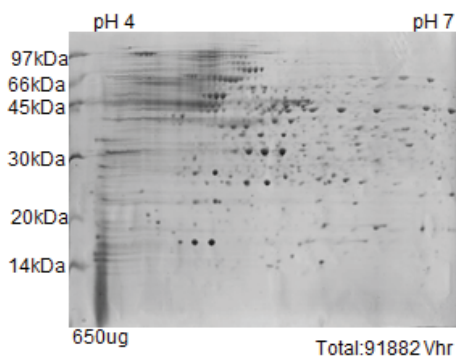
Hidratação da tira: 650µg de proteína/1% IPG buffer/50mM DTT/solução de reidratação.

Programa de focalização: 75µA/tira	Voltage (V)	Time (h)	Vhr
1 Step and hold	50	2:00	-
2 Step and hold	200	4:00	-
3 Step and hold	500	1:00	-
4 Step and hold	1000	1:00	5200
5 Gradient	8000	-	13500
6 Step and hold	8000	-	60000
Total:			78 000 Vhr

FONTE: a autora (2018).

A parte ácida continuou não resolvida, embora o restante do gel tenha ficado satisfatório. Foi feita nova modificação no programa de isoeletrofocalização, porém, a parte ácida não apresentou redução dos *streaks*. Os parâmetros e resultados estão representados na figura 34.

FIGURA 34 - GEL 2-D TESTE 5.



Hidratação da tira: 650µg de proteína/1% IPG buffer/50mM DTT/solução de reidratação.

Programa de focalização: 75µA/tira	Voltage (V)	Time (h)	Vhr
1 Step and hold	50	2:00	-
2 Step and hold	200	4:00	-
3 Step and hold	500	1:00	-
4 Step and hold	1000	1:00	-
5 Gradient	8000	-	13500
6 Step and hold	8000	-	76000
Total:			93 000 Vhr

FONTE: a autora (2018).

Foi realizado outro teste utilizando maior tempo de focalização e hidratando a tira com 650µg de proteínas, 1,5% de IPG buffer, 50mM de DTT e solução de hidratação (programa descrito na tabela 20). A focalização não ocorreu, o gel ficou com muitas manchas horizontais e sem bandas definidas. Em protocolos extensos de focalização, superiores a 100 kVh totais, pode ocorrer *overfocusing*, levando a esse padrão de manchas, devido ao fluxo eletro-osmótico de água, resultante do movimento do tampão e das próprias proteínas pelo efeito do campo elétrico (GE Healthcare Handbook).

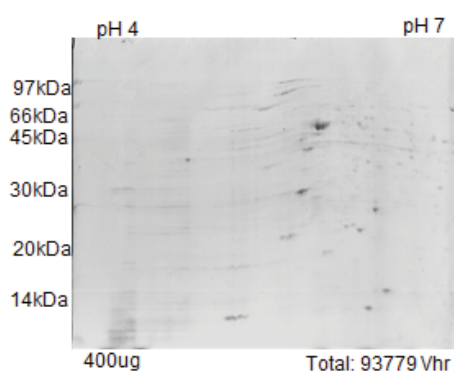
TABELA 20 - PROGRAMA DE FOCALIZAÇÃO UTILIZADO NO TESTE 6.

Programa de focalização: 50µA/tira	Voltage (V)	Time (h)	Vhr
1 Step and hold	50	4:00	-
2 Step and hold	100	4:00	-
3 Step and hold	200	4:00	-
4 Step and hold	500	3:00	-
5 Gradient	1000	2:00	-
6 Gradient	1500	4:00	-
7 Gradient	8000	-	20000
8 Step and hold	8000	14:00	-
Total: 141 368 Vhr			

FONTE: a autora (2018).

Para o teste seguinte, a concentração de proteínas foi diminuída e o programa de isoleletrofocalização alterado, como descrito na figura 35.

FIGURA 35 - GEL 2-D TESTE 7.



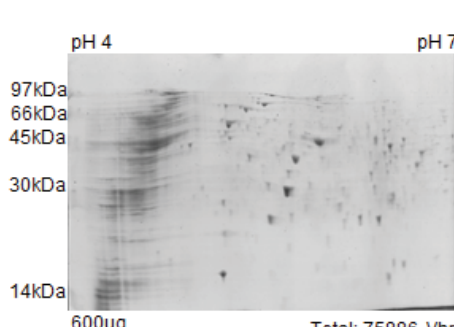
Hidratação da tira: 400µg de proteína/1,5% IPG buffer/50mM DTT/solução de reidratação.

Programa de focalização: 75µA/tira	Voltage (V)	Time (h)	Vhr
1 Step and hold	50	2:00	-
2 Step and hold	100	4:00	-
3 Step and hold	200	4:00	-
4 Step and hold	500	2:00	-
5 Step and hold	1000	2:00	-
6 Gradient	8000	-	13500
7 Step and hold	8000	-	76000
Total:			94 200 Vhr

FONTE: a autora (2018).

A redução da quantidade de proteínas agravou o problema da isoleletrofocalização, que se demonstrou insatisfatória em todo o gel. Para o novo teste (FIGURA 36), a quantidade de proteínas foi novamente aumentada e o protocolo de isoleletrofocalização alterado.

FIGURA 36 - GEL 2-D TESTE 8.



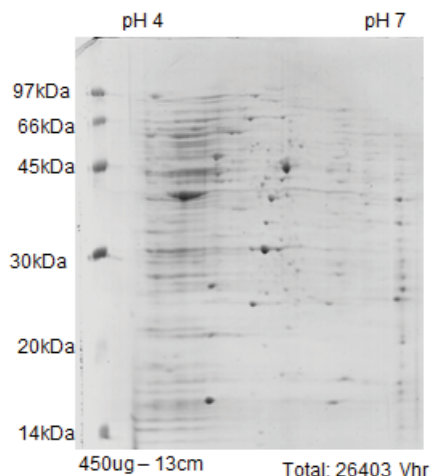
Hidratação da tira: 600µg de proteína/1% IPG buffer/50mM DTT/solução de reidratação.

Programa de focalização: 75µA/tira	Voltage (V)	Time (h)	Vhr
1 Step and hold	50	2:00	-
2 Step and hold	200	4:00	-
3 Step and hold	500	1:00	-
4 Step and hold	1000	1:00	-
5 Gradient	8000	-	13500
6 Step and hold	8000	-	60000
Total:			75886 Vhr

FONTE: a autora (2018).

Sem solucionar o problema da isoeletrofocalização na parte ácida, optamos por utilizar uma tira de 13cm, pH 4-7 e um programa já padronizado pela autora anteriormente. Os parâmetros e gel estão representados na figura 37.

FIGURA 37 - GEL 2-D TESTE 9.



Hidratação da tira: 400 μ g de proteína/1,5% IPG buffer/50mM DTT/solução de reidratação.

Programa de focalização: 75 μ A/tira	Voltage (V)	Time (h)	Vhr
1 Step and hold	50	16:00	-
2 Step and hold	500	-	500
3 Step and hold	1000	-	800
4 Step and hold	8000	-	11300
5 Step and hold	8000	-	13000
Total:			26403 Vhr

FONTE: a autora (2018).

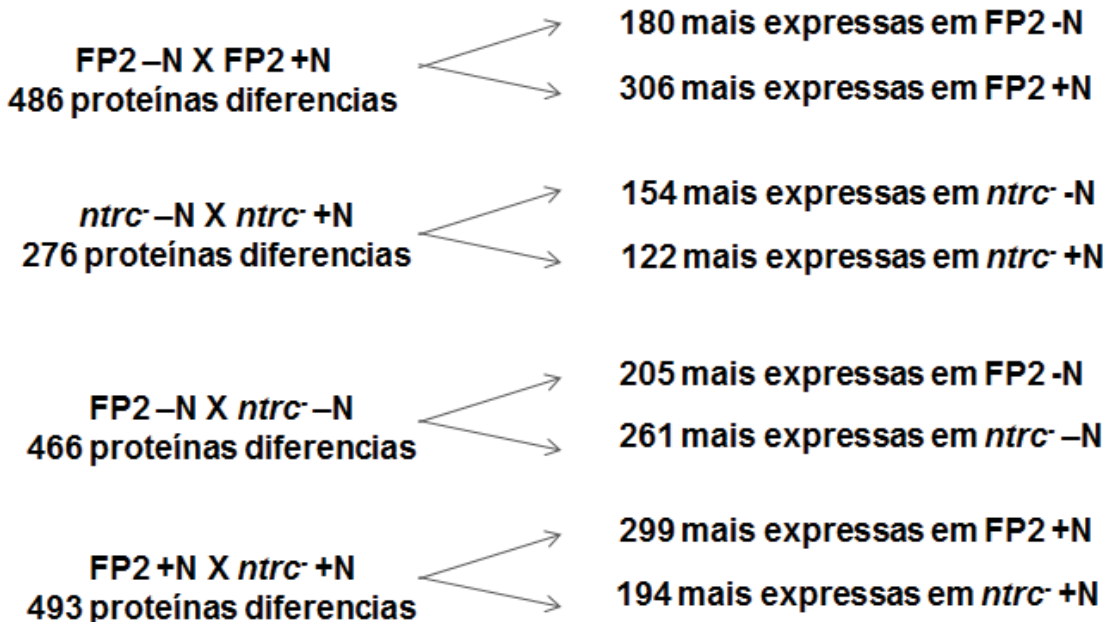
O padrão do gel se repetiu e a parte ácida continuou não focalizando. Possivelmente, o problema seja inerente à amostra. Não foi possível padronizar o protocolo para 2D-DIGE e a metodologia inicialmente proposta para a análise proteômica foi alterada para uma abordagem por *shotgun label-free*. Devido ao volume de dados gerado por esse método de análise, limitamos este trabalho ao estudo da estirpe selvagem FP2 e seu mutante *ntrC*, em alto e baixo nitrogênio. As amostras das demais estirpes foram produzidas e as análises serão abordadas em outro trabalho.

Análise do proteoma de *A. brasiliense* FP2 e seu mutante *ntrc* em alto e baixo nitrogênio

Foram produzidas amostras em quadruplicata de *A. brasiliense* FP2 e sua estirpe mutante *ntrc*, em alto e baixo nitrogênio, nas condições previamente descritas. A análise proteômica *shotgun label-free* foi realizada através do colaborador Dr. Gustavo Antônio de Souza, da unidade de Espectrometria da Universidade de Oslo, Noruega. Foi utilizado espectrômetro de massas Orbitrap Q-Exactive (Thermo Fisher Scientific) do tipo quadrupolo. Proteínas com foldchange acima de 2 e p-value menor que 0,05 foram consideradas diferenciais. Foram identificadas 2254 proteínas na análise, das quais 1721 são diferenciais. As

comparações e o número de proteínas diferenciais em cada uma delas estão descritas na figura 38.

FIGURA 38 - NÚMERO DE PROTEÍNAS DIFERENCIAIS IDENTIFICADAS EM CADA COMPARAÇÃO. A condição de alto nitrogênio está representada por +N e de baixo por -N.



FONTE: a autora (2018).

No manuscrito apresentado na primeira parte deste trabalho estão descritas as proteínas diferenciais identificadas nas comparações entre alto e baixo nitrogênio na estirpe selvagem e no mutante *ntrC*. Nas tabelas 21 e 22 estão as proteínas diferenciais encontradas nas demais comparações, entre estirpes.

TABELA 21 - PROTEÍNAS DIFERENCIAIS ENTRE *A. brasiliense* FP2 E O MUTANTE *ntrC* EM BAIXO NITROGÊNIO.

t-test p-value	FC	Protein IDs	Protein
Upregulated:			
1.45E-05	1189.43	gi 392384431	beta-ketoacyl-ACP reductase
1.86E-07	1117.61	gi 392384452	amino acid ABC transporter substrate-binding protein
3.12E-10	1101.39	gi 392383070	urea ABC transporter substrate-binding protein
2.93E-06	591.30	gi 392379722	ABC-type branched-chain amino acid transport systems, periplasmic component
1.73E-08	533.90	gi 392380681	ammonia channel protein
4.35E-08	273.58	gi 392379716	dihydroorotase
1.03E-05	273.57	gi 392383795	ABC transporter substrate-binding protein
7.54E-06	229.98	gi 392378005	amino acid ABC transporter substrate-binding protein
1.41E-05	206.45	gi 392377482	ABC transporter substrate-binding protein

8.52E-06	192.86	gi 392384455	amidohydrolase
5.79E-06	154.67	gi 392384453	hypothetical protein
1.85E-06	135.98	gi 392384473	acetyltransferase
5.20E-05	86.05	gi 392383066	ABC transporter ATP-binding protein
0.000142	83.03	gi 392384450	ABC transporter ATP-binding protein
1.74E-05	79.32	gi 392378794	S-adenosyl-L-methionine (SAM)-dependent methyltransferase PhcB
5.31E-06	76.91	gi 392383952	amino acid ABC transporter substrate-binding protein
0.000205	68.65	gi 392384046	ABC transporter substrate-binding protein
0.000135	60.02	gi 392384448	2-amino-thiazoline-4-carboxylic acid hydrolase
4.80E-06	49.70	gi 392381713	conserved protein of unknown function
1.32E-05	47.05	gi 392380596	ABC transporter ATP-binding protein
7.71E-05	46.05	gi 392384143	adenosylcobalamin-dependent methylmalonyl-CoA mutase small subunit (MCM-beta)(N-terminal fragment), partial
4.37E-07	44.89	gi 392377295	conserved protein of unknown function; putative Radical SAM domain
5.10E-07	39.68	gi 392384445	FMN reductase
5.26E-05	39.67	gi 392384454	putative FAD dependent oxidoreductase
1.27E-07	35.84	gi 392384045	N-carbamoylsarcosine amidase
0.044778	35.49	gi 392381052	hypothetical protein
7.90E-05	33.68	gi 392383069	branched-chain amino acid ABC transporter permease
4.42E-05	33.05	gi 392380332	amino acid ABC transporter substrate-binding protein
0.00027	31.97	gi 392382671	Crp-type transcriptional activatory protein (fragment), partial
7.68E-05	31.70	gi 392379721	gamma-glutamyltransferase (fragment), partial
0.000797	31.16	gi 392384437	chromosome partitioning protein
4.08E-06	29.80	gi 392378105	nitrate ABC transporter substrate-binding protein
2.54E-06	27.17	gi 392377569	peptidase S41
3.69E-08	27.10	gi 392381762	azoreductase
1.38E-05	23.64	gi 392384043	amidase (fragment), partial
0.000183	21.65	gi 392384044	putative Glutamyl-tRNA(Gln) amidotransferase subunit A (Glu-ADT subunit A)
4.01E-05	21.33	gi 392384447	putative sensory transducer protein
0.012667	19.51	gi 392384067	polyisoprenoid-binding protein
0.014662	18.50	gi 392384456	hypothetical protein
0.003679	16.12	gi 392384149	ribonucleotide-diphosphate reductase subunit alpha
0.000177	16.01	gi 392384436	putative chromosome-partitioning protein parB
0.000251	14.11	gi 392382462	molybdopterin molybdenumtransferase MoeA
2.96E-05	12.88	gi 392380304	branched-chain amino acid ABC transporter substrate-binding protein
0.000257	12.45	gi 392383973	hypothetical protein
2.62E-05	12.12	gi 392379972	ABC transporter substrate-binding protein
0.001392	11.95	gi 392381934	anthranilate synthase
0.001146	11.33	gi 392381292	16S rRNA processing protein RimM

0.052632	10.78	gi 392378258	Rrf2 family transcriptional regulator
0.00123	10.63	gi 392379713	agmatinase
0.017304	10.56	gi 392378572	transcriptional regulator
1.09E-06	10.13	gi 392381004	nitrogen regulatory protein P-II 1
0.000507	9.89	gi 392377481	spermidine/putrescine ABC transporter ATPase
0.001426	9.77	gi 392384458	O-methyltransferase
0.03545	9.63	gi 392384438	phosphatidylethanolamine N-methyltransferase
1.32E-05	9.21	gi 392379727	carbon monoxide dehydrogenase
0.014824	9.01	gi 392378308	acyl-CoA synthetase
0.004888	8.97	gi 392379712	amino acid ABC transporter substrate-binding protein
1.64E-05	8.73	gi 392382764	DNA-binding response regulator
6.21E-05	8.29	gi 392380326	amidohydrolase
0.03593	8.12	gi 392381633	protein of unknown function
2.00E-07	8.10	gi 392383067	ABC transporter ATP-binding protein
0.011272	8.10	gi 392383253	conserved exported protein of unknown function; deacetylase domain
0.006014	7.81	gi 392378234	iron-dicitrate transporter subunit; ATP-binding component of ABC superfamily; KpLE2 phage-like element
0.000635	7.74	gi 392377486	hydantoin-racemase
0.000734	7.66	gi 392379730	hypothetical protein
0.028229	7.57	gi 392380133	hypothetical protein
0.001115	7.44	gi 392380085	putative transcriptional regulator, TetR family
1.13E-06	7.10	gi 392383998	putative Metallo-hydrolase/oxidoreductase superfamily protein; Beta-lactamase-like
0.005031	7.01	gi 392380710	CBS domain-containing protein
0.020397	6.98	gi 392380333	hypothetical protein
0.007546	6.95	gi 392382907	hypothetical protein
0.006936	6.87	gi 392378220	PKHD-type hydroxylase
0.001146	6.75	gi 392378644	hypothetical protein
0.006168	6.71	gi 392378731	X-Pro dipeptidyl-peptidase
0.059953	6.44	gi 392383748	TonB system transport protein ExbD
0.05644	6.39	gi 392382607	DNA-binding response regulator
0.000144	6.33	gi 392381692	dioxygenase
3.64E-06	6.10	gi 392378226	iron ABC transporter substrate-binding protein
0.022986	5.98	gi 392380606	aminoacyl-tRNA deacetylase
0.003632	5.72	gi 392380783	formamidopyrimidine-DNA glycosylase
0.032838	5.49	gi 392380868	ATP-dependent protease subunit HslV
0.016279	5.46	gi 392384150	oxygen-dependent ribonucleotide reductase, beta subunit
0.006501	5.39	gi 392382401	amino acid ABC transporter substrate-binding protein
0.025188	5.37	gi 392379071	nitrite reductase, copper-containing
0.009233	5.36	gi 392379323	glutathione S-transferase
0.001061	5.23	gi 392382452	RNA polymerase factor sigma-32
0.000253	5.12	gi 392377994	putative ornithine cyclodeaminase

0.001545	5.03	gi 392383015	elongation factor G
3.83E-06	5.00	gi 392379728	carbon monoxide dehydrogenase
0.000425	4.92	gi 392383652	anti-sigma factor antagonist
0.002753	4.90	gi 392377642	hypothetical protein
0.000463	4.85	gi 392382482	Holliday junction ATP-dependent DNA helicase RuvA
0.001731	4.82	gi 392379393	cyclic nucleotide-binding protein
0.02316	4.79	gi 392378138	quinolinate synthetase
0.048402	4.73	gi 392380180	conserved exported protein of unknown function
0.002557	4.72	gi 392382593	protein of unknown function
0.000173	4.61	gi 392378016	cobalt ABC transporter substrate-binding protein
0.038266	4.52	gi 392378522	sulfate transporter subunit
0.001168	4.45	gi 392384245	ABC transporter substrate-binding protein
7.75E-06	4.38	gi 392379032	mandelate racemase
0.001149	4.37	gi 392381498	bacterioferritin
0.001588	4.35	gi 392378831	glutathione-dependent reductase
0.005747	4.35	gi 392383954	polar amino acid ABC transporter ATP-binding protein
0.019068	4.30	gi 392382529	transcriptional repressor
5.54E-06	4.29	gi 392379894	peptide ABC transporter substrate-binding protein
0.000666	4.21	gi 392379812	hypothetical protein
0.057044	4.20	gi 392378353	protein of unknown function
5.18E-05	4.19	gi 392378882	IMP dehydrogenase
0.013608	4.16	gi 392378413	hypothetical protein
0.000431	4.03	gi 392380182	hypothetical protein
2.49E-06	3.94	gi 392378830	NAD(P)H:quinone oxidoreductase
6.48E-06	3.90	gi 392377167	nitrogen regulation protein NR(I)
0.039806	3.89	gi 392380935	cyclic nucleotide-binding protein
0.003567	3.87	gi 392378104	nitrate ABC transporter permease
0.000179	3.85	gi 392382402	ABC transporter permease
0.017602	3.84	gi 392384040	multidrug ABC transporter ATP-binding protein
0.022343	3.78	gi 392377888	conserved exported protein of unknown function
0.002204	3.77	gi 392377615	hybrid sensor histidine kinase/response regulator
0.010576	3.75	gi 392378232	putative histidine kinase
0.000518	3.74	gi 392379726	ABC transporter ATP-binding protein
0.000202	3.70	gi 392383726	methylmalonate-semialdehyde dehydrogenase (acylating)
0.00214	3.70	gi 392378187	N5-glutamine S-adenosyl-L-methionine-dependent methyltransferase
0.008772	3.69	gi 392383594	methyl-accepting chemotaxis protein
1.29E-05	3.60	gi 392381440	methyl-accepting chemotaxis protein
0.009465	3.57	gi 392381198	hypothetical protein
2.32E-06	3.55	gi 392384086	ATP-dependent acyl-CoA ligase
0.000168	3.53	gi 392378223	iron ABC transporter ATP-binding protein
0.002299	3.45	gi 392382887	conserved exported protein of unknown function
0.002717	3.45	gi 392383950	N-formylglutamate deformylase

0.020359	3.44	gi 392380521	two-component sensor histidine kinase, partial
0.001705	3.42	gi 392380023	putative oligopeptide ABC transporter (substrate-binding protein)
0.015163	3.42	gi 392380573	glycerol-3-phosphate dehydrogenase
0.013658	3.40	gi 392379033	ABC transporter substrate-binding protein
0.005114	3.38	gi 392380209	hypothetical protein
0.005439	3.38	gi 392380858	Fe-S oxidoreductase
0.010272	3.35	gi 392379081	GntR family transcriptional regulator
0.003956	3.32	gi 392382578	bacterioferritin
0.010674	3.31	gi 392377229	histidine kinase
0.003946	3.28	gi 392383632	AMP nucleosidase
0.02539	3.10	gi 392381391	fluoroacetate dehalogenase
0.025146	3.10	gi 392378316	putative sensor histidine kinase
0.017468	3.09	gi 392379924	exported protein of unknown function
0.046532	3.09	gi 392380891	phosphoenolpyruvate synthase regulatory protein
0.002771	3.07	gi 392384088	ABC transporter
0.004966	3.02	gi 392377991	hypothetical protein
0.033717	2.98	gi 392378244	CopG family transcriptional regulator
0.038633	2.97	gi 392378473	chromosome segregation ATPase
0.051071	2.95	gi 392380777	spermidine/putrescine ABC transporter,substrate-binding component
0.00771	2.95	gi 392380635	conserved protein of unknown function
0.00321	2.92	gi 392383940	glycine/betaine ABC transporter substrate-binding protein
2.06E-05	2.90	gi 392377535	D-3-phosphoglycerate dehydrogenase-like protein
0.01696	2.88	gi 392378378	quercetin 2,3-dioxygenase
0.01243	2.88	gi 392381711	methyl-accepting chemotaxis protein
0.003176	2.87	gi 392380874	imidazole glycerol phosphate synthase cyclase subunit
0.006817	2.82	gi 392378401	ribonucleoside-diphosphate reductase, adenosylcobalamin-dependent
0.030507	2.81	gi 392377400	squalene synthase HpnD
0.008411	2.78	gi 392379395	hypothetical protein
0.000203	2.76	gi 392384090	enoyl-CoA hydratase
0.012335	2.72	gi 392379195	LysR family transcriptional regulator
0.004127	2.71	gi 392384146	5-methyltetrahydropteroylglutamate--homocysteine S-methyltransferase
0.01421	2.70	gi 392381702	phosphate starvation protein PhoH
0.001348	2.66	gi 392384156	carboxyvinyl-carboxyphosphonate phosphorylmutase
2.05E-05	2.64	gi 392380183	peptidase
0.005949	2.64	gi 392381217	hypothetical protein
0.035041	2.63	gi 392382712	hypothetical protein
0.0126	2.62	gi 392381207	ornithine cyclodeaminase
0.015762	2.54	gi 392378438	transcriptional regulator
0.006262	2.48	gi 392381341	hypothetical protein
0.022387	2.48	gi 392380651	heme ABC exporter, ATP-binding protein CcmA
0.008063	2.46	gi 392380931	ABC transporter ATP-binding protein

0.037147	2.44	gi 392379902	RNase adaptor protein RapZ
0.003612	2.41	gi 392382870	two-component transcriptional regulator involved in heavy-metal (Cu/Zn) homeostasis
0.000735	2.40	gi 392383138	methyl-accepting chemotaxis protein
0.022916	2.36	gi 392379901	PTS permease nitrogen regulatory IIA protein, partial
0.04535	2.35	gi 392382866	MFS transporter
0.000251	2.34	gi 392383996	bifunctional protein putA [Includes: Proline dehydrogenase; Delta-1-pyrroline-5-carboxylate dehydrogenase]
0.012474	2.32	gi 392377431	hypothetical protein
0.023398	2.31	gi 392379312	polyamine ABC transporter substrate-binding protein
0.003619	2.30	gi 392383844	ABC transporter ATP-binding protein
0.013645	2.29	gi 392378236	periplasmic-binding protein
0.005876	2.27	gi 392381489	hypothetical protein
0.001075	2.27	gi 392382075	heat-shock protein
0.001323	2.27	gi 392381066	phage shock protein PspA
0.046568	2.22	gi 392381965	acetolactate synthase small subunit
0.038697	2.18	gi 392383946	conserved protein of unknown function
0.005981	2.18	gi 392379796	nuclease PIN
0.010697	2.17	gi 392383696	putative O-succinylbenzoate--CoA ligase (menE)
0.02915	2.16	gi 392378812	GGDEF domain-containing protein
0.00083	2.15	gi 392384279	3-isopropylmalate dehydrogenase
0.015696	2.15	gi 392382322	ABC transporter ATP-binding protein
0.001762	2.14	gi 392378129	protein of unknown function
0.021062	2.14	gi 392383963	pyridoxal 4-dehydrogenase
0.003308	2.11	gi 392382528	putative cobalamin synthesis protein CobW-like
0.003721	2.10	gi 392382483	Holliday junction DNA helicase RuvB
0.001657	2.10	gi 392383778	2-dehydro-3-deoxy-6-phosphogalactonate aldolase
0.004045	2.09	gi 392377271	cytochrome C protein
0.015919	2.09	gi 392383170	farnesyltranstransferase
0.032383	2.08	gi 392384031	C4-dicarboxylate ABC transporter
0.000199	2.07	gi 392383471	alpha/beta hydrolase
0.000515	2.07	gi 392382575	glycogen debranching enzyme
0.010573	2.06	gi 392380694	phenylalanine-tRNA ligase subunit alpha
0.000312	2.06	gi 392383681	acetyl-CoA acetyltransferase with thiolase domain (fragment), partial
0.049261	2.05	gi 392380825	putative divalent cation transporter (hemolysin and CBS domains)
0.014204	2.05	gi 392382591	methylenetetrahydrofolate reductase [NAD(P)H]
0.015954	2.03	gi 392381424	50S ribosomal protein L27
Downregulated:			
6.47E-08	474.06	gi 392384504	glycerol-3-phosphate dehydrogenase
0.000135	377.48	gi 392384510	ABC transporter substrate-binding protein
3.09E-08	274.74	gi 392380237	oxaryl-CoA decarboxylase
0.000579	109.28	gi 392378810	response regulator

3.04E-08	100.24	gi 392381543	tripartite ATP-independent periplasmic transporter, DctQ component
2.19E-06	89.01	gi 392381576	acetoin:2,6-dichlorophenolindophenol oxidoreductase subunit alpha
1.41E-06	85.08	gi 392381231	site-specific tyrosine recombinase
0.007958	66.33	gi 392378783	2-aminobenzoate-CoA ligase
1.44E-05	60.23	gi 392381577	pyruvate dehydrogenase subunit beta
1.09E-05	57.11	gi 392381579	shikimate 5-dehydrogenase
0.000197	49.03	gi 392384512	glycerol kinase
0.013648	46.79	gi 392377868	conserved protein of unknown function
0.000185	45.03	gi 392384505	ABC transporter ATP-binding protein
7.44E-06	42.97	gi 392379004	amino acid-binding protein
5.27E-07	42.31	gi 392380229	formyl-CoA transferase
0.002863	39.85	gi 392382435	agmatine deiminase
0.000155	39.70	gi 392378686	type VI secretion protein EvpB
3.41E-05	33.32	gi 392377679	ABC transporter ATP-binding protein
0.000349	30.14	gi 392381648	putative short chain dehydrogenase
6.83E-07	30.11	gi 392379885	putative sperimidine/putrescine transport protein (ABC superfamily, atp_bind)
0.00029	28.74	gi 392377166	PAS domain-containing sensor histidine kinase
2.41E-06	26.63	gi 392380243	amino acid dehydrogenase
1.11E-06	26.63	gi 392381546	hypothetical protein
2.80E-06	25.30	gi 392382531	conserved hypothetical protein; beta-Ig-H3/Fasciclin domain
2.02E-06	24.80	gi 392378463	acetyl-CoA acetyltransferase
0.000154	22.80	gi 392379746	3-ketoacyl-ACP reductase
0.01486	19.99	gi 392380782	hypothetical protein
0.000261	17.79	gi 392384513	oxidoreductase
0.002789	16.31	gi 392380519	ABC transporter substrate-binding protein
0.000465	15.88	gi 392382197	ABC transporter substrate-binding protein
0.003572	14.17	gi 392377674	3-hydroxybutyrate dehydrogenase
0.002019	13.90	gi 392384506	ABC transporter ATP-binding protein
0.002209	13.14	gi 392383076	nitrate ABC transporter substrate-binding protein
0.001283	12.78	gi 392378256	peroxiredoxin
0.000241	12.13	gi 392378371	AMP-dependent synthetase
0.000208	11.96	gi 392380358	hypothetical protein
0.007269	11.84	gi 392377678	ABC transporter permease
0.00313	11.60	gi 392379146	hypothetical protein
0.002886	11.19	gi 392378070	chemotaxis protein
3.19E-07	10.23	gi 392377496	hypothetical protein
4.63E-05	10.20	gi 392379078	ABC transporter permease
0.002011	9.97	gi 392382827	cytochrome c oxidase subunit II
1.03E-06	9.97	gi 392380095	glucose dehydrogenase precursor
8.15E-05	9.46	gi 392377680	ABC transporter ATP-binding protein
0.005502	9.42	gi 392383564	conserved protein of unknown function
0.009671	9.38	gi 392379787	saccharopine dehydrogenase

0.007037	9.19	gi 392383073	oxidoreductase
0.009848	9.03	gi 392377454	regulator of disulfide-bond formation, SirA family protein
0.002068	8.98	gi 392378687	type VI secretion protein
0.00013	8.84	gi 392378851	hypothetical protein
2.93E-05	8.77	gi 392381995	hypothetical protein
0.009169	8.68	gi 392379974	serine acetyltransferase
0.007289	8.62	gi 392383487	hydrolase
0.017016	7.73	gi 392379079	aldehyde dehydrogenase
0.0126	7.60	gi 392378685	conserved protein of unknown function
0.000236	7.34	gi 392377425	hypothetical protein
0.007772	7.20	gi 392378172	arabinose 5-phosphate isomerase
0.00745	7.11	gi 392382073	isomerase
0.059828	6.93	gi 392378216	hypothetical protein
0.000951	6.64	gi 392379737	aldehyde dehydrogenase
0.032919	6.32	gi 392378867	hypothetical protein
0.013291	6.03	gi 392382167	pyrroloquinoline quinone biosynthesis protein PqqD
2.22E-05	5.92	gi 392377675	acetoacetyl-coenzyme A synthetase
0.000287	5.91	gi 392382000	protein of unknown function
0.001035	5.89	gi 392382729	adenylyl-sulfate kinase
0.004229	5.80	gi 392382682	outer membrane protein assembly factor
0.024171	5.60	gi 392377421	segregation/condensation protein A
0.000181	5.46	gi 392378073	methyl-accepting chemotaxis sensory transducer (fragment), partial
4.31E-05	5.45	gi 392377272	carbon monoxide dehydrogenase subunit G
0.000157	5.43	gi 392381330	enoyl-CoA hydratase
0.007257	5.33	gi 392381362	microcin C ABC transporter permease YejB
0.000309	5.25	gi 392380202	response regulator
0.000571	5.24	gi 392382072	N-acetyltransferase
0.042313	5.18	gi 392379391	hypothetical protein
0.028728	5.15	gi 392380145	2-methylcitrate dehydratase
0.010291	5.15	gi 392380921	DNA-binding response regulator
0.000218	5.10	gi 392382168	pyrroloquinoline quinone biosynthesis protein C
0.008772	5.09	gi 392381386	histidine kinase
3.73E-06	5.03	gi 392380545	NAD-glutamate dehydrogenase
0.005326	4.92	gi 392382217	thioesterase
2.65E-05	4.87	gi 392379136	branched-chain amino acid ABC transporter substrate-binding protein
0.011814	4.84	gi 392381228	CBS domain-containing protein
0.000635	4.73	gi 392377603	Guanylate kinase (GMP kinase)
0.047708	4.71	gi 392384034	ABC transporter
0.000393	4.66	gi 392382957	flagellar motor switch protein FliM
0.000202	4.65	gi 392382862	hybrid sensor histidine kinase/response regulator
5.84E-05	4.60	gi 392380246	SAM-dependent methyltransferase (fragment), partial
0.044319	4.54	gi 392383129	leucyl/phenylalanyl-tRNA--protein transferase

0.001871	4.48	gi 392383807	MBL fold hydrolase
0.012837	4.43	gi 392378465	acyl-CoA dehydrogenase
0.013728	4.39	gi 392382655	cobyric acid synthase CobQ
0.048464	4.32	gi 392379285	hypothetical protein
0.005895	4.28	gi 392379747	dehydratase
0.000304	4.26	gi 392382890	DNA primase
0.000732	4.24	gi 392378075	protein of unknown function
0.016083	4.16	gi 392383902	Dak phosphatase
0.000113	4.12	gi 392380028	short chain dehydrogenase
0.000446	4.11	gi 392381232	malate synthase A
0.001169	4.09	gi 392383905	dihydrodipicolinate synthase family protein
0.001807	4.08	gi 392383072	hypothetical protein
0.000251	4.04	gi 392382858	alkylhydroperoxidase
0.049713	4.00	gi 392378436	chemotaxis glutamate methylesterase CheB
0.00732	3.96	gi 392380533	peptidase S16
0.031582	3.96	gi 392382717	phosphate acyltransferase
0.000296	3.87	gi 392381859	alcohol dehydrogenase
0.058512	3.83	gi 392378896	hydrolase
0.008744	3.79	gi 392378997	acyl-CoA dehydrogenase
0.00663	3.77	gi 392380686	membrane protein
0.002888	3.69	gi 392382605	C4-dicarboxylate ABC transporter
0.001281	3.62	gi 392379740	ABC transporter substrate-binding protein
0.000736	3.61	gi 392381539	oxidoreductase
0.00681	3.60	gi 392382924	VWA domain-containing protein
0.000827	3.57	gi 392383231	hypothetical protein
0.00232	3.53	gi 392378026	sugar ABC transporter
0.004385	3.51	gi 392377409	protein of unknown function
2.95E-05	3.48	gi 392381171	cation acetate symporter
0.001246	3.47	gi 392382126	phosphatidate cytidylyltransferase
3.07E-06	3.46	gi 392381516	3,4-dihydroxy-2-butanone 4-phosphate synthase
0.001472	3.44	gi 392378255	ABC transporter substrate-binding protein
0.052085	3.41	gi 392382856	hypothetical protein
0.008856	3.39	gi 392379179	lipopolysaccharide biosynthesis (fragment), partial
0.004485	3.38	gi 392377659	murein L,D-transpeptidase
0.000751	3.35	gi 392384520	response regulator
0.002811	3.30	gi 392379303	ABC transporter substrate-binding protein
0.0038	3.27	gi 392378215	conserved protein of unknown function
0.000152	3.27	gi 392384516	citrate (Si)-synthase
1.74E-05	3.27	gi 392382040	hypothetical protein
0.018691	3.25	gi 392382679	peroxiredoxin
0.001797	3.24	gi 392381484	phosphoribosylformylglycinamide synthase
0.000553	3.20	gi 392381032	isocitrate lyase
6.62E-05	3.18	gi 392383065	hypothetical protein
0.001809	3.16	gi 392380560	DUF1674 domain-containing protein

0.000665	3.14	gi 392378407	conserved protein of unknown function
0.008254	3.12	gi 392380240	haloacid dehalogenase
0.002832	3.12	gi 392378024	fumarylacetoacetate hydrolase
0.029379	3.07	gi 392378157	3-oxoacyl-ACP reductase
0.001468	3.06	gi 392378071	hypothetical protein
1.85E-06	3.06	gi 392382138	glutathione S-transferase
0.003071	3.06	gi 392377627	hybrid sensor histidine kinase/response regulator
0.011945	3.01	gi 392383781	ATP-dependent chaperone ClpB
0.000622	3.00	gi 392381665	CoA transferase
0.006359	3.00	gi 392377566	altronate hydrolase
0.009921	2.97	gi 392378575	acetoin utilization protein
0.001312	2.97	gi 392378566	coproporphyrinogen III oxidase
0.003415	2.94	gi 392378749	nucleotidyltransferase
0.002134	2.93	gi 392380004	2-hydroxychromene-2-carboxylate isomerase
8.13E-05	2.91	gi 392381924	conserved protein of unknown function
0.000876	2.91	gi 392378675	RNA polymerase sigma factor RpoE
0.004864	2.89	gi 392379110	translation initiation factor IF-3
2.64E-05	2.85	gi 392379933	beta-ketoacyl-ACP reductase
0.000395	2.84	gi 392382745	cobalamin biosynthesis protein CobD
0.002412	2.82	gi 392377591	hypothetical protein
0.005855	2.81	gi 392379365	two-component system sensor histidine kinase/response regulator
0.001454	2.79	gi 392378657	methylmalonyl-CoA carboxyltransferase
0.012919	2.78	gi 392382356	aminodeoxychorismate lyase
0.003233	2.77	gi 392380638	magnesium transporter
0.007888	2.75	gi 392381917	propionyl-CoA synthetase
0.007042	2.74	gi 392382387	C4-dicarboxylate ABC transporter
2.94E-05	2.73	gi 392377478	ABC transporter substrate-binding protein
0.000553	2.72	gi 392384521	conserved protein of unknown function
0.000294	2.70	gi 392379758	mononuclear molybdenum enzyme YedY
4.40E-07	2.69	gi 392382215	enoyl-CoA hydratase
0.04989	2.69	gi 392382481	crossover junction endodeoxyribonuclease
0.034358	2.67	gi 392380949	transporter
0.000543	2.66	gi 392380962	high-affinity branched-chain amino acid ABC transporter (substrate-binding protein) (fragment), partial
0.017331	2.64	gi 392384535	hypothetical protein
0.001122	2.64	gi 392377806	methyl-accepting chemotaxis protein
0.015807	2.64	gi 392383631	cell division protein
0.027852	2.63	gi 392379394	hypothetical protein
0.027847	2.62	gi 392381887	hypothetical protein
0.000135	2.62	gi 392383091	ABC transporter, substrate-binding component
0.002228	2.61	gi 392377798	hypothetical protein
3.71E-05	2.61	gi 392380056	ATP synthase subunit beta
0.00025	2.60	gi 392382164	3-deoxy-8-phosphoctulonate synthase

6.41E-05	2.58	gi 392378204	hypothetical protein
0.010355	2.58	gi 392383619	CoA ester lyase
0.001199	2.57	gi 392382683	membrane protein
0.002273	2.56	gi 392381931	conserved hypothetical protein with 2 CBS domains
0.005741	2.54	gi 392378072	exported protein of unknown function
0.000428	2.54	gi 392377673	thiol:disulfide oxidoreductase
0.001253	2.53	gi 392379802	heptosyltransferase
0.000496	2.51	gi 392378822	putative tyrosine/serine phosphatase
0.013133	2.49	gi 392377887	ferrous iron transporter B
0.000814	2.49	gi 392378448	cobyric acid a,c-diamide synthase
0.001412	2.49	gi 392378842	protein phosphatase
0.001944	2.49	gi 392381940	3-methyl-2-oxobutanoate hydroxymethyltransferase
0.047944	2.48	gi 392379290	hypothetical protein
0.001014	2.47	gi 392381091	peptide-methionine (R)-S-oxide reductase
0.006017	2.47	gi 392377471	hypothetical protein
0.006473	2.47	gi 392378950	alcohol dehydrogenase
0.038075	2.46	gi 392377885	conserved protein of unknown function
0.002628	2.45	gi 392381674	conserved exported protein of unknown function
0.00039	2.45	gi 392380087	acriflavine resistance protein B
0.001059	2.45	gi 392378782	putative transcriptional regulator, MarR family
0.000726	2.44	gi 392383176	hypothetical protein
0.024873	2.43	gi 392380173	diguanylate cyclase
0.00011	2.38	gi 392381685	formate dehydrogenase subunit gamma
0.002038	2.38	gi 392381147	ATP-dependent DNA helicase RecQ
0.008154	2.38	gi 392380011	hypothetical protein
0.033693	2.38	gi 392379289	hypothetical protein
0.000737	2.38	gi 392378578	1-deoxy-D-xylulose-5-phosphate synthase
0.006352	2.36	gi 392383907	conserved exported protein of unknown function
0.002523	2.36	gi 392377182	nucleoside triphosphate pyrophosphohydrolase
0.045588	2.35	gi 392378442	ATP synthase
0.000219	2.34	gi 392382116	carboxymethylenebutenolidase
0.016845	2.34	gi 392377795	hypothetical protein
0.000896	2.32	gi 392382214	CoA-binding protein
0.000859	2.32	gi 392377593	phosphoribosylglycinamide formyltransferase
0.00597	2.32	gi 392382776	phytoene desaturase
0.058402	2.31	gi 392381044	putative endonuclease/exonuclease/phosphatase
0.006498	2.31	gi 392380020	lipoate-protein ligase B
0.005615	2.31	gi 392382486	protein TolR
0.006253	2.30	gi 392382747	diguanylate cyclase
0.000638	2.30	gi 392378699	type VI secretion protein
0.001614	2.29	gi 392377408	ATPase AAA
0.000451	2.29	gi 392382407	putative acetyltransferase
0.004056	2.28	gi 392382038	putative phosphoglycolate phosphatase

0.00508	2.27	gi 392383629	diaminopimelate epimerase
0.013136	2.26	gi 392381155	putative ATP-dependent RNA helicase with P-loop hydrolase domain (rhIE gene)
0.030614	2.25	gi 392383088	amP-dependent synthetase and ligase
0.007428	2.25	gi 392379403	copper ABC transporter, permease component (modular protein)
0.005041	2.24	gi 392379965	acylphosphatase
0.021528	2.21	gi 392377377	pantetheine-phosphate adenylyltransferase
0.000937	2.20	gi 392381311	oxidoreductase
0.000398	2.20	gi 392382161	preprotein translocase subunit SecG
0.000999	2.19	gi 392380439	Fe-S oxidoreductase
0.034395	2.19	gi 392378884	hypothetical protein
0.017602	2.19	gi 392383046	polysaccharide export protein
0.012118	2.19	gi 392381025	2-oxoglutarate synthase
0.002647	2.18	gi 392383638	response regulator
0.00469	2.18	gi 392381099	C4-dicarboxylate ABC transporter
0.000491	2.18	gi 392383664	hypothetical protein
0.051918	2.17	gi 392377165	tRNA-dihydrouridine synthase
0.020637	2.17	gi 392383212	lipoprotein
0.000926	2.15	gi 392383337	transcription elongation factor GreA
0.014571	2.15	gi 392380354	chromosome partitioning protein, partial
0.006984	2.15	gi 392380022	aldehyde dehydrogenase
0.000124	2.15	gi 392379938	phosphohydrolase
0.000203	2.15	gi 392378904	pyruvate dehydrogenase (acetyl-transferring) E1 component subunit alpha
0.036533	2.14	gi 392383086	cupin
0.002179	2.12	gi 392383957	molybdopterin dinucleotide-binding region
0.004528	2.12	gi 392377826	aminoglycoside phosphotransferase
0.006553	2.11	gi 392380832	MucR family transcriptional regulator
0.009971	2.11	gi 392377175	putative GTP-binding protein (HflX-like)
0.015286	2.10	gi 392377631	FAD-dependent oxidoreductase
0.016833	2.10	gi 392380236	NADH-quinone oxidoreductase subunit F
0.006281	2.09	gi 392379459	flagellin
0.00288	2.09	gi 392378866	16S rRNA-binding GTPase
0.026423	2.08	gi 392383148	hypothetical protein
0.000977	2.08	gi 392382714	hypothetical protein
0.013956	2.08	gi 392382031	ATPase AAA
0.00031	2.08	gi 392383276	conserved protein of unknown function; putative coiled-coil domain
0.001647	2.07	gi 392383052	ABC transporter substrate-binding protein
0.0001	2.06	gi 392377461	ABC transporter substrate-binding protein
0.051155	2.06	gi 392377205	ABC transporter substrate-binding protein
0.012882	2.05	gi 392378519	histidinol-phosphate transaminase
0.003257	2.04	gi 392378852	transcriptional regulator
0.003927	2.04	gi 392382489	peptidoglycan-associated lipoprotein
0.000726	2.04	gi 392381213	diguanylate cyclase

0.039689	2.04	gi 392377162	competence damage-inducible protein A
0.012512	2.03	gi 392381088	cold-shock protein

FONTE: a autora (2018).

TABELA 22 - PROTEÍNAS DIFERENCIAIS ENTRE *A. brasiliense* FP2 E O MUTANTE *ntrC* EM ALTO NITROGÊNIO.

t-test p-value	FC	Protein IDs	Protein
Upregulated:			
1.35E-06	1870.55	gi 392384431	beta-ketoacyl-ACP reductase
2.69E-06	747.88	gi 392384452	amino acid ABC transporter substrate-binding protein
1.66E-07	240.28	gi 392384453	hypothetical protein
3.09E-06	153.69	gi 392384445	FMN reductase
1.01E-08	142.30	gi 392384455	amidohydrolase
3.24E-05	96.96	gi 392384451	high-affinity branched-chain amino acid ABC transporter (permease protein) (fragment), partial
2.06E-05	86.62	gi 392383952	amino acid ABC transporter substrate-binding protein
0.000321	63.27	gi 392384448	2-amino-thiazoline-4-carboxylic acid hydrolase
0.02871	60.80	gi 392383747	proton channel of the Tol-Pal system (fragment), partial
3.22E-05	52.51	gi 392384454	putative FAD dependent oxidoreductase
0.000636	44.87	gi 392381915	protein of unknown function
4.74E-06	41.30	gi 392384438	phosphatidylethanolamine N-methyltransferase
3.02E-05	40.72	gi 392379840	phosphate acetyltransferase
6.79E-08	35.40	gi 392378794	S-adenosyl-L-methionine (SAM)-dependent methyltransferase PhcB
1.36E-05	34.27	gi 392384437	chromosome partitioning protein
0.000659	31.72	gi 392380947	S-adenosylmethionine decarboxylase related
0.001162	29.70	gi 392382671	Crp-type transcriptional activatory protein (fragment), partial
6.35E-07	29.69	gi 392384436	putative chromosome-partitioning protein parB
5.31E-07	28.31	gi 392383051	MarR family transcriptional regulator
2.34E-06	27.71	gi 392384447	putative sensory transducer protein
3.48E-06	27.15	gi 392377295	conserved protein of unknown function; putative Radical SAM domain
0.008096	25.60	gi 392378514	hypothetical protein
0.000152	25.32	gi 392378501	Uptake hydrogenase large subunit precursor
0.000585	25.31	gi 392383746	exported protein of unknown function
5.05E-06	21.90	gi 392380632	phosphotyrosine protein phosphatase
1.76E-05	19.77	gi 392384450	ABC transporter ATP-binding protein
0.003045	18.38	gi 392383748	TonB system transport protein ExbD
0.002353	16.56	gi 392384456	hypothetical protein
0.000108	16.16	gi 392381842	protein of unknown function, partial
6.42E-05	16.09	gi 392383652	anti-sigma factor antagonist
0.008413	14.55	gi 392382103	NADH-quinone oxidoreductase subunit M
0.003625	13.67	gi 392383950	N-formylglutamate deformylase
9.74E-05	12.97	gi 392384473	acetyltransferase

3.58E-05	12.75	gi 392379397	U32 family peptidase
0.012659	12.55	gi 392381657	hypothetical protein
0.000138	12.25	gi 392380710	CBS domain-containing protein
1.77E-07	12.15	gi 392379656	cytochrome c
0.000779	11.41	gi 392378504	Uptake hydrogenase small subunit precursor (Hydrogenlyase) (Membrane-bound hydrogenase small subunit)
0.005693	11.13	gi 392384484	Tlp1
0.00944	10.82	gi 392383591	homoserine O-succinyltransferase
8.59E-05	10.47	gi 392383594	methyl-accepting chemotaxis protein
0.00013	9.87	gi 392384458	O-methyltransferase
0.004812	9.80	gi 392378572	transcriptional regulator
0.000753	9.62	gi 392384449	branched-chain amino acids ABC transporter; ATP-binding component
0.001863	8.76	gi 392384067	polyisoprenoid-binding protein
0.001539	8.70	gi 392377282	hypothetical protein
0.00023	8.53	gi 392378226	iron ABC transporter substrate-binding protein
0.03642	8.42	gi 392380886	death-on-curing protein
0.008609	8.00	gi 392382599	dehydrogenase
9.38E-06	7.97	gi 392378882	IMP dehydrogenase
0.001102	7.81	gi 392383677	3-methylcrotonyl-CoA carboxylase subunit alpha
0.001941	7.70	gi 392383613	diguanylate cyclase
0.002189	7.62	gi 392384485	putative methyl-accepting chemotaxis protein
0.000242	7.54	gi 392379393	cyclic nucleotide-binding protein
0.009722	7.23	gi 392380458	chromosome partitioning protein
0.000175	7.00	gi 392380182	hypothetical protein
0.049974	6.71	gi 392381219	hypothetical protein
9.11E-06	6.69	gi 392382912	oxidoreductase
0.021791	6.58	gi 392378234	iron-dicitrate transporter subunit; ATP-binding component of ABC superfamily; KpLE2 phage-like element
0.008098	6.56	gi 392380755	integral membrane protein linked to a cation pump
0.019894	6.53	gi 392383253	conserved exported protein of unknown function; deacylase domain
1.62E-05	6.00	gi 392378500	hydrogenase 2 maturation endopeptidase
0.004205	5.99	gi 392379071	nitrite reductase, copper-containing
0.001748	5.95	gi 392383973	hypothetical protein
0.002338	5.95	gi 392378488	hydrogenase expression/formation protein HypE
0.000292	5.92	gi 392384245	ABC transporter substrate-binding protein
8.97E-05	5.86	gi 392380133	hypothetical protein
0.001286	5.86	gi 392382322	ABC transporter ATP-binding protein
0.000383	5.80	gi 392380302	hypothetical protein
0.00839	5.70	gi 392379033	ABC transporter substrate-binding protein
0.002298	5.59	gi 392379404	ABC transporter ATP-binding protein
0.012971	5.58	gi 392380649	transporter
0.037502	5.49	gi 392381270	two component sensor histidine kinase; membrane protein

6.35E-05	5.42	gi 392378016	cobalt ABC transporter substrate-binding protein
0.002485	5.38	gi 392378198	exported protein of unknown function
0.007074	5.33	gi 392382976	hypothetical protein
0.007975	5.31	gi 392382967	flagellar assembly protein FliX
0.002325	5.24	gi 392378492	hydrogenase accessory protein HypB
0.000375	5.23	gi 392378730	cell filamentation protein Fic
0.000556	5.18	gi 392383015	elongation factor G
6.23E-05	5.15	gi 392383847	acetylpolyamine amidohydrolase
7.84E-06	5.04	gi 392378223	iron ABC transporter ATP-binding protein
0.000572	5.02	gi 392379395	hypothetical protein
0.05495	5.02	gi 392382529	transcriptional repressor
3.33E-05	4.98	gi 392377563	C4-dicarboxylate ABC transporter
0.000113	4.95	gi 392384019	2-keto-4-methylthiobutyrate aminotransferase
0.030445	4.90	gi 392378729	putative hemerythrin-like, metal-binding (MHR) protein (bacteriohemerythrin)
0.005219	4.87	gi 392379408	hypothetical protein
0.005017	4.83	gi 392381691	two-component sensor histidine kinase
0.052873	4.76	gi 392378258	Rrf2 family transcriptional regulator
0.000377	4.71	gi 392378353	protein of unknown function
6.66E-06	4.69	gi 392383368	hypothetical protein
1.88E-05	4.68	gi 392380759	cytochrome c oxidase, cbb3-type subunit II
0.029194	4.61	gi 392384269	hypothetical protein
0.00101	4.53	gi 392379032	mandelate racemase
0.000217	4.47	gi 392379406	TAT-dependent nitrous-oxide reductase
0.004932	4.38	gi 392380180	conserved exported protein of unknown function
0.003692	4.38	gi 392380392	dTDP-glucose 4,6-dehydratase
5.49E-05	4.32	gi 392383643	chemotaxis response regulator CheY
5.99E-06	4.32	gi 392378423	hypothetical protein
0.040691	4.28	gi 392379713	agmatinase
0.019516	4.25	gi 392378308	acyl-CoA synthetase
0.017422	4.22	gi 392381172	conserved protein of unknown function; putative CBS domain
0.00083	4.20	gi 392377535	D-3-phosphoglycerate dehydrogenase-like protein
0.024546	4.15	gi 392380859	oxidoreductase subunit with NAD(P)-binding domain and ferredoxin-like domain
0.026058	4.02	gi 392382663	protein of unknown function
2.22E-05	3.96	gi 392383138	methyl-accepting chemotaxis protein
2.60E-06	3.95	gi 392381337	oxygen-independent coproporphyrinogen III oxidase
0.029158	3.94	gi 392383259	aldolase
0.000624	3.91	gi 392383948	IclR family transcriptional regulator
0.006184	3.86	gi 392383795	ABC transporter substrate-binding protein
0.015651	3.86	gi 392381489	hypothetical protein
3.34E-06	3.81	gi 392380183	peptidase
0.008607	3.79	gi 392381707	cell division topological specificity factor MinE
0.009459	3.79	gi 392384266	protein of unknown function

8.10E-06	3.77	gi 392382402	ABC transporter permease
0.009886	3.74	gi 392381354	flagellar motor switch protein FliG
0.000132	3.74	gi 392380757	cytochrome c oxidase, cbb3-type subunit III
0.004101	3.74	gi 392381711	methyl-accepting chemotaxis protein
0.000127	3.73	gi 392378406	cell division ATP-binding protein FtsE
9.49E-05	3.71	gi 392377994	putative ornithine cyclodeaminase
0.003397	3.69	gi 392381486	hypothetical protein
2.93E-05	3.63	gi 392378668	hypothetical protein
1.79E-05	3.62	gi 392381058	cytochrome c biogenesis protein CcsA
0.007758	3.57	gi 392377400	squalene synthase HpND
0.004148	3.54	gi 392380661	cytochrome c biogenesis protein
4.61E-05	3.51	gi 392383844	ABC transporter ATP-binding protein
0.00173	3.48	gi 392383793	peptidase
5.51E-06	3.45	gi 392381453	indolepyruvate/phenylpyruvate decarboxylase
0.000141	3.44	gi 392378673	formate acetyltransferase
0.012793	3.43	gi 392379391	hypothetical protein
0.002293	3.41	gi 392379159	hypothetical protein
0.001182	3.40	gi 392380760	cytochrome c oxidase, cbb3-type subunit I
0.000162	3.40	gi 392380418	putative Glycosyl transferase protein
0.000606	3.39	gi 392381025	2-oxoglutarate synthase
0.050729	3.38	gi 392379353	ABC transporter substrate-binding protein
0.003979	3.38	gi 392381292	16S rRNA processing protein RimM
7.24E-05	3.37	gi 392382593	protein of unknown function
0.045178	3.36	gi 392381379	methyltransferase UbiE
0.004653	3.35	gi 392378413	hypothetical protein
0.023376	3.33	gi 392383653	conserved protein of unknown function
0.001981	3.33	gi 392380891	phosphoenolpyruvate synthase regulatory protein
0.021235	3.32	gi 392377857	TPR repeat-containing protein (fragment), partial
0.003078	3.32	gi 392378879	acriflavin resistance protein
0.000242	3.31	gi 392380184	methylamine utilization protein MauG
0.007346	3.29	gi 392383646	chemotaxis signal transduction protein CheW
0.053396	3.28	gi 392381074	ATP-binding protein
0.025255	3.22	gi 392378411	multidrug resistance efflux pump (EmrB-like) (fragment), partial
0.001131	3.22	gi 392382482	Holliday junction ATP-dependent DNA helicase RuvA
0.002366	3.21	gi 392380651	heme ABC exporter, ATP-binding protein CcmA
0.009187	3.18	gi 392382676	conserved protein of unknown function; putative histidine triad hydrolase domain
0.000153	3.18	gi 392381026	2-oxoglutarate synthase
8.85E-05	3.17	gi 392383946	conserved protein of unknown function
0.034707	3.15	gi 392378329	arginase
0.00032	3.13	gi 392384086	ATP-dependent acyl-CoA ligase
0.004225	3.12	gi 392380874	imidazole glycerol phosphate synthase cyclase subunit
0.001187	3.11	gi 392381391	fluoroacetate dehalogenase

0.000801	3.09	gi 392378470	membrane protein
0.000437	3.08	gi 392378674	sigma-54-dependent Fis family transcriptional regulator
0.031596	3.08	gi 392382319	hypothetical protein
0.000648	3.06	gi 392382223	class I poly(R)-hydroxyalkanoic acid synthase
0.010825	3.06	gi 392377431	hypothetical protein
0.044787	3.03	gi 392377796	GGDEF domain-containing protein
0.000259	3.01	gi 392383940	glycine/betaine ABC transporter substrate-binding protein
0.044606	3.00	gi 392378482	ribonuclease HII
0.013308	2.99	gi 392380783	formamidopyrimidine-DNA glycosylase
0.010536	2.99	gi 392382727	phosphoadenosine phosphosulfate reductase
0.000382	2.97	gi 392384251	conserved exported protein of unknown function
0.000539	2.96	gi 392380938	colanic acid biosynthesis glycosyltransferase WcaL
4.25E-07	2.95	gi 392378598	glyoxalase
3.60E-05	2.93	gi 392382289	enoyl-[acyl-carrier-protein] reductase
1.39E-05	2.89	gi 392380790	inorganic pyrophosphatase
0.004184	2.88	gi 392382119	DNA polymerase III subunit alpha
0.000393	2.86	gi 392380181	hypothetical protein
0.001377	2.85	gi 392382075	heat-shock protein
0.013856	2.84	gi 392383212	lipoprotein
0.002867	2.82	gi 392381308	DNA polymerase V
0.000128	2.80	gi 392381994	polyphosphate kinase 2
0.007595	2.75	gi 392380911	major outer membrane protein OmaA
0.024084	2.73	gi 392378187	N5-glutamine S-adenosyl-L-methionine-dependent methyltransferase
6.16E-05	2.72	gi 392377888	conserved exported protein of unknown function
0.001083	2.72	gi 392382562	2-dehydro-3-deoxy-D-gluconate 5-dehydrogenase
0.002138	2.70	gi 392381751	Rrf2 family transcriptional regulator, partial
0.029234	2.70	gi 392384085	methyl-accepting chemotaxis protein
0.040469	2.67	gi 392383655	transcriptional regulator
0.000133	2.65	gi 392383237	phosphate acetyltransferase
0.001279	2.65	gi 392383990	hypothetical protein
0.008129	2.64	gi 392383846	Zn-dependent hydrolase
0.002407	2.64	gi 392380573	glycerol-3-phosphate dehydrogenase
0.002852	2.62	gi 392382231	glycerol dehydrogenase
2.11E-06	2.62	gi 392383170	farnesyltranstransferase
0.000359	2.61	gi 392382461	molybdopterin synthase sulfur carrier subunit
0.007834	2.61	gi 392382930	ATPase AAA
0.01579	2.61	gi 392382111	hypothetical protein
0.006483	2.60	gi 392381427	ABC transporter ATP-binding protein
0.006705	2.60	gi 392383772	3-ketoacyl-CoA reductase
0.004457	2.58	gi 392380743	transcriptional repressor for high-affinity phosphate uptake
0.000642	2.55	gi 392382360	4-hydroxy-tetrahydrodipicolinate synthase
0.000319	2.55	gi 392382528	putative cobalamin synthesis protein CobW-like

3.86E-05	2.55	gi 392377581	RNA degradosome polyphosphate kinase
0.032153	2.55	gi 392379677	ABC transporter substrate-binding protein
0.014453	2.54	gi 392382095	NADH-quinone oxidoreductase subunit E
0.013322	2.53	gi 392382082	malonyl-CoA decarboxylase
0.01607	2.53	gi 392380840	adenylate cyclase
0.02942	2.51	gi 392381096	hypothetical protein
0.037094	2.49	gi 392384150	oxygen-dependent ribonucleotide reductase, beta subunit
0.000527	2.48	gi 392380684	glycogen synthase
0.022604	2.48	gi 392382099	NADH-quinone oxidoreductase subunit I
0.052931	2.47	gi 392382955	hypothetical protein
0.028211	2.46	gi 392381402	methyl-accepting chemotaxis protein (fragment), partial
0.000187	2.46	gi 392383998	putative Metallo-hydrolase/oxidoreductase superfamily protein; Beta-lactamase-like
0.000207	2.45	gi 392378310	methionine ABC transporter substrate-binding protein
0.016171	2.44	gi 392378418	DNA topoisomerase IV, subunit A (fragment), partial
0.048767	2.43	gi 392381460	response regulator, partial
0.001253	2.42	gi 392379901	PTS permease nitrogen regulatory IIA protein, partial
0.005611	2.41	gi 392382706	3,4-dihydroxy-2-butanone-4-phosphate synthase
0.020137	2.41	gi 392378802	hemerythrin
0.013179	2.41	gi 392383654	hypothetical protein
0.053827	2.39	gi 392384040	multidrug ABC transporter ATP-binding protein
0.00377	2.39	gi 392377686	precorrin-6A reductase
0.000106	2.39	gi 392381024	rubererythrin
0.001531	2.39	gi 392380948	spermidine synthase
0.030782	2.38	gi 392383636	chitin deacetylase
0.011533	2.37	gi 392380764	putative RNA methyltransferase
0.00072	2.36	gi 392381965	acetolactate synthase small subunit
0.002767	2.36	gi 392383162	2-isopropylmalate synthase
0.005523	2.35	gi 392380737	cysteine synthase A
0.025662	2.35	gi 392378227	PadR family transcriptional regulator
0.0005	2.34	gi 392383996	bifunctional protein putA [Includes: Proline dehydrogenase; Delta-1-pyrroline-5-carboxylate dehydrogenase]
0.022018	2.34	gi 392382187	esterase
0.008033	2.33	gi 392382179	peroxiredoxin
0.000831	2.33	gi 392378414	GGDEF domain-containing protein
0.011724	2.32	gi 392380842	universal stress protein
0.001954	2.31	gi 392382712	hypothetical protein
0.035698	2.30	gi 392381198	hypothetical protein
0.006685	2.27	gi 392380442	molybdenum storage protein beta subunit (Mo storage protein beta subunit) (MoSto beta subunit)
0.000289	2.26	gi 392377991	hypothetical protein
6.96E-05	2.25	gi 392379844	5-dehydro-4-deoxy-D-glucuronate isomerase
0.032145	2.25	gi 392378416	DNA repair protein RecO

0.004183	2.24	gi 392378424	conserved protein of unknown function; putative coiled-coil and glutathione domains
0.010975	2.24	gi 392381312	hypothetical protein
0.000648	2.22	gi 392381485	phosphoribosylaminoimidazolesuccinocarboxamide synthase
0.014983	2.22	gi 392381288	hypothetical protein
0.007511	2.22	gi 392381207	ornithine cyclodeaminase
0.019571	2.21	gi 392382271	D-amino acid dehydrogenase small subunit
0.001335	2.21	gi 392383681	acetyl-CoA acetyltransferase with thiolase domain (fragment), partial
0.000681	2.21	gi 392378786	hypothetical protein
0.00181	2.20	gi 392382870	two-component transcriptional regulator involved in heavy-metal (Cu/Zn) homeostasis
0.026392	2.20	gi 392382813	hypothetical protein
0.001185	2.20	gi 392382439	ABC transporter ATP-binding protein
0.015234	2.20	gi 392384271	hypothetical protein
0.000692	2.20	gi 392382335	oxidoreductase
0.035585	2.19	gi 392382591	methylenetetrahydrofolate reductase [NAD(P)H]
0.010914	2.19	gi 392379312	polyamine ABC transporter substrate-binding protein
0.043637	2.19	gi 392380078	altronate oxidoreductase
0.000358	2.17	gi 392383778	2-dehydro-3-deoxy-6-phosphogalactonate aldolase
0.005125	2.17	gi 392381368	hypothetical protein
0.000805	2.17	gi 392377562	sorbitol dehydrogenase
0.001493	2.17	gi 392380565	hypothetical protein
0.014835	2.16	gi 392383969	chromosome partitioning protein
0.001033	2.16	gi 392382680	GTP-binding protein
0.044703	2.16	gi 392382224	hypothetical protein
0.008263	2.16	gi 392383932	hypothetical protein
5.45E-05	2.15	gi 392383642	hypothetical protein
0.003517	2.15	gi 392381424	50S ribosomal protein L27
0.019869	2.15	gi 392380647	histidine/lysine/arginine/ornithine ABC transporter ATP-binding protein HisP
0.003166	2.15	gi 392381425	50S ribosomal protein L21
0.000509	2.15	gi 392384277	hypothetical protein
0.034871	2.14	gi 392380627	mannose-1-phosphate guanylyltransferase
0.00139	2.14	gi 392379974	serine acetyltransferase
0.001725	2.13	gi 392378330	ornithine--oxo-acid transaminase
0.002974	2.13	gi 392382575	glycogen debranching enzyme
0.003953	2.13	gi 392382404	arginine ABC transporter ATP-binding protein
0.010204	2.12	gi 392381314	5-aminolevulinate synthase
0.006026	2.12	gi 392383236	acetate kinase
0.013166	2.11	gi 392378965	taurine ABC transporter substrate-binding protein
0.000168	2.11	gi 392382427	DNA polymerase III subunit delta'
0.037363	2.10	gi 392381678	hypothetical protein
0.000847	2.10	gi 392380873	1-(5-phosphoribosyl)-5-[(5-phosphoribosylamino)methylideneamino]imidazole-4-carboxamide isomerase

0.037062	2.10	gi 392378759	short-chain dehydrogenase
0.000234	2.09	gi 392382725	sulfite reductase
0.026514	2.09	gi 392383941	glycine/betaine ABC transporter permease
0.001348	2.08	gi 392377419	putative spermidine/putrescine ABC transporter,(ATP-binding protein)
0.004747	2.08	gi 392378520	cyclohexadienyl dehydrogenase
0.004319	2.07	gi 392383942	proline/glycine betaine ABC transporter ATP-binding protein
0.006745	2.07	gi 392382998	30S ribosomal protein S14
0.050973	2.06	gi 392382263	GntR family transcriptional regulator
0.004383	2.06	gi 392380100	mannonate dehydratase
0.000669	2.06	gi 392383336	carbamoyl phosphate synthase large subunit
0.007373	2.05	gi 392378114	protein of unknown function
0.017031	2.05	gi 392384088	ABC transporter
0.043152	2.05	gi 392377623	branched-chain amino acid aminotransferase
0.059352	2.05	gi 392382804	hypothetical protein
8.89E-05	2.04	gi 392379297	serine/threonine-protein kinase PknK, partial
0.001411	2.03	gi 392382996	50S ribosomal protein L18
0.017172	2.02	gi 392380801	glycerophosphoryl diester phosphodiesterase
0.00972	2.01	gi 392380893	shikimate dehydrogenase
6.71E-06	2.01	gi 392380635	conserved protein of unknown function
0.003553	2.01	gi 392382350	30S ribosomal protein S18
Downregulated:			
8.41E-07	746.43	gi 392381576	acetoin:2,6-dichlorophenolindophenol oxidoreductase subunit alpha
1.60E-07	632.83	gi 392384504	glycerol-3-phosphate dehydrogenase
2.80E-06	336.71	gi 392384510	ABC transporter substrate-binding protein
1.45E-07	221.25	gi 392381577	pyruvate dehydrogenase subunit beta
2.96E-06	153.34	gi 392381543	tripartite ATP-independent periplasmic transporter, DctQ component
1.72E-07	78.15	gi 392381579	shikimate 5-dehydrogenase
0.000146	75.73	gi 392380358	hypothetical protein
1.55E-06	60.15	gi 392380237	oxaryl-CoA decarboxylase
6.61E-07	52.01	gi 392380229	formyl-CoA transferase
0.000104	50.52	gi 392382197	ABC transporter substrate-binding protein
7.91E-06	48.93	gi 392384505	ABC transporter ATP-binding protein
4.90E-05	44.34	gi 392383076	nitrate ABC transporter substrate-binding protein
5.95E-07	42.42	gi 392384512	glycerol kinase
0.000574	39.96	gi 392380519	ABC transporter substrate-binding protein
9.17E-08	39.43	gi 392380243	amino acid dehydrogenase
0.000108	35.36	gi 392377678	ABC transporter permease
1.34E-05	34.60	gi 392381228	CBS domain-containing protein
2.23E-05	29.66	gi 392379004	amino acid-binding protein
7.60E-06	27.70	gi 392381546	hypothetical protein
0.00011	27.46	gi 392378686	type VI secretion protein EvpB
0.000123	24.61	gi 392380217	hypothetical protein

5.24E-05	24.51	gi 392379740	ABC transporter substrate-binding protein
0.000169	24.06	gi 392383073	oxidoreductase
0.000137	21.55	gi 392378687	type VI secretion protein
9.03E-07	19.21	gi 392377496	hypothetical protein
0.000752	18.22	gi 392377679	ABC transporter ATP-binding protein
0.017898	17.98	gi 392377868	conserved protein of unknown function
9.04E-06	15.86	gi 392379746	3-ketoacyl-ACP reductase
5.47E-06	15.59	gi 392379136	branched-chain amino acid ABC transporter substrate-binding protein
7.58E-05	14.46	gi 392379078	ABC transporter permease
0.000407	13.46	gi 392384513	oxidoreductase
7.13E-07	13.32	gi 392382138	glutathione S-transferase
0.002897	13.06	gi 392381859	alcohol dehydrogenase
0.030019	12.10	gi 392378681	ClpV1 family T6SS ATPase
4.47E-06	12.08	gi 392378463	acetyl-CoA acetyltransferase
0.001219	11.95	gi 392378256	peroxiredoxin
0.001366	10.83	gi 392382827	cytochrome c oxidase, subunit II
0.002249	10.68	gi 392380055	prolipoprotein diacylglycerol transferase
0.01025	10.47	gi 392381718	4-alpha-hydroxy-tetrahydropterin dehydratase (fragment), partial
2.53E-07	10.32	gi 392379737	aldehyde dehydrogenase
0.027488	10.27	gi 392380319	DNA-binding response regulator
0.007599	10.13	gi 392378075	protein of unknown function
0.0123	8.85	gi 392379287	protein of unknown function
0.001868	8.80	gi 392377165	tRNA-dihydrouridine synthase
0.001732	8.70	gi 392378997	acyl-CoA dehydrogenase
3.47E-05	8.42	gi 392381386	histidine kinase
4.06E-05	8.10	gi 392381362	microcin C ABC transporter permease YejB
0.02184	8.10	gi 392379079	aldehyde dehydrogenase
0.013923	8.03	gi 392382745	cobalamin biosynthesis protein CobD
8.10E-05	7.99	gi 392378371	AMP-dependent synthetase
9.19E-06	7.95	gi 392378468	histidine kinase
0.010166	7.85	gi 392382563	acyl-CoA dehydrogenase
0.00554	7.77	gi 392380145	2-methylcitrate dehydratase
0.004361	7.22	gi 392381633	protein of unknown function
0.00013	6.88	gi 392380202	response regulator
4.35E-05	6.81	gi 392377675	acetoacetyl-coenzyme A synthetase
0.000169	6.70	gi 392377272	carbon monoxide dehydrogenase subunit G
0.002162	6.15	gi 392383857	Crp/Fnr family transcriptional regulator
0.000293	6.13	gi 392382683	membrane protein
0.015451	5.66	gi 392383781	ATP-dependent chaperone ClpB
2.25E-05	5.50	gi 392380545	NAD-glutamate dehydrogenase
4.48E-05	5.47	gi 392378685	conserved protein of unknown function
0.037916	5.39	gi 392383284	response regulator
0.000381	5.37	gi 392377680	ABC transporter ATP-binding protein

0.00758	5.06	gi 392381501	glycosyl transferase family 51
0.016947	4.94	gi 392379394	hypothetical protein
0.056435	4.82	gi 392383348	2-dehydropantoate 2-reductase
0.003868	4.74	gi 392379403	copper ABC transporter, permease component (modular protein)
0.003281	4.67	gi 392380075	dihydroxy-acid dehydratase
0.000145	4.65	gi 392382072	N-acetyltransferase
0.001505	4.63	gi 392382481	crossover junction endodeoxyribonuclease
7.12E-05	4.59	gi 392382682	outer membrane protein assembly factor
0.000234	4.54	gi 392380932	hypothetical protein
0.002038	4.54	gi 392379303	ABC transporter substrate-binding protein
0.008346	4.46	gi 392381539	oxidoreductase
0.041936	4.44	gi 392383323	peptide methionine sulfoxide reductase
0.000239	4.39	gi 392383086	cupin
0.015822	4.38	gi 392377627	hybrid sensor histidine kinase/response regulator
0.000273	4.33	gi 392378073	methyl-accepting chemotaxis sensory transducer (fragment), partial
0.025706	4.29	gi 392378699	type VI secretion protein
0.007748	4.27	gi 392377498	conserved protein of unknown function
0.000167	4.23	gi 392377674	3-hydroxybutyrate dehydrogenase
0.000516	4.21	gi 392379802	heptosyltransferase
5.95E-06	4.19	gi 392381516	3,4-dihydroxy-2-butanone 4-phosphate synthase
1.44E-05	4.15	gi 392378456	putative transcriptional regulator, HTH-XRE family
0.021247	4.11	gi 392382679	peroxiredoxin
0.017961	4.01	gi 392378386	ABC transporter substrate-binding protein
0.006272	3.98	gi 392378465	acyl-CoA dehydrogenase
0.008319	3.93	gi 392381805	Rrf2 family transcriptional regulator
0.000122	3.92	gi 392379747	dehydratase
0.025612	3.84	gi 392384034	ABC transporter
0.000116	3.82	gi 392382078	nitrogen regulatory protein P-II
0.001338	3.79	gi 392380023	putative oligopeptide ABC transporter (substrate-binding protein)
0.022955	3.75	gi 392383224	transcriptional activator, LuxR/FixJ family
0.000357	3.74	gi 392382040	hypothetical protein
0.007415	3.73	gi 392379787	saccharopine dehydrogenase
0.04161	3.72	gi 392378070	chemotaxis protein
0.000527	3.65	gi 392377478	ABC transporter substrate-binding protein
0.012761	3.63	gi 392378072	exported protein of unknown function
0.000806	3.63	gi 392379121	regulatory lipoprotein
0.038187	3.62	gi 392382386	carbon-monoxide dehydrogenase small subunit
0.002038	3.51	gi 392382810	ATP-dependent acyl-CoA ligase
3.36E-05	3.50	gi 392377639	NUDIX hydrolase
0.038908	3.49	gi 392377172	D-amino acid aminotransferase
0.005918	3.45	gi 392380004	2-hydroxychromene-2-carboxylate isomerase
0.001876	3.41	gi 392383231	hypothetical protein

0.002233	3.37	gi 392381659	septum formation initiator
0.017975	3.31	gi 392382764	DNA-binding response regulator
0.010757	3.30	gi 392381417	nicotinate-nicotinamide nucleotide adenyltransferase
0.003254	3.28	gi 392383905	dihydrodipicolinate synthase family protein
0.036227	3.28	gi 392379742	putative Oxoglutarate dehydrogenase (succinyl-transferring)
0.000819	3.22	gi 392377166	PAS domain-containing sensor histidine kinase
0.007861	3.13	gi 392382259	hydroxypyruvate isomerase
0.000291	3.10	gi 392384516	citrate (Si)-synthase
0.000232	3.07	gi 392382116	carboxymethylenebutenolidase
0.013788	3.06	gi 392382531	conserved hypothetical protein; beta-Ig-H3/Fasciclin domain
0.000232	3.03	gi 392377298	hypothetical protein
0.051744	3.00	gi 392378892	hypothetical protein
0.02072	3.00	gi 392383564	conserved protein of unknown function
0.007611	2.99	gi 392380686	membrane protein
8.30E-05	2.97	gi 392383907	conserved exported protein of unknown function
0.00497	2.96	gi 392378074	chemotaxis glutamate methylesterase CheB
0.042449	2.93	gi 392379387	transcriptional regulator
0.017835	2.92	gi 392380533	peptidase S16
0.000221	2.87	gi 392381791	acyl-CoA dehydrogenase
0.026223	2.87	gi 392383892	SapC family protein
8.40E-05	2.87	gi 392378024	fumarylacetoacetate hydrolase
0.004153	2.84	gi 392379968	agmatinase
0.015957	2.81	gi 392382869	two-component sensor histidine kinase; putative heavy-metal sensor (Cu/Zn)
0.004192	2.78	gi 392377471	hypothetical protein
0.019883	2.76	gi 392378173	LPS export ABC transporter periplasmic protein LptC
0.000128	2.74	gi 392380087	acriflavine resistance protein B
0.015647	2.73	gi 392383087	protein of unknown function
0.002029	2.73	gi 392383088	amP-dependent synthetase and ligase
0.020563	2.71	gi 392379889	arginase
0.014545	2.68	gi 392379744	acyl-CoA dehydrogenase
0.000342	2.68	gi 392384521	conserved protein of unknown function
0.000585	2.68	gi 392383065	hypothetical protein
8.80E-05	2.65	gi 392381330	enoyl-CoA hydratase
0.030598	2.61	gi 392378026	sugar ABC transporter
0.000363	2.60	gi 392379894	peptide ABC transporter substrate-binding protein
0.048714	2.58	gi 392381702	phosphate starvation protein PhoH
8.94E-06	2.55	gi 392380730	cold-shock protein
0.007781	2.53	gi 392381940	3-methyl-2-oxobutanoate hydroxymethyltransferase
0.01265	2.52	gi 392383492	hypothetical protein
0.003431	2.52	gi 392381032	isocitrate lyase
0.007333	2.50	gi 392381727	putative transcriptional regulator, Crp/Fnr family
0.000234	2.48	gi 392382858	alkylhydroperoxidase

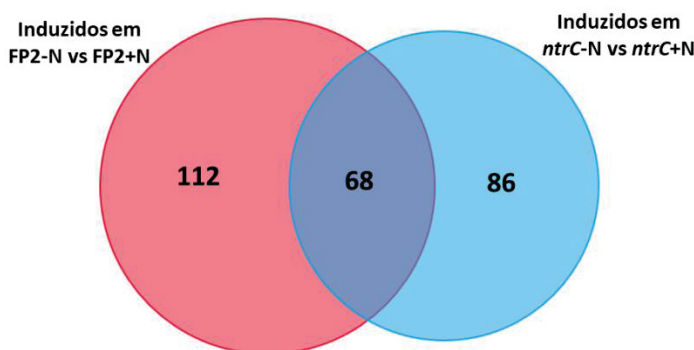
0.053863	2.48	gi 392380240	haloacid dehalogenase
0.006569	2.44	gi 392384520	response regulator
0.024567	2.44	gi 392378151	long-chain-fatty-acid-CoA ligase
0.04699	2.43	gi 392380988	heat-inducible transcriptional repressor HrcA
0.004593	2.42	gi 392378787	imidazolonepropionase
0.045676	2.42	gi 392380313	TetR family transcriptional regulator
0.053197	2.40	gi 392377262	iron-sulfur cluster assembly scaffold protein
0.000868	2.40	gi 392378071	hypothetical protein
0.000344	2.39	gi 392380011	hypothetical protein
0.006871	2.37	gi 392382038	putative phosphoglycolate phosphatase
0.003494	2.35	gi 392380949	transporter
0.013967	2.34	gi 392380705	CarD family transcriptional regulator
0.007038	2.33	gi 392383382	ABC transporter permease
0.001718	2.32	gi 392381099	C4-dicarboxylate ABC transporter
0.001634	2.29	gi 392379736	putative D-lactate dehydrogenase
0.021171	2.26	gi 392380236	NADH-quinone oxidoreductase subunit F
0.019787	2.26	gi 392382937	histidine kinase
0.000642	2.25	gi 392378407	conserved protein of unknown function
0.013802	2.24	gi 392381890	hypothetical protein
0.008476	2.23	gi 392380014	thiamine biosynthesis protein ThiS
0.052226	2.22	gi 392384281	hypothetical protein
0.034284	2.22	gi 392382217	thioesterase
0.021024	2.22	gi 392378255	ABC transporter substrate-binding protein
0.004494	2.19	gi 392380691	two-component response regulator (modular protein)
0.014676	2.18	gi 392383733	asparagine synthetase B
0.005308	2.18	gi 392382321	ABC transporter permease
0.010681	2.16	gi 392382329	membrane protein
0.002096	2.15	gi 392378904	pyruvate dehydrogenase (acetyl-transferring) E1 component subunit alpha
0.023156	2.13	gi 392380826	16S rRNA maturation RNase YbeY
0.056145	2.12	gi 392377571	PleD family two-component system response regulator
0.002058	2.10	gi 392377402	superoxide dismutase
0.020963	2.09	gi 392380015	glycine oxidase
0.005535	2.08	gi 392379459	flagellin
0.003389	2.08	gi 392378782	putative transcriptional regulator, MarR family
0.0105	2.08	gi 392378319	septum formation inhibitor Maf
0.006115	2.08	gi 392378097	chromosome partitioning protein
0.002264	2.07	gi 392382988	N-formylglutamate amidohydrolase
5.93E-05	2.07	gi 392383091	ABC transporter, substrate-binding component
0.016804	2.06	gi 392384535	hypothetical protein
0.04096	2.05	gi 392382126	phosphatidate cytidylyltransferase
3.11E-05	2.05	gi 392377673	thiol:disulfide oxidoreductase
0.006605	2.05	gi 392380246	SAM-dependent methyltransferase (fragment), partial

0.058221	2.04	gi 392377740	TIGR02302 family protein
0.035838	2.02	gi 392382862	hybrid sensor histidine kinase/response regulator
0.026568	2.01	gi 392384522	putative methyl-accepting chemotaxis sensory transducer
0.0012	2.00	gi 392380086	MexH family multidrug efflux RND transporter periplasmic adaptor subunit

FONTE: a autora (2018).

A fim de selecionar potenciais alvos para regulação por NtrC, foi feito um gráfico de Venn (FIGURA 39) com dois grupos de proteínas induzidas: um em amostras de FP2 baixo nitrogênio, quando NtrC está fosforilado e ativo, e outro de proteínas induzidas no mutante *ntrc* baixo nitrogênio, que são reguladas também pela ausência de nitrogênio, porém de forma independente de NtrC.

FIGURA 39 - GRÁFICO DE VENN COM O NÚMERO DE PROTEÍNAS INDUZIDAS EM FP2 E *ntrC* EM BAIXO NITROGÊNIO.

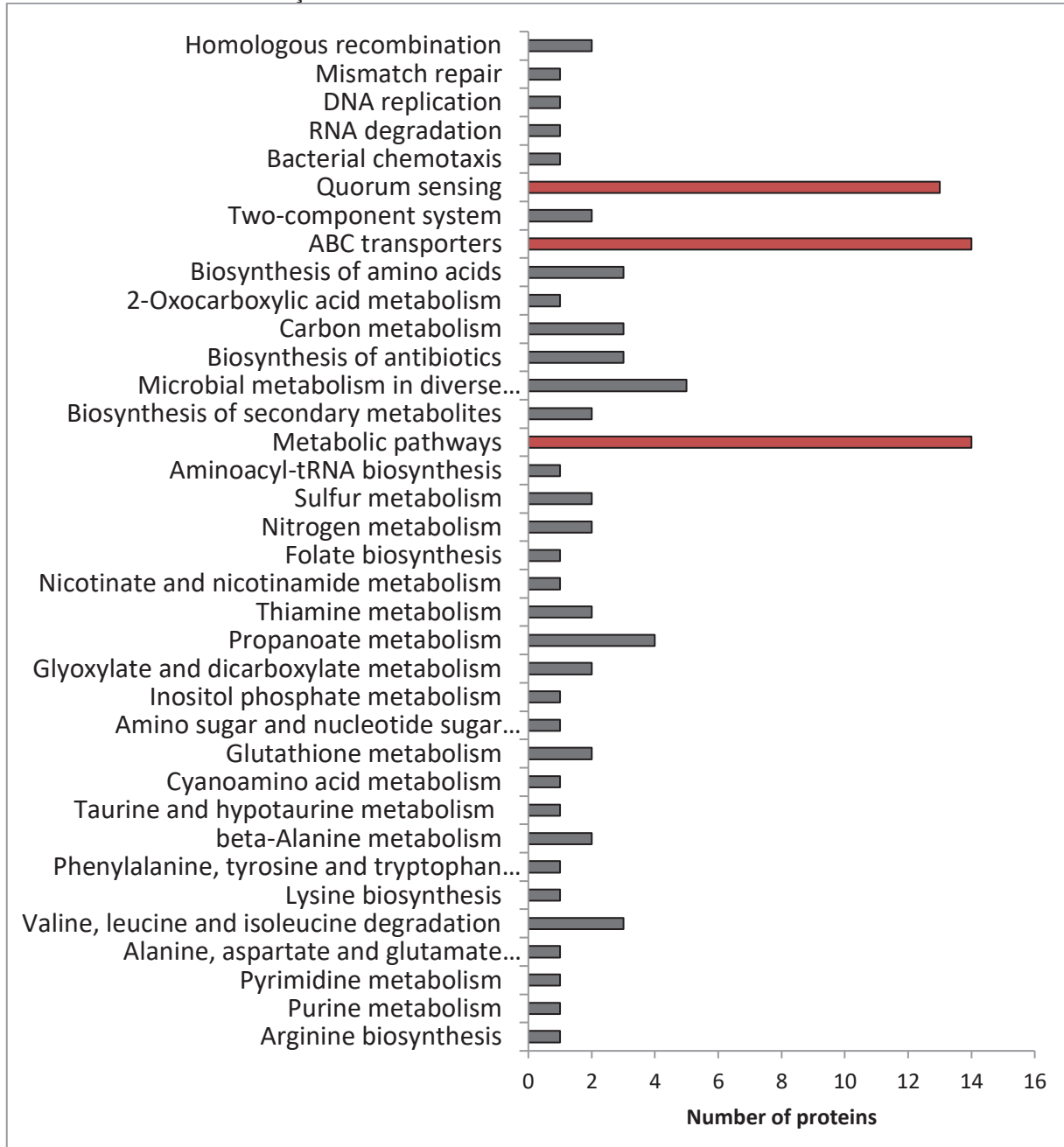


FONTE: a autora (2018).

A intersecção representa um grupo de 68 proteínas que são reguladas pela ausência de nitrogênio, porém, não são ativadas por NtrC, uma vez que o mutante não expressa esse ativador. Por outro lado, as proteínas induzidas exclusivamente em FP2 apresentam potencial para serem induzidas por NtrC, representando um grupo de 112 proteínas que são o foco principal deste estudo.

A classificação KEGG (Cluster of Orthologous Groups) completa desse grupo de proteínas (FIGURA 40), mostrou que a maioria delas (destacadas em vermelho) são transportadores ABC, ou está envolvida em quorum sensing ou vias metabólicas. Detalhes e discussão desse grupo de proteínas estão mostrados no manuscrito da primeira parte deste trabalho.

FIGURA 40 - CLASSIFICAÇÃO KEGG DO GRUPO DE PROTEÍNAS COM POTENCIAL REGULAÇÃO POR NtrC.



FONTE: a autora (2018).

Há ainda um grupo de proteínas hipotéticas ou não caracterizadas. Embora, não foi possível atribuir uma função a elas, NtrC provavelmente ativa direta ou indiretamente essas proteínas em resposta à limitação de nitrogênio.

Análise bioinformática

Foi realizada uma análise em parceria com o departamento de bioinformática da Universidade do Missouri para buscar sítios de ligação de NtrC na região promotora dos genes candidatos. Como não há sequência de ligação para NtrC descrita para *Azospirillum brasiense* FP2 e Sp.245, inicialmente foi realizada uma busca por um motivo em comum na região até 300 pb *upstream* às sequências dos 112 genes candidatos à indução por NtrC. Não foi encontrado nenhum motivo conclusivo e a abordagem foi mudada. Foram feitas buscas por motivos em comum nos promotores de genes conhecidamente regulados por NtrC (*amtB*, *glnZ* e o próprio *ntrC*). Foi encontrado um motivo que teve sua sequência comparada aos sítios de ligação de NtrC já definidos de *E. coli*, *Pseudomonas putida* e *Azospirillum brasiliense* Sp7, uma vez que a sequência apresenta um grau de conservação. Esse motivo poderia ser o sítio de ligação de NtrC em Sp245, mas não ocorreu alinhamento de sequências com os sítios já conhecidos de outros organismos e a análise foi inconclusiva. Uma nova abordagem foi utilizada buscando na região promotora dos genes candidatos os sítios de ligação de NtrC dos organismos supracitados. Além disso, considerando que NtrC ativa a transcrição de genes de forma dependente de sigma 54, foi também realizada uma busca pelo sítio de ligação desse fator alternativo. As proteínas descritas na tabela 23 apresentaram motivos com similaridade de bases (destacadas em verde) em relação aos sítios de ligação de NtrC dos organismos mencionados.

Dentre os 112 genes candidatos, 23 apresentaram um possível sítio de ligação de sigma 54 (tabela 24), com alta similaridade à sequência consenso (bases em verde). Dentre estes, está *glnZ* e *ntrC*, conhecidamente regulados por NtrC e sigma 54. Os 21 genes remanescentes são fortes candidatos à regulação por NtrC, embora mais estudos sejam necessários para avaliar a atividade desses promotores. As proteínas destacadas em negrito na tabela 24 apresentam possíveis sítios de ligação para NtrC e sigma 54, aumentando a possibilidade de regulação por NtrC.

TABELA 23 - PROTEÍNAS COM POSSÍVEIS SÍTIOS DE LIGAÇÃO DE NtrC NA REGIÃO PROMOTORAS DOS GENES. Em verde estão as bases que apresentaram similaridade com o motivo utilizado na busca.

<i>A. brasiliense</i> Sp7 - TGCTTATNNNCTGGCA					
Matched Sequence	p-value	ID	Gene	Proteome FC	Protein name
TGCTTCTCCTCTGGAG	8.21E-06	gi 392383934	<i>ohr</i>	2.87	organic hydroperoxide resistance protein, OsmC superfamily
TGCCATTATTGGCA	2.60E-05	gi 392381004	<i>glnZ</i>	7.92	nitrogen regulatory protein P-II 1
TGCCGATGCCAGCGCA	4.25E-05	gi 392382708	<i>nusB</i>	2.61	transcription antitermination factor NusB
CGCCCATGAGCTGGCC	4.54E-05	gi 392378468		15.37	histidine kinase with CBS domain
CGCCGATCGATTGGCA	7.26E-05	gi 392381004	<i>glnZ</i>	7.92	nitrogen regulatory protein P-II 1
CACCTATGGCTGGTCA	7.33E-05	gi 392379971		2.93	putative spermidine/putrescine transport protein (ABC superfamily, atp_bind)
TGCTTTGGTTGGCG	7.66E-05	gi 392377569		10.75	peptidase S41
TGCCCATGCATCGGCA	7.66E-05	gi 392377481		4.99	spermidine/putrescine ABC transporter ATPase
TGTTTGGGCTTGCA	7.72E-05	gi 392377740		2.39	TIGR02302 family protein
<i>E. coli</i> - TGCACNNNNNTGGTGCA					
Matched Sequence	p-value	ID	Gene	Proteome FC	Protein name
TCCACGCTGGGGTGCA	4.72E-06	gi 392380988	<i>hrcA</i>	2.71	heat-inducible transcriptional repressor HrcA
CGCACCCGGTGGAGCG	3.12E-05	gi 392382791		2.14	alcohol dehydrogenase
TGCACGCCGGGATGCT	3.24E-05	gi 392379730			hypothetical protein
TGCGCCATGGGGTGCG	3.48E-05	gi 392382255	<i>thiC</i>	2.51	phosphomethylpyrimidine synthase ThiC
CGCACCCGTTGGGCC	4.32E-05	gi 392382683		2.37	membrane protein
TCTCGGGGTGGTAA	4.44E-05	gi 392379802		2.47	heptosyltransferase
CGCACCCCCATGCCGA	4.63E-05	gi 392382255	<i>thiC</i>	2.51	phosphomethylpyrimidine synthase ThiC
TGCACGGGATTGGGCC	4.63E-05	gi 392383241		3.06	hybrid sensor histidine kinase/response regulator, partial
TGCACCGCCAGCGTGG	6.72E-05	gi 392380988	<i>hrcA</i>	2.71	heat-inducible transcriptional repressor HrcA
TCCACCGTGGGTGAC	7.44E-05	gi 392382481	<i>ruvC</i>	3.36	crossover junction endodeoxyribonuclease
TGCCCGCCTTTGGCA	8.76E-05	gi 392384046		39.96	ABC transporter substrate-binding protein
TGCACAGCAAAGTGC	9.16E-05	gi 392378731		10.59	X-Pro dipeptidyl-peptidase

<i>Pseudomonas putida</i> - TGCACCCATAATGGTGCA					
Matched Sequence	p-value	ID	Gene	Proteome FC	Protein name
GGCAGCGTAATGCTGCA	5.23E-06	gi 392381228		3.79	CBS domain-containing protein
TGCAGCATTACGCTGCC	4.95E-05	gi 392381228		3.79	CBS domain-containing protein
TGCCAATAATTACGCA	7.17E-05	gi 392381004	glnZ	7.92	nitrogen regulatory protein P-II 1

FONTE: a autora (2018).

TABELA 24 - PROTEÍNAS COM POSSÍVEIS SÍTIOS DE LIGAÇÃO DE SIGMA 54 NA REGIÇÃO PROMOTORA DOS SEUS GENES. Em verde estão as bases que apresentaram similaridade com o motivo utilizado na busca. As proteínas em negrito apresentam também possível sítio de ligação de NtrC.

Sigma 54 -TGGCACGNNNNTTGC					
Matched Sequence	p-value	ID	Gene	Proteome FC	Protein name
TTGCACGGGGATTGC	1.94E-06	gi 392383241		3.06	hybrid sensor histidine kinase/response regulator, partial
TGGCACGGATTCTGC	3.42E-06	gi 392384046		39.96	ABC transporter substrate-binding protein
TGGCATGGAACTTGC	3.89E-06	gi 392377481		4.99	spermidine/putrescine ABC transporter ATPase
CGGCACGCCATGC	6.15E-06	gi 392381749		3.94	putative Methyl-accepting chemotaxis protein with multiple PAS domains
TGCCCCGACGGTAGC	7.42E-06	gi 392377639		2.17	NUDIX hydrolase
TGGCACGGGCCGTGT	9.23E-06	gi 392377481		4.99	spermidine/putrescine ABC transporter ATPase
TGGCCTGGGGCTTGC	9.31E-06	gi 392377167	ntrC	3.34	nitrogen regulation protein NR(I)
TGGCCTGCCCGTTGC	9.41E-06	gi 392378148		2.77	succinyl-diaminopimelate desuccinylase
TGGCACGGCAACACGC	1.34E-05	gi 392383934		2.87	organic hydroperoxide resistance protein, OsmC superfamily
AGGCACCCAGGTTGC	1.43E-05	gi 392379744		3.53	acyl-CoA dehydrogenase
TGGCACGGCTGGCTGA	1.50E-05	gi 392383137		6.00	hypothetical protein
CGGAACGGCATTGC	1.65E-05	gi 392384143	mutA	9.26	adenosylcobalamin-dependent methylmalonyl-CoA mutase small subunit (MCM-beta)(N-terminal fragment), partial
TGGCACACCTCCCTGC	2.03E-05	gi 392381749		3.94	putative Methyl-accepting chemotaxis protein with multiple PAS domains
CGGCACGGGGTTTC	2.03E-05	gi 392381341		6.16	hypothetical protein

AGGCACGGTAATTGC	2.33E-05	gi 392379924	2.41	exported protein of unknown function
TGGCACAGCGTTGA	2.77E-05	gi 392381713	14.46	chemotaxis sensory transducer
TGGCCCAAGGATTGC	3.07E-05	gi 392380826	2.01	16S rRNA maturation RNase YbeY
CGGCACGCTGTTGG	3.63E-05	gi 392378005	gi nH	amino acid ABC transporter substrate-binding protein
TGGCACGAAACGGTTC	3.79E-05	gi 392381052	218.62	hypothetical protein
TGGCCCCGTTGTTCC	7.17E-05	gi 392382255	thiC	phosphomethylpyrimidine synthase ThiC
CGGCACGATTGTGA	8.20E-05	gi 392381004	gi nZ	nitrogen regulatory protein P-II 1
CGGCCGGCGGGTGGC	9.77E-05	gi 392381633	11.30	protein of unknown function
CGGCACGCCGCCGC	9.80E-05	gi 392379403	4.62	copper ABC transporter, permease component (modular protein)

FONTE: a autora (2018).

Análise metabolômica

Para comparar as respostas metabólicas de *A. brasiliense* FP2 e do mutante *ntrC*, culturas bacterianas foram produzidas em triplicata nas mesmas condições descritas para a análise proteômica. Os metabólitos intracelulares foram extraídos da fase polar para análise GC-MS, como descrito no manuscrito deste trabalho. Os compostos foram identificados por comparação do tempo de retenção e massa experimentais com a biblioteca do Centro de Metabolômica da Universidade do Missouri. Os metabólitos foram comparados entre as amostras utilizando Metaboanalyst e considerados diferenciais quando o “fold change” estava acima de 2 e o p-value menor que 0,05. O enfoque da análise metabolômica apresentado no manuscrito foram as comparações entre baixo e alto nitrogênio para a mesma estirpe bacteriana. No entanto, foram feitas as análises comparativas também entre as estirpes na mesma disponibilidade de nitrogênio. Os metabólitos diferenciais encontrados na análise entre selvagem e mutante, ambos em baixo ou alto nitrogênio, estão apresentados nas tabelas 25 e 26. Em alto nitrogênio foram encontrados 30 compostos diferenciais, dos quais 12 foram identificados (3 na estirpe selvagem e 9 na mutante), principalmente açúcares. Em baixo nitrogênio são 64 compostos diferenciais, incluindo 14 identificados em FP2 e 14 no mutante, dentre esses a maioria é composta por aminoácidos e poliaminas. Dois compostos identificados como D-manose (*m/z* 319,2), com pequena variação no tempo de retenção, são mais abundantes na estirpe mutante em alto nitrogênio, comparada com a selvagem e também na estirpe selvagem em baixo nitrogênio quando comparada com o mutante na mesma condição. O aumento desses açúcares no selvagem em baixo nitrogênio e no mutante em alto nitrogênio indica uma alta atividade do metabolismo de carboidratos e energia nestas amostras. Foi mostrado no manuscrito deste trabalho que a estirpe selvagem em alto nitrogênio, quando comparada com baixo nitrogênio, apresenta abundância de diversos aminoácidos, principalmente os de cadeia ramificada, o que foi atribuído ao estado bem nutrido da célula em alto nitrogênio. Porém, na comparação entre selvagem e mutante em baixo nitrogênio (tabela Y), esses mesmos compostos apresentaram maior abundância na estirpe selvagem, mesmo com baixa disponibilidade de N. Interessantemente, o ácido úrico (*m/z* 456,2), que apresentou maiores foldchanges nas comparações entre alto e baixo nitrogênio para a mesma estirpe (manuscrito),

não apresentou abundância diferencial quando as comparações foram realizadas entre as estirpes. Portanto, o aumento do ácido úrico ocorre em alta disponibilidade de nitrogênio em ambas as estirpes quando comparadas com a condição de baixo N, indicando que as vias de síntese desse composto não são reguladas por NtrC. Putrescina (*m/z* 174,1) está mais abundante em alto nitrogênio em ambas estirpes em relação ao baixo N (manuscrito), porém, quando a comparação é entre estirpes, o mutante apresentou um aumento desse composto em relação à selvagem quando ambas estão em baixo nitrogênio. A concentração de poliaminas intracelulares é correlacionada positivamente com a taxa de crescimento, o que explicaria a abundância de putrescina em alto N para ambas estirpes. No entanto, a alta taxa de morte celular na estirpe mutante em baixo N, devido à falta de nutrientes e à ausência de um sistema eficiente na assimilação alternativa de N, pode levar a um aumento de putrescina.

TABELA 25 - DIFFERENTIAL METABOLITES BETWEEN *A. brasiliense* FP2 AND *ntrC* UNDER HIGH NITROGEN.

FP2 high N vs <i>ntrC</i> high N	Retention time (min)	<i>m/z</i>	FC	log2(FC)
Unknown	9.9969	172.1	91.66	6.5182
Unknown	31.2578	257.1	11.66	3.544
Unknown	13.5311	159.1	6.33	2.6631
Unknown	29.9889	353.2	5.24	2.3897
Unknown	10.7788	173.1	5.17	2.3713
Unknown	13.4449	159.2	4.67	2.2242
Laminaribose Meox 2	31.8343	204.1	2.89	1.5295
Citramalic Acid, O,O,O-TMS	17.4566	247.1	2.64	1.3981
Unknown	29.4829	338.3	2.56	1.3543
Unknown	20.0339	231.2	2.36	1.2398
Unknown	33.534	236.1	2.30	1.202
Adenosine, 5-methylthio- 3TMS	33.5353	236.1	2.30	1.202
Unknown	33.5489	236.1	2.30	1.202
<i>ntrC</i> high N vs FP2 high N	Retention time (min)	<i>m/z</i>	FC	log2(FC)
Arabinose methoxyamine 4TMS	20.3391	307.1	3.31	1.7254
Unknown	24.8873	159	3.25	1.7008
Unknown	21.6392	205.1	3.14	1.6486
Unknown	19.2553	233.1	3.12	1.6408
Pyroglutamic acid 2TMS	18.36	156.1	2.87	1.5222
Xylose, O,O,O,O-TMS, MEOX1	20.3459	217.1	2.78	1.4727
Unknown	10.7476	186.2	2.74	1.4559
L-Glutamic Acid, N,O,O-TMS	19.627	246.1	2.71	1.4394
Unknown	21.6718	217.1	2.67	1.4189
Unknown	23.4162	205.1	2.36	1.2404
D-Mannose, O,O,O,O-O-TMS, o-	23.6414	319.2	2.35	1.2355

methyloxime 2					
D--Mannose, O,O,O,O,O-TMS, MEOX1	23.3497	319.2	2.34	1.2278	
Hexadecenoic acid, 9-Z- 1TMS	25.1247	311.3	2.29	1.1947	
Octadecenoic acid, 9-Z- 1TMS	27.3818	339.3	2.25	1.1682	
Unknown	25.1674	241.2	2.23	1.1556	
Boric Acid, O,O,O-TMS	9.204	221.1	2.15	1.1076	
Unknown	9.3044	191.1	2.09	1.0668	

FONTE: a autora (2018).

TABELA 26 - DIFFERENTIAL METABOLITES BETWEEN *A. brasiliense* FP2 AND *ntrC* UNDER LOW NITROGEN.

FP2 low N vs <i>ntrC</i> low N	Retention time (min)	<i>m/z</i>	FC	log2(FC)
Unknown	9.9969	172.1	95.09	6.5712
Methyl 9-Z-octadecenoate	26.1447	264.2	20.96	4.3892
Unknown	13.3127	158	9.96	3.3155
Unknown	13.3181	158	9.21	3.2027
Unknown	15.8743	306.1	8.61	3.1066
Unknown	15.913	306.2	8.61	3.1066
Unknown	25.9975	220.2	6.75	2.7553
Unknown	26.0016	220.2	6.75	2.7553
Phosphoric Acid, O,O,O-TMS	14.092	299.1	5.21	2.3825
Maltose Monohydrate MEOX2 TMS	32.9893	361.2	3.98	1.993
L-Valine, N-trimethylsilyl-, trimethylsilyl ester	13.1994	218.1	3.82	1.9353
D--Mannose, O,O,O,O,O-TMS, MEOX1	23.3497	319.2	2.91	1.5405
Unknown	31.2578	257.1	2.90	1.5344
D--Mannose, O,O,O,O,O-TMS, o-methyloxime 2	23.6414	319.2	2.84	1.504
L-Phenylalanine, N,O-TMS	19.9627	218.1	2.79	1.4797
Glycine 3TMS	14.8394	174.1	2.77	1.4691
L-Isoleucine, N,O-TMS	14.5321	158.2	2.66	1.4131
Unknown	23.4162	205.1	2.59	1.3707
L-Lysine, N,N,N,O-TMS	23.777	174.1	2.35	1.2303
L-Glutamic Acid, N,O,O-TMS	19.627	246.1	2.21	1.1455
Succinic Acid 2 TMS	14.8543	247.1	2.11	1.075
Unknown	23.0317	160.1	2.10	1.0715
Unknown	23.0378	160.1	2.10	1.0715
ISOMALTOSE MEOX1 TMS	32.3104	204.2	2.03	1.025
Laminaribose Meox 2	31.8343	204.1	2.00	1.0008
<i>ntrC</i> low N vs FP2 low N	Retention time (min)	<i>m/z</i>	FC	log2(FC)
Unknown	21.6392	205.1	5.93	2.5669
Unknown	19.2553	233.1	4.20	2.0703
L-Putrescine, N,N,N,N-TMS	21.5267	174.1	4.17	2.0611
Unknown	21.6718	217.1	4.06	2.0223
Unknown	10.7476	186.2	3.73	1.8994
Levulinic acid, 5-amino- 1MEOX 3TMS MP	21.7396	174.1	3.65	1.8687
Unknown	13.5012	233.2	3.37	1.7521
Unknown	12.5334	188.2	3.13	1.646

Tristrimethylsilylhydroxylamine	11.6117	249.1	3.00	1.5854
Octadecenoic acid, 9-Z- 1TMS	27.3818	339.3	2.92	1.5458
Unknown	28.1536	339.3	2.88	1.5263
Unknown	26.9959	299.3	2.85	1.5133
Citramalic Acid, O,O,O-TMS	17.4566	247.1	2.84	1.5039
Unknown	26.2803	325.3	2.78	1.4741
Unknown	26.3176	325.3	2.78	1.4741
Unknown	25.1674	241.2	2.74	1.452
Unknown	31.5698	230.1	2.67	1.4177
Boric Acid, O,O,O-TMS	9.204	221.1	2.66	1.4113
Unknown	27.1213	339.3	2.64	1.3982
Hexadecenoic acid, 9-Z- 1TMS	25.1247	311.3	2.60	1.3781
Unknown	9.1335	156.2	2.58	1.3655
Unknown	9.3044	191.1	2.58	1.3654
Unknown	27.5493	342.3	2.40	1.2631
Stearic Acid, O-TMS	27.5527	342.3	2.40	1.2631
4-HYDROXYPYRIDINE,O-TMS	10.2966	152.1	2.37	1.2427
Nonanoic Acid TMS	15.7272	215.1	2.37	1.2421
Hexadecanoic Acid, O-TMS	25.3322	313.3	2.33	1.2226
Unknown	9.8666	243.9	2.33	1.2205
Tetradecanoic Acid, O-TMS	22.9082	285.2	2.27	1.1836
Oxalic Acid TMS	12.2696	219.2	2.22	1.153
Unknown	9.1559	158.2	2.22	1.1488
Glutaric acid, 2-hydroxy- 3TMS	18.9304	247.1	2.21	1.1469
Unknown	18.9325	247.1	2.21	1.1469
Unknown	9.4068	155.2	2.20	1.1357
Unknown	9.3993	155.1	2.19	1.1282
Unknown	12.1909	191.1	2.16	1.109
Unknown	29.3961	295.2	2.04	1.0321
Unknown	46.5443	207.1	2.02	1.0166
Unknown	30.836	369.3	2.01	1.0067

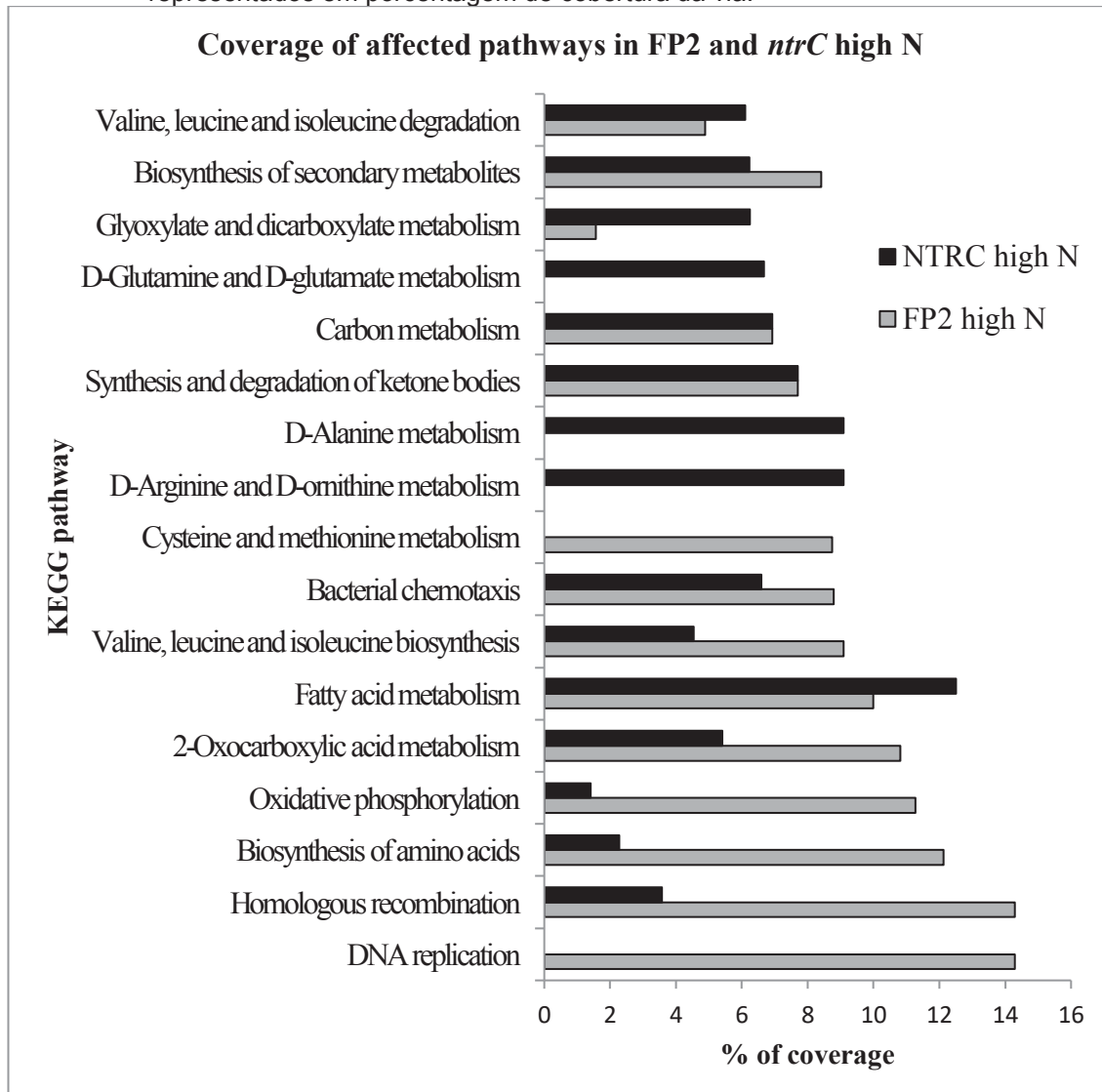
FONTE: a autora (2018).

Integração de proteoma e metaboloma utilizando análise de vias KEGG

O *Azospirillum brasilense* Sp.245 possui 124 vias metabólicas, de acordo com KEGG (Kyoto Encyclopedia of Genes and Genomes). As proteínas e metabólitos diferenciais de cada comparação foram mapeados de acordo com a via a qual pertencem. No manuscrito apresentado neste trabalho, foram descritas as vias mais afetadas pela disponibilidade de nitrogênio em cada estirpe. As 10 vias mais afetadas em cada amostra, nas comparações entre selvagem e mutante, alto e baixo N, estão apresentadas nas figuras 41 e 42. A figura se baseia na porcentagem de cobertura de cada via, integrando dados do proteoma e metaboloma. A limitação de nitrogênio induziu no mutante principalmente vias

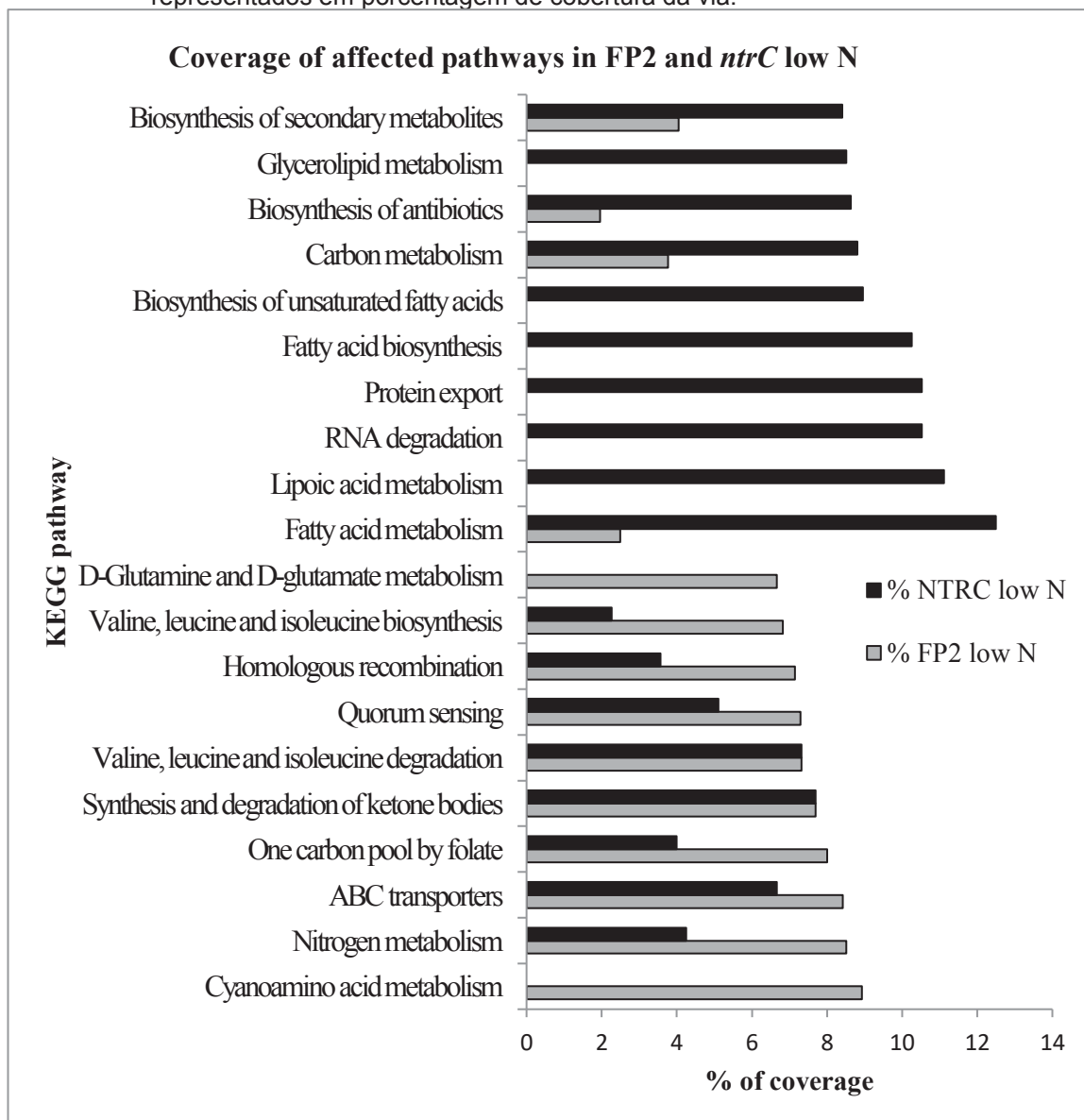
relacionadas ao metabolismo e síntese de ácidos graxos, sugerindo que esses processos não são regulados por NtrC. Por outro lado, as vias induzidas no selvagem em baixo N são potencialmente induzidas por NtrC, e incluem principalmente vias relacionadas ao metabolismo de nitrogênio, transportadores ABC e quorum sensing. Em alto nitrogênio, a via mais afetada no mutante também é relacionada ao metabolismo de ácidos graxos. Portanto, a alteração observada nessa via é provavelmente uma adaptação à falta de NtrC e não à ausência de N. No selvagem em alto nitrogênio, as vias mais induzidas são relacionadas à síntese de aminoácidos e replicação de DNA, em decorrência do estado nutricional das células.

FIGURA 41 - DEZ VIAS MAIS AFETADAS NAS ESTIRPES SELVAGEM E MUTANTE EM ALTO NITROGÊNIO. Os resultados incluem análise proteômica e metabóloma e estão representados em porcentagem de cobertura da via.



FONTE: a autora (2018).

FIGURA 42 - DEZ VIAS MAIS AFETADAS NAS ESTIRPES SELVAGEM E MUTANTE EM BAIXO NITROGÊNIO. Os resultados incluem análise proteômica e metabolômica e estão representados em porcentagem de cobertura da via.



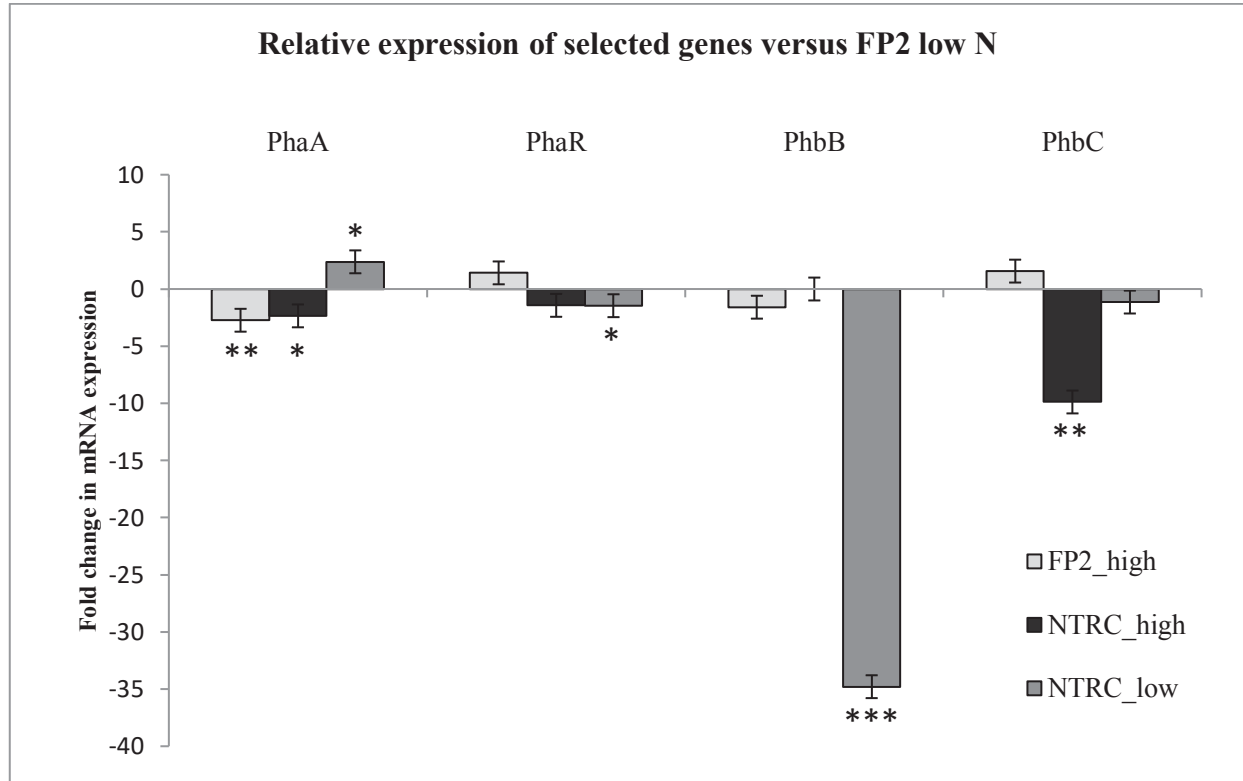
FONTE: a autora (2018).

Análise qRT-PCR de genes diferencialmente expressos

Além dos genes selecionados para validação da análise proteômica (descritos no manuscrito deste trabalho), também foram feitas qRT-PCR para genes envolvidos na síntese de Polyhydroxybutyrate (PHB). Esse composto é um polímero que forma grânulos de armazenamento de carbono, que são envolvidos em lipídeos e proteínas denominadas fasinas. Os três genes envolvidos na síntese de PHB são *phbA* (β -ketothiolase), *phbB* (acetoacetyl coenzyme A reductase), e *phbC* (PHB synthase) e também o gene *phaR*, que codifica o repressor das fasinas, tiveram sua

expressão avaliada por qRT-PCR em cada amostra. A expressão relativa foi calculada em função de FP2 em baixo nitrogênio e está representada na figura 43.

FIGURA 43 – EXPRESSÃO RELATIVA DOS GENES SELECIONADOS COMPARADOS AO CONTROLE *A. brasiliense* FP2 BAIXO N. Asteriscos representam p-value = 0.05*; 0.01** and 0.001***.



FONTE: a autora (2018).

